Engineering rFVIIa-loaded platelets; a novel approach to treating acute bleeding

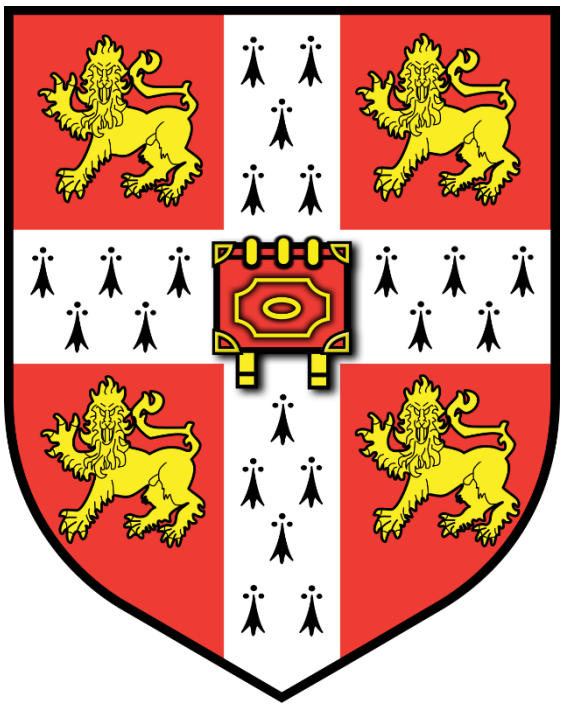

Souradip Mookerjee
St Catharine's College

This thesis is submitted on November 2020 for the degree of Doctor of Philosophy

Declaration

This dissertation is the result of my own work and includes nothing which is the outcome of work done in collaboration except as declared in the Preface and specified in the text. It is not substantially the same as any that I have submitted, or am concurrently submitting, for a degree or diploma or other qualification at the University of Cambridge or any other University or similar institution except as declared in the Preface and specified in the text.

I further state that no substantial part of my dissertation has already been submitted, or is being concurrently submitted, for any such degree, diploma or other qualification at the University of Cambridge or any other University or similar institution except as declared in the Preface and specified in the text. This dissertation does not exceed the prescribed limit of 60,000 words.

Souradip Mookerjee
November 2020

Abstract

Engineering rFVIIa-loaded platelets; a novel approach to treating acute bleeding

Souradip Mookerjee, St Catharine's College

Haemorrhage remains a leading cause of mortality around the world, resulting from both trauma and surgery. Current treatments for acute haemorrhage include blood products such as fresh frozen plasma, as well as platelet transfusion and recombinant clotting factors such as rFVIIa. However, the use of recombinant clotting factors is limited due to cost and adverse side effects resulting from increased thrombosis, such as increased rate of myocardial infarction and cerebrovascular accidents.

Platelets are small anucleate cells that exist in very large quantities in our blood and, along with cross-linked fibrin from the coagulation cascade, are involved in forming a haemostatic plug upon exposure to damaged endothelium in a wound. They are metabolically active and undergo a process of platelet activation when stimulated by pro-thrombotic agonists such as thrombin resulting from the coagulation cascade. This then triggers a process whereby the contents of their granules are released locally to facilitate coagulation.

This thesis explores the possibility of loading these platelet granules with recombinant clotting factors, in this case rFVIIa which has already been shown in clinical trials to result in a significant decrease in mortality from acute haemorrhage. The targeted delivery of this drug is explored, both through endocytosis and genetic engineering of megakaryocytes differentiated *in vitro* from induced pluripotent stem cells (iPSCs). These are evaluated with *in vitro* assays to model the process of clot formation, as well as an *in vivo* model of haemostasis to compare their efficacy to conventional treatments. Overall, this serves as a proof of concept of the engineering of platelet granules as a novel drug delivery system.

Acknowledgements

I would firstly like to thank Dr Robert Semple, Professor Stefan Marciniak, Lesley Flood, Hannah Dennis and everyone else associated with the MB/PhD programme for giving me the opportunity to undertake this period of research alongside my medical studies, as well as all of their ongoing support and believing in me throughout. I would also like to thank Dr Annett Mueller and Dr Thomas Moreau for being excellent supervisors in my first year, and Dr Holly Foster and Dr Amie Waller in my second and third years.

I would not be where I am today without Dr Cedric Ghevaert who has been an amazing PI to work with as well as a trusted mentor and friend, as well as everyone else in the Ghevaert Lab who has helped me over the years including but not limited to Dr Moyra Lawrence, Dr Amanda Evans and Dr Dan Howard.

All of this would not have been possible without Dr Oliver and Professor Marciniak who both extended an offer to me to study at Cambridge many years ago, for whom I have been eternally grateful and no doubt changed the course of my life. Unfortunately, Dr Oliver passed away unexpectedly during the writing of this thesis, but he is fondly remembered by countless people including myself at St Catharine's College whom he taught and provided pastoral advice to.

I would not have been able to survive the changing world of 2020 without the crucial support from my family, especially my parents, Dr Joydeep and Dr Sutapa Mookerjee and my sisters, Saloni and Sohana who welcomed me back home as the country went into lockdown and I began to write this thesis. I may have starved to death long before November if it were not for their nourishment, both culinary and emotionally.

Finally, I would like to thank the support of the Rosetrees Trust and James Baird Fund, who funded my research through these three years, and whose continued support, friendliness and encouragement has helped me become a better researcher.

Table of Contents

List of Figures

List of Tables

List of Abbreviations

AAVS1	Adeno-Associated Virus Integration Site 1
B2M	β2-microglobulin
cbMK	Cord blood-derived megakaryocyte
CFU-S	Colony forming units in the spleen
CLP	Common lymphoid progenitor
CMP	Common Myeloid Progenitor
CRISPR	Clustered regularly interspaced short palindromic repeats
DSB	Double Strand Break
DTS	Dense tubular system
EB	Erythroblast
ENDO	Endostatin/COL18A2
F7F	FVII modified with a furin cleavage site
F7TF	FVII modified with a furin cleavage site and a thrombin cleavage site
FACS	Fluorescence Activated Cell Sorting
FC	Flow cytometry
FFP	Fresh frozen plasma
FoPMK	Forward-programmed megakaryocyte
GP1b	Glycoprotein 1b
GR	Golgi remnants
HLA	Human Leukocyte Antigen
HPA	Human Platelet Antigen
HSC	Haematopoietic Stem Cell
iPSC	Induced Pluripotent Stem Cell
IVC	Inferior vena cava
MEP	Megakaryocyte-erythroid progenitor
MF	microfilaments
MK	Megakaryocyte
MkP	Megakaryocyte Progenitor

MPP	Multipotent Progenitor
MS3	MasterShef 3
MS4	MasterShef 4
MTC	Microtubular coil
OCS	Open Canalicular System
PF4	Platelet Factor 4
PLP	Platelet-like particle
PS	Phosphotidylserine
RBC	Red blood cell
TALEN	Transcription activator-like effector nucleases
TFPI	Tissue Factor Pathway Inhibitor
THBS	Thrombospondin
VEGF	Vascular Endothelial Growth Factor
vWF	Von Willebrand Factor
vWF-F7TF	Fusion protein of the SPD2 domain of vWF to FVII modified with a thrombin and furin cleavage site
ZFN	Zinc Finger Nuclease

1 INTRODUCTION

1.1 An introduction to platelets

Platelets are anucleate, discoid cells with a radius of 2.6μm-2.9μm (Figure 1.1). They are the smallest cells circulating in human blood at an average concentration of 150-400x10^9 per litre. They last for around ten days in the circulation meaning that daily, megakaryocytes release 1/10^{th} of the platelet mass into the circulation and that 1/10^{th} of the circulating platelets are cleared in the spleen and the liver (Kaplan and Saba, 1978). Their primary physiological function is in haemostasis where they can sense damaged endothelium and accumulate at the site of injury, initiating blood clot formation to block the circulatory leak although recent work has shown them to be important in many immunological functions (Semple, Italiano and Freedman, 2011). Although they lack a nucleus, platelets remain metabolically active and can sustain de novo translation from remnant mRNAs (Weyrich *et al.*, 2004).

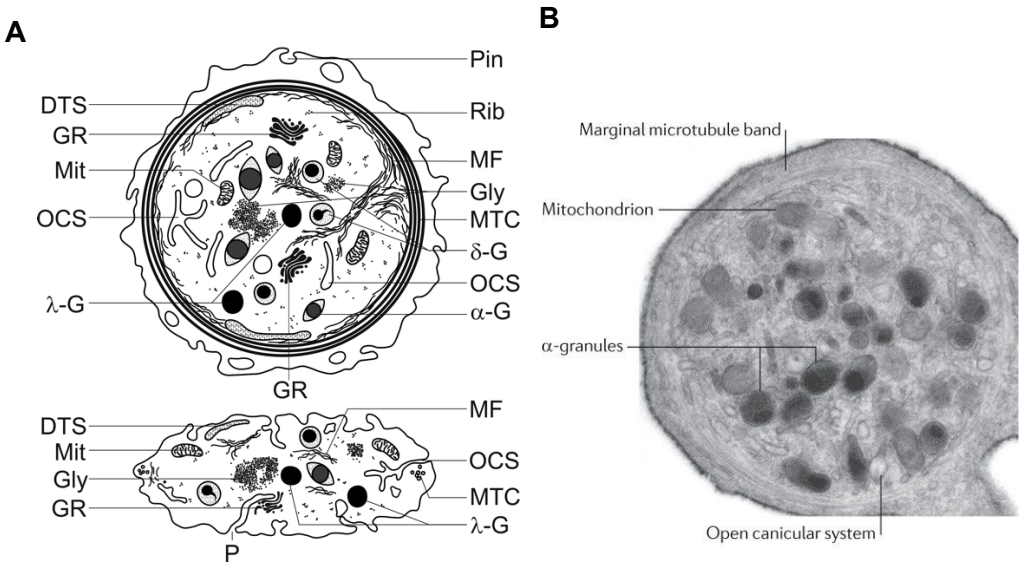

Figure 1.1. *Schematic and real electron micrograph of the ultrastructure of platelets.* ***(A)*** *A schematic of platelet ultrastructure in the equatorial plane (upper image) and in cross section (lower image). Reprinted under the CC BY license from Transmission Electron Microscopy of Platelets From Apheresis and Buffy-Coat-Derived Platelet Concentrates (Neumüller, Ellinger and Wagner, 2015)* ***(B)*** *An electron micrograph of a platelet showing some of these features highlighted in real platelets. (Reprinted by permission from Springer Customer Service Centre GmbH: Springer Nature, Nature Reviews Immunology: Platelets and the Immune Continuum. Semple, Italiano and Freedman © 2011; permission conveyed through Copyright Clearance Center, Inc)*

Abbreviations: DTS = dense tubular system, Gly = glycogen, α = α-granules, δ = δ-granules or dense bodies, λ = λ-granules or lysosomes, GR = Golgi remnants, MF = microfilaments, Mit = Mitochondria, OCS = open canalicular system, P = pores of the OCS, Pin = pinocytosis, Rib = ribosomes, MTC = microtubular coil.

1.2 *Megakaryopoiesis and thrombopoiesis in vivo*

Platelets arise from larger (10-65μm) polyploid cells known as megakaryocytes (MKs) that are, in turn, derived from haematopoietic stem cells (HSCs) in the bone marrow (Levine, Hazzard and Lamberg, 1982). The process of these stem cells differentiating to form megakaryocytes is known as megakaryopoiesis, while the process by which these polyploid multinucleate megakaryocytes fragment to form platelets is known as thrombopoiesis (Kaushansky, 2005; Geddis, 2010) (Figure 1.2).

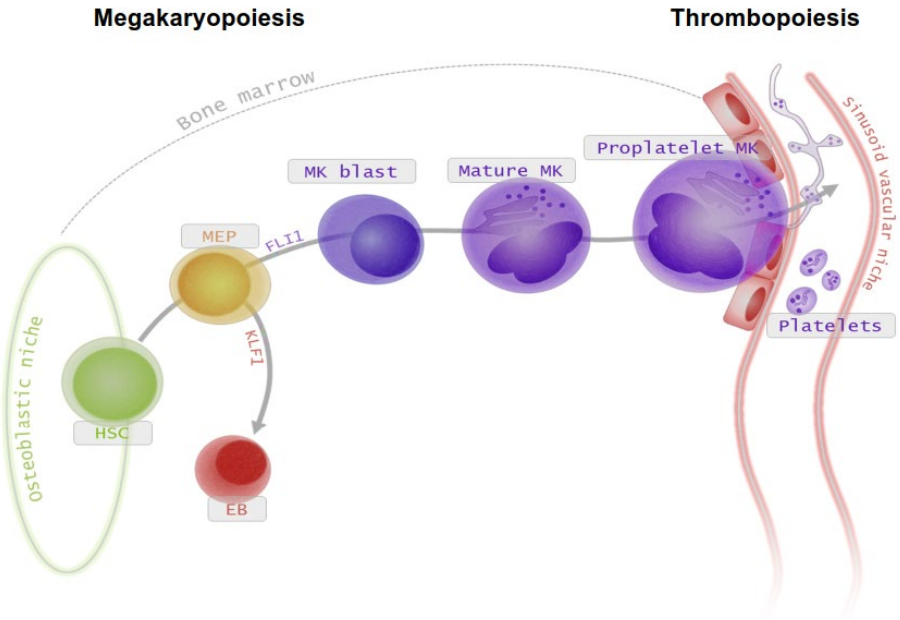

Figure 1.2. *An overview of differentiation from HSCs to megakaryocytes in vivo, followed by thrombopoiesis to give rise to platelets in the circulation. (Figure by Thomas Moreau, unpublished, reproduced with permission).*

1.2.1 *An introduction to stem cells*

A stem cell is defined as a cell that has the properties of being able to self-renew and to differentiate to produce more specialised cells, leading to a loss of some of the stem cell's development potential. Pioneering work in the 20th century defined the power of a single cell to fully regenerate tissues destroyed by radiation (Weissman, 2014). This idea arose originally from studies in the haematopoietic system, after the atom bomb was deployed, it became clear in animal models that the lowest lethal dose effectively eliminated the blood-forming system, resulting in death within two weeks (Weissman, 2014). At the height of the cold war, there was much research on how to counteract these effects through bone marrow transplantation. The dominant theory of the day was that a transplant from an unirradiated donor released factors that drove the repair of the irradiated host cells (Jacobson *et al.*, 1951). Two important papers reversed this notion, using

either mice bearing a chromosome marker or rats with their own histochemically-trackable chromosomes as a bone marrow donor to show that at least early post-treatment survival was driven by the regeneration of blood-formation by the donor cells rather than by host cells repaired by the postulated factors (Ford *et al.*, 1956; Nowell *et al.*, 1956).

Type of Stem Cell	**Differentiates into**	**Example of cell:**
Totipotent	All embryonic and extraembryonic tissues	Zygote
Pluripotent	All embryonic tissues	Embryonic stem cell (ESC), induced pluripotent stem cell (iPSC)
Multipotent	All lineages of a tissue/organ	Haematopoietic stem cell (HSC), neural stem cell (NSC)
Oligopotent	A limited number of lineages	Common myeloid progenitor (CMP), common lymphoid progenitor (CLP)
Bipotent	Two different lineages	Megakaryocyte erythroid progenitor (MEP)
Unipotent/Progenitor cell	One lineage	Macrophage progenitor

Table 1.1. *A summary of the different types of stem cells identified in vivo, categorised by their potential for differentiation.*

McCulloch and Till gave bone marrow transplants to heavily irradiated mice and showed that these cells migrated to the spleen and were able to form nodules there that reconstituted the haematopoietic system of these animals (McCulloch and Till, 1960; Becker, McCulloch and Till, 1963). Within each nodule, they identified donor cells of several different lineages (erythrocyte-forming, platelet-forming and leukocyte-forming) and used abnormal chromosome marker studies to establish the clonal nature of these nodules. This, combined with the direct linear relationship between the number of cells transplanted and number of nodules formed, led to the conclusion that each nodule represented the progeny of a single transplanted bone marrow cell. They also demonstrated that cells within the colony could give rise to additional colonies after serial transplantation into a second recipient (the now classic assay of self-renewal potential). Based around the numbers of bone marrow cells required for a successful transplant, they also concluded that this cell capable of both self-renewal and differentiation was rare in the bulk population. Furthermore, these nodules (that they named

'colony forming units in the spleen', or 'CFU-S'), were noted to have a variable capacity for self-renewal, giving rise to the idea of functional heterogeneity and that not all stem cells are created equal (Siminovitch, McCulloch and Till, 1963). Subsequent work over the decades established that the zygote itself was a 'totipotent' stem cell, and as these cells divided and specialised into various bodily tissues, they became more restricted to only forming cells within each lineage (Zakrzewski *et al.*, 2019) and that regulation of clonal expansion may be stochastic (Wiesner *et al.*, 2018). Eventually, the cell giving rise to all the lineages of the blood system became known as a haematopoietic stem cell, and other identified stem cell types are outlined in Table 1.1.

1.2.2 *HSC maintenance in bone marrow*

Stromal co-cultures were used to maintain HSC cultures *in vitro*, and it became clear that *in vivo* HSC survival was also dependent upon support from populations of non-haematopoietic cells in the bone marrow (Dexter, Allen and Lajtha, 1977). Functional colony forming assays made clear that these HSCs were not randomly distributed in the bone marrow, but existed within a well-defined spatial organisation in the endosteal region of the bone marrow (Lord, Testa and Hendry, 1975). Combined with observations that recovery of CFU-S in the recipient proceeded differently depending upon the cytotoxic regime used to bring about the depletion, and that the theoretical 'immortality' a stem cell should possess was at odds with experimental findings suggesting an 'age-structure', the existence of a 'stem cell niche' was hypothesised, drawing parallels with the field of ecology (Schofield, 1978). Schofield's theory outlined that these stem cells were in a defined anatomical location and that removal of stem cells from this niche resulted in differentiation, and that this specialised microenvironment had additional functions, such as the ability to impose a stem-like state onto differentiated cells, and a mechanism to limit the accumulation of genetic mutation in stem cells by restricting their cell cycle until necessary.

HSCs were identified by flow cytometry through a combination of antibodies and fluorophores too complex to replicate with immunofluorescence (Spangrude, Heimfeld and Weissman, 1988; Morrison and Scadden, 2014). The development of tools required to directly image HSC localisation with confidence in haematopoietic tissues took over 25 years. A simplified cell surface marker selection and the identification of genetic markers made it possible to generate GFP-tagged mice (Nombela-Arrieta *et al.*, 2013; Morrison and Scadden, 2014; Acar *et al.*, 2015; Chen *et al.*, 2016). Analysis of the localisation of these cells in tissue sections showed that most HSCs reside in areas adjacent to the sinusoidal

blood vessels in the bone marrow and spleen, leading to the proposal of a perivascular niche for HSCs (Kiel *et al.*, 2005).

Soluble factors that are non-cell-autonomously required to maintain HSC populations were discovered through conditional genetic deletion studies of the factor receptor in HSCs. These include SCF (that binds to its receptor KIT, expressed by HSCs) (Barker, 1994), CXCL12 (through binding to its receptor CXCR4) (Nagasawa *et al.*, 1996) and TPO (binding to c-Mpl) (Kimura *et al.*, 1998). Many other factors have also been identified that do not appear to be required for HSC maintenance under steady state conditions but can promote HSC regeneration after injury, including angiogenin (Goncalves *et al.*, 2016), angiopoietin-like protein 3 (Zheng *et al.*, 2011), FGF1 (Zhao *et al.*, 2012), FGF2 (Itkin *et al.*, 2012), IL-6 (Bernad *et al.*, 1994), Notch-2 (Varnum-Finney *et al.*, 2011) and pleiotropin (Himburg *et al.*, 2014).

Cell ablation studies were used to identify other cell types involved in maintaining this microenvironment. This identified many stromal cell populations, including osteoblasts (Visnjic *et al.*, 2004), CXCL12-adundant reticular (CAR, also described as perivascular stromal) cells (Omatsu *et al.*, 2010), leptin receptor-expressing (LEPR+) cells (Zhou *et al.*, 2014), Nes-CreER+ (Nestin+) cells (Méndez-Ferrer *et al.*, 2010) and Ng2-CreER+ cells (Kunisaki *et al.*, 2013), as well as differentiated haematopoietic cells themselves such as megakaryocytes (Bruns *et al.*, 2014) and macrophages (Chow *et al.*, 2011). In each case, HSCs entered the cell cycle and/or became depleted after the ablation of the respective cell populations, suggesting a loss of the niche environment.

These studies remain controversial; some have commented upon how there has been no cell type that has yet been ablated and *not* shown to induce HSC activation or depletion (Crane, Jeffery and Morrison, 2017). This has led to speculation that there is widespread cross-talk where many cells indirectly regulate other cells in the bone marrow. This is apparent when vascular cells are ablated, leading to a disruption of blood flow through the bone marrow (e.g. Nes-CreER is expressed by bone marrow endothelial cells (Ono *et al.*, 2014)). In one case, HSCs were only depleted weeks after osteoblast ablation when the entire bone marrow became pancytopenic (Visnjic *et al.*, 2004). Observations through immunofluorescence show that few HSCs reside close to bone surfaces where osteoblasts are located and that osteoblasts do not even express the crucial niche factor SCF (Ding *et al.*, 2012).

There is evidence for MKs having a direct role on HSC maintenance by inhibiting HSC cell division through several redundant signalling factors. Megakaryocytes are situated physically close to HSCs in the perivascular region and produce TGFb which has been shown to inhibit HSCs *in vivo* (Zhao *et al.*, 2014). Conditional deletion of TGFb from MKs also increase HSC proliferation *in vivo*. They are also a source of CXCL4 (also known as platelet factor 4, PF4) and Cxcl4-deficient mice have increased HSC numbers and proliferation (Bruns *et al.*, 2014). The administration of recombinant CXCL4 or TGFβ reduces the proliferation that is otherwise seen.

Overall, HSCs exist in the bone marrow predominantly in well-defined anatomical locations in the perivascular or perisinusoidal regions and depend upon many non-cell-autonomous factors. SCF and CXCL12 appear the most important and well-studied, along with cell-cell interactions; especially with cells that produce the mentioned factors, including the perivascular stromal cells. These HSCs exist in a dynamic equilibrium between factors pulling them towards division to undergo haematopoiesis and quiescence in order to maintain their stem-cell-like properties in equal measure. The maintenance of HSCs in culture *in vitro* indefinitely as they exist *in vivo* remains, as of yet, impossible.

1.2.3 *HSC differentiation of megakaryocyte precursor cells*

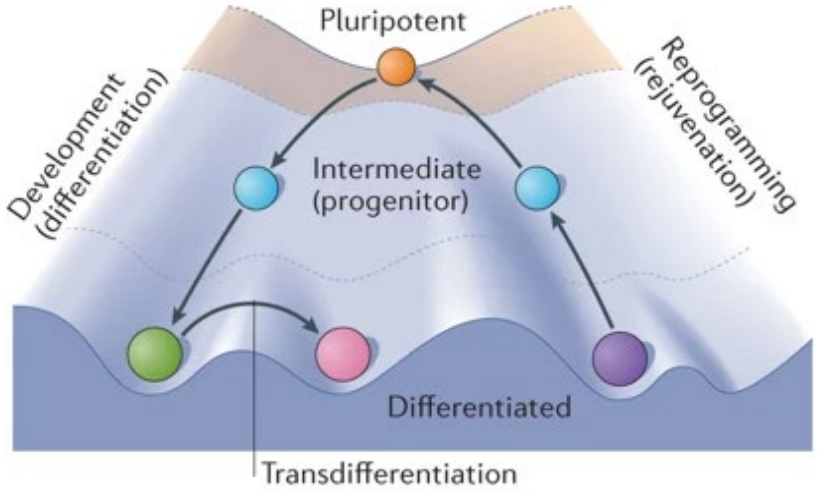

Figure 1.3. *Waddington's landscape, illustrating the idea that acquisition of cell fate can occur unidirectionally, from an immature (pluripotent) to a mature (differentiated) state, depicted as a ball rolling down from the top of a 'mountain' to the bottom of a 'valley'. (Reprinted by permission from Springer Customer Service Centre GmbH: Springer Nature, Nature Reviews Molecular Cell Biology: A decade of transcription factor-mediated reprogramming to pluripotency. Takahashi and Yamanaka © 2016; permission conveyed through Copyright Clearance Center, Inc)*

During differentiation, HSCs progressively become more restricted in their lineage. In 1957, Waddington described how mammalian development is unidirectional, akin to a ball rolling down a mountain to the bottom of various valleys to represent the potential differentiation trajectories of multipotent cells (Waddington, 1957). Over time, a series of landmark experiments have also shown that cell fate is both flexible and reversible, for example, the cloning of a sheep from the nucleus of a differentiated cell (Wilmut *et al.*, 1997) and the discovery of induced pluripotent stem cells (iPSCs), where differentiated cells can be induced to return to a state of pluripotency (Takahashi and Yamanaka, 2006). Nonetheless, bearing these caveats in mind, this still serves as a useful model to describe the differentiation pathway of pluripotent stem cells into megakaryocytes, with each valley the ball passes down representing the various epigenetic programming the cell acquires through this process (see Figure 1.3).

Many groups have used lineage tracing techniques to investigate how the differentiation potential of HSCs become progressively restricted (Figure 1.4). Cell surface markers of discrete subpopulations of developing blood cells are analysed by flow cytometry and fluorescence-assisted cell sorting (FACS) and various functional assays (including *in vitro* colony assays and *in vivo* transplantation assays) are used to characterise their differentiation potential, giving rise to the classical idea of a 'haematopoietic tree', a highly ordered and deterministic process (Figure 1.4). HSCs lose their ability to self-renew while retaining full lineage potential in the form of multipotent progenitors (MPPs) (Morrison and Weissman, 1994). Eventually, they appear to form bipotent megakaryocyte-erythroid progenitors (MEPs) either directly or through a common myeloid progenitor (CMP), followed by megakaryocyte progenitors (MkPs) (Nakorn, Miyamoto and Weissman, 2003).

The success of these marker-based approaches is dependent upon the existence of cell-surface markers specific for distinct progenitors, and that captured cell populations are not perturbed during functional assays; both assumptions are coming under scrutiny (Sun *et al.*, 2014). Despite the unequivocal evidence for the hierarchical and branching nature of haematopoietic differentiation, recent single cell transcriptomic approaches have revealed unexpected, considerable heterogeneity in the classically sorted populations from Figure 1.4 (Paul *et al.*, 2015). This study combined massively parallel single cell RNA-seq (MARS-Seq) with indexed FACS and further functional assays and found that FACS markers were poor predictors for the single-cell-based transcriptomic clustering of cells. Rather than being a simple deterministic organised process, single cell data suggests these intermediate cells exist along a gradient with transplantation

experiments suggesting a high degree of plasticity. For example, CD41+ MK progenitors in transplantation assays demonstrated the ability to still form erythrocyte lineages.

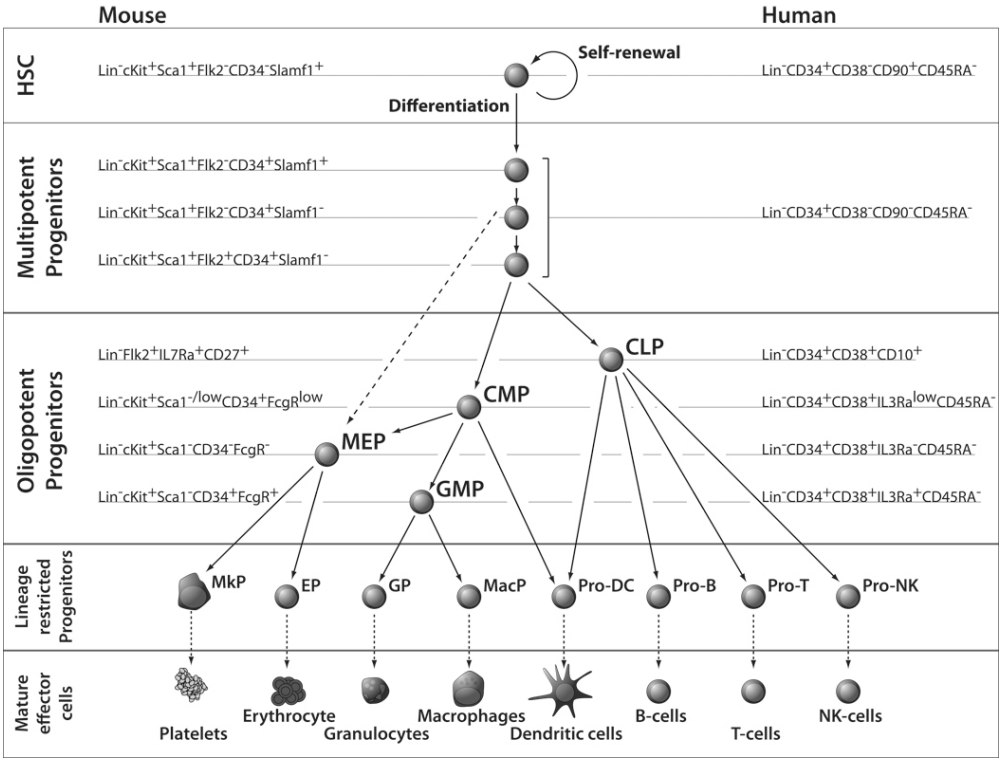

Figure 1.4. *Model of the hematopoietic hierarchy. The HSC resides at the top of the hierarchy and is defined as the cell that has both the self-renewal capacity and the potential to give rise to all hematopoietic cell types (multipotency). HSCs first lose self-renewal capacity, then lineage potential step-by-step as it commits to a certain lineage. The cell surface phenotype of each population is shown for the mouse and human systems. In the mouse, evidence suggests that some of MPPs directly give rise to MEP without passing through CMP (dashed arrow). CLP, common lymphoid progenitor; CMP, common myeloid progenitor; DC, dendritic cell; EP, erythrocyte progenitor; GMP, granulocyte/macrophage progenitor; GP, granulocyte progenitor; HSC, hematopoietic stem cell; MacP, macrophage progenitor; MEP, megakaryocyte/erythrocyte progenitor; MkP, megakaryocyte progenitor; NK, natural killer; Lin, lineage markers. © 2010 John Wiley & Sons, Inc. Reprinted from Seita and Weissman, 2010 by permission conveyed through Copyright Clearance Center, Inc.*

Complicating matters, MKs and HSCs share many features in common, including dependence upon TPO signalling through the c-Mpl receptor, as well as sharing many surface markers between them, including CD41, CD150 and CD9 and mRNA transcripts of proteins such as von Willebrand Factor (VWF). There are of course, important differences; CD42b is only expressed by mature megakaryocytes and not in any progenitor (Nishikii, Kurita and Chiba, 2017). There may be important physiological reasons for these similarities; TPO is the major physiological regulator of platelet homeostasis, and *in vitro* can directly instruct HSC precursors to differentiate towards a megakaryocytic lineage (Choi

et al., 1995; Stoffel, Wiestner and Skoda, 1996). When the platelet count is low, an increase in TPO levels triggers an increase in HSC differentiation towards megakaryocytes and platelet formation (Bartley *et al.*, 1994). Although c-Mpl deficient mice have an 85% reduction in their platelet count, they are still able to produce platelets, suggesting redundancy and a role for other mediators in this process (Gurney *et al.*, 1994).

As the differentiation process is thought to be largely mediated by the transcriptional state in the cell, three groups of the driving transcription factors involved in megakaryopoiesis have also been identified; the GATA family, core binding factor (CBF) and ETS transcription factors. The presence of binding sites for the GATA family of zinc-finger transcription factors is a canonical feature of megakaryocytic promoters. GATA1 and its binding partner FOG1 have both shown to be important as a central broker in megakaryopoiesis and erythropoiesis (Stachura, Chou and Weiss, 2006). Mutations in GATA1 lead to an X-linked thrombocytopaenia, and as many as four distinct biochemical classes of mutation have been described in X-linked disorders of megakaryocyte development (Nichols *et al.*, 2000). Distinct structural elements of GATA1 appear to contribute to different parts of megakaryopoiesis as evidenced through *ex vivo* rescue assays (Kuhl *et al.*, 2005).

Several megakaryocytic promoters contain CBF (also known as RUNX) sites. The CBF family of transcription factors consists of the three homologous DNA-binding proteins RUNX1-3 and a non-DNA binding component, CBFβ. Mature megakaryocytes express high levels of RUNX1 and low levels of RUNX3 (Levanon *et al.*, 2001), while inducible inactivation of either RUNX1 or its binding partner CBFβ in mice causes a rapid and profound disruption in megakaryopoiesis with limited effects on erythropoiesis (Ichikawa *et al.*, 2004). This is likely mediated through its effects on expression and signalling of c-Mpl.

ETS transcription factor binding sites occur next to most megakaryocytic gene promoters, often adjacent to GATA sites (Bastian *et al.*, 1999). Three transcription factors in the ETS family are known to be involved in driving megakaryopoiesis, FLI1, GAPBα and TEL1. In mouse models, depletion of any of these three transcription factors leads to a specific drop in platelet counts with no effect on haemoglobin levels (Hart *et al.*, 2000; Hock *et al.*, 2004; Pang *et al.*, 2006). FLI1 was also discovered from mutations in humans that lead to a thrombocytopaenia and a characterisation of megakaryopoiesis from CD34+ HSCs derived from patients showed a deficiency in differentiation, recapitulated when a mouse model

was created and rescue experiments showed that this phenotype was dependent upon FLI1 expression (Raslova *et al.*, 2004).

As well as positive regulators of megakaryopoiesis, antagonists have also been discovered. Through a random chemical mutagenesis screen in mice, the transcription factor c-Myb was identified as a potent negative modulator of megakaryopoiesis, acting through the recruitment of the p300 coactivator; mutations in either lead to the same marked elevation in platelet count and tissue megakaryocytes. It is likely that this acts at the level of the MEP; wild-type cultured MEPs gave rise to predominantly erythroid cells, c-Myb-/- MEPs gave rise to predominantly megakaryocytes, an effect reversed by retroviral transduction of functional c-Myb (Mukai *et al.*, 2006).

1.2.4 *MK production, endomitosis and cytoplasmic maturation*

Once committed to the megakaryocytic lineage, MK progenitors differentiate into immature megakaryocytes with a limited capacity for self-renewal and must undergo a series of characteristic maturation steps to become terminally differentiated. Interestingly, the mere translocation of megakaryocyte progenitors to the vicinity of bone marrow vascular sinusoids is sufficient to induce maturation, with the cytokines SDF-1 and FGF-4 implicated in this process (Avecilla *et al.*, 2004).

Endomitosis is the first maturation step that takes place. This is a primarily TPO-driven process through which MKs become polyploid through cycles of DNA replication without cell division (Ebbe, 1976; Gurney *et al.*, 1994). The study of this process was facilitated through the use of *in vitro* culture systems using TPO. During their life cycle, MKs first undergo a proliferative mitotic (2n) stage in which their progression through the cell cycle is identical to other haematopoietic cells. Subsequently, during endomitosis, MKs can acquire a DNA content of 4n, 8n, 16n, 32n, 64n and even 128n in a single polylobulated nucleus (Zimmet and Ravid, 2000).

This polyploidy is likely required to produce the large quantities of mRNA and protein to be packaged into platelets, but the relationship between high polyploidy and efficient platelet production is highly debated (Zimmet and Ravid, 2000). For example, nicotinamide is often used to increase ploidy of human and mouse MKs in culture (Giammona *et al.*, 2006), but administration of this to mice does not increase their platelet counts (Konieczna *et al.*, 2013). Overexpression of cell cycle regulators such as cyclin D3 have been also shown to enhance MK ploidy

in vivo without any increase in platelet count (Zimmet *et al.*, 1997), affecting the G1 phase of the cell cycle (see Figure 1.5).

There is evidence to suggest that endomitosis is due to an inhibition of late cytokinesis. During normal mitosis, cytokinesis occurs through the formation of a cleavage furrow, a contractile ring comprising of myosin II and F-actin, that generates the mechanical forces necessary for cell separation (Lordier *et al.*, 2008). RhoA, a small GTPase regulating the actin cytoskeleton, is required to generate this contractile force and the microtubule-associated GEF-H1 activates RhoA at the cleavage furrow (Birkenfeld *et al.*, 2007), while ECT2 is involved in RhoA localisation and activation (Petronczki *et al.*, 2007).

Studies in primary MKs reveals that RUNX1 downregulates MYH10 (myosin IIB heavy chain) (Lordier *et al.*, 2012), and that both GEF-H1 and ECT are downregulated at the mRNA and protein level during polyploidization (Gao *et al.*, 2012). Interestingly, GEF-H1 downregulation appears to be required for 2n cells to become 4n, while ECT downregulation appears to be necessary for polyploidization beyond 4n, suggesting different mechanisms are involved in the initial 2n to 4n transition and subsequent endomitotic events.

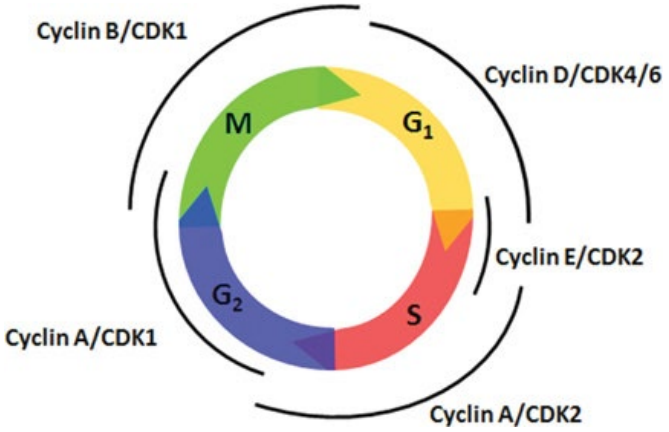

Figure 1.5. *Cyclin–CDK regulation of the mammalian cell cycle. The cell cycle consists of a DNA synthesis (S) phase and a mitotic (M) phase, separated by two gap (G1 and G2) phases. In mammalian cells different cyclin–CDK complexes regulate progression of cells through the different phases of the cell cycle. Republished with permission of Portland Press Ltd, from Control of cell cycle progression by phosphorylation of cyclin-dependent kinase (CDK) substrates, Suryadinata, Sadowski and Sarcevic, Bioscience Reports 30(4) © 2010; permission conveyed through Copyright Clearance Center, Inc.*

Although inhibition of cleavage furrow formation physically prevents MKs from dividing, there may be a separate process that regulates the repeated cycles of DNA replication and limits their exit from mitosis. Studies in megakaryocytic transformed cell lines show that this switch to polyploidization may also be mediated through degradation of cyclin B and consequent reduced activity of the

cyclin B-dependent Cdc2 kinase (Datta *et al.*, 1996). Many studies have identified roles for G1/S phase regulators, such as cyclins D and E, supporting the hypothesis that up-regulation of G1 phase components may be important in promoting endomitotic DNA replication for the development of high ploidy MKs (see Figure 1.5) (Muntean *et al.*, 2007; Eliades, Papadantonakis and Ravid, 2010).

The other main maturation phase MKs must undergo is cytoplasmic maturation. This process describes the development of a highly invaginated membrane reservoir system throughout the MK cytoplasm continuous with the plasma membrane known as the invaginated membrane system (IMS) or the demarcation membrane (DMS). This requires a high amount of protein and lipid synthesis and so only occurs after endomitosis has taken place. The IMS is thought to act as a membrane reservoir for the surface area required for proplatelet formation, as demonstrated by direct labelling to observe membrane dynamics *in vitro* (Schulze *et al.*, 2006). The IMS also requires cytoskeletal support; spectrin, a protein that forms the plasma membrane skeleton in many cell types has been shown to form a 2D lattice that stabilises and underlies the IMS in MKs, and MKs expressing a spectrin tetramer disrupting construct have an underdeveloped IMS with insufficient membrane to form proplatelets (Patel-Hett *et al.*, 2011).

Other major hallmarks of MK maturation include the formation of structures that are not important to the MK itself, but are crucial to the function of the resultant platelets from the MK. These include the formation of a dense tubular system, found to be the site of prostaglandin synthesis in platelets (Gerrard, White and Peterson, 1978), the open canalicular system, a surface-connected channelled system important as a conduit for discharge of granule products during platelet activation (Escolar and White, 1991), and the formation and loading of these granules with proteins and other substances.

1.2.5 *Platelet granules and their biogenesis*

There are three main types of granules in platelets, α-granules, dense (or δ-granules) and lysosomal granules, of which the α-granules are the most abundant, numbering between 50 and 80 per platelet and comprising about 10% of the platelet volume (Harrison and Cramer-Martin, 1993). The contents of these α-granules are heterogeneous, containing substances that are either membrane-bound proteins that become exposed onto the surface of platelets (e.g. P-selectin) or proteins that are released into the interstitial space (Figure 1.8). In many ways, they are analogous to the Weibel-Palade bodies found in endothelial cells,

containing many similar proteins as cargo, such as vWF (Heijnen, 2019). The dense granules contain ADP, serotonin and other small-molecule, non-protein mediators of platelet-platelet signalling.

α–granules have four distinct morphological zones identified by electron microscopy. From the outside in they are the peripheral membrane, tubular and vesicular structures, an electron-lucent area and an electron-dense nucleoid. Mass spectrometry experiments to probe the proteome of these α-granules has identified over 280 different proteins with many whose physiological role is not yet clear (Maynard *et al.*, 2007). These proteins include those that are important for haemostasis (such as von Willebrand Factor, factor V and thrombospondin) as well as innate immunity (such as CXCL1, platelet factor 4 [PF4] and RANTES), perhaps reflecting the dual role of platelets in haemostasis and as an immune cell (Thomas and Storey, 2015).

Platelet granule formation begins in the MK but continues in the circulating platelet. Platelet α-granules contain proteins that arrive broadly from one of two sources (see Figure 1.6); from biosynthesis, predominantly at the MK level (such as PF4), through the trans-Golgi network, with some vestigial synthesis in platelets and through endocytosis and pinocytosis at both the MK and platelet levels (for proteins such as fibrinogen and IgG) (Harrison and Cramer-Martin, 1993).

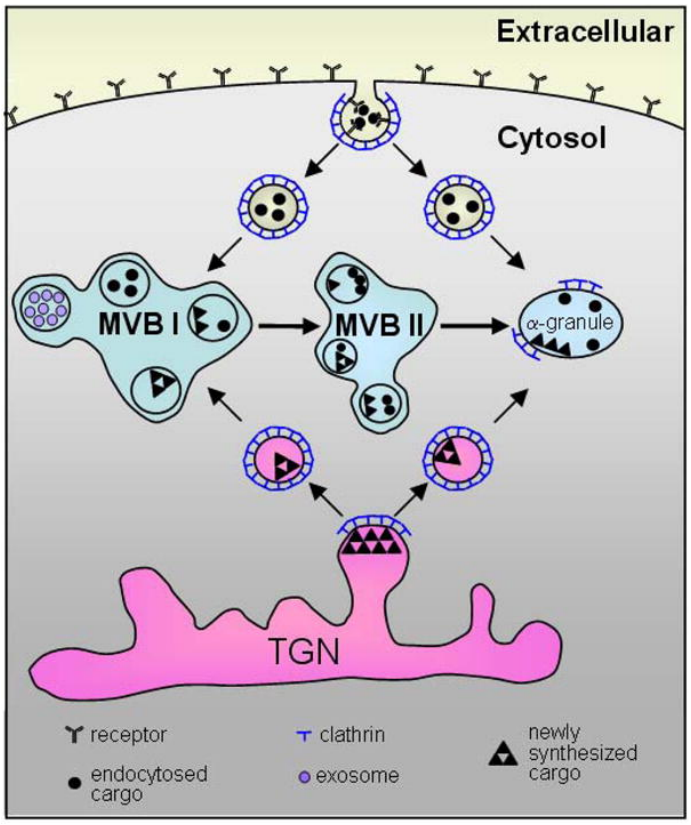

Figure 1.6. *α–Granule cargo derives from budding of the trans-Golgi network (TGN) and endocytosis of the plasma membrane. MVB - multivesicular bodies* (Blair and Flaumenhaft, 2009)[1]

In the megakaryocyte, α–granules appear to be derived in part from the budding of small vesicles from the trans-Golgi network as seen through immunogold staining for α–granules proteins such as PF4 in rat megakaryocytes and studies of various α–granule cargo proteins have suggested different mechanisms for the targeting and retention of different granule proteins (Hegyi, Heilbrun and Nakeff, 1990). Studies of PF4 led to the identification of a four amino acid signal sequence in an exposed hydrophilic loop required for the sorting of PF4 into α–granules, with analogous sequences identified in other platelet chemokines such as RANTES and NAP-2 (El Golli *et al.*, 2005). Mice lacking the dominant platelet glycosaminoglycan, serglycin, fail to store soluble proteins containing basically charged regions, such as PF4, PDGF or NAP-2, suggesting serglycin may serve to retain chemokines containing an exposed cationic region (Blair and Flaumenhaft, 2009).

Another mechanism suggested for the incorporation of larger soluble proteins into α–granules is through the aggregation of protein monomers. Large multimeric

[1] Reprinted from Blood Reviews 23(4), Blair and Flaumenhaft, Platelet α-granules: Basic biology and clinical correlates, 177-189, Copyright 2009, with permission from Elsevier.

self-assembling proteins such as multimerin, a factor V binding protein found in platelet α–granules, have been proposed to sort to immature vesicles through homoaggregation (Hayward *et al.*, 1999). In MKs, VWF also self-assembles into large multimeric structures and is packaged into a discrete tubular structure within α–granules. The expression of vWF in cell lines possessing a regulated secretory pathway (e.g. RIN 5F or 293T cells) can also drive the *de novo* formation of α–granule-like structures complete with recruitment of membrane proteins such as P-selectin, but this does not occur in cell lines lacking such a secretory pathway (e.g. CHO or 3T3 cells) (Blagoveshchenskaya *et al.*, 2002). One group took advantage of this biosynthesis route by fusing the signalling domain of VWF (the SPD2 domain) with FVIII and introduced this as a lentiviral gene therapy in haemophilic dogs to restore haemostasis (Du *et al.*, 2013).

Evidence for endocytosis as a mechanism for granule biogenesis was discovered through observations that these granules contain large amounts of proteins that are unlikely to be synthesised by megakaryocytes. For example, immunoglobulins (e.g. IgG) are well-known to be produced by B cells as part of the adaptive immune system through complex processes of recombination and hypermutation that simply do not occur in megakaryocytes. Guinea pigs injected with horseradish peroxidase (HRP) were studied and their MKs and subsequent platelets were found to contain HRP inside of the α–granules. This HRP was able to be released from these platelets upon stimulation with thrombin, showing that proteins could be endocytosed, packaged into α–granules and released upon exposure to a platelet agonist (Handagama, George, *et al.*, 1987). Studies in dogs evaluating the accumulation of fibrinogen and immunoglobulin show that the levels of endocytosed but not endogenous proteins increase as platelets age, suggesting that constitutive trafficking to platelet α–granules continues throughout the lifespan of the platelet (Heilmann *et al.*, 1994).

There has also been evidence to show this may also work for other proteins that are not usually present in granules, including Factor VII. MEG-01 megakaryoblastic cells were incubated with recombinant activated Factor VII and flow cytometry combined with immunofluorescence was used to show this becomes taken up into the granules of these cells, as well as the subsequently produced platelets. The authors suggest this could explain the prolongation of the beneficial effects of this clinical drug beyond its usual two hour half-life in the blood (Schut *et al.*, 2017).

In many other cell models, vesicle trafficking and maturation is mediated through an orchestrated assemblage of coat proteins (e.g. clathrin, COPII), adapter

proteins (e.g. AP1, AP2, AP3), fusion machinery (e.g. SNAREs) and monomeric GTPases (e.g. Rabs) and it is thought that similar processes take place in MKs. Vesicles budding from either the trans-Golgi network or the plasma membrane from endocytosis are subsequently directed towards multivesicular bodies (MVBs). MVBs appear to be a key megakaryocyte-platelet storage and sorting compartment, that are abundant in early megakaryocytes and decline with cellular maturation, serving as an intermediate stage of granule formation. Kinetic studies in MKs demonstrate the transport of endocytosed proteins proceeds from endosomes to immature MVBs (MVB I, with internal vesicles alone) to mature MVBs (MVB II, with internal vesicles and an electron dense matrix) to α–granules (Heijnen *et al.*, 1998).

Recent data also suggests there are two distinct sub-types of α–granules; broadly, one containing pro-angiogenic proteins, such as VEGF, and the other containing anti-angiogenic proteins, such as endostatin. Proteins appear to be differentially packaged into one and not the other, with no overlap of proteins existing in both (Sehgal and Storrie, 2007; Italiano *et al.*, 2008). The physiological role of the differential packaging of α–granules remains unclear, as well as whether further subtypes exist. Furthermore, other studies, have disputed the existence of separate specialised granule subtypes, favouring the explanation that this observation is due to stochastic protein sorting to α-granules. This is backed by immunofluorescence data showing that VEGF and endostatin co-localise 41% of the time, suggesting these observations are possibly microscope-setting-dependent (Kamykowski *et al.*, 2011).

Other approaches to studying granule formation are through the studies of diseases that lead to a lack of α-granules in platelets. Some of these studies led to the discovery of VPS33B, VPS16B and NBEAL2 being essential to granule biogenesis, though the precise mechanisms remain unclear (Chen *et al.*, 2017). Overall, there appear to be many different redundant mechanisms and processes responsible for granule formation in platelets, some of which are similar to other cell types studied and others that appear unique to MKs.

1.2.6 *Platelet assembly and release*

Proplatelets are long (up to millimetres in length), thin cytoplasmic processes emanating from megakaryocytes, characterised by multiple platelet-sized swellings linked together by thin cytoplasmic bridges. Developing platelets were assumed to be encased in plasma membrane only as proplatelets are formed, supported by the observation that platelet membrane antigenicity and structure

more closely resembles those of the IMS than of the surface of the MK. Direct visualisation with GFP-tagged proteins further demonstrated the IMS to be the origin of proplatelet and platelet membranes (Schulze *et al.*, 2006b).

The classical theory suggested that the megakaryocyte fragment into platelets, with the IMS serving the function of subdividing the MK cytoplasm into platelet areas (Becker and De Bruyn, 1976) but the evidence for these subdivisions remained elusive. This was later supplanted by the 'flow model', postulating that platelets derived exclusively from the interconnected platelet-sized beads along proplatelets, and that the IMS did not function to divide platelet fields, but to act as a reservoir of surface membrane to be evaginated during proplatelet formation (Radley and Haller, 1982).

Proplatelets have been observed (1) *in vivo* (Schmitt *et al.*, 2001), (2) in a wide range of mammalian species including mice, rats, guinea pigs, humans and others (Handagama, Feldman, *et al.*, 1987; Tablin, Castro and Leven, 1990; Choi *et al.*, 1995), (3) extending from megakaryocytes in the bone marrow through junctions in the endothelial lining of blood sinuses, hypothesised to subsequently be released into the circulation and undergo further fragmentation into platelets (Lichtman *et al.*, 1978), and (4) to be absent in mice lacking two distinct haematopoietic transcription factors, failing to produce proplatelets in culture and leading to a severe thrombocytopaenia *in vivo* (Shivdasani *et al.*, 1997; Lecine *et al.*, 1998).

Through the discovery of TPO, *in vitro* megakaryocyte culture systems have been developed that have successfully reconstituted the platelet formation process allowing this process to be directly visualised as it takes place. Counter-intuitively, TPO appears to also inhibit proplatelet formation by mature human megakaryocytes *in vitro* (Ito *et al.*, 1996). Mice containing fluorescent markers in their megakaryocytes combined with intravital microscopy have allowed these processes to also be visualised directly in the cranial bone marrow in living mice, showing that proplatelets extend through the endothelium into capillaries and these megakaryocytic fragments are released into the circulation, exceeding the size typically expected for platelets, suggesting these undergo further fragmentation later on, which is the modification in the 'modified' flow model (Patel, Hartwig and Italiano, 2005).

Proplatelet formation appears dependent upon microtubule formation; drugs that depolymerise microtubules such as nocodazole or vincristine also block proplatelet formation *in vitro*. The microtubule cytoskeleton of megakaryocytes

undergoes a dramatic rearrangement. Studies of murine megakaryocytes transduced with EB3-GFP (end binding protein 3, to mark growing microtubules) have revealed that immature MKs lacking proplatelets show a centrosomal-coupled microtubule nucleation/assembly reaction where microtubules assemble only from centrosomes and grow outwards to the cell cortex (Patel *et al.*, 2005). Just before proplatelet formation however, as observed through fluorescence time-lapse microscopy, centrosomal assembly ceases, microtubules begin to consolidate into the cortex and microtubule assembly occurs continuously throughout the entire proplatelet structure. Organelles, including platelet granules, are transported along these microtubule bundles into the proplatelets, powered by microtubule motor proteins. They appear to be captured in developing platelets by microtubule coils, which persist in mature platelets.

In recent years, evidence for the classical fragmentation model of platelet formation (termed MK rupture) has emerged as an alternative to the proplatelet model in the context of IL-1a-dependent emergency platelet release in response the administration of an inflammatory stimulus to mice (Nishimura *et al.*, 2015). This process appears to be independent of serum TPO levels, and entails rapid cytoplasmic fragmentation followed by the release of much larger numbers of platelets than would be expected under normal homeostasis, primarily into blood vessels.

Still controversial in the field is the primary location of platelet production. Although megakaryocytes arise in the bone marrow, they have been documented to migrate into the blood and therefore platelet production may also occur at non-marrow sites (Michelson, 2007). In the developing foetus, thrombopoiesis occurs from megakaryocytes resident in first the yolk sac and then the foetal liver, suggesting that the bone marrow microenvironment, although sufficient, is not necessary for platelet release (Brouard *et al.*, 2017). The two main alternative locations of platelet formation are in the blood and in the lungs.

Behnke and Forer have suggested that the final stage of platelet formation takes place in the blood (Behnke and Forer, 1998). In this model, megakaryocyte fragments that are released from the bone marrow into the blood become transformed into platelets while in circulation. This theory is supported by the presence of megakaryocytes as well as megakaryocyte fragments that are sometimes beaded (and can represent between 5-20% of the circulating platelet mass in plasma) in the blood, and reports that these megakaryocyte fragments, when isolated from platelet-rich plasma taken from rats, elongate and undergo

curving and bending motions, eventually fragmenting to form disc-shaped structures resembling platelets.

Aschoff first described pulmonary megakaryocytes in 1893, suggesting they arose in the bone marrow, migrated into the blood and because of their massive size, were lodged in the capillary bed of the lung where they fragmented and released platelets (Aschoff, 1893). This was supported by data showing (1) the presence of MKs in the lungs, and (2) there were more MKs in the blood entering the lungs than the blood exiting, while there were more platelets in blood exiting the lungs than entering. More recently, Lefrançais et al used 2-photon microscopy in GFP reporter mice to show similar results, as well as video footage of the process of proplatelet formation taking place from MKs in the capillary bed of the lungs, but the calculations for what percentage of the total platelet production of the body this represents is debated (Lefrançais *et al.*, 2017).

Overall, it is likely that all three sites, bone marrow, blood and the lungs play roles in platelet formation. At present, it appears that megakaryocytes in the bone marrow produce the majority of proplatelets which later undergo fragmentation further in the circulation, perhaps due to shear forces. This is likely supplemented by some platelet production also taking place in the lungs.

1.2.7 *Platelets and their physiology; activation to thrombus formation*

In vivo observations show that flowing blood segregates into an RBC-rich core and an RBC-depleted near-wall region (Figure 1.7), which is where the majority of the platelets are located (Tangelder *et al.*, 1985). This margination effect is greater in arterioles than in venules, suggesting that this effect is due to high shear rates. This margination is thought to have an important physiological function, allowing platelets to react quickly when the vessel wall and endothelium is damaged.

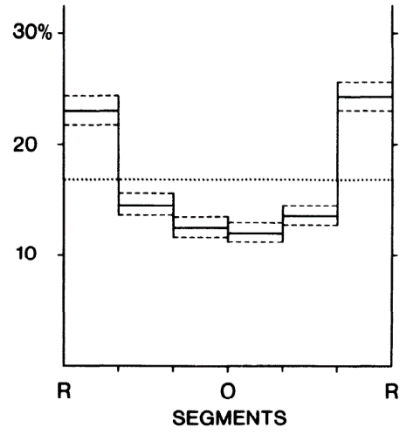

Figure 1.7. *Generalised frequency distribution of platelets in a blood vessel (solid line) with 95% confidence intervals (dashed lines) as calculated from 15 measurements in 13 vessels in 10 animals (total platelet number 6,571) demonstrating that platelets are pushed to the outer parts of the blood vessel in contact with endothelium. Distribution expected in the case of a uniform distribution is indicated by dotted line. Reprinted by permission from The American Physiological Society © 1985 Tangelder et al., Distribution of blood platelets flowing in arterioles, Am J Physiol. 1985 Mar;248(3 Pt 2):H318-23.*

Under resting physiological conditions, the endothelium of blood vessels release nitric oxide and prostacyclin, inhibiting platelet activation and preventing aggregation (Lüscher, 1993). Upon vessel injury and damage to the endothelium, platelets can interact with subendothelial components that have become exposed, such as collagen. This leads to a sequence of tightly controlled processes; tethering, rolling, activation and firm adhesion, resulting in the formation of stable platelet adhesion and thrombus formation (Michelson, 2007).

The mechanisms for these processes vary between vessels of low shear rate (veins and arteries) compared with high shear rates in the microvasculature. In vessels with a low shear rate, the exposure of platelets to collagen, laminin and fibronectin appear to play the predominant role in tethering and recruiting flowing platelets; exposed collagen can directly bind to the platelet glycoprotein (GP) Ia/IIa and GPVI receptors (Savage, Saldívar and Ruggeri, 1996). In vessels with a high shear rate, von Willebrand Factor (vWF) can form a bridge between exposed collagen and the GP Ib/V/IX complex on the platelet membrane (Andrews and Berndt, 2004) to tether platelets. This tethering is insufficient to produce stable binding, but it acts to decelerate platelets, allowing them to roll in the direction of blood flow. This rolling process puts non-activated platelets into close and continuous contact with the exposed extracellular matrix, allowing further platelet-matrix interactions to stabilise the adhesion.

Collagen type I and II are particularly potent adhesion molecules exposed by the subendothelial extracellular matrix. The subsequent binding of these collagens to platelet GPVI receptors induces their activation. Other mediators from neighbouring activated platelets additionally can trigger further activation of platelets, such as ADP, serotonin (both released from platelet dense granules) and thrombin (from the coagulation cascade) by binding to G-protein coupled receptors (GPCRs) on platelet membranes such as PAR1/4 for thrombin, and $P2Y_{12}$ for ADP (Figure 1.8A) (Thomas and Storey, 2015).

These various signals converge on an intracellular messenger, calcium. Platelet activation causes an increase in intracellular Ca^{2+}, in turn resulting in a physical shape change and causing activated platelets to flatten and spread. Calcium signalling also causes the activation of integrins on the membrane surface that promote strong aggregation and adhesion by the formation of fibrinogen bridges. Finally upon activation, platelets also release their granules through mechanisms similar to what has been described in the release of synaptic vesicles at neuronal junctions, through the binding of v-SNAREs on granule membranes with t-SNAREs on platelet plasma membranes driving the fusion of these lipid membranes in a controlled manner, releasing the contents of the granules into the extracellular space (Blair and Flaumenhaft, 2009).

The primary v-SNARE mediating platelet α–granule secretion is VAMP-8, with VAMP-3 and with VAMP-2 serving subordinate functions (Ren *et al.*, 2007). Platelet t-SNAREs include syntaxins and SNAP-23. Syntaxins 2 and 4 have been shown to participate in α–granule release. Coiled-coil domains within v-SNAREs and t-SNAREs interact, forming a twisted 4-helical bundle, bringing the opposing negatively charged membranes of the granule and target membrane into close apposition, generating the energy required for membrane fusion. Pore formation with a subsequent release of granule content follows, with an expansion of the total platelet membrane surface area (Figure 1.8B) (Ren, Ye and Whiteheart, 2008).

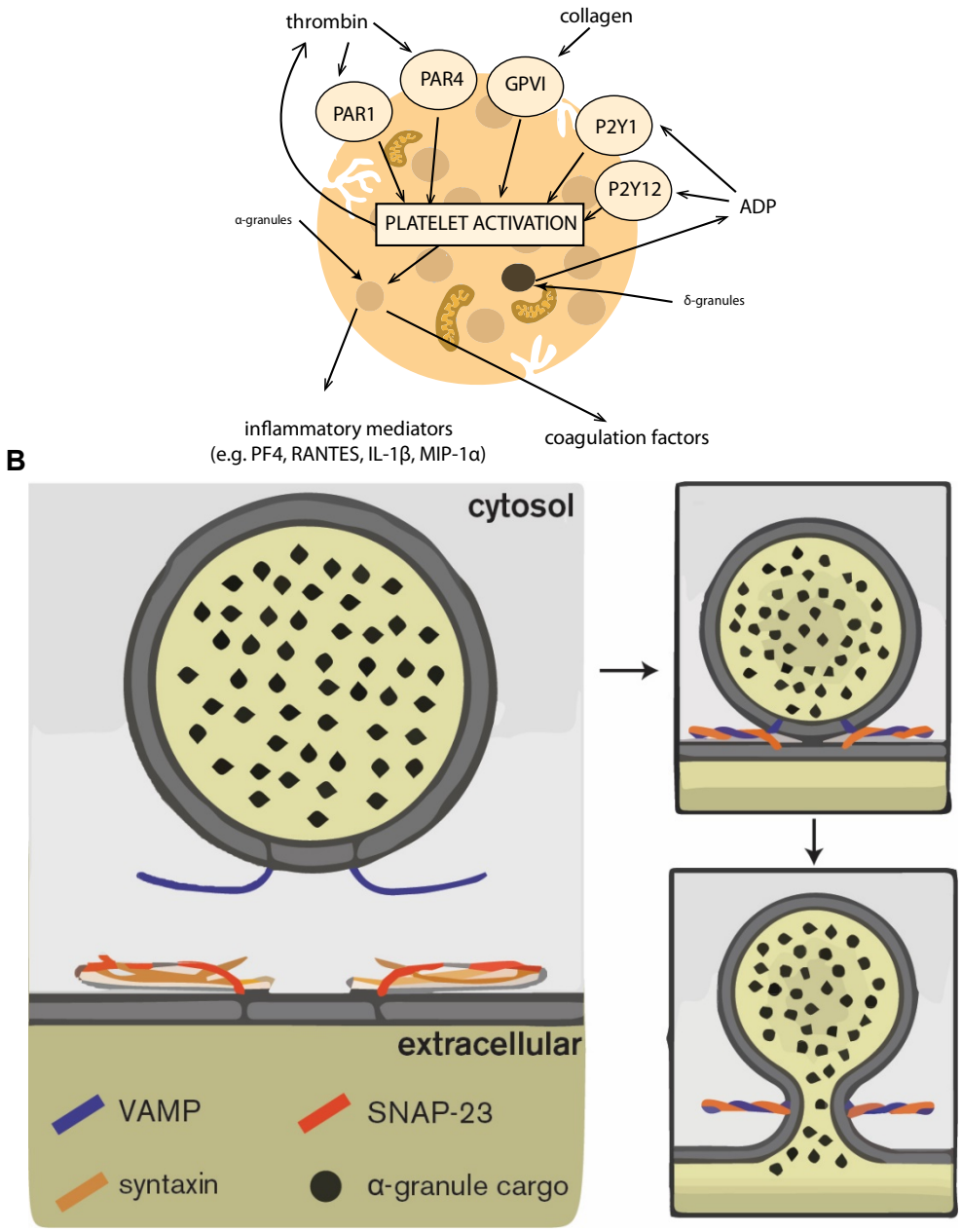

Figure 1.8. *Diagram of the triggers and receptors involved in platelet activation and the subsequent release of the contents of α-granules. (A) Thrombin from the coagulation cascade, as well as collagen and ADP all trigger platelet activation, resulting in several key morphological changes including degranulation. Redrawn based on Thomas and Storey, 2015. (B) Granules are normally prevented from being released in a resting platelet by repulsion between the negatively charged vesicle membrane and negatively charged plasma membrane. Upon activation, the v-SNARES and t-SNARES interact to physically overcome these repulsive forces. The lipid membrane of the granule fuses with the surface membrane, releasing the contents of the granule into the OCS while delivering the membrane components of the granule into the surface of the platelet (e.g. P-selectin). Adapted from Blair and Flaumenhaft, 2009*[2].

[2] Reprinted from Blood Reviews 23(4), Blair and Flaumenhaft, Platelet α-granules: Basic biology and clinical correlates, 177-189, Copyright 2009, with permission from Elsevier.

Ultimately this signalling results in an 'inside-out' signalling cascade that leads to the priming of integrin $_{IIb}\beta_3$ (also known as the CD41/61 complex). Platelet surface membranes express several integrins, including $\alpha_{IIb}\beta_3$ (fibrinogen receptor), $\alpha_v\beta_3$ (vitronectin receptor), $\alpha_2\beta_1$ (collagen receptor), $\alpha_5\beta_1$ (fibronectin receptor) and $\alpha_6\beta_1$ (laminin receptor) that all share similar signal transduction mechanisms. The most abundant of these is $\alpha_{IIb}\beta_3$, which is normally kept in a low-affinity resting state in circulating platelets. Activation of the Ca^{2+} signalling cascade, through CalDEG-GEF1 and its downstream target Rap1, results in the binding of talins and kindlins to the cytoplasmic domain of this integrin, inducing changes in its extracellular domain to an activated state (Crittenden *et al.*, 2004). Ligand binding to this activated form of $\alpha_{IIb}\beta_3$ not only mediates further platelet adhesion and aggregation but also results in a second 'outside-in' signalling pathway that has similar effects to the GPCR-mediated signalling pathway described earlier. There is much cross-talk between these pathways, and the end result is further platelet spreading, granule secretion, as well as stable adhesion and eventually clot retraction (Shattil and Newman, 2004).

1.3 Induced pluripotent stem cells, in vitro megakaryopoiesis and bioreactors

1.3.1 *Induced pluripotent stem cells for regenerative medicine*

As previously described in Table 1.1, pluripotent stem cells have the property of being able to differentiate into any tissue type in the body and hold great potential in regenerative medicine. Mouse and human embryonic stem cells are undifferentiated, pluripotent stem cells that can be maintained indefinitely in culture. However, for many decades the field had been fraught with ethical issues, as these stem cells were once only obtainable from embryonic tissues from aborted foetuses.

Gurdon et al demonstrated that all differentiated, somatic cells retain the necessary information to regenerate an entire organism (Gurdon, Elsdale and Fischberg, 1958). This culminated with experiments in the 1990s where a whole sheep was cloned from a skin fibroblast from an adult, demonstrating that even somatic cells might be manipulated to return to a stem-like state (Wilmut *et al.*, 1997). This would be far more desirable than obtaining these stem cells from embryonic sources, both from an ethical standpoint and from a histocompatibility standpoint if these were to be used to regenerate tissues for eventual transplant or transfusion. Unlike other stem cell therapies, platelets have no nucleus and cannot divide, so risks classically associated with these therapies like oncogenicity are much reduced.

To tackle the many issues that remain with donor-derived platelet products and in order to better study megakaryocyte biology there have been several different attempts at recreating megakaryopoiesis *in vitro*. Although *in vivo* HSCs appear to be able to self-renew without limit, once they are removed from their niche they do not appear to maintain their stem-like state indefinitely. There remain many unknowns about the factors that maintain this niche *in vivo*, and this can only be partially replicated through complex combinations of cytokines in tissue culture and so only survive for several days in tissue culture at present (Frisch and Calvi, 2014).

Much more recently, induced pluripotent stem cells (iPSCs) have shown great promise as a more practical source of stem cells, being derived through driving the expression of four specific transcription factors (Oct3/4, Sox2, Klf4 and c-Myc) in easily-acquired skin fibroblasts to induce a pluripotent-like cell state (Takahashi and Yamanaka, 2006). These transcription factors are highly expressed in embryonic stem (ES) cells, and driving their over-expression appears to be able to induce pluripotency in both mouse and human somatic cells, indicating they likely regulate a key switch in the developmental signalling network necessary for pluripotency.

In recent years, much attention has turned to the possibility of guiding iPS cells (which can be maintained indefinitely in tissue culture) through haematopoietic differentiation and megakaryopoiesis. Simultaneously, there has been much work in designing bioreactors for these megakaryocytes to recreate the shear forces thought to be necessary for thrombopoiesis *in vitro*.

1.3.2 *Recreating MK differentiation in vitro from iPS cells*

The classical approach to creating megakaryocytes from iPS cells has been ‘directed differentiation’, to recreate the process of paracrine signalling that occurs *in vivo* to differentiate iPS cells through sequential changes in the culture media. Much of this early work was done with mouse and human embryonic stem cells, and this has in more recent years been translated into iPSC cultures. Each new culture media contains different combinations of cytokines to guide the iPS cells through a process modelled after embryogenesis (Lu *et al.*, 2011).

In mice and humans, two distinct haematopoietic programs, designated primitive haematopoiesis and definitive haematopoiesis, occur during embryonic/foetal development and both give rise to megakaryocytes. These programs can be distinguished by the subtype of globin expressed in erythroid cells. The first, primitive wave of haematopoiesis develops from an extra-embryonic mesoderm

population in the yolk sac. These yolk sac progenitors give rise to nucleated erythrocytes, macrophages and primitive megakaryocytes. Towards the end of the primitive wave, definitive erythro-myeloid progenitors emerge from the yolk sac and colonise the foetal liver, where they act as the major source of haematopoiesis prior to the emergence of HSCs. Another wave, this time of definitive haematopoiesis, occurs in the aorto-gonads-mesonephros region and this is responsible for the generation of long-term HSCs having multi-lineage potential as well as enucleated erythrocytes, myeloid cells, lymphocytes and crucially, definitive megakaryocytes. These HSCs then colonise the foetal liver, before transitioning to the bone marrow where they reside for the remainder of adult life (Mikkola and Orkin, 2006).

While megakaryocytes are generated in both waves, functional differences between them have been well-documented. Primitive megakaryocytes are less proliferative, display a lower ploidy and each megakaryocyte releases a relatively small number of platelets. By contrast, definitive megakaryocytes undergo more rounds of endomitosis and give rise to on the order of 10^3-10^4 platelets per MK (Wang and Zheng, 2016). There is recent evidence to suggest that Wnt signalling (Sturgeon *et al.*, 2014) and IGF_2BP_3 (Elagib *et al.*, 2017) acts as a master switch driving immature foetal haematopoiesis to the adult form.

The first attempts to differentiate human ES cells through haematopoiesis was through co-culture with certain mouse stromal cell lines derived from haematopoietic tissue (Kaufman *et al.*, 2001). In particular, co-culture with the OP9 stromal cell line was able to differentiate up to 25% of the human ES cells into CD34+ HSCs within 8-9 days of culture, displaying the phenotype of primitive haematopoietic progenitors and going on to produce lymphoid and myeloid cells when subsequently co-cultured with the MS-5 stromal cell line (Vodyanik *et al.*, 2005). Kinetic studies have shown the differentiating populations progress through a primitive streak stage defined by either BRACHYURY or MIXL1 expression, then to KDR+ (Flk-1+) or PDGFR+ mesoderm, and subsequently to a yolk sac haematopoietic program (Zambidis *et al.*, 2005). Studies comparing these MKs to those from adult bone marrow have found iPSC-derived primitive megakaryocytes are smaller, have lower ploidy and release fewer platelets when infused into mice (Wang *et al.*, 2015).

This was followed by studies aiming to eliminate the use of both serum and stromal cells, barriers in translation to clinical contexts. BMP4 was discovered as a crucial signal to induce the formation of the primitive streak-like population required for the subsequent development of haematopoietic mesoderm, and

when supplemented with recombinant VEGF, FGF2, TPO and SCF were able to differentiate these hESCs to megakaryocytes as observed by functional assays and were able to produce functional platelet-like particles (Pick *et al.*, 2007). Much of this work has been directly translated to iPSC culture.

In more recent years, this process has been refined further and differentiation protocols driving definitive haematopoiesis have been developed through the timed modulation of the Wnt pathway (Sturgeon *et al.*, 2014). Both haematopoietic programs transition through a hemogenic endothelial intermediate and develop from KDR+ mesoderm progenitors that are distinguishable by CD235a expression. Generation of the primitive progenitors (KDR+CD235a+) depends on stage-specific activin-nodal signalling and inhibition of the Wnt pathway, while specification of the definitive progenitors (KDR+CD235a-) required Wnt signalling in the same timeframe.

However, one of the key issues with directed differentiation has been the yield and number of generated megakaryocytes and the quantity of platelets produced. The process of directed differentiation involves recreating the whole of haematopoiesis, and so cells that have differentiated down a non-megakaryocytic route are generated at each stage, resulting in a relatively low yield of megakaryocytes per input iPSC (Gaur *et al.*, 2006).

1.3.3 *Improving the purity of the differentiation process with 'forward-programming'*

One approach developed by Eto et al to improve the number of MKs produced through directed differentiation has been the immortalisation of MK progenitors obtained through directed differentiation, through overexpression of BMI1 and BCL-XL to suppress senescence and apoptosis and c-Myc to promote proliferation (Nakamura *et al.*, 2014). This has proven successful in scaling up the production of megakaryocytes to enable animal model experiments but it also raises several clinical safety concerns with regards to the safety of potentially infusing immunocompatible immortalised cells into a patient; primarily due to the risk of tumorigenicity and lack of an immune response against these cells. This technique also requires very precise control over Myc expression levels and subsequent silencing of all three exogenous genes to achieve full MK maturation. The complex nature of the genetic modifications involved and the manual screening and clonal selection resulting in a limited success rate for this immortalisation technique have proven barriers to this being widely adopted.

An alternative approach was developed by Moreau et al that can give rise to a far greater purity and yield of megakaryocytes compared with directed differentiation, known as ‘forward-programming’ (Moreau *et al.*, 2016). MK-specific transcription factors (TFs) forming complexes able to interact with chromatin modelers were hypothesised to be able to rewire the hiPSC gene regulatory network to induce differentiation. This came out of RNAseq experiments comparing the transcription factor expression between iPSCs and cord blood-derived megakaryocytes, followed by overexpressing combinations of these factors in iPSCs through lentiviral vectors. This had been following discoveries on the plasticity of cell identity controlled by limited sets of transcription factors altering the epigenetic landscape (Cherry and Daley, 2012).

iPSCs were then maintained in iPSC medium (containing FGF2 and Activin A) for two days, followed by a MK medium (containing TPO and SCF) for a further five days, requiring no mesoderm induction. Crucially, these culture conditions after transduction with a GFP control showed no evidence for megakaryocytes in the culture, demonstrating these culture conditions alone were not capable of inducing differentiation.

Overexpression of a combination of GATA1, FLI1 and TAL1 was uniquely able to produce CD41+CD42+ megakaryocytes from iPSCs in a highly efficient manner, maturing into platelet-producing cells that could be cryopreserved, maintained, and amplified *in vitro* for over 90 days. The culture was further optimised by introducing a mesoderm induction step with FGF2 and BMP4 and embryoid body culture instead of a 2D iPSC culture.

There remain issues with these differentiation systems. Functional, qPCR and more recently, scRNAseq data suggests that forward programming appears to produce primitive megakaryocytes rather than the definitive MKs found in adult bone marrow. Gene expression profiles were compiled from iPSCs, fetal liver MKs and cbMKs to create a ‘trajectory’ of MK development and to examine the genes most differentially expressed between these cultures. When compared to the gene expression profile in FoP-MKs, although many of these differentially expressed genes appeared to be similarly expressed to cbMKs, some key MK genes appeared to either be unchanged from the levels expected in iPSCs or in between the levels expressed by iPSCs and cbMKs (e.g. vWF). It remains an ongoing area of research in the lab to find factors that may help further mature the MKs produced. This controversy is not unique to the field of iPSC-derived MKs, but to many other fields attempting to derive adult tissues from iPSCs, such as with cardiomyocytes (Karakikes *et al.*, 2015).

1.3.4 *Stem cell editing to produce better megakaryocytes and platelets*

The potential for platelets derived from standardised iPSC lines raise the possibility of improving upon them using genome editing techniques. Such modifications could include the addition or removal of TFPI to promote or reduce clotting, combinations of growth factors (difficult to currently deliver together at high doses to specific tissues using traditional pharmacokinetics) to promote cardiac regeneration in myocardial infarction or rFVIIa to promote clotting in areas of bleeding. Evidence supporting the modulation of TFPI come from monoclonal antibodies inhibiting it currently undergoing development as a procoagulant (Lauritzen *et al.*, 2019). Evidence for growth factors promoting cardiac regeneration come from studies on thymosin-β4 in cell culture (Smart *et al.*, 2007). Recombinant factor VIIa was chosen here due to its proven efficacy in clinical practice as a low-hanging fruit to investigate the principle of delivering proteins in a targeted manner using platelets. If proven successful, this would open the possibility for other proteins with currently more speculative benefits to be delivered in this way.

Technology to perform targeted gene replacement (or gene insertion) in both yeast and mouse ES cells has been available since 1979, utilising homologous recombination for gene replacement and powerful selection procedures (often requiring both positive selection to maintain the cells that have taken up the modification and negative selection against the common products of random integration) (Scherer and Davis, 1979; Gordon and Ruddle, 1981; Capecchi, 2005). The absolute frequency of homologous recombination has always been low, on the order of one in every 10^4-10^7 cells, limiting its utility in other experimental systems. The challenge in extending gene targeting can therefore be largely viewed as one of increasing the frequency of recombination.

In recent years, several new techniques have emerged that have made this process fast and accurate, inspired by discoveries that natural recombination events are initiated through the formation of double strand breaks (DSBs) (Rudin, Sugarman and Haber, 1989). In the absence of a replacement template, a targeted DSB can introduce targeted mutagenesis. When two double strand breaks are introduced ‘bracketing’ a genomic locus, the entire locus can be knocked out in a targeted manner.

The first advancement in this field came from the development of zinc finger nucleases (ZFNs); synthetic proteins based around zinc finger proteins (a family of transcription factors) fused to the endonuclease Fok1. These originated from observations that natural type IIS restriction enzyme Fok1 has physically

separable domains for binding and cleavage, that the cleavage domain has no apparent sequence specificity, and when this cleavage domain was fused to alternative recognition domains constructed from novel assemblies of zinc fingers (where each finger binds primarily 3bp of DNA in a remarkably modular fashion), that this cleavage activity could be redirected to specific targets (Kim, Cha and Chandrasegaran, 1996).

The design of combinations of zinc finger assemblies to target specific regions of interest remained complex for many years however, and new technologies that could make this targeting process easier emerged. Transcription activator-like effector nucleases (TALENs) were developed as an alternative to ZFNs for genome editing and DSB introduction, based around the same cleavage domain of Fok1. However, instead of using zinc finger assemblies for gene targeting, it was fused to a novel DNA binding domain composed of highly conserved repeats derived from transcription activator-like effector (TALEs), proteins secreted by *Xanthomonas* bacteria. Crucially, these DNA binding domains could be designed easily and rapidly with a simple 'protein-DNA code' that relates modular DNA-binding TALE repeat domains to individual bases in a target-binding site (Li *et al.*, 2011).

Both above-mentioned technologies require the expression of custom-designed proteins, each of which act as specific endonucleases to a target DNA sequence. A recent breakthrough has been the development of endonucleases designed around clustered regularly interspaced short palindromic repeats (CRISPR), where a single endonuclease (Cas9 and others) can be introduced with a short guide RNA to target its activity to a desired location (Jinek *et al.*, 2012; Cong *et al.*, 2013). Originally this was discovered as part of a bacterial immune system, allowing for the same endonuclease to be retargeted using only fragments of RNA. There are many advantages to this approach over designing a novel protein assembly for each modification; oligonucleotide synthesis is comparatively faster, more straightforward to perform and far less expensive, paving the way for much a greater scale of modifications to be made. CRISPR technology has been expanded to include the possibility of not only introducing double stranded breaks (and so perform gene knockout, mutagenesis and replacement), but also as a targetable activatory/inhibitory transcription factor, and at scale for large-scale CRISPR knockout screens (Bikard *et al.*, 2013; Hart *et al.*, 2015).

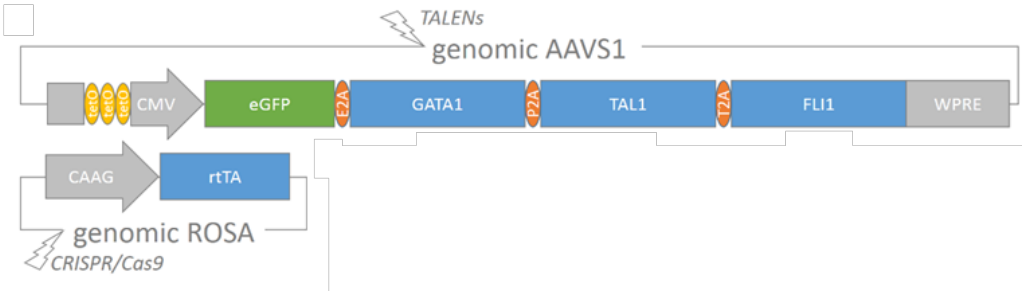

Figure 1.9. *Schematic view of the inducible expression cassette and genomic integration sites in the inducible MKFoP system. Reproduced with permission from Thomas Moreau, unpublished.*

Use of lentivirus has proven to be a barrier towards clinical translation of these technologies. One use of genome editing in our lab was to reduce the need for lentivirus to overexpress TFs. This was done by inserting a doxycycline-inducible cassette inserted by Dr Amanda Dalby to the genomic safe harbour site AAVS1 to protect it from being epigenetically silenced (Figure 1.9). This allows expression of the three transgenes necessary for differentiating the iPS cells to megakaryocytes along with a reporter GFP upon exposure to doxycycline and allows for differentiation to occur without exposure to lentiviruses, rendering it more suitable for GMP-grade manufacturing.

The dominant cause of alloimmune platelet transfusion refractoriness (observed in 5-15% of patients) is due to the production of alloantibodies against HLA class I. Knockout of HLA Class I expression by using CRISPR to delete β2-microglobulin, a protein required to stabilise HLA-A, B, C and E, on the surface of platelets could result in universal platelets suitable for any transfusion. Suzuki et al have shown that this is not only possible but that the resultant PLPs are also inert to NK cell mediated immunity, the normal immune process to remove cells not expressing HLA Class I (Suzuki *et al.*, 2020). The HLA-matching of donor platelets may be one day supplemented with a supply of universally immuno-compatible platelets, especially for patients that show a high refractoriness to transfusion.

Taken together, genome editing has been used successfully in iPSC-derived MK culture to simplify protocols and to introduce clinically desirable modifications to the megakaryocyte. There has even been some work in using these technologies to introduce mutations to study genetic diseases of megakaryopoiesis that have proven difficult to study in MKs from patients due to the rarity of megakaryocytes in bone marrow aspirates and the complex nature of many of these genetic diseases that previous technologies have been unable to replicate (Albers *et al.*, 2012). The potential for off-target effects of CRISPR and other gene editing tools in MKs demands caution and further work however, and the study of genome-

wide changes introduced through these techniques has become possible only recently through the advent of next-generation sequencing technologies.

1.3.5 *Replicating thrombopoiesis in vitro through bioreactor design*

Although the precise location of platelet formation *in vivo* remains controversial, it has been widely accepted that each adult MK can give rise to 10^3 platelets. A resting culture of cbMK or FoP-MKs can give rise to proplatelets and subsequent PLPs but is comparatively far less efficient; it has been estimated that the yields are between 1-2 PLPs per MK from a static culture. This is thought to be due to the importance of mechanical factors (e.g. shear forces) that physically separate PLPs from MKs, as well as soluble factors produced by the niche that stimulate platelet release. However, the complex interactions within the 3D microenvironments regulating thrombopoiesis remain poorly understood.

Bioreactors attempt to recreate some of these mechanical factors to more closely simulate the bone marrow microenvironment and niche in which these MKs normally live and thrive and have proven important in scaling up the production of platelets from these *in vitro* MK culture systems. There have been several complementary approaches to their design.

Thon et al developed a microfluidic device that was biologically-inspired to recapitulate a simplified 2D version of the dimensions of human venules in the bone marrow and provide a physiological shear stress to extract viable platelets from iPSC-derived MKs (Thon *et al.*, 2014). A two-channel design was used to recreate this shear stress; the two channels sit on top of one another, separated by a membrane containing small holes. They were able to show that adult mouse MKs seeded into the upper channel were retained in the membrane through video light microscopy. Differential flow in both chambers was able to provide shear stress to stimulate proplatelet formation and this allowed their device to siphon off the platelets from these proplatelet extrusions. They showed that shear stress-induced proplatelet formation was driven by the cytoskeleton using a GFP-tagged tubulin marker, and that this process also occurred in iPSC-derived megakaryocytes obtained through directed differentiation, to obtain a yield of around 14 PLPs per input MK.

One approach suggested by Ito et al is to use a turbulent flow-based bioreactor. They hypothesised that shear forces alone could not explain the discrepancy between the order of magnitude differences between those produced by shear forces in bioreactors similar to Thon et al. Through observations made *in vivo*, they suggested that turbulence could also induce thrombopoiesis and designed a

bioreactor based on this principle, a vertical reciprocal motion liquid culture bioreactor (Ito *et al.*, 2018). They describe a liquid culture containing two oval shaped mixing blades fixed at right angles to each other, repeating an up-down reciprocal motion to generate turbulent flow, and showed it was possible to generate between 70-80 PLPs per input MK compared with the 14 seen with the Thon bioreactor.

There have been attempts seeking to recreate a 3D structure to mimic the bone microenvironment, as opposed to the 2D microfluidic devices develop by Thon et al. One such approach used a two-layer collagen scaffold (extensively cross-linked collagen type I, which has been widely used as a 3D scaffold structure for other tissue regeneration projects). This follows on from previous work showing that carbodiimide crosslinking of collagen leads to the ablation of integrin-dependent cell stimulation while adding stability and strength. The two-layer collagen scaffolds were integrated into a twin chamber culture system, where one side allowed for seeding of MKs into the scaffold and retention of MKs within its porous structure, while cross-flow subjected them to shear forces to induce platelet release (Shepherd *et al.*, 2018).

Another distinct approach is that of the SilkFusion project, an EU-wide collaboration using silk fibroin protein to assemble 3D scaffolds mimicking the bone marrow niche architecture and functionalise this material with proteins to recreate the extracellular matrix (ECM) composition found *in vivo* (Di Buduo *et al.*, 2015). They were able to show that the silk is a similar stiffness to the *in vivo* microenvironment and can direct human MK behaviour, functionalisation with ECM proteins could support MK development and that co-culture with endothelial cells increases proplatelet formation and platelet release.

Individually, these approaches have paved way for a much higher yield of platelets from iPSC-derived MKs, and insights into their mechanisms of platelet release combined with an appraisal of their relative strengths and limitations will no doubt lead to improvements in these technologies in the near future towards reaching a 10^3 platelet per MK yield as is possible *in vivo*.

1.4 An introduction to coagulation

1.4.1 *The classical 'waterfall' model of haemostasis*

As well as platelets, another important factor for haemostasis is the central role that the vast amounts of proenzymes produced by the liver play in the role of maintaining haemostasis. The classical waterfall model was introduced by Davie,

Ratnoff and Macfarlane describing the cascade of enzyme-mediated amplification of the clotting process, based upon *in vitro* experiments with human donor blood (Davie and Ratnoff, 1964; Macfarlane, 1964). Initially, the molecular identity of many of the factors involved with procoagulant activity were unknown and were labelled in roman numbers from Factor I to XII in order of their discovery. Other proteins were also discovered that showed an anticoagulant activity, such as protein C, S and Z.

Further studies have revealed the identities of these factors (see Table 1.2). These circulate as zymogens in the blood, and once activated are suffixed with ‘a’ to indicate their activation. Most of these factors are proteins produced by the liver, apart from factors III (tissue factor) and IV (calcium). Factors II, VII, IX, and X as well as protein C, S and Z are dependent upon a post-translational modification (vitamin K dependent gamma carboxylation of glutamic acid residues) that enables them to bind calcium and other divalent cations and thus participate in this coagulation cascade (Vermeer, 1984).

Clotting factor number	Clotting factor name	Function
I	Fibrinogen	Clot formation
II	Prothrombin	Activation of I, V, VII, VIII, XI, XIII, protein C, platelets
III	Tissue Factor	Co-factor of VIIa
IV	Calcium	Facilitates coagulation factor binding to phospholipids
V	Proaccelerin, labile factor	Cofactor of X-prothrombinase complex
VI	Unassigned	
VII	Proconvertin, stable factor	Activates factor IX, X
VIII	Antihaemophilic factor A	Cofactor of IX-tenase complex
IX	Antihaemophilic factor B or Christmas factor	Activates X, forms tenase complex with factor VIII
X	Stuart-Prower factor	Thrombinase complex with factor V; activates factor II
XI	Plasma thromboplastin antecedent	Activates factor IX
XII	Hageman Factor	Activates factor XI, VII and prekallikrein
XIII	Fibrin-stabilising factor	Crosslinks fibrin

Table 1.2. *A table of the clotting factors that have been assigned Roman numerals. (Based upon Wright, 1962)*

Knowledge of this coagulation cascade has led to the development of many drugs to modulate its various components to promote an anticoagulated state for patients at risk of thrombosis. Drugs such as warfarin antagonise the production of vitamin K dependent clotting factors, by competing with vitamin K for binding sites on vitamin K epoxide reductase (VKOR), competitively inhibiting the post-translational modifications necessary for these factors to function (Czogalla *et al.*, 2017). The factor VII and anticoagulant protein C has a much shorter half-life than

the procoagulant factors II, IX and X in blood (Stirling, 1995). The loss of protein C leads to a lack of inhibition of coagulation, while the loss of Factor VII inactivates the extrinsic pathway (but the intrinsic pathway is left undisturbed). Thus, warfarin initially causes a brief pro-coagulant state followed by a prolonged anti-coagulant state when the rest of the vitamin K-dependent factors are removed from circulation. For this reason and to over the delay between initiation of warfarin therapy and depletion of vitamin K-dependent factors, clinically it is often supplemented with heparin initially, which acts as an anticoagulant through activating the enzyme inhibitor antithrombin III (ATIII), which then inactivates thrombin, Factor Xa and other proteases (Hirsh *et al.*, 2001).

The extrinsic pathway described here has been shown to be vital in initiation of clotting. In this model, FVII is activated to FVIIa through contact with tissue factor (factor III) and forms a complex of FVIIa-TF. This complex goes on to activate Factor X to Xa. Both extrinsic and intrinsic pathways converge on Factor X (Figure 1.10), the steps after which are called the common pathway. Factor Xa, in combination with Factor Va, converts prothrombin to thrombin, and subsequently thrombin converts fibrinogen to fibrin, forming a fibrin clot. The intrinsic pathway described acts as an amplification loop, being both initiated by either thrombin activating FXI or contact activation of FXII from negatively charged surfaces and resulting in the formation of more thrombin, through a cascade of FXII, FXI, IX, VIII resulting in activation of Factor X (Macfarlane, 1964). Clinically, the extrinsic and common pathways are measured through the prothrombin time (PT), while activation of the intrinsic and common pathways are measured through the activated partial thromboplastin time (aPTT) and the understanding of the calcium dependence of this process led to the use of calcium chelators for blood collection (Erban, Kinman and Schwartz, 1989).

This model has also helped to understand genetic defects in coagulation. For example, haemophilia A and B are caused by a lack of Factor VIII and IX respectively, which affects the same intrinsic pathway (Castaman and Matino, 2019). Clinically, the missing factors are replaced (through factor concentrates or recombinant factors) or the intrinsic pathway is bypassed by supplementing the extrinsic pathway with further FVIIa (although the mechanism through which this may work remains controversial for reasons described in more detail in section 1.4.2). Clinical samples showing defects in coagulation can also be mixed with known normal plasma; a correction of the PT or aPTT implies the defect is due to a lack of a coagulation factor, while a continuation of abnormal test results implies the presence of inhibitors, which can develop as an immune response to repeated transfusions of factor concentrates (Miller, 2019).

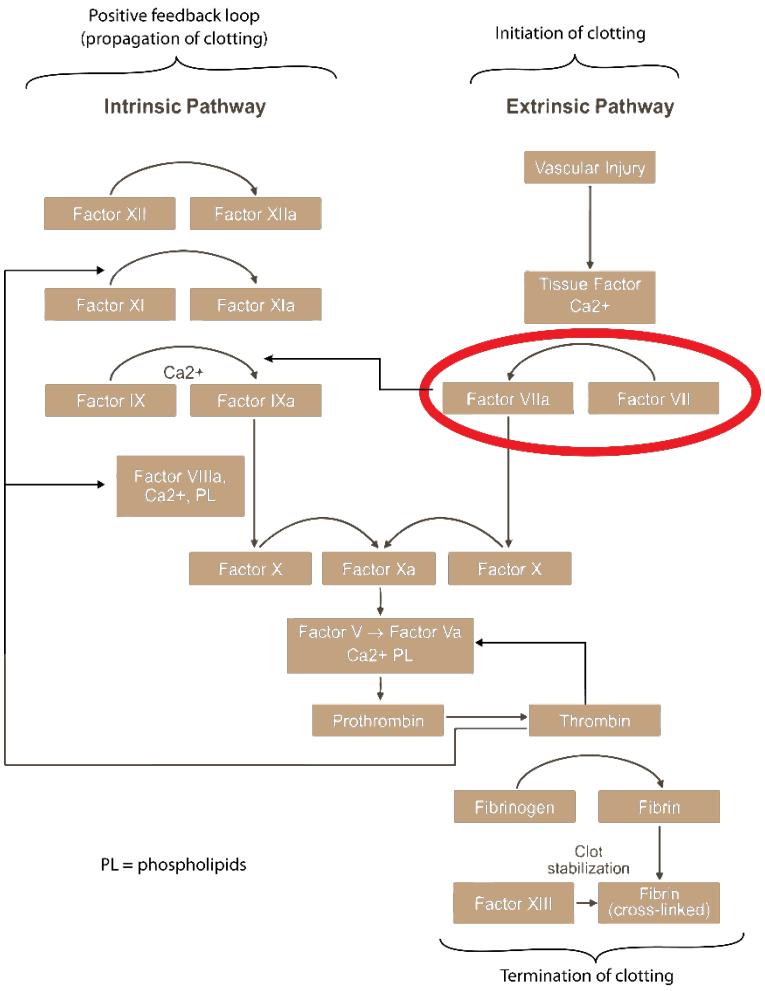

Figure 1.10. *The classical waterfall model of coagulation, redrawn based on information from* (Peters and Harris, 2018). *Circled is the central activation of Factor VII to Factor VIIa of the extrinsic pathway, vital in the initiation of clotting. PL = phospholipids.*

The two cascades of extrinsic and intrinsic cascades (Figure 1.10) may suggest that they operate as independent and redundant pathways, but clinical manifestations of individual factor deficiencies demonstrate that this is not the case. Further evidence for the intrinsic pathway acting as a signal amplification loop comes from studies of mutations in its component enzymes. Deficiencies of the initial parts of the intrinsic pathway (FXII, HMWK or PK) cause a marked elongation of aPTT but are not associated with a tendency for bleeding in humans or mice (Cheng *et al.*, 2010). Deficiencies of the next downstream enzyme, FXI, is associated with variable haemostatic deficits in humans (because the extrinsic pathway can bypass its requirement through the direct activation of FIX by FVIIa), while deficiencies in FIX or FVIII is universally associated with serious bleeding tendencies, suggesting that the cascading nature of this system is crucial for signal amplification (Wang *et al.*, 2005; Grover and Mackman, 2019). Each

molecule upstream can activate multiple molecules of the downstream component, and in turn each of these can activate multiple molecules of their downstream component. This pattern continues throughout the cascade; thus defects in the more downstream components are more apparent in the phenotype.

Platelets are notably absent from this model of coagulation, not fitting with the observations that thrombocytopenic patients bleed considerably regardless of the correct functioning of all enzymes described in the waterfall model, and we know that thrombi *in vivo* consist not just of fibrin but also a mesh of platelets and red blood cells. This waterfall model was developed through studying coagulation *in vitro* and has proven vital for understanding and measuring coagulation defects in a clinical laboratory setting, but it has become clear over many decades that this does not accurately represent the processes that lead to coagulation *in vivo.*

1.4.2 *A more modern cell-based model highlights the synergy between the clotting factors and platelets*

In recent years, there have been attempts to combine the understanding of platelet biology with the coagulation cascade. The more recent modern cell-based model of coagulation proposed by Hoffman and Monroe suggests that the described coagulation cascade occurs on the surface of platelets and endothelial cells, progressing in three overlapping stages; (1) initiation which takes place on a tissue-factor bearing cell, (2) amplification in which platelets and cofactors are activated to set the stage for large scale thrombin generation, and (3) propagation, in which large amounts of thrombin are generated on the surface of platelets as seen in Figure 1.11 (Hoffman and Monroe, 2001).

The initiation of clotting takes place after the injury of vascular endothelium, exposing tissue factor to circulating FVII. The endothelial membrane acts as a place for the activation of FVII, FV and FX, leading to the production of thrombin (and subsequently, fibrin) as described in the extrinsic pathway in the classical model (Hoffman and Monroe, 2001). During amplification, platelets adhere to the collagen-vWF complex initiating their aggregation. Activated platelets then bind FIXa and FVIIIa and promote the release of FV which is subsequently activated by thrombin and FXa, similar to the intrinsic pathway in the classical model. During the propagation phase, the FIXa-FVIIIa complex adhering to the surface of platelets activates FX and binds to FVa. The FVa-FXa complex then converts prothrombin into thrombin, initiating the conversion of fibrinogen to fibrin, resulting

in a fibrin burst with subsequent clot formation. Many of these mentioned factors feed back to continue this process until a suitable haemostatic plug has formed.

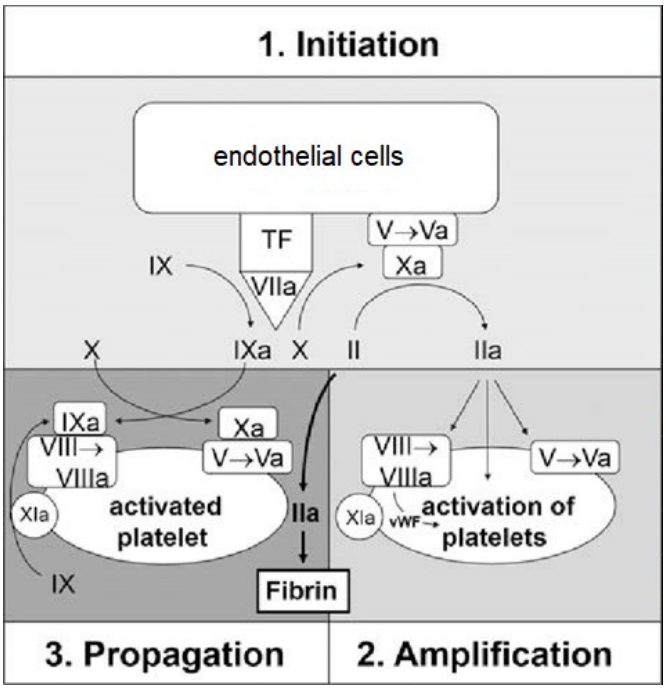

Figure 1.11. *A cell-based model of coagulation.* (Hoffman and Monroe, 2001; Bezinover *et al.*, 2018). *Reprinted by permission from Wolters Kluwer Health, Inc: Perioperative Coagulation Management in Liver Transplant Recipients, Transplantation 102(4) © 2018.*

This cell-centric model of haemostasis may help explain some clinical features that an enzyme-centric model does not (Hoffman and Monroe, 2001). For example, in haemophilia, the classical model cannot explain why the extrinsic pathway cannot produce enough FXa to (at least partially) compensate for a lack of factor VIII/IX. TFPI has been hypothesised to shut off the FVIIa/TF pathway before it can make enough FXa to support generation of haemostatic amounts of thrombin (Wood *et al.*, 2014). While this may play a role, the cell-based model suggests another intriguing possibility; that the bleeding tendency in haemophilia is caused not because of a lack of production of FXa, but because it is produced on the wrong cell surface. FXa produced on the surface of a TF-bearing cell is unlikely to reach the platelet surface without being inhibited by ATIII or TFPI. These two inhibitors at their normal plasma levels inhibit FXa so efficiently that it has a half-life of a minute or less in solution (Jesty *et al.*, 1996). By contrast, FIXa is inhibited much less rapidly by ATIII and not at all by TFPI and so it can migrate from the TF-bearing cell to the platelet surface to form the platelet tenase complex (Hoffman and Monroe, 2001). This model suggests therefore that the bleeding

tendency in haemophilia is a failure specifically of platelet-surface FX activation and thrombin generation.

Furthermore, there is evidence that TF can become expressed on the surface of monocytes within minutes when stimulated by activated platelets through the action of P-selectin (Ivanov *et al.*, 2019). There is also indication that this TF can end up on the surface of these platelets through microparticles produced by these monocytes (Siddiqui *et al.*, 2002). Flow cytometry data also suggest that platelets have an inactive form of TF on their surface that becomes functional upon release. However, the relevance of this in health and disease remains somewhat unexplored.

1.5 Current therapies for the treatment of haemorrhage

The causes of thrombosis, pathological clot formation in the absence of bleeding, are well-structured by Virchow's triad, which relies on the pillars of hypercoagulability, endothelial damage and blood flow stasis. The induction of haemostasis for the treatment of haemorrhage also relies on exacerbating one or more of these pillars, either surgically through using substances to promote blood flow stasis, or medically through augmenting blood to be hypercoagulable. The choice of therapy often depends heavily on the cause of the haemorrhage.

Surgically, blood flow stasis is often treated through compression, sutures and electro-cauterisation as well as topical haemostatic agents ranging from physical substrates such as bone wax, gelatine foams, mineral zeolite and cyanoacrylate, through to absorbable agents containing oxidised cellulose, microfibrillar collagen, chitosan and biologic agents such as thrombin and fibrin (Achneck *et al.*, 2010).

Therapies used to promote hypercoagulability of blood focus around blood-derived sources of replacement coagulation factors. Fresh frozen plasma (FFP) is transfused to replace coagulation factors lost during massive haemorrhage (Dickneite and Pragst, 2009). Cryoprecipitate is another blood product derived from repeated freeze-thawing of FFP to produce a source of more concentrated clotting factors including Factor VIII, vWF and fibrinogen. It is most commonly used to replenish fibrinogen levels in acquired coagulopathy in the context of cardiac surgery, trauma, obstetric haemorrhage and liver transplantation (Nascimento, Goodnough and Levy, 2014). Prothrombin complex concentrates (PCC) are blood products enriched in the vitamin K-dependent clotting factors II, VII, IX and X. FFP, cryoprecipitate and PCC all serve to replace lost coagulation factors and so have their use during massive ongoing perioperative or post-

partum haemorrhage, and in reversal of warfarin therapy by replacing the vitamin K-dependent factors back into the blood (Sarode *et al.*, 2013; Ghadimi, Levy and Welsby, 2016).

As well as factors to promote the clotting cascade, tranexamic acid (TXA), a synthetic lysine analogue, is a widely used treatment used to inhibit plasmin generation and thus the process of fibrinolysis. Patients with polytrauma and those undergoing surgical procedures on organs rich in plasminogen activators (e.g. liver, kidney, pancreas) are at a high risk of hyperfibrinolysis and in these cases, antifibrinolytics such as TXA can be used for prophylaxis and treatment of bleeding (Pabinger *et al.*, 2017).

For patients with haemophilia disorders, factor replacement therapy with FVIII or FIX as required is often standard therapy. Upon the development of inhibitory antibodies, patients may also be trialled on Factor Eight Inhibitor Bypass Activity (FEIBA), a blood product containing zymogen Factors II, IX and X as well as activated factor VII, often considered to be an activated form of PCC (Turecek *et al.*, 2004; Dager, Roberts and Nishijima, 2019). Recombinant activated FVII is also used as an alternative to this blood product to achieve a similar effect, and both can be used off-license in severe haemorrhage in non-haemophiliacs (described in further detail in section 1.5.4).

Finally, as mentioned in previous sections, haemostasis requires both coagulation factors and platelets and thus platelet transfusion is a hugely successful therapy for patients suffering from thrombocytopenia due to chemotherapy, leukaemia, or massive blood loss.

1.5.1 *Transfusion of platelets as a therapy for bleeding*

Pioneering work by W. Duke in 1910 first established that it was possible to reverse the risk of bleeding with a case series of thrombocytopenic patients transfused with fresh whole blood, whose bleeding ceased and platelet counts increased (Duke, 1910). It took another fifty years to confirm the role of thrombocytopaenia as the key cause of bleeding in the haemorrhagic disorders of leukaemia and to show that selective platelet transfusion could relieve these. An autopsy series compared deaths retrospectively in acute leukaemia patients before and after 1959 when platelet transfusion became available, and found that strikingly, haemorrhage was the second leading cause of death after infection and that this dropped from 67% (1953-1959) to 37% (1960-63) (Hersh *et al.*, 1965). By the end of the 1960s, platelet transfusion had become a routine procedure in

haematology departments and had also moved from only treating acute bleeding to also being used prophylactically to prevent them. Along with antibiotics for infections, this both directly extended patient survival and gave their physicians more time to try new chemotherapies to treat the underlying leukaemia.

Over the next several decades evidence emerged that these platelets could be stored for up to 3 days at 22°C with no loss of haemostatic function and subsequent advances made it possible to extend this to 5 and then 7 days (Murphy and Gardner, 1971). As well as platelets extracted from pooled donated whole blood (the buffy coat procedure that requires four pooled blood units), new technologies such as automated apheresis allowed the possibility of more frequent donations from single platelet donors and thus a way to meet the inventory needs of transfusion services supporting increasing numbers of chemotherapy patients (Simon, 1994).

Platelet concentrates also became widely adopted for treating other causes of haemorrhage, such as that due to trauma (e.g. on the battlefield), postpartum and during surgery (especially cardiac surgery). Although widely practiced, there is still a lack of consensus in the literature upon the evidence for perioperative platelet transfusion to maintain haemostasis (Levy *et al.*, 2017).

1.5.2 *Modern platelet transfusion practices around the world*

Presently, up to 2.9 million transfusions of platelets take place each year in Europe (Stroncek and Rebulla, 2007). Platelet transfusion strategies are driven by either the need to stop active bleeding (therapeutic) or to prevent its occurrence in at-risk groups (prophylactic). The most common situations are for patients receiving chemotherapy, requiring surgery (especially cardiac surgery) or having experienced severe haemorrhage (e.g. from pregnancy or childbirth, trauma, largely from road traffic accidents, or severe anaemia in the young, often caused by malaria), often being combined with other blood products such as fresh frozen plasma and red blood cells (RBCs) in a massive transfusion protocol.

Just like other blood products, platelets must be tested for immuno-compatibility between donors and hosts. A mismatch can quite quickly lead to hyperacute rejection and other suboptimal clinical outcomes. Until the turn of the 20th century, blood transfusions were a dangerous and unsafe practice, outlawed in many parts of the world. Landsteiner's pioneering work in 1900 laid the foundation for transfusion medicine with the discovery of the ABO blood type system which made these procedures much safer (Landsteiner, 1900). As well as the ABO blood groups common to RBCs and platelets, platelets also have other specific

antigens that must be matched that are not required for RBC transfusions, such as human leukocyte antigens (HLA) and human neutrophil antigens (HNA) and human platelet antigens (HPA) (Estcourt *et al.*, 2017). Often these are not as important in a patient receiving their first platelet transfusion, but this becomes more important if they begin to receive repeated transfusions and post-pregnancy due to the development of alloimmunisation.

In most high-income countries, there is an adequate supply of blood with its use largely pre-planned and predictable, with most blood transfusions (79%) taking place in the over 60 group (WHO, 2016). Blood donors and their donated blood are rigorously screened, and so the frequency of disease transmission through transfusion is low, although tragically marred by recent scandals in the 1980s with the large-scale infection of patients with HIV and Hepatitis B when strict screening and testing for infectious agents was less common. However, many of these factors that are no longer as prevalent in higher-income countries remain major ongoing issues in lower-income countries, where most blood transfusions (67%) are given to children below the age of 5. This reflecting the different demands on medical care in different parts of the world. In sub-Saharan Africa, blood shortages (the leading cause of maternal mortality due to post-partum haemorrhage) and unsafe blood (leading to many instances of transmission of HIV and hepatitis) represent major challenges in transfusion medicine (WHO, 2015). These are thought to be due to the result of a relative paucity of donors (combined with a free market, quickly leading to blood products becoming unaffordable for many), the unwillingness of relatives to donate due to cultural differences as well as inadequate supply chains, storage and transport infrastructure (Bates *et al.*, 2008).

1.5.3 *Current limitations of platelet transfusion*

In recent years with advances in chemotherapy and increases in trauma surgery, demand for platelet products is steadily increasing while at the same time, the supply from donors has remained largely constant (see Figure 1.12) (Cowan, 2017). Many countries rely on voluntary non-remunerated donors, as commercial blood donation has been demonstrated to result in blood with a higher prevalence of both HIV and Hepatitis B antigen (Ahmed, Ibrahim and Hassan, 2007; Ala *et al.*, 2012).

There have been no major advances to improve the storage of platelets beyond 7 days, compared with 35-40 days for red blood cells, making these a comparatively highly perishable blood product (Smethurst, 2016; García-Roa *et*

al., 2017). Due to their short shelf life, it can be difficult for their supply to keep up with their demand, especially over holiday periods when fewer donors are available, after natural events such as snowstorms, and maintaining the logistics of a blood supply chain is difficult in remote areas (American Red Cross, 2019). Platelet concentrates are kept at room temperature, increasing risk of bacterial contamination, and their haemostatic and metabolic function is known to deteriorate over time in storage, in a process named platelet storage lesion (Thon, Schubert and Devine, 2008; Védy *et al.*, 2009). Furthermore, the prophylactic use of platelets requires the use of repeated transfusions that increases the risk of more allo-immunity against these products. This requires progressively stricter HLA matching, which reduces the pool of potential donors and it can very quickly become difficult to obtain compatible blood (Levy and Woodfield, 1984).

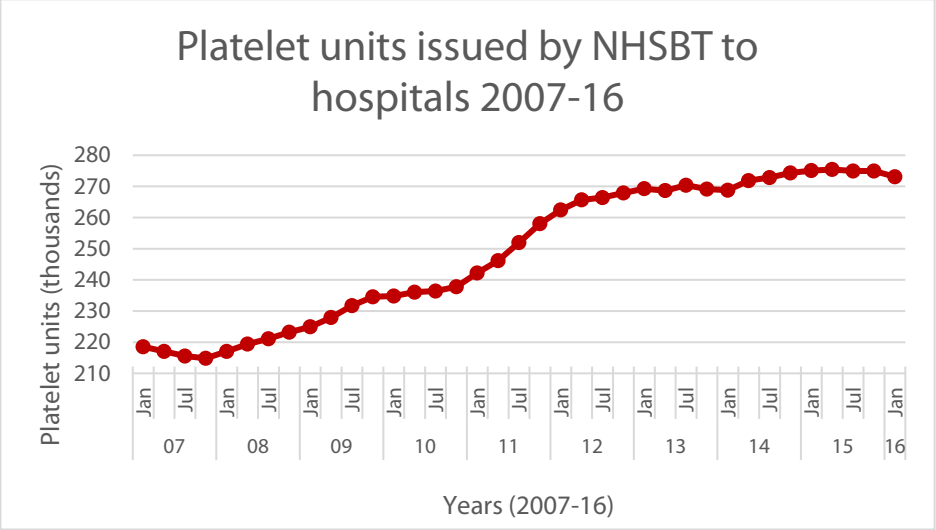

Figure 1.12. *Demand for platelet units increasing over time in the UK, replotted with data from Strategies to reduce inappropriate use of platelet transfusions (Cowan, 2017) under CC BY. NHSBT = National Health Service Blood and Transplant.*

1.5.4 *NovoSeven (a recombinant FVIIa) as a clinical treatment for bleeding*

The above-mentioned cell-based theory of haemostasis also may explain some features of the efficiency of high dose recombinant FVIIa in promoting haemostasis in haemophiliacs. Recombinant factor VIIa (*eptacog alfa* or its brand name, *NovoSeven*), was originally developed as a 'bypass factor' to treat bleeding tendencies in haemophiliacs that had developed inhibitors to exogenous FVIII and FIX (Hedner and Kisiel, 1983).

Factor VII, a serine protease, is encoded in chromosome 13q34, by a sequence approximately 12.8kb in length containing 9 exons and 8 introns (O'Hara *et al.*,

1987) located 2.8kb upstream from the Factor X gene (Miao *et al.*, 1992). Alternative splicing leads to the expression of two isoforms, A and B. Isoform B is the prevailing form in the liver and does not include exon 1b, thus encoding a shorter signal peptide than isoform A (O'Hara *et al.*, 1987). Both isoforms encode for the same mature protein of a single-chain peptide with 406 amino acids, with a molecular weight of 50kDa (Mirzaahmadi *et al.*, 2011). This zymogen protein is converted into its active form by the cleavage of a peptide bond between Arg152-Ile153, physiologically triggered by exposure to tissue factor as described in Figure 1.13, while both resultant peptides, the heavy and the light chain, are held together by two disulphide bonds. The zymogen undergoes a conformational change to expose the active site of the enzyme (Figure 1.13). *Eptacog alfa* is produced in Chinese Hamster Ovary (CHO) cells through expressing the recombinant form of zymogen Factor VII. It is activated to FVIIa as a consequence of the purification process (Jurlander *et al.*, 2001).

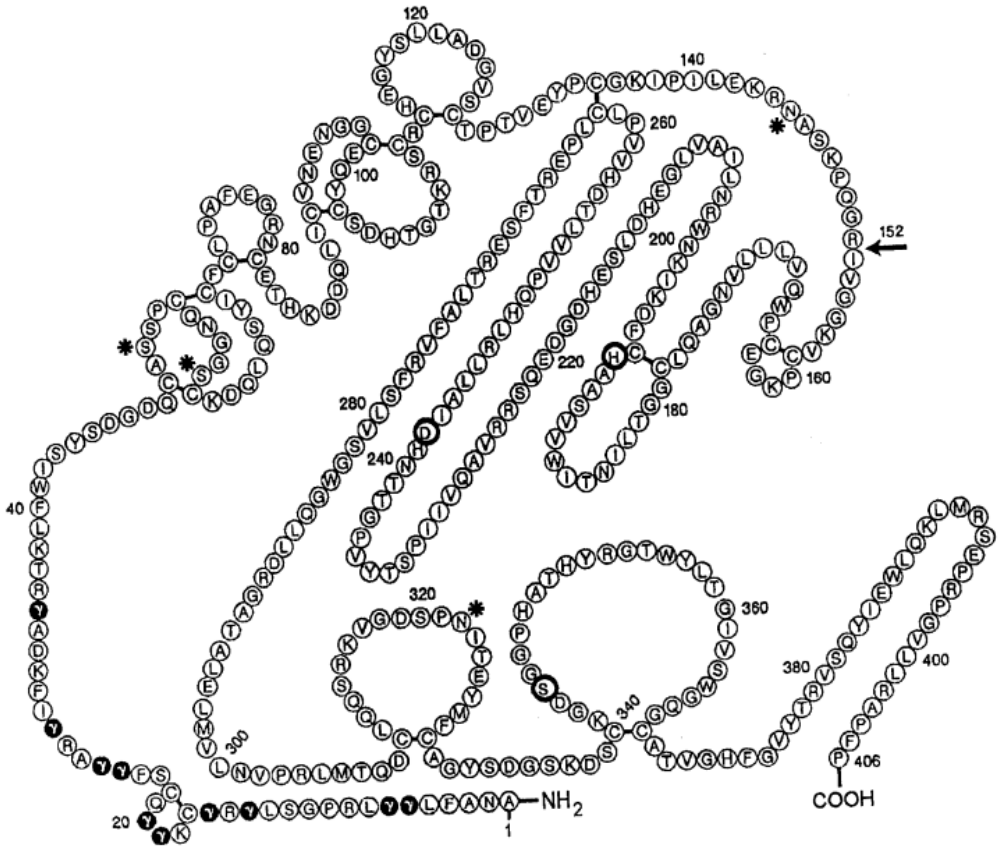

Figure 1.13. *The structure of human Factor VII, taken from* (Jurlander *et al.*, 2001)*. * indicates glycosylation sites, γ indicates gamma-carboxyglutamic acid, bold circles indicate catalytic site residues, arrow indicates the cleavage site for activation after Arg152. © Georg Thieme Verlag KG.*

The doses of rFVIIa required for a clinical effect in haemophiliacs produce plasma levels that are several orders of magnitude greater than the Kd for FVIIa binding to TF, leading many to conclude that it is unlikely that rFVIIa works through this classical extrinsic pathway TF-dependent mechanism (Augustsson and Persson, 2014). In the literature, it is well-documented that FVIIa has very little (although not zero) proteolytic activity in the absence of its co-factor. In the cell-based model of haemostasis, the platelet surface may behave as a phosphotidylserine (PS)-containing lipid surface in supporting the activity of FVIIa. FVIIa has been demonstrated to bind to activated, but not unactivated platelets with an affinity similar to that for synthetic PS-containing lipid vesicles, and that once bound to the surface of an activated platelet, it can activate FX (Rao and Rapaport, 1990). The amount of FXa generated through this mechanism is thought to be sufficient to support near-normal levels of thrombin generation in an experimental model of FVIII and FIX deficiency. This is consistent with a model of coagulation in which platelet surface FXa generation is necessary to support platelet prothrombinase assembly (Ivanciu, Krishnaswamy and Camire, 2014).

As the cell-based model of haemostasis suggests the haemostatic defects in haemophilia is due to a failure of platelet surface thrombin generation, restoration of platelet surface thrombin generation by high dose FVIIa through this mechanism is plausible. In support of this, it has been found the levels of rFVIIa that must be obtained *in vivo* correlate well with the levels needed for restoration of platelet surface thrombin generation *in vitro*. This platelet surface mechanism would also explain why high dose FVIIa is effective in establishing haemostasis in non-haemophilic patients with thrombocytopenia or other platelet function defects (Hoffman and Monroe, 2001). In models of these conditions, the addition of high levels of FVIIa enhances the amount of thrombin generated by each platelet.

Tissue Factor Pathway Inhibitor (TFPI) is also a known potent negative regulator of the extrinsic pathway of coagulation by forming a complex with FXa; the FVIIa:TF complex generated from the extrinsic pathway forms a quaternary complex, FVIIa:TF:FXa:TFPI, which feeds back to inhibit the firm step of the extrinsic pathway (Hedner and Erhardtsen, 2000). Two isoforms are known, with platelets containing TFPIα and endothelial cells containing TFPIβ. Platelet TFPI has been shown to play a physiological role in limiting thrombus growth in chimeric mouse studies (Maroney *et al.*, 2011). One theory suggests that the high dose of rFVIIa required for clinical efficacy is to overcome this initial negative feedback loop. Evidence for this idea has been mixed, with a recent study showing that in the presence of concizumab, a monoclonal antibody that inhibits

TFPI, where we might expect the potency of rFVIIa to increase if the above hypothesis were true. The potency of rFVIIa increased when measured on human blood with *in vitro* assays, but not when measured *in vivo* in rabbits when measuring blood loss as a primary endpoint (Lauritzen *et al.*, 2019).

In summary, the mechanism of action of rFVIIa is thought not to be due to augmentation of the extrinsic pathway or by binding to tissue factor in a manner similar to endogenous FVII activation, but instead through increasing FXa on the surface of activated platelets. This allows for the bypass of deficiencies in factors that mediate signal transduction between tissue-factor-bearing cells and platelets in haemophilia as well as the augmentation of platelet thrombin generation in thrombocytopenia. It is this latter point has led to the use of rFVIIa off-license as a treatment for severe bleeding after massive haemorrhage.

Bleeding after cardiac surgery is a serious complication, and excessive blood loss necessitates transfusion of allogeneic blood products as described earlier as well as surgical re-exploration. Between 5-7% of patients lose greater than 2L of blood within the first 24 hours after surgery and up to 5% require re-operation to treat this bleeding (Clifford and Kor, 2016). Both transfusion and re-operation are associated with prolonged intensive care and hospital stays as well as reduced survival rates. Retrospective studies have also shown that alternatives, such as PCC and FEIBA do not provide any advantage over rFVIIa, in terms of blood loss, incidence of re-exploration and thromboembolic events (Rao *et al.*, 2014; Mehringer *et al.*, 2018).

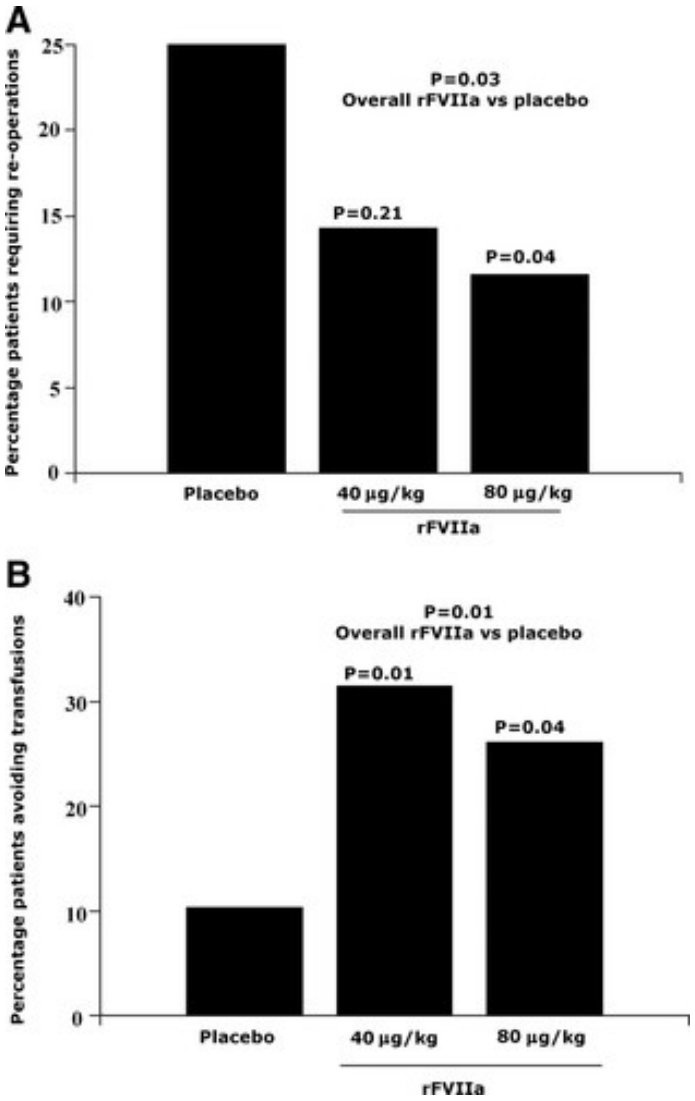

Figure 1.14. *Randomised controlled trial of NovoSeven in patients undergoing cardiac surgery. (A) Percentage of patients requiring reoperations because of bleeding. Percentages are based on the number of patients randomized and dosed (placebo, n=68 patients; 40 µg/kg rFVIIa, n=35 patients; 80 µg/kg rFVIIa, n=69 patients).* P *values were determined in comparison to placebo treatment values with* χ^2 *tests. (B) Percentage of patients avoiding transfusions after administration of trial drug. Percentages are based on the number of patients randomized and dosed (placebo, n=68 patients; 40 µg/kg rFVIIa, n=35 patients; 80 µg/kg rFVIIa, n=69 patients).*(Gill *et al.*, 2009). *Reprinted by permission from Wolters Kluwer Health, Inc: Safety and Efficacy of Recombinant Activated Factor VII, Circulation 120(1) © 2009.*

Clinical randomised controlled trials of rFVIIa have been undertaken to determine whether rFVIIa used off-license may be able to improve outcomes in these situations (Figure 1.14). In one such trial, patients who had undergone cardiac surgery and were bleeding were randomised to either a placebo or rFVIIa at two doses (40µg/kg and 80µg/kg) (Gill *et al.*, 2009). Primary end-points were to measure the number of adverse events and secondary end-points were to measure rates of re-operation, amounts of blood loss and the rates of transfusion being used as a therapy. Outcomes from this trial showed a statistically significant

difference in the secondary end-points; significantly fewer patients in the rFVIIa group underwent a re-operation in a dose-dependent manner and significantly fewer required allogeneic transfusions. There were more serious adverse events reported (including strokes) in the groups that received rFVIIa compared with placebo, although these results did not reach statistical significance. The study concluded that it may be beneficial but must be used with caution.

Apart from the potential adverse side-effects, other barriers to the use of rFVIIa in preventing bleeding include cost. With an average adult male of 70kg, a 80µg/kg dose would be 5.6mg, which costs around $11,700.00 per injection (NICE, 2020). As recombinant protein drugs have a short half-life (in this case, of 1-2 hours), it is likely that repeated injections would be required. Lowering the cost of using rFVIIa clinically would add to the market case for the use of this therapy, however there may be numerous other advantages including an improved safety profile and the ability to use the same technology to deliver combinations of multiple proteins such as growth factors in the future.

1.6 Project aims

The aims of my PhD are to investigate the possibility of using platelet α–granules as a delivery vehicle for rFVIIa, which might lead to a reduction in the number of platelets needed for a transfusion, as well as the amount of rFVIIa required to achieve haemostasis.

In order to do this using the forward-programming system, I will modify the zymogen FVII gene to become self-activating and fused this with a vWF SPD2 motif to direct the protein sorting machinery of megakaryocytes to package this into α–granules. I will investigate whether through transduction of in vitro-derived megakaryocytes, if it is possible to create a non-immortalised cell culture of human megakaryocytes that produce platelets loaded with rFVIIa. I will further characterised the functionality of this rFVIIa to demonstrate it shows efficacy despite the modifications made and characterised the haemostatic effect of the resultant platelets through *in vitro* assays.

In turn, I will use endocytosis to demonstrate it is possible for both megakaryocytes and platelets to passively take up rFVIIa into their granules and release it upon activation.

Finally, I will also develop a mouse model for human platelet transfusion and haemostasis with thrombocytopaenic immunodeficient NRG/J mice, establish the controls and test the efficacy of both donor derived-platelets and donor-derived platelets loaded with rFVIIa to investigate the additional benefit that this might provide.

2 MATERIALS AND METHODS

2.1 Molecular Biology

2.1.1 *Buffers*

2.1.1.1 Tyrode's buffer

Compound	Concentration
NaCl	137mM
KCl	2.7mM
$CaCl_2$	1.8mM
$Mg_2Cl_2 \cdot 6H_2O$	1mM
NaH_2PO_4	0.2mM
$NaHCO_3$	12mM
Glucose	5.5mM

2.1.1.2 TAE buffer (50x stock)

Compound	Concentration
Tris base	2M
Glacial acetic acid	1M
0.5M EDTA (pH 8.0)	50mM

2.1.1.3 PBE Flow buffer

Compound	Concentration
EDTA	2mM
BSA	0.5%
Make up to 1L in PBS	

2.1.1.4 TAP lysis buffer

Compound	Concentration
Tris-HCl (pH 8.0)	10mM
NaCl	150mM
NP-40	0.1%
Make up to 100mL in deionised water	

2.1.1.5 4% PFA

Compound	Concentration
16% Formaldehyde solution (no methanol) (28908, Thermo)	10ml
Make up to 40mL with PBS	

2.1.1.6 Acid-citrate dextrose (ACD)

Compound	Concentration
Sodium citrate	37mM
Citric acid	25mM
Dextrose	82mM
Make up to 100mL in deionised water	

2.1.1.7 AHD-575 (Haemoglobin lysis reagent)

Compound	Concentration
Triton X-100	2.5%
NaOH	10mM
Make up to 100mL in deionised water	

2.1.1.8 0.1M Carbonate/Bicarbonate antibody adsorption buffer (pH 9.6)

Compound	Concentration
Sodium bicarbonate	12.5mM
Sodium carbonate (anhydrous)	87.5mM
Make up to 500mL in deionised water	

2.1.1.9 ELISA Wash Buffer

Compound	Concentration
Tween-20	0.05%
Make up to 500mL in PBS	

2.1.1.10 Immunofluorescence permeabilization buffer

Compound	Concentration
BSA (A9418-5G, Sigma-Aldrich)	1%
Goat Serum (G9023-5ML, Sigma-Aldrich)	10%
Glycine	0.3M
PBS-Tween 20	0.1%

2.1.1.11 Immunofluorescence primary antibody buffer

Compound	Concentration
BSA (A9418-5G, Sigma-Aldrich)	1%
PBS-Tween 20	0.1%
Antibody	1:1000

2.1.1.12 ACK buffer

Compound	Concentration
NH_4Cl	150mM
$KHCO_3$	10mM
Na_2EDTA	0.1mM

2.1.1.13 LB Broth

Compound	Amount
Tryptone	10g
NaCl	10g
Yeast extract	5g
Made up to 1L with distilled water	

2.1.1.14 Ampicillin LB-Agar Plates

Compound	Amount
Bacto agar	15g
LB Broth	1L

100mg/ml ampicillin	0.5mL

2.1.1.15 TBS-Tween, pH 8.0

Compound	Concentration
Tris base	0.05 M
NaCl	138mM
KCl	2.7mM
Tween-20	0.05%

2.1.1.16 AE6 media

Compound	Concentration
DMEM/F12 (Life Technologies)	500mL
$NaHCO_3$	0.054%
L-Ascorbic Acid (Thermo Fisher Scientific)	64mg/L
Insulin (Life Technologies)	20mg/L
Transferrin (Life Technologies)	11mg/L
Selenium (Life Technologies)	0.0134mg/L

2.1.2 *Antibodies*

Clone	Host species	Antigen	Dilution	Used for	Company	Cat no.
polyclonal	Rabbit	FVII - recombinant protein fragment corresponding to a region between amino acids 209 and 444 (heavy chain only)	1:1000	IF	Abcam	ab97614

polyclonal	Goat	FVII - recombinant protein fragment between amino acids 39 and 444 (both light and heavy chains)	1:1000	IF	R&D	AF2338
EP6185(2)	Rabbit	FVII	1:100	FC, chromogenic, WB	Abcam	ab151543
HIP8	Mouse	anti-CD41a-H7	1:100	FC	BDPharmingen	561422
HIP1	Mouse	anti-CD42b-APC	1:100	FC	BDPharmingen	551061
HIP1	Mouse	anti-CD235a-PE	1:100	FC	BDPharmingen	555570
MOPC-21	Mouse	Isotype H7	1:100	FC	BDPharmingen	555749
MOPC-21	Mouse	Isotype APC	1:100	FC	BDPharmingen	555751
MOPC-21	Mouse	Isotype PE	1:100	FC	BDPharmingen	560167
polyclonal	Goat	anti-rabbit-Alexa488	1:1000	FC	Invitrogen	A11034
polyclonal	Donkey	anti-goat-HRP conjugate	1:10000	WB	Signalway Antibody	L3042-2

polyclonal	Goat	anti-rabbit-HRP conjugate	1:10000	WB	Southern Biotech	4030-05
polyclonal	Rabbit	GAPDH	1:1000	WB	Abcam	ab9485
1C2	Hamster	Anti-CD42d PerCy5.5	1:100	FC	BioLegend	148507
ALMA.16 (RUO)	Mouse	Anti-CD42-APC	1:100	FC	BDPharmingen	558819
HTK888	Hamster	Isotype PerCy5.5	1:100	FC	BioLegend	400931
Polyclonal	Rabbit	Anti-mouse thrombocyte	1:25	Platelet depletion	Cedarlane Lab	CLA31440
Monoclonal	Rabbit	Anti-GP1b	0.6µg/g bw	Platelet depletion	Emfret Analytics	R300
Polyclonal	Rabbit	Anti-Factor VII	1:100	FC	Abcam	ab197656
polyclonal	Rabbit	Anti-Factor VII	1:100	FC	Abcam	ab97614
VG1	Mouse	Anti-VEGF	1:1000	IF	Novus Biologicals	NB100664SS
Monoclonal	Mouse	Anti-endostatin	1:1000	IF	Santa Cruz Biotechnology	sc-514355
Polyclonal	Goat	Anti-Mouse-488 Secondary	1:1000	IF	Thermo Fisher	A21121
Polyclonal	Goat	Anti-Rabbit-647	1:1000	IF	Thermo Fisher	A21244

A6.1	Mouse	Anti-thrombospondin	1:1000	IF	Abcam	ab1823

2.1.3 *PCR Primers*

All primers were ordered from Sigma-Aldrich, UK. See specific methods and results sections for details on their use.

Name	**Purpose**	**Sequence**
LC_FO	Amplification of F7 light chain	GCCGGATCCGCCAACGCGTTCCTGGAG
LC_2RKR_RE		CCTCTTCCTCCTCTTCCTTCGGCCTTGGGGTTTGCT
2RKR_HC_FO	Amplification of F7 Heavy chain	AGGAAGAGGAGGAAGAGGATTGTGGGGGGCAAGGTG
HC_RE		GTTGCGGCCGCCTAGGGAAATGGGGCTCGCA
Thrombin_LC_FO	Amplification of F7 light chain with added thrombin cleavage sequence in 5’	GCCGGATCCCTGACCCCCAGAGGCTGGAGACTGGCCAACGCGTTCCTGGAG
Pcdna4_fo2	PCR colony screening (pcDNA4 plasmid transformed)	AAGGGCGACACGGAAATGTT
Pcdna4_re2		ATGGACTTGAGGCACACTGG
F7_Seq_fo	Sequencing of Factor VII gene	TACGTGCTGGGGATGATGACCTG
pWPT_DWF7TF_Frag1_Fo	Gibson assembly (single fragment) of DW-F7TF	GCTGTCCTCAGCAGTCCCCTGTCTCATGGCAGCAAAAGGACGCGTCTGACCCCCAGAGGCTGG

pWPT_DWF7TF_Frag1_Re		TTTTGTAATCCAGAGGTTGATTATCGGAATTCCCTCGAGGTCGACCTAGGGAAATGGGGCTCGCAGG
pWPT_noDWF7TF_Frag1_FO	Gibson assembly (two fragment) of noDW-F7TF	CATGAGTCCAGGGGCTATAGCCCTTTGCTCTGCCCGTTGCTCAGCAAGTTACTTGGG
pWPT_noDWF7TF_Frag1_RE		CTCCAGCCTCTGGGGGTCAGGGTCCTTCTTCCACAACCTCC
pWPT_noDWF7TF_Frag2_FO		GAGGTTGTGGAAGAAGGACCCTGACCCCCAGAGG
pWPT_noDWF7TF_Frag2_RE		TTTTGTAATCCAGAGGTTGATTATCGGAATTCCCTCGAGGTCGACCTAGGGAAATGGGGCTCGCAGG
RRE_qPCR_FO	Primers for lentiviral titration by qPCR	tttgttccttgggttcttgg
RRE_qPCR_RE		gatgccccagactgtgagtt
HMBS_qPCR_FO		attaccccgggagactgaac
RRE_qPCR_RE		ggctgttgcttggacttctc

Table 2.1. *A list of PCR primers used in the project, containing their label, function and DNA sequence.*

2.1.4 *PCR*

Human foetal liver cDNA was obtained (kind gift from Dr Ludovic Vallier) from which the F7 gene was amplified by Dr Annett Mueller.

Preparative PCR for cloning used the high fidelity Phusion (M0530, New England BioLabs) or Platinum Taq (11304-011, Invitrogen) polymerases. Both were utilised using the optimal annealing temperature (Tm) for each given primer pair and a maximum of 35 amplification cycles. Each reaction was set up as follows:

Polymerase (as described above)	0.1µL (2U/reaction)
10X Buffer (provided with polymerase)	5µL
50mM MgCl2 (provided with polymerase)	1.5µL
10mM dNTP mix (18427-088, Invitrogen)	1µL
Water, nuclease-free	To 50µL

This was followed by thermal cycling as described below:

Step	**Temperature, ºC**	**Time**	**Cycles**
Initial denaturation	94	2mins	1
Denaturation	94	30s	25-35
Annealing	Tm-5	30s	
Extension	72	1min/kb	
Hold	4	Indefinitely	1

For all PCR colony screening, 2x PCR Master Mix (K0171, Thermo Scientific) was used. Each PCR reaction was set up as follows:

PCR Master Mix (2x)	25µL
Forward primer	1µM
Reverse primer	1µM
Template DNA	Pipette tip used to extract small amount from colony
Water, nuclease-free	To 50µL

Samples were then amplified by thermal cycling as follows:

Step	Temperature, ºC	Time	Cycles
Initial denaturation	95	3mins	1
Denaturation	95	30s	25-40
Annealing	Tm-5	30s	
Extension	72	1min/kb	
Final extension	72	10mins	1

After which they were analysed on a 1% TAE agarose gel with a Kb+ ladder (10787018, Invitrogen), running at 80V and 400mA for 30mins. DNA fragments in gels were visualised through adding 1X SYBR safe DNA Gel stain (stock concentration at 1:10,000) (S33102, Thermo Fisher Scientific) and subsequent use of a UV light box.

2.1.5 *Cloning*

Restriction cloning was performed on the plasmid pcDNA4/TO/Myc-His B (V103020, Thermo Scientific) using BamHI (R0136, NEB) and NotI (R0189, NEB) for double digestion. DNA was incubated with restriction enzymes in NEBuffer 3.1 (B7203, NEB) and incubated at 37°C for 1 hr. Purification was performed using a 1% agarose gel in TAE buffer with a Kb+ ladder (10787018, Invitrogen), running at 80V and 400mA for 30mins.

DNA was extracted from gels and purified through gel melting and a column spin preparation (28704, Qiagen) and PCR products were purified with a column spin preparation (28104, Qiagen). DNA fragments in gels were visualised through SYBR safe DNA Gel stain (S33102, Thermo Fisher Scientific) and subsequent use of a UV light box. Relevant DNA fragments were excised with a scalpel and weighed. Gel slices were combined with buffer QG at a ratio of 3:1, followed by incubation at 50ºC for 10 minutes to dissolve the gel slice. One gel slice volume equivalent of isopropanol was added to the sample and was centrifuged (17,900g for 1 minute) with the provided QIAquick spin column to bind DNA into the embedded silicon membrane. The flow-through was discarded, and the DNA bound to the column was washed with buffer PE and centrifuged (17,900g for 1 minute) again. Subsequently, DNA was redissolved from the column with nuclease-free water and eluted into a clean microcentrifuge tube. DNA concentration and purity were quantified using a NanoDrop Spectrophotometer ND-1000 (Thermo Scientific).

Ligation was performed by incubation of DNA purified from PCR products and excised gels with the T4 ligase (M0202, NEB). This was performed by incubating

2µl of 10X T4 DNA Ligase buffer, 1µl of 200,000 units/ml T4 ligase, 50ng of vector DNA, insert DNA at a molar ratio of 3:1 and nuclease-free water to make the volume up to 20µl. The reaction was incubated for 16 hours at 4°C.The required mass of insert was calculated as follows:

$$\text{required mass of insert (g)} = \text{molar ratio} \times \text{mass of vector (g)} \times \frac{\text{insert length (kb)}}{\text{vector length (kb)}}$$

Transformation was performed with the TOP10 bacterial strain (C404010, Thermo Scientific). A vial of cells was thawed for transformation and 5µL of a ligation reaction was gently pipetted into the vial. Vials were incubated on ice for 30 minutes, followed by a heat shock at 42ºC in a pre-warmed water bath for 30 seconds. Vials were place immediately on ice and 250µL of SOC media was added. Vials were shaken at 37ºC for 1 hour at 225rpm in a shaking incubator. 20µL of the vial was transferred onto ampicillin LB-agar plates (for recipe see 2.1.1.14) and grown overnight to isolate transformant colonies. Individual bacterial clones were then grown in liquid culture with LB broth (for recipe see 2.1.1.13) (Media Lab, CIMR) supplemented with 100µg/ml ampicillin (10835242001, Sigma-Aldrich) for 16 hours at 37°C and 250rpm shaking in aerobic conditions.

The pWPT-VWF lentiviral plasmid was a kind gift from Dr Wilcox, Wisconsin USA. The single fragment assembly proceeded with double restriction digestion of the plasmid with MluI (R0198) and SalI (R0138) in NEBuffer 3.1 (B7203) (New England BioLabs). The two-fragment assembly proceeded with a sequential digest of BlpI (R0585) for 1hr at 37°C, followed by adjustment of the salt concentration to 100mM by addition of NaCl, and addition of SalI (R0138) with subsequent incubation for 1hr at 37°C. Gibson cloning was then performed as per manufacturer instructions with 2x Gibson Assembly Master Mix (E2611S, New England BioLabs).

Cloning steps and primers were designed on SnapGene v4.2.2 (GSL Biotech) which was also used to align sequencing data and produce plasmid maps. Sequencing was performed through capillary-read Sanger sequencing by Source Biosciences, UK.

2.2 Cell culture techniques

2.2.1 *Cell lines and storage*

All mammalian cell culture was performed under sterile conditions, in the absence of antibiotics and in standard humidified incubators kept at 37°C and 5% CO_2 normoxic atmosphere.

Cell line	Source	Media	Splitting	Other
HEK293T cells (human embryonic kidney)	American Tissue Culture Collection (ATCC)	Dulbecco's Modified Eagle Medium with GlutaMax-I (31966-021, Gibco), supplemented with 10% fetal bovine serum (FBS) (10270, Gibco).	1:20 every three days in T75 flasks using TrypLE (12563-029, Gibco) to generate a single cell suspension from the adherent cell layer	All experiments were performed while the cells were between passage 20 and 30.
HepG2 cells (human hepatocellular carcinoma)	American Tissue Culture Collection (ATCC)	Advanced Dulbecco's Modified Eagle Medium (12491-015, Gibco) supplemented with 10% FBS (10270, Gibco).	split 1:6 every seven days in T25 flasks using TrypLE (12563-029, Gibco) to generate a single cell suspension from the adherent cell layer.	All experiments were performed while the cells were between passages 10 and 20.
CHRF-288-11s	Katrin Voss (Witte *et al.*, 1986)	RPMI 1640 (A10491-01, Gibco) supplemented with 10% FBS	split 1:6 every three days	
BobC-iPSC	(Yusa *et al.*, 2011)	AE6 media is supplemented with fibroblast growth factor 2 (FGF2) 15ng/ml (R&D) and Human Activin A 15ng/ml	Every day	

		(Cambridge Stem Cell Institute)		
BobC-FoPMK	Derived from BobC-iPSC and transduction as per (Moreau *et al.*, 2016)	Serum-free GMP SCGM (20802-0500, CellGenix)	Monday, Weds, Friday	All experiments were performed between day 20-100 of forward programming

2.2.2 *Transfection*

Transfection of plasmid DNA was performed using TurboFect reagent (R0532, Thermo Scientific) as per manufacturer instructions. 1µg of plasmid DNA was diluted in 100µL of serum-free RPMI 1640 media (12633-012, Gibco), before being mixed with 2µL of TurboFect reagent and vortexed. Turbofect/DNA complexes were allowed to form for 15 minutes. HEK293T cells were seeded into a 6 well plate and the Turbofect/DNA mixture was introduced when the cells were at 80-90% confluency and gently rocked to spread evenly across the cells.

2.2.3 *Sample collection and cell lysis*

The collection of cell supernatants was performed 48 hours after transfection and aspirated from the 6 well plates. The cell layers were washed with phosphate-buffered saline (PBS) and detached using a 5-minute, 37°C incubation with TrypLE Select (12563-029, Gibco), washed by dilution with PBS (1:10), taken into a 15ml tube and centrifuged to collect the cell pellets after a 300g centrifugation for 5 minutes at r.t. The supernatants were aspirated, and the cells lysed in 300µL of either M-PER cell lysis buffer (78501, Thermo Fisher) with Pierce Protease Inhibitors (88666, Thermo Fisher) or TAP lysis buffer (2.1.1.4), without inhibitors by vortexing the mixture and incubating on ice for 5 minutes. This was then centrifuged at 14000g for 10 minutes to remove cell debris.

2.2.4 *Forward Programming of iPSCs to Megakaryocytes*

iPS cells with genomic modifications to contain GATA1, TAL1 and FLI1 under the control of a doxycycline-inducible promoter were used for forward programming. iBobC and iPBG3 cell lines were received from Dr Amanda Dalby. Forward programming is largely similar to as described previously in (Moreau *et al.*, 2016). Briefly, iPS cells were seeded onto 0.5µg/cm^2 vitronectin-coated plates (A14701, Life Technologies) as single cells and cultured with AE6 (500ml of DMEM/F12 [11330-032, Gibco], 7.5% $NaHCO_3$, 1x 99% LAA [A92902, Sigma-Aldrich], 1x ITS (10 µg/ml recombinant human insulin, 5.5 µg/ml human transferrin (substantially

iron-free), and 5 ng/ml sodium selenite) [I3146, Sigma-Aldrich]), FGF2 (15ng/ml, SRP4037, Sigma-Aldrich), Activin A (15ng/ml, A4941, Sigma-Aldrich) and 10mM Y-27632 (ROCK inhibitor) (SCM075, Sigma-Aldrich). After 24 hours, cells were washed with PBS and switched to mesoderm media (AE6 with FGF2 (20ng/ml) and BMP4 (10ng/ml, 314-BP-010, R&D Systems) and 1µg/ml doxycycline added. After 48 hours, the medium was changed for MK-supporting culture conditions as CellGRO-SCGM (20802-0500, CellGenix) supplemented with rhTPO (288-TP-025/CF, R&D) at 20ng/ml and rhSCF (PHC2111, Gibco) at 25ng/ml, maintaining 1µg/ml doxycycline for iBobC and 0.25µg/ml for iPBG3 in order to induce the transgenic expression of the three transcription factors instead of lentiviral vectors. and refreshing medium component every 3 days. For further details regarding the development and detailed phenotyping of forward-programmed lines, see Moreau *et al.*, 2016.

2.2.5 *Flow cytometry for cell culture monitoring*

CHRFs were analysed by flow cytometry by extracting 100µL from culture within a T75 flask, combined with 300µl of PBE Flow Buffer (2.1.1.3), 1µg/ml DAPI (D9542, Sigma-Aldrich) and count beads (335925, BD Biosciences). Data collection was performed on a Gallios Flow Cytometer (Beckman-Coulter) with gates set to exclude non-viable cells (DAPI+) and to measure GFP expression and count beads. Results were analysed with Kaluza Analysis v1.5 (Beckman Coulter).

Forward Programmed megakaryocytes were stained in the dark for 20mins with antibodies (anti-CD41a-H7, anti-CD42b-APC, anti-CD235a-PE) (including unstained, single stained and isotype controls) before being diluted in PBS, spun down at 300g for 5 minutes and resuspended in flow buffer and 1µg/ml DAPI and flow cytometry was performed as described above. Antibody details (catalogue numbers, source company, clone type) are available on page 73.

2.2.6 *Intracellular flow cytometry staining*

Wash steps for all cells were performed by adding 1ml of PBE flow buffer (2.1.1.3), spinning at 300g for 5mins and aspirating the supernatant. Wash steps for samples containing platelets were performed by adding 750ng/ml prostaglandin I2 (PGI_2) (P6188, Sigma) and 1ml of PBE flow buffer (2.1.1.3) before spinning down at 1500g and aspirating the flow buffer.

Firstly, samples were incubated with 1:50 (1 unit) of Zombie-Violet (423113, BioLegend) for 20mins followed by a wash step. Samples were then fixed with 4% PFA for 15mins in the dark at room temperature, followed by another wash step. Samples were permeabilised with Reagent B in Fix-and-perm kit (GAS002S5, Thermo) and incubated with primary antibodies (2.1.1.12) at the appropriate dilution for 20mins. After a wash step, samples were incubated with Reagent B again along with secondary antibodies (2.1.1.12) in the dark for 20mins. Samples underwent another wash step, followed by resuspension in PBE

flow buffer (2.1.1.3) and data was collected using the Gallios Flow Cytometer as described above (2.2.5).

2.2.7 *Lentiviral production and titration*

Lentiviruses were produced as described previously (Moreau *et al.*, 2016). Briefly, HEK293T cells were transfected (2.2.2) with the individual pWPT plasmid (12255, Addgene) containing the sequences of interest and co-transfected with packaging plasmids psPAX2 (12260, Addgene) and pMD2.G (12259, Addgene). Cells were washed after 24 hours and supernatants containing virus were collected at 48 hours and concentrated using Lenti-X Concentrator (631232, Takara Bio). One volume of supernatant was combined with three volumes of Lenti-X Concentrator and mixed by gentle inversion. The mixture was incubated at 4ºC for 30 minutes, and then centrifuged at 1500g for 45 minutes held at 4ºC. The resulting supernatant was removed, following careful resuspension of the pellet in 1/100th of the original volume in CellGro (20802-0500, CellGenix). qPCR titrations of lentiviruses were also performed as described previously by the lab in an MX3000P (Stratagene). Briefly, HCT116 cells transduced with various multiplicities of infection (MOIs) of GFP-bearing lentivirus was run on a flow cytometer and used as a control curve. Then all cell lysates from cells transduced with unknown titres of virus and GFP control virus were analysed by qPCR for HMBS (hydroxymethylbilane synthase, as a housekeeping gene present in the cells) and RRE (Rev-responsive element, to measure the presence of the vector), along with known dilutions of a qPCR lentivirus standard. Functional data from the flow cytometry was used to create a conversion curve between qPCR ratios of viral Rev-response element (RRE) to cellular hydroxymethylbilane synthase (HMBS) with GFP expression (in transduction units/ml). A Poisson distribution was used to model infection by the lentivirus and calculate the effective transduction units present in each viral sample.

2.2.8 *Transduction of cells with lentivirus*

Cells were counted, and 1x10^5 cells were resuspended in 300µl of media (2.2.1) in a 24 well plate, and the appropriate amount of lentivirus was added (with an MOI of between 2 and 10) carefully to transduce the cells along with protamine sulfate at a final concentration of 10µg/ml (P3369-10G, Sigma-Aldrich). Cells were washed in PBS after 24 hours, and the culture was scaled up over the next three splits into a 6 well plate (and in the case for CHRFs but not for FoP-MKs, T25 flask and eventually into T75 flasks).

2.3 Protein experiments

2.3.1 *Immunofluorescence*

Fibrinogen (F3879-1G, Sigma) (200µg/ml) was adsorbed onto glass cover slips for 1hr at r.t. Cells (counted to 1x10^6) incubated onto these coated cover slips for 1hr were fixed with 1% formaldehyde at 37°C for 10 mins, and then washed in

PBS. Permeabilisation buffer (page 72) was added and cover slips were incubated at room temperature for 1hr, followed by primary antibody buffer (page 73) for 1hr at room temperature, and then washed three times in PBS for five minutes each. They were then incubated with secondary antibody buffer (1% BSA, 1:1000 secondary antibody, goat anti-rabbit-Alexa488) for 1hr at room temperature in the dark and washed again 3x (5 mins each) with PBS in the dark. The first wash step included 1µg/ml DAPI (D9542, Sigma-Aldrich) to stain nuclei. These were fixed onto slides with ProLong Diamond Antifade Mountant (P36961, Invitrogen).

2.3.2 *Western Blotting*

Protein concentrations were analysed via a BCA assay (23225, Thermo Scientific). BSA standards were made through diluting the provided BSA stocks, to 2000, 1500, 1000, 750, 500, 250, 125, 25 and 0µg/ml. BCA Working reagent was prepared by mixing 50 parts of the provided reagent A with 1 part of the provided reagent B. 25µL of each sample or standard was pipetted onto a microplate, along with 200µl of working reagent. The plate was covered and left in the dark at 37ºC for 30mins. Colour changes were measured at 562nm with a SpectraMax M5 spectrophotometer, and the standard curve was used to interpolate protein concentrations of the samples.

Samples were then normalised for protein concentration and were denatured using a reducing agent (NP0004, Invitrogen) and sample buffer (NP0007, Invitrogen) by incubating this mixture at 90ºC for 10 minutes. Samples loaded into a 4-12% Bis-Tris gel (NP0321BOX, Life Technologies) were run at 180V for 1hr with 2.5µl of a MagicMark XP Protein Ladder (LC5602, Thermo Scientific) with a running buffer containing 50ml of 20x MOPS SDS Running Buffer (NP0001, Life Technologies), 1L of dH_2O and 500µL of antioxidants (NP0005, Life Technologies). Samples were then wet-transferred onto nitrocellulose membrane at 30V for 1hr, with transfer buffer containing 50ml of 20x Transfer Buffer (NP0006, Life Technologies), 100ml of methanol, 1ml of anti-oxidants (NP0005, Life Technologies) and 850ml of dH_2O.

Blocking was performed with 5% skimmed milk (70166-500G, Sigma-Aldrich) in TBS-Tween (for recipe see 2.1.1.15) (T9039-10PAK, Sigma-Aldrich) for 2hrs, followed by primary antibody in 5% skimmed milk (for concentrations of antibodies, see 2.1.1.12) overnight at 4°C on a plate rocker. TBS-Tween (for recipe see 2.1.1.15) (T9039-10PAK, Sigma-Aldrich) was then used for washing (3x10mins). The appropriate secondary antibody was incubated (see section 2.1.1.15). Imaging was performed through use of ECL Prime reagent (RPN2232, Amersham) by adding a 1:1 mixture of the provided reagent A (luminol) and reagent B (peroxide) at r.t. in the dark for 5 minutes followed by imaging using a LICOR Odyssey Fc Imaging System.

After imaging, for additional antibody stainings membranes were stripped with stripping buffer (46430, Thermo Scientific) for 15mins at room temperature. Membranes were then reblocked, stained and developed with appropriate follow-up antibodies as described in the previous paragraph.

2.3.3 *ELISA*

A Factor VII sandwich ELISA (ab190810, Abcam) was performed. Samples and standards were incubated with an antibody cocktail solution (supplied with kit) at room temperature for 1hr in a plate shaker at 400rpm. TMB Substrate (supplied with kit) was added and incubated for 10mins in the dark, before the reaction was stopped with 0.16M sulphuric acid. Microplates were read using a SpectraMax M5 (Molecular Devices) at 450nm and data was analysed with SoftMax Pro v7.0.3.

2.3.4 *Chromogenic Factor VII Assay*

A chromogenic factor VII assay (ab108830, Abcam) was performed. Monoclonal FVII antibody (ab151543) was adsorbed to a 96 well Nunc MaxiSorb microplate by incubating 100uL of 0.1M carbonate/bicarbonate buffer (pH 9.6) with a rabbit monoclonal anti-FVII antibody (described in 2.1.1.15) per well. Samples and standards were allowed to bind on a microplate (either the one provided with the kit or the one prepared in the lab) at room temperature for 1hr, and then the plate was washed 5x in ELISA wash buffer (page 72). Tissue Factor, chromogenic Factor Xa substrate and Factor X (all supplied with kit) were added, and the plate was incubated at 37°C for 30mins. The rate of colour change over time was measured at 405nm every minute for 60 minutes with plate shaking before each reading. Data was analysed with SoftMax Pro v7.0.3. NovoSeven (*eptacog alfa*) (#00169-7201-01, Novo Nordisk) was used as a positive control at the indicated serial dilutions.

2.3.5 *Thrombin generation assay*

The thrombin generation assay (5006010, Technoclone) was performed as follows. This assay was performed on black immunostandard 96 well plates for fluorescence assays (475515, Thermo Fisher). A thrombin calibration curve was generated by adding a 1:2, 1:4, 1:20 and 1:200 dilution of the calibrator in duplicate. 40µL of each of these samples was added to the 96 well plate, followed by 50µL of the TGA substrate (5006235, Technoclone). Fluorescence was measured for 10 minutes in 30 second intervals on a SpectraMax M5 pre-warmed to 37ºC with the protocol files provided with the kit. This was then exported onto the Excel spreadsheet given with the kit in order to calculate the concentration of thrombin in the TGA substrate. Platelet samples were measured by adding 40µL of the samples in duplicate to the 96 well plate, followed by 10µL of the RC Low buffer (5006212, Technoclone) provided with the kit. Finally, 50µL of TGA substrate was added before immediately placing the plate into a SpectraMax M5 pre-warmed to 37ºC using the given protocol files. Analysis was performed

according to the Excel spreadsheet provided by the manufacturer to measure all relevant parameters of the thrombin generation curve.

2.3.6 *Whole blood sampling and platelet preparation*

Blood was drawn first using an EDTA vacutainer which was then discarded, and then, following this, without a tourniquet over sodium citate by vacutainers with full written informed consent given by the donor under local ethics approval (Blood donor ethics no: HBREC.2018.13).

An additional 10% acid citrate dextrose (ACD, Sigma) was added to the blood before centrifugation at 100g at room temperature (r.t.) for 20 mins. The platelet rich plasma (PRP) layer was collected and supplemented with 750ng/ml PGI_2 (P6188, Sigma) before centrifugation at 1400g at r.t. for 10mins. The supernatant was removed and the platelet pellet carefully resuspended in Tyrode's buffer (page 71) supplemented with 10% ACD and 750ng/ml PGI_2 (P6188, Sigma). Finally, platelets were centrifuged at 1400g at r.t. for 10mins and platelets carefully resuspended in a Tyrode's buffer to the indicated concentration. Platelet concentrations were calculated by diluting 10µl of platelets in 10ml of ISOTON solution (12754878, Fisher Scientific), and then measured using a Z2 Coulter Counter (6605700, Beckman-Coulter).

2.3.7 *Endocytosis of rFVIIa in MKs and platelets*

Platelets were first prepared as in section 2.3.6. MKs and platelets were incubated with 0.01µg/µl rFVIIa for 2 hours at room temperature to allow endocytosis to take place. Platelet samples were then inhibited with 750ng/ml PGI_2 (P6188, Sigma), washed with Tyrode's and centrifuged (1400g for 10mins), followed by resuspension in Tyrodes buffer to wash off any unabsorbed rFVIIa. MKs were washed with PBE, spun down at 300g, and resuspended in PBE. These samples were then used for further analysis in intracellular flow, releasate assay and immunofluorescence staining.

2.3.8 *Animal housing*

Mice were housed in pathogen free conditions. Animals were kept in a standard temperature- and humidity-controlled environment and had free access to water at Central Biomedical Services (Cambridge, UK) and cared for by trained staff. This research has been regulated under the Animals (Scientific Procedures) Act 1986 Amendment Regulations 2012 following ethical review by the University of Cambridge Animal Welfare and Ethical Review Body (AWERB). Experiments were performed under Project Licence P667BD734 by trained, Personal Licence (PIL) holders.

2.3.9 *Tail vein bleed*

Peripheral blood samples were withdrawn from the tail vein (to a maximum volume of 20 µL) to measure full blood counts. Mice were heated for 5mins at 30ºC in a hot box. They were then transferred into a murine restraint stand. A 27G needle (BD Microlance 3 needles @ 27G x ½, cat no.:#300635, BD) was used to puncture a superficial vessel, and blood was collected into EDTA coated capillary tubes (SARSTEDT Microvette CB 300 K2E, ref.: 16.444). Pressure was applied to ensure haemostasis, before mice were returned to cages. Blood samples were then analysed using a Vet abc Plus+(scil) automatic haemocytometer.

2.3.10 *IVC bleed*

Mice were terminated by a rising CO2 concentration. They were then moved onto a corkboard where they were held in place and a midline incision was made into the peritoneum in order to isolate the inferior vena cava (IVC). 1ml of blood was withdrawn from the IVC into either 100µL of ACD (as prepared in 2.1.1.6) or 0.1M EDTA to ensure anticoagulation. The right femoral artery was transected to ensure exsanguination and completion of the schedule 1 protocol.

2.3.11 *Antibody depletion*

Mice were injected with 0.6µg/g body weight anti-CD42b (#R300, Emfret Analytics) in PBS intraperitoneally. Mice were bled from the tail vein at necessary timepoints into EDTA-coated capillary tubes (Microvette CB300, Sarstedt) to confirm depletion prior to tail transection assay. Platelet counts were determined using a Vet abc Plus+(scil) automatic haemocytometer. On one occasion, mice were followed up at 1, 4, 24, 48, 96 and 120 hours post depletion in order to assess the platelet depletion window.

2.3.12 *Tail transection assay*

Immunodeficient NRG/J mice were depleted specifically of their platelets using 0.6µg/g BW anti-CD42b antibody (Emfret Analytics, Germany) a minimum of one hour prior to a tail vein bleed both to confirm depletion and give an accurate haemoglobin level. Following confirmation of depletion (by tail vein bleed as in 2.3.9), mice were injected intraperitoneally using a mixture of ketamine (100mg/kg) and xylazine (10mg/kg) and transferred to a chamber set to 38degrees for 5minutes. Mice were then immediately intravenously (IV) injected in a tail vein with either Tyrode's buffer, washed donor or *in vitro* bioreactor derived platelets. Immediately following IV injection, mouse tails were transected 2mm from the tail tip, and placed into 40ml warmed phosphate buffered saline. Every 4 mins tails were moved into fresh 40ml of saline for a total of 20mins. Following a maximum 20mins of bleeding time, mice were euthanised and blood was collected from the inferior vena cava into 100µl of 0.5M EDTA.

2.3.13 *Haemoglobin assay*

The haemoglobin assay was based on the modified Triton-X/NaOH method from the QuantiChrom Haemoglobin Assay Kit (#DIHB-250, BioAssay Systems). For the standards, 50µL water (blank) and 50µL of calibrator were added in duplicate to wells of a 96 well plate. This gives a linear response in the range of 0-200mg/dl of haemoglobin. 50µL of each unknown sample was added in duplicate to the 96 well plate. 200µL of the AHD-575 reagent was added to all wells, this was incubated for 5 mins at room temperature to allow for the colour change, and then read on a plate reader at 400nm. The diluted calibrator is equivalent to 100mg/dL Hb. From the raw values, a Hb concentration was obtained using the formula:

$$[Hb]_{sample} = \frac{OD_{sample} - OD_{blank}}{OD_{calibrator} - OD_{blank}} \times 100$$

From the Hb concentration values, it is possible to infer the volume of blood loss from an animal with the following formula:

$$\text{Blood loss} = \frac{[Hb]_{falcon\ tube} \times Volume_{falcon\ tube}}{[Hb]_{tail\ vein\ bleed}}$$

Post platelet depletion haemoglobin levels were analysed on a haematology analyser (scil Vet abc Plus+, scil animal care company) as a reference baseline haemoglobin level for each individual mouse.

2.3.14 *Mouse MK isolation and culture*

Mouse bone marrow (BM) cells were prepared by extracting femoral and tibial bones from mice, with the muscle stripped and bone marrow exposed through fracture of the epiphysis. Media (DMEM containing 10% FBS and 5% pen-strep) was used to flush out bone marrow with a syringe. Extracted marrow was collected in 50ml falcon tubes, which were subsequently centrifuged for 5mins at 200g held at 4ºC and supernatant aspirated. The cell pellets were resuspended in 6ml ACK buffer (2.1.1.12) per mouse, and filtered through a 70µm filter into a fresh falcon tube, followed by further centrifugation at 200g for 5mins held at 4ºC. Cells were resuspended and subsequently cultured in mouse MK media consisting of 5ml CellGro per mouse (Cellgenix, Freiburg, Germany) with 50 ng/mL recombinant murine thrombopoietin (TPO; PeproTech) at 37°C under 5% CO2 for 5 days.

Mature MKs were purified using a 1.5%/3% bovine serum albumin (BSA) gradient. Cells were pooled into a 15ml falcon, washed with PBS and centrifuged at 120g for 5 mins held at r.t. BSA gradients were prepared by diluting 30% BSA 1:10 for a 3% gradient and 1:20 for a 1.5% gradient. Supernatants were poured off and cells resuspended in 4ml of PBS. Cells were layered on top of the BSA gradient and left to stand for 45 mins. The top 10ml was then transferred (or

discarded if this was the second BSA gradient for this culture) to a 15ml falcon, centrifuged at 200g for 5mins, the supernatant was discarded and cells were resuspended in 5ml of MK media (CellGro supplemented with TPO as described above). Cells were then incubated at 37ºC for a further three days. For the remaining 2ml of the BSA gradient, 20ml of PBS was added, centrifuged at 120g for 5mins, the supernatant was poured off and the pellet was resuspended in the desired concentration of MK media.

2.3.15 *Releasate assays*

Releasate assays were performed by incubating donor platelets (prepared as in 2.3.6) or PLPs with and without agonist (1 unit of thrombin/reaction or 10μM TRAP6/10μM MeS-ADP) for 30 minutes at 37ºC. PGI_2 (P6188, Sigma) was added at 750ng/ml to inhibit any unactivated platelets, samples were spun down at 1400g for 10mins, and the supernatant was used for other assays.

2.3.16 *Genomic sequencing and analysis*

Genomic DNA was isolated (DNeasy kit, Qiagen) from each parental cell line, all clones and subclones and used for whole-genome sequencing using the Illumina HiSeqX10 platform. Fragments of 150bp paired-end trimmed sequencing reads were aligned to the GRCh37 reference genome using BWA. Marking of duplicates and their removal took place using biobambam, and mutations were then called using CaVEMaN. All somatic mutations were then filtered through standardised quality control filters (Alexandrov *et al.*, 2013), filtering for Mean Alignment Score (ASMD) of reads greater than 130, and no clipped bases were considered, identifying SNVs. Annotated SNPs from the general population taken from dbSNP were then removed as well as any variants with an allelic frequency less than 0.2. For indels, the PINDEL algorithm was used to call these variants, and only those with a standard filtering score of >250 and an allelic frequency of >0.2 were considered.

3 Genetically engineering a FVII that can self-target to α–granules in a FOP-MK culture system

3.1 Introduction

3.1.1 *Forward programming as a technique for high purity megakaryocyte differentiation from stem cells*

Although there exist many techniques to differentiate megakaryocytes from iPSCs, in this project the forward-programming methodology was adopted. With an average yield of 200,000 MKs per input iPSC, this is much higher than had been previously reported from directed differentiation, reported to be on average 26.3 and 11.7 times more mature MKs compared to directed differentiation from two different cell lines (Moreau *et al.*, 2016). The purity of the culture was also far greater on average, the percentage of cells that became CD41+/CD42+ was 97.7±0.8% for the forward-programming technique compared to 21.3±2.9%. This suggests that it is possible to combine the benefits of the large numbers of MKs from the immortalisation technique but without similar safety risks. This high efficiency of differentiation combined with the serum and stromal cell free culture, minimal cell manipulation and low cytokine requirements established this technology as a promising platform for both basic biology and clinical applications. In a clinical context, the long-term culture expansion allows a cumulative production of $2x10^{11}$ MKs releasing (without the use of bioreactor technology) around $1x10^{12}$ platelets, the equivalent of 3 transfusion units, from only $1x10^{6}$ iPSCs.

In culture, these mature FoPMKs produced proplatelet structures containing P-selectin-positive α–granules. Electron microscopy of the platelets produced from these FoPMKs compared to those produced from cbMKs showed that both contained the typical platelet ultrastructure, including a high α–granule content. *In vitro* derived platelets from FoPMKs showed surface expression of the main thrombocyte receptors, normal mean volume on a blood analyzer and an increased immature platelet fraction compared to donor blood. Platelet survival was assayed in an *in vivo* NSG mouse model; the FoPMK platelets were detectable for several hours, while showing a shorter half-life than primary donor platelets. Finally, functionally the produced platelet-like particles (PLPs) appear able to be able to react to thrombin stimulation and take part in clot formation *in vitro*, with visible sequential rolling, binding, and spreading.

3.1.2 *Preliminary work on targeting proteins to α-granules (performed by Dr Annett Mueller)*

Previously, FVIII has been targeted to the α-granules of canine megakaryocytes as a gene therapy for haemophilia A through fusion with the vWF signal peptide

and D2 domain (SPD2), a protein normally present in α-granules (Du *et al.*, 2013). vWF is a protein normally expressed in α-granules, and so its signalling domain was chosen to direct other proteins to be trafficked in a similar way. The ability to target proteins into the α-granules of forward-programmed megakaryocytes has been demonstrated by Dr Annett Mueller through the fusion of vWF SPD2 to GFP; immunohistochemistry (IHC) data shows good co-localisation of the GFP with a marker of α-granules (Figure 3.1). Both constructs were under control of a megakaryocyte-specific ITGA2B promoter. The cells are also stained for thrombospondin, a marker for α-granules. Figure 3.1A shows transduction with a lentivirus containing this ITGA2B promoter fused to eGFP without any targeting domain, and this eGFP is mostly located within the cytoplasm. Figure 3.1B shows transduction of the same construct, with a vWF-SPD2 domain from Du and colleagues inserted between the ITGA2B promoter and the eGFP, demonstrating co-localisation of GFP with thrombospondin, suggesting that the protein has been targeted to the α-granules.

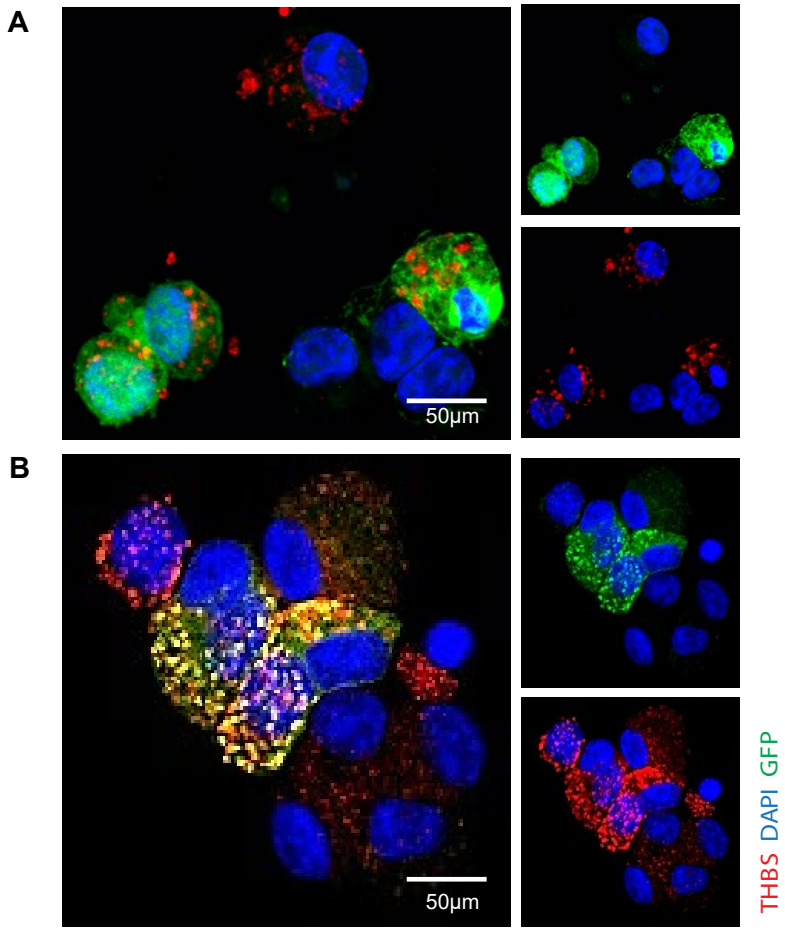

Figure 3.1. *Fluorescence microscopy data taken from forward-programmed megakaryocytes transduced with a construct containing the ITGA2B promoter fused to either (A) only eGFP or (B) the SPD2 domain of vWF fused to eGFP (data generated by Dr Annett Mueller). THBS – thrombospondin (red, ab1823, secondary A21244).*

3.1.3 *Previous work on a self-activating FVII*

Previously, the zymogen Factor VII (FVII) cDNA coding sequence had been cloned from adult liver tissue by TA cloning into the plasmid pCRII by Dr Annett Mueller. This could be used to produce the zymogen form of Factor VII (FVII), but for the purpose of loading the granules to be used in a similar way to rFVIIa, the factor VII needed to be produced and stored in an activated form into the platelet α-granules.

The zymogen form is converted physiologically to the active form in the blood by cleavage of a peptide bond between Arg152-Ile153 (Chaing *et al.*, 1994), located between the light and heavy chains, after exposure to tissue factor. In one study, this cleavage site was disrupted by the insertion of a specific binding site (RKRRKR) for the intracellular protease furin to result in a constitutively activated FVIIa (Margaritis *et al.*, 2004). This modified FVII sequence has previously been expressed long-term as a gene therapy *in vivo* in a mouse model to elevate plasma rFVIIa levels (Aljamali *et al.*, 2008).

3.1.4 *Thrombin cleavage sequence for separation of FVII from vWF*

To avoid unwanted effects on FVII enzymatic function and to prevent it from being tethered to the activated platelet by the vWF domain, the separation of FVII from the vWF peptide upon its release from the α-granules at the site of injury would be required (Figure 3.2).

Thrombin was chosen as a suitable enzyme to cleave off the activated factor VII from vWF, as it concentrates in areas of bleeding thus allowing an accurate time and space control of protein cleavage specifically at sites of injury. The thrombin cleavage sequence (LTPRGWRL) was chosen from a study on the optimal cleavage sequence for human thrombin using phage display technology (Gallwitz *et al.*, 2012). This was then codon-optimised for *H. sapiens* to ensure maximal protein translation using a tool and codon table available online (Nakamura, Gojobori and Ikemura, 2000; Stothard, 2000) and integrated into a PCR primer. This was specifically chosen due to being based around human thrombin instead of the commonly used sequence (LVPRGS), based on bovine thrombin (Waugh, 2011).

3.1.5 *Assays to measure the functional activity of Factor VIIa*

Specific assays to measure the activity of FVIIa activity exist in the literature, notably a chromogenic FVII assay (Avvisati *et al.*, 1980). This involves the immobilisation of FVII from a sample on a plate with an antibody similar to an ELISA, and then uses the addition of Factor X as a substrate for Factor VII, and

the addition of a chromogenic substrate for Factor Xa that can be read on a plate reader to give an enzyme kinetics readout.

Other clotting assays that can be performed in vitro include the thrombin generation assay (TGA). There is somewhat of a gap between the aPTT and PTT (that measure ex vivo coagulation) and in vivo coagulation, which involves an interplay between the coagulation cascade and platelets; the TGA was developed to fill this gap. Coagulation of the test sample (either platelet poor or platelet-rich plasma) is activated by a small amount of tissue factor and phospholipids, and the reaction of thrombin generation is measured continuously through the means of a thrombin-specific fluorogenic substrate (Tripodi, 2016). As such, several parameters can be measured of the coagulation reaction at once, including the lag time between stimulation with tissue factor and thrombin spike, the peak thrombin generation, the area under the curve representing the total thrombin generation and the rate of increase of thrombin generation (the velocity index). Many of these parameters have correlations to a hyper- or hypo- coagulable state in patients (van Veen, Gatt and Makris, 2008).

In recent years, microfluidic devices have become popular for measuring coagulation with very small samples. For example, the in vitro thrombus under flow (IVTUF) assay is able to measure incorporation of differentially labelled platelet samples and assess their interaction with a collagen-coated substrate while under flow, attempting to recapitulate the *in vivo* environment more closely than traditional assays (Provenzale *et al.*, 2019). Other assays using microscopic pillars have been used (‘NanoPosts’) to measure the contractile force of individual platelets which may change after exposure to a procoagulant environment (Feghhi *et al.*, 2016).

3.2 Aims

3.2.1 *Cloning strategy*

The aims for modifying the FVII sequence were to (1) ensure the FVII would be self-activating without the need for tissue factor, (2) to be directed to the α-granules by fusion with the vWF SPD2 domain and (3) to be able to cleave off this domain in areas of bleeding through the insertion of a thrombin cleavage site (summarised in Figure 3.2). Overlapping-extension PCR was used to amplify the light and heavy chains independently containing the furin cleavage sequence in the amplification primers (Figure 3.3A) before being joined back together. A further PCR reaction would be used to extend this combined product to contain a thrombin cleavage site (Figure 3.3B) (vWF-F7TF, containing the **vWF** domain fused to **FVII** modified with a **t**hrombin and **f**urin site).

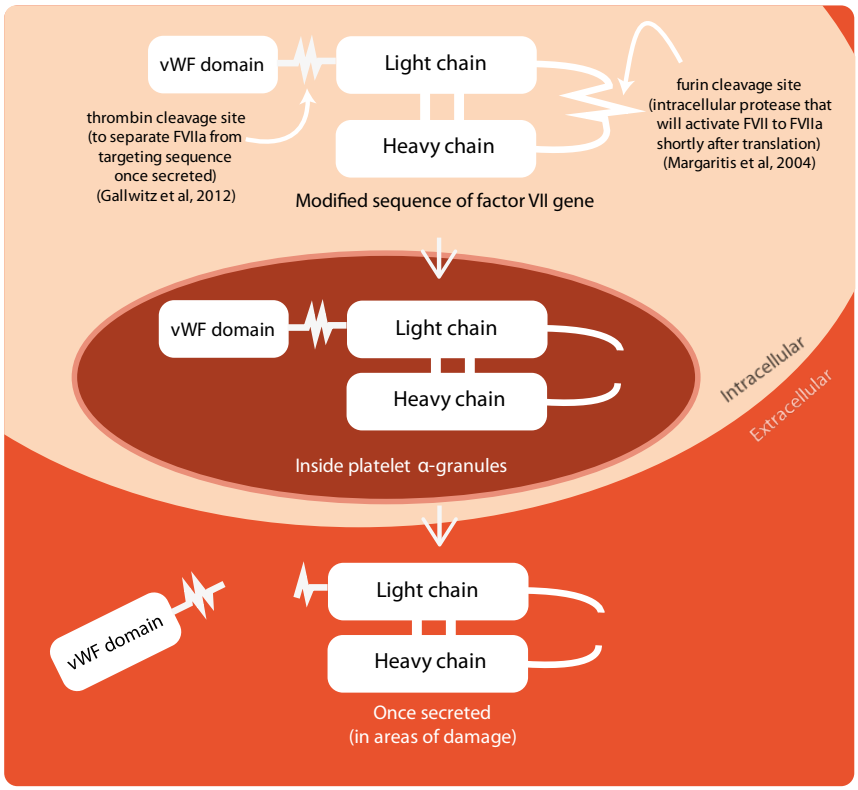

Figure 3.2. *Schematic of the intended design of the modified FVII sequence in FoP-MKs.*

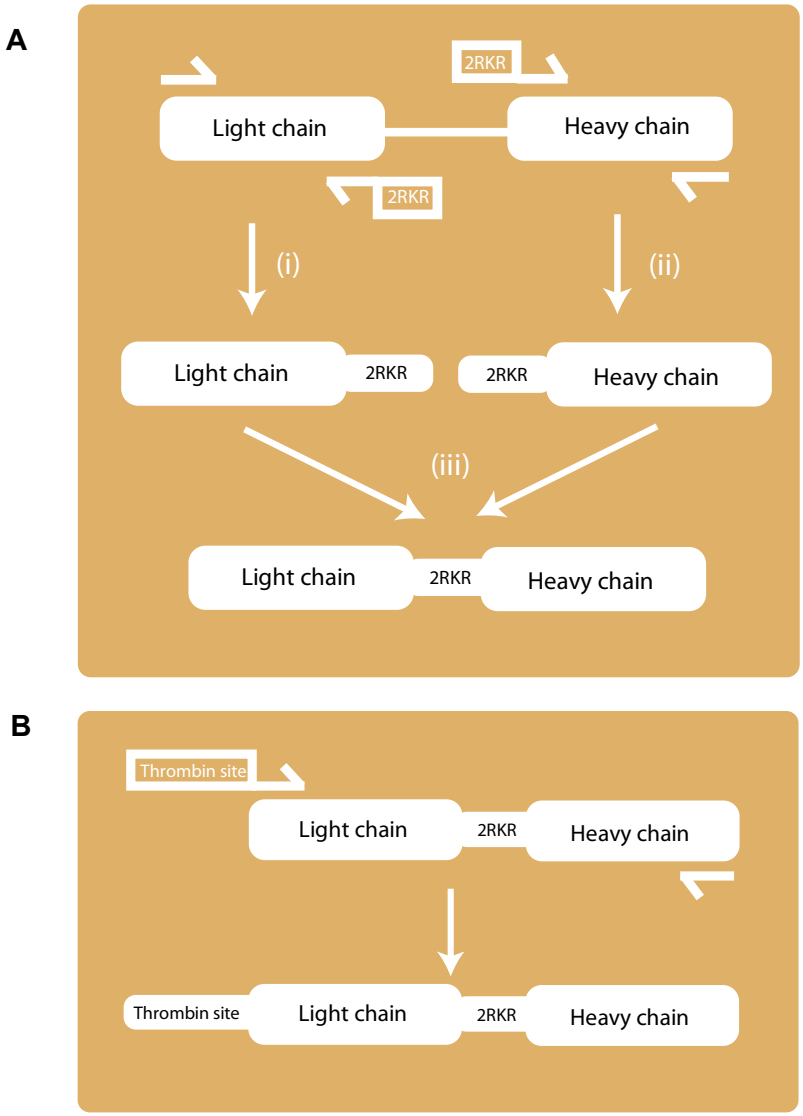

Figure 3.3. *Schematic of the overlaying-extension PCR strategy used to* ***(A)*** *insert a 2RKR (furin cleavage sequence) between the light and heavy chains of Factor VII, followed by* ***(B)*** *a thrombin cleavage site before the light chain of FVII.*

3.2.2 *Structural assays in transduced CHRFs and FoPMKs*

Next, lentivirus containing the generated construct was transduced into a megakaryoblast cell line to discover a suitable antibody, confirm successful expression. Assays were established such as intracellular flow cytometry, ELISA, Western blot. The lentivirus was then transduced into FoPMKs and the same assays were repeated to confirm the successful expression of the vWF-F7TF fusion sequence. Immunofluorescence was then used to examine the localisation of the fusion protein and compare this to several α-granule markers.

3.2.3 *Functional assays for FVII in FoPMKs and subsequent platelets*

Next, assays were performed to measure the function of this modified fusion protein. The furin and thrombin cleavage sites were experimentally tested through addition of exogenous enzyme and analysis by Western blot. A chromogenic enzymatic assay was also performed on the lysates of these transduced MKs. Platelets produced from these MKs were collected and also analysed for the presence of FVII by intracellular flow cytometry, before being analysed by a thrombin generation assay to compare their function to platelets from untransduced FoPMKs and human donor platelets.

3.3 A furin cleavage site was inserted between the light and heavy chains by overlapping-extension PCR

Replacement of the normal FVII activation cleavage site with a furin cleavage site was performed through overlapping-extension PCR. Primers were designed for the heavy and light chain separately to amplify out each chain, while adding the sequence with the furin cleavage sequence (RKRRKR) in their nucleic acid 5' and 3' ends respectively (details in section 2.1.3 for the primers LC_FO, LC_2RKR_RE, 2RKR_HC_FO, HC_RE). BamHI and NotI restriction enzyme sites were also added to the primers such that they could allow for later restriction cloning before the light chain and after the heavy chain sequence. The resulting sequence containing the furin sequence is labelled F7F.

The plasmid containing zymogen FVII was used as a template to perform the independent preparative PCRs for the light and heavy chains so that they could then be combined into one sequence (Figure 3.3). The amplification of the heavy chain required further optimisation when standard buffer did not allow efficient amplification of the heavy chain (Figure 3.4A) – the polymerase was switched to a Platinum Taq, the buffer was changed to a HF buffer and a temperature gradient was used (Figure 3.4B). The use of a HF buffer or Platinum Taq was sufficient to amplify this heavy chain, and the results from the HF buffer were subsequently used in an overlapping-extension PCR reaction to join them together (Figure 3.4C). The final PCR products were sequenced to confirm their integrity to the original template; alignment was successful and no frameshifts or point mutations were observed (Figure 3.4D).

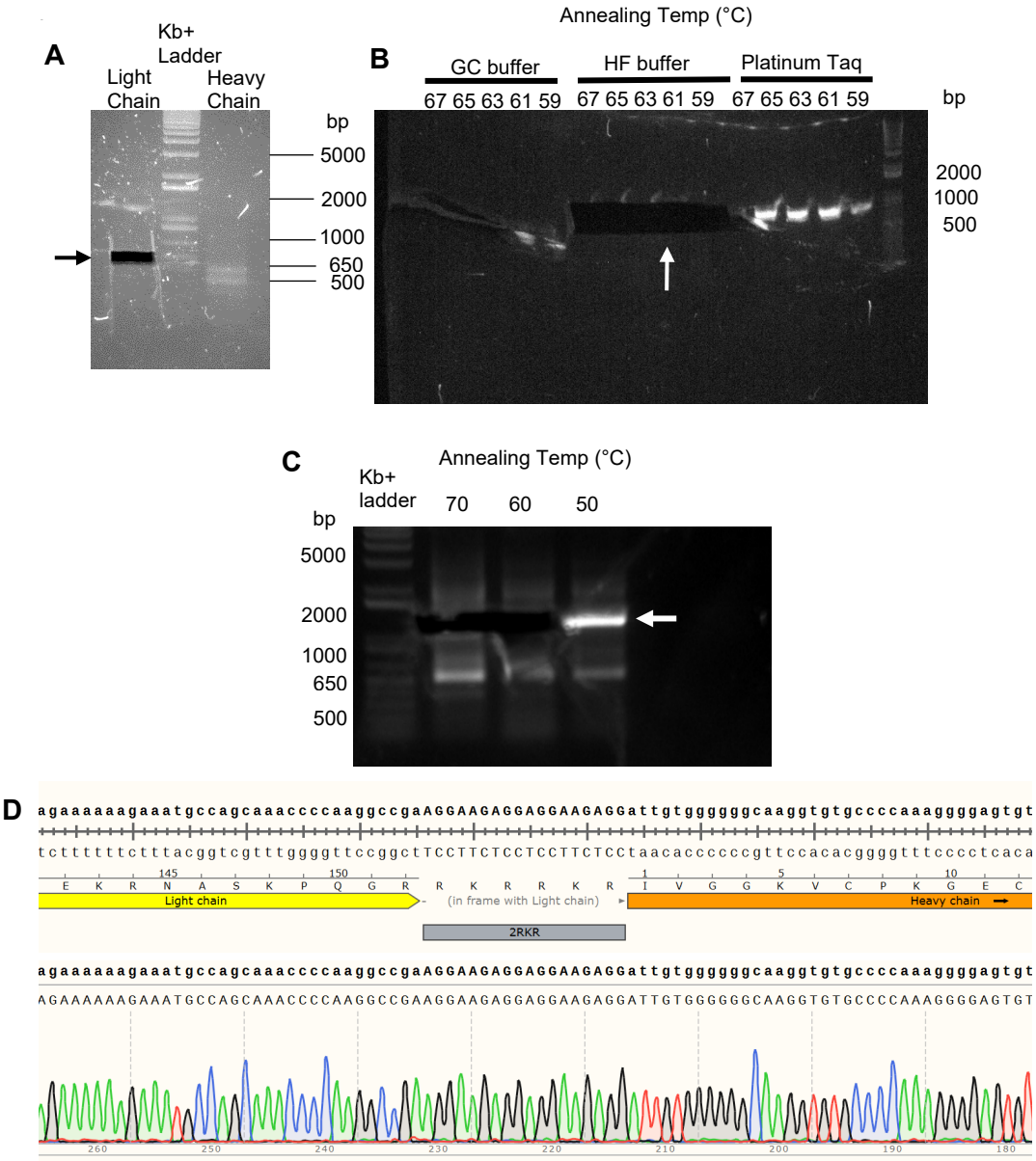

Figure 3.4. *Amplification of light and heavy chain to insert furin cleavage sequence from template Factor VII cloned out of primary adult liver cDNA.* ***(A)*** *Agarose gel (1%) was run after the PCR reaction to amplify the light and heavy chains from the template, using GC buffer. Arrow indicates the light chain extracted for further cloning.* ***(B)*** *Agarose gel (1%) used to optimise the annealing temperature and buffer conditions Bands seen in the GC buffer are artefacts from handling the gel. Indicated is a row of bands extracted for further cloning.* ***(C)*** *Agarose gel (1%) after performing the final PCR overlaying-extension reaction combining the products from (A) and (B), under three different annealing temperatures. Bands from two conditions were excised (indicated) and DNA was extracted for further cloning.* ***(D)*** *Sanger sequencing confirmed the insertion of a sequence encoding for the furin cleavage site.*

3.4 Insertion of a thrombin cleavage site by PCR

The F7TF sequence was obtained by PCR using the F7F sequence as a template and a forward primer containing this thrombin cleavage site (details in section 2.1.3 for the primers Thrombin_LC_FO and HC_RE). The result was run on a gel to separate the different DNA sequences present in the reaction, the expected size band for F7TF extracted and sent for sequencing to confirm the insertion of the thrombin cleavage sequence (Figure 3.5). The yellow box represents an error in the base calling algorithm, and the chromatogram below shows the missing base is likely a C, corresponding with the engineered sequence, confirming there were no unexpected mutations in the sequence.

Figure 3.5. *Sequencing was used to confirm the insertion of the thrombin cleavage sequence before the light chain of FVII.*

3.5 Gibson assembly for cloning into pWPT-VWF

Next a plasmid was created using a vector backbone capable of generating lentiviruses, and to transduce cell lines resistant to classical transfection (e.g. forward-programmed megakaryocytes) and establish stable clones. A construct from the David Wilcox group was chosen (Du *et al.*, 2013) containing a CD41 promoter fragment to restrict expression to megakaryocytes and the SPD2 domain from vWF to target proteins to α-granules of megakaryocytes and platelets (Figure 3.6). As a control, a version of the plasmid without the vWF targeting sequence would be cloned as well.

The cloning for these constructs was performed using the Gibson assembly method of utilising overlapping PCR primers (Gibson *et al.*, 2009). Insertion of the F7TF sequence fused to the vWF α-granule targeting (GT) sequence was a one-fragment insertion (resulting in the fusion sequence vWF-F7TF) (Figure 3.7A and

Figure 3.7B). For the cloning of a construct without the GT sequence, there were no easily accessible restriction sites to extract this targeting sequence without also removing part of the ITGA2B promoter fragment so this was performed using a two-fragment assembly, where the part of the promoter that would be excised was amplified by PCR and assembled back in to the plasmid alongside F7TF (Figure 3.7C and Figure 3.7D).

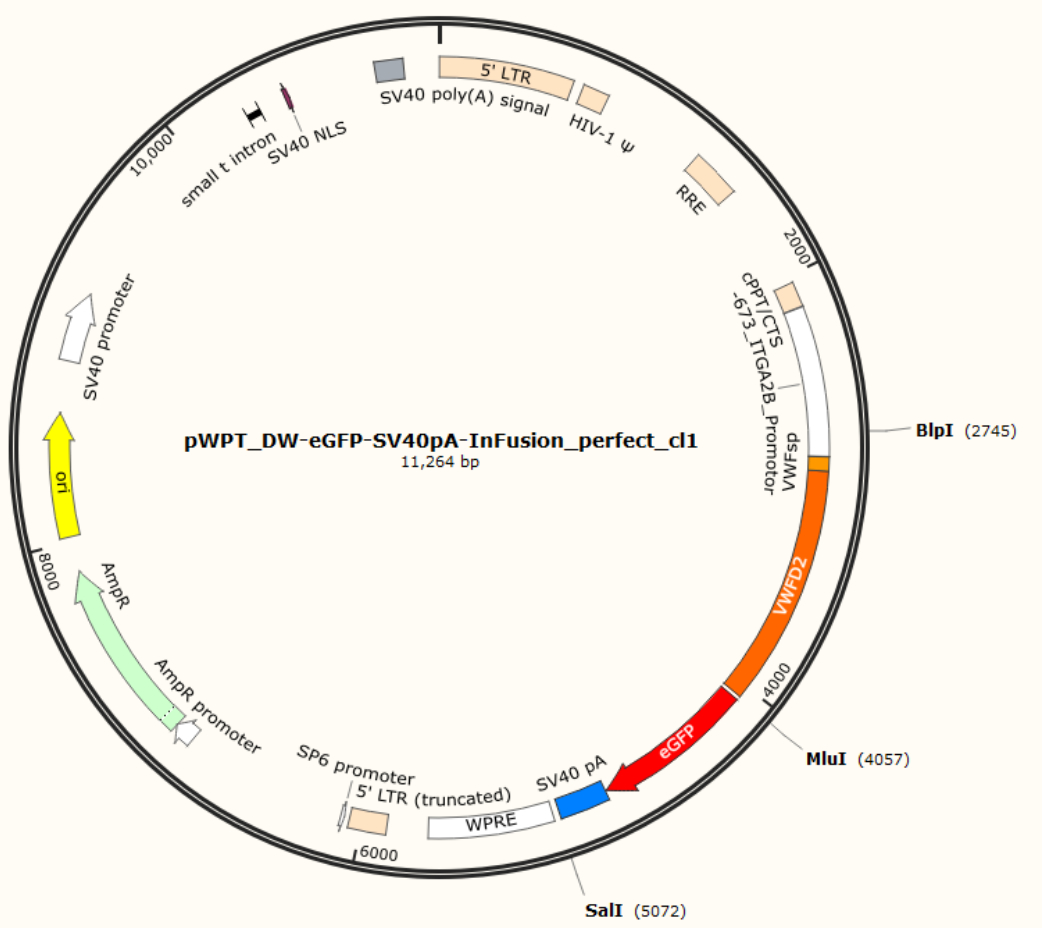

Figure 3.6. *The unmodified pWPT plasmid with the VWF targeting sequence attached to eGFP under control of a megakaryocyte-specific promoter (CD41, or ITGA2B) (Du et al., 2013) with the three different unique restriction sites highlighted.*

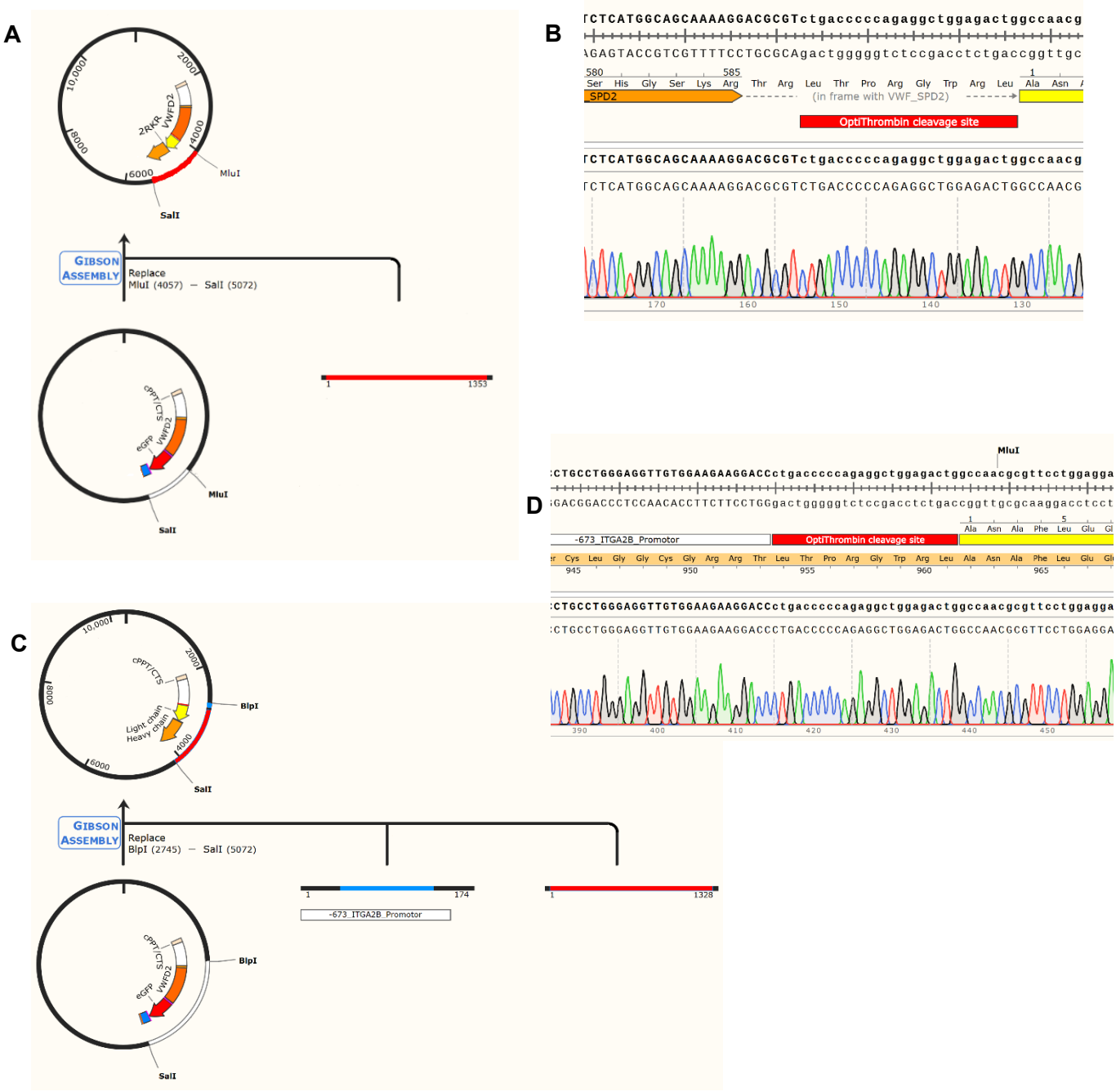

Figure 3.7. *The cloning strategy for inserting modified Factor VII into a pWPT lentiviral plasmid using Gibson assembly.* ***(A)*** *Insertion of the F7TF sequence fused to the vWF via a simple one-fragment assembly* ***(B)*** *Sanger sequencing chromatogram showing the insertion of F7TF into the pWPT backbone after the vWF domain.* ***(C)*** *Insertion of the F7TF sequence without the vWF sequence via a two-fragment assembly.* ***(D)*** *Sanger sequencing chromatogram showing the insertion of F7TF into the pWPT backbone without the vWF domain.*

3.6 Lentivirus was produced and titred from the previously described plasmids

Lentivirus from the plasmids described in Figure 3.7B and Figure 3.7C were generated (see section 2.2.7) and titrated by qPCR (Figure 3.8). The average viral titre for the pWPT lentivirus containing vWF fused to the modified FVII sequence was calculated to be 8.73E+08 ± 5.39E+05 (mean ± SD). The average viral titre for the pWPT lentivirus containing the modified FVII sequence without vWF was 7.16E+08 ± 2.92E+08 (mean ± SD). Cells were transduced with these viral samples as described in section 2.2.8.

A

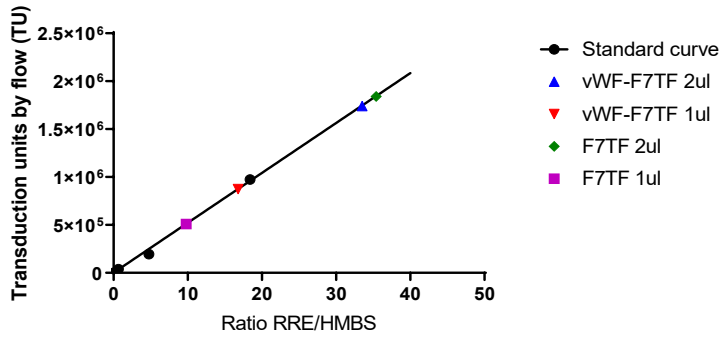

B

sample	Average titre (TU/ml)	Standard Deviation
vWF-F7TF	8.73E+08	5.39E+05
F7TF	7.16E+08	2.92E+08

Figure 3.8. *Linear regression between the qPCR copy number ratio calculated for the GFP virus. The GFP was used to control for the transduction efficiency of the cells, to ensure they were responding to transduction in an expected way, while the qPCR controls were to establish that the qPCR reaction was working as expected. n=1* ***(A)*** *The linear regression displayed graphically* ***(B)*** *This linear regression was used to calculate the equivalent GFP-flow titres in TU for the two types of virus produced*.

3.7 CHRF cells were transduced with the virus to establish FVII assays and confirm production of the modified protein

CHRFs, a cell line derived from megakaryoblasts were cultured and transduced with the produced lentiviruses in order to generate large amounts of protein to set up assays that could measure FVII.

The ELISA showed that the lentivirus containing vWF-F7TF was successfully expressing this protein, while F7TF showed no evidence for expression of FVII. A standard curve was established with known concentrations of FVII (Figure 3.9A). An ELISA on the lysates was performed, and significant ($p<0.001$) amounts of FVII was detected in the positive control, NovoSeven, and the lysates of cells transduced with vWF-F7TF but not the lysates from cells transduced with F7TF without the vWF signalling domain (Figure 3.9B). As the amount detected reached the upper limit of the ELISA, samples were diluted 1:10 and run again on an ELISA to accurately quantify the FVII concentration in the vWF-F7TF lysate (Figure 3.9C). Finally, the supernatants from the vWF-F7TF culture also showed

some detectable FVII, suggesting that the vWF-F7TF ended up in the resultant platelets produced by these cells (Figure 3.9D).

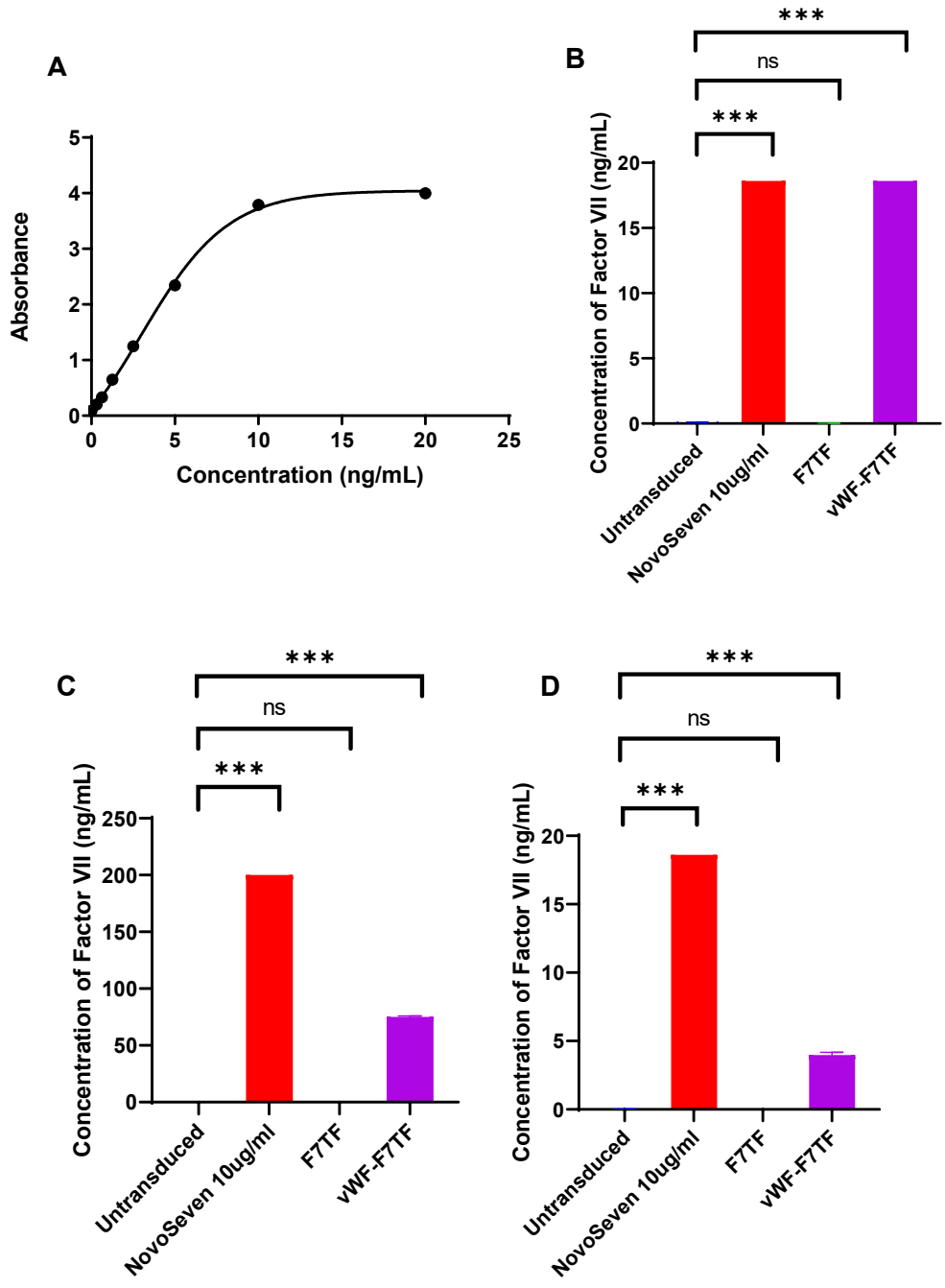

***Figure 3.9**. ELISA results from CHRF cells transduced with either of the two lentiviruses. (A) Concentration curve for ELISA (B) Concentration of FVII from lysates taken from untransduced CHRFs, CHRFs transduced with modified FVII lacking the vWF leader sequence (FVII) and CHRFs transduced with cells transduced with the vWF-FVII fusion protein sequence (vWF-FVII). (C) 1:10 dilution series of all lysate samples. (D) Concentration of FVII detected in supernatants from the same cell cultures as (B). NovoSeven was used as a positive control. 1x10^6 cells in each sample were lysed for this assay. *** p<0.001 One-way ANOVA with Tukey's multiple comparisons test. n=3*

3.8 An antibody was found to analyse intracellular FVII expression by flow cytometry

A flow cytometry-based assay to detect intracellular FVII was developed. HepG2 cells (details in section 2.2.1), derived from a hepatocellular carcinoma known to produce FVII was used as a positive control and all three antibodies showed some positive signal compared to the secondary only control (Figure 3.8).

From Figure 3.11D, only antibody 2, a rabbit monoclonal raised against FVII, was able to differentiate between untransduced CHRFs and CHRFs transduced with vWF-F7TF. Antibody 1 (Figure 3.11C) appeared not to be able to differentiate between the transduced and untransduced cells, suggesting it may be binding to some other protein non-specifically. Antibody 3 (Figure 3.11E) appeared able to give differential staining between transduced and untransduced CHRFs, but paradoxically it appeared to give a weaker signal in the presence of FVII.

Antibody 2 was chosen and used to set up a gating strategy, demonstrated in Figure 3.12. Three concentrations were trialled for the antibody on untransduced and vWF-F7TF transduced cells (Figure 3.12C and D). All three concentrations showed a good discrimination between the untransduced and transduced samples. A concentration of 1:20 showed an increased percentage positive for FVII in both the untransduced and transduced samples, indicating a higher non-specific binding. A 1:1000 dilution was achieved by first diluting the antibody 1:10 and subsequently 1:100 in the sample incubation step, to avoid the pipetting of very small volumes. It showed increased variability between stains thought to be due to issues with fully mixing the pre-dilution solution. A 1:100 concentration was therefore chosen from this data for all future intracellular flow experiments as it gave a good discrimination between untransduced and transduced cells and low variability.

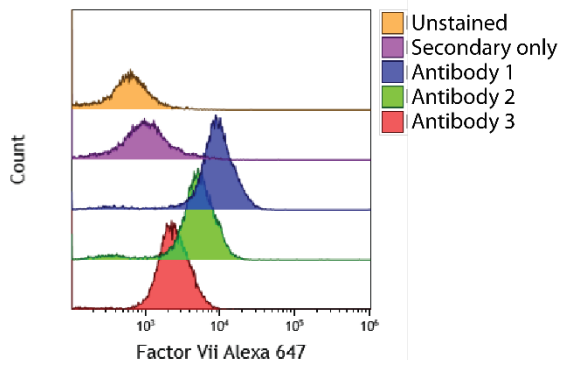

Figure 3.10. *All three antibodies were used to stain HepG2 cells (known to be positive for FVII). Shown are the unstained, secondary only controls, and results from the three different antibodies (antibody 1, ab197656) (antibody 2, ab151543) (antibody 3, ab97614 (secondary, A21244) (details in section 2.1.1.15)*

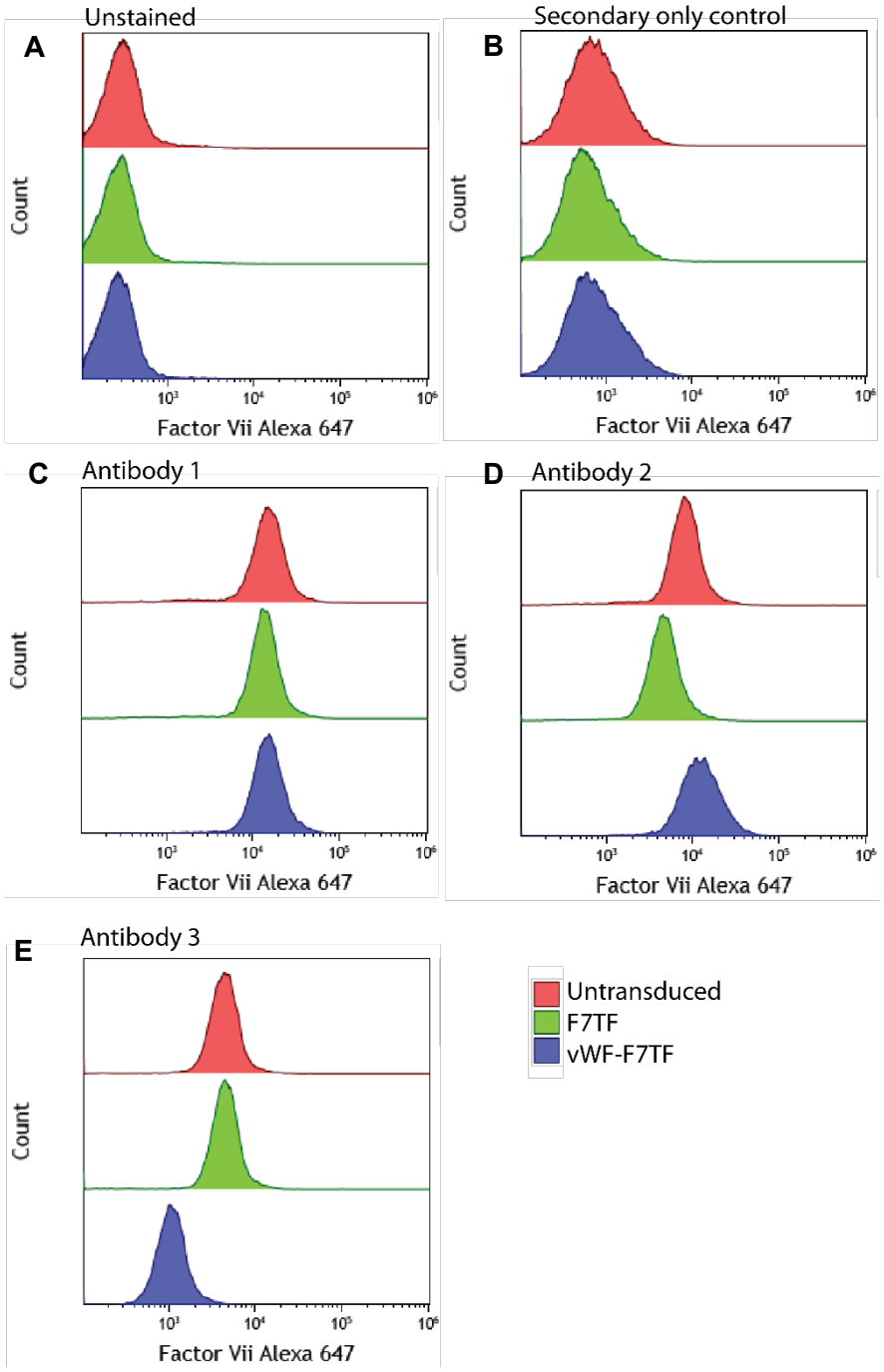

Figure 3.11. *Flow cytometry data from three different antibodies on untransduced CHRFs and CHRFs transduced with vWF-F7TF or F7TF. Representative overlay flow plots shown, n=3 for each antibody. (A) Unstained cell control (B) Secondary only control (C) Staining for antibody 1 (ab197656) (B) Staining for antibody 2 (ab151543) (C) Staining for antibody 3 (ab97614) (details in section 2.1.1.15)*

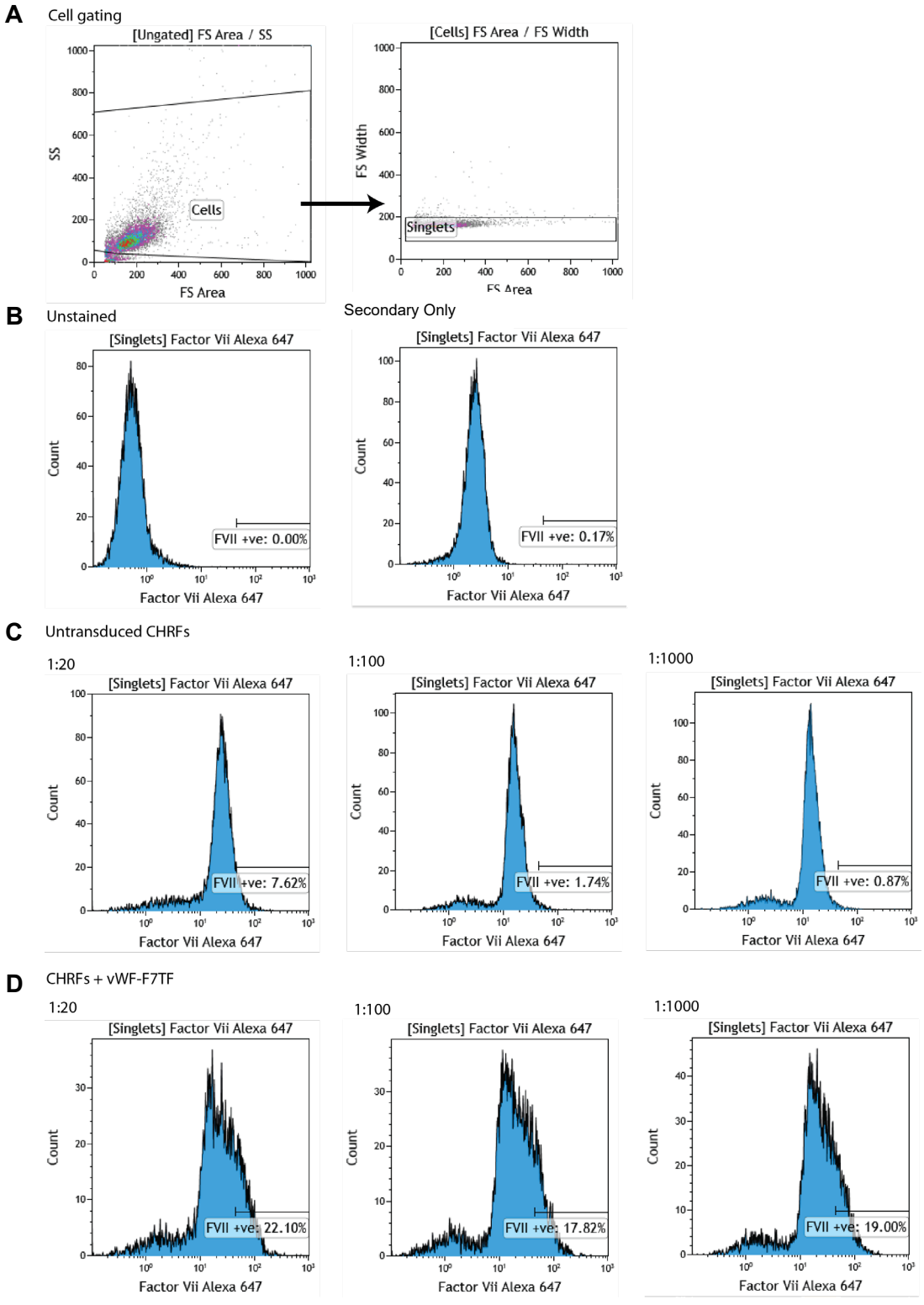

Figure 3.12. *Gating strategy using antibody 2 from the panel in Figure 3.10. (A) Cell gating, used subsequently in the other representative flow plots. (B) Unstained and secondary only control results from staining untransduced CHRFs (C) Untransduced CHRFs with the primary antibody incubated at three concentrations. (D) CHRFs transduced with vWF-F7TF using three different primary antibody concentrations.*

3.9 This antibody was further validated by Western blot and used to verify the presence of the fusion protein

This antibody is able to detect FVII at ~52kDa in HepG2 as expected, along with a ~90kDa protein in the CHRFs transduced with vWF-FVII (Figure 3.13) showing that the full fusion protein with the vWF SPD2 domain is being expressed. No band is seen in the CHRFs transduced without the vWF sequence or in untransduced CHRFs. A non-specific band is noted in the 50kDa range for untransduced forward programmed megakaryocytes (FoP-MKs), but no other non-specific bands were noted.

The presence of the ~90kDa band in the cells transduced with vWF-F7TF is of the expected size, containing both the vWF sequence (~40kDa) and the F7TF protein (~52kDa) as one fusion protein and no such band is seen in the untransduced cell lysates, validating the antibody to be binding to the expected protein (both in its native denatured sequence in HepG2 cells and modified denatured sequence in CHRFs).

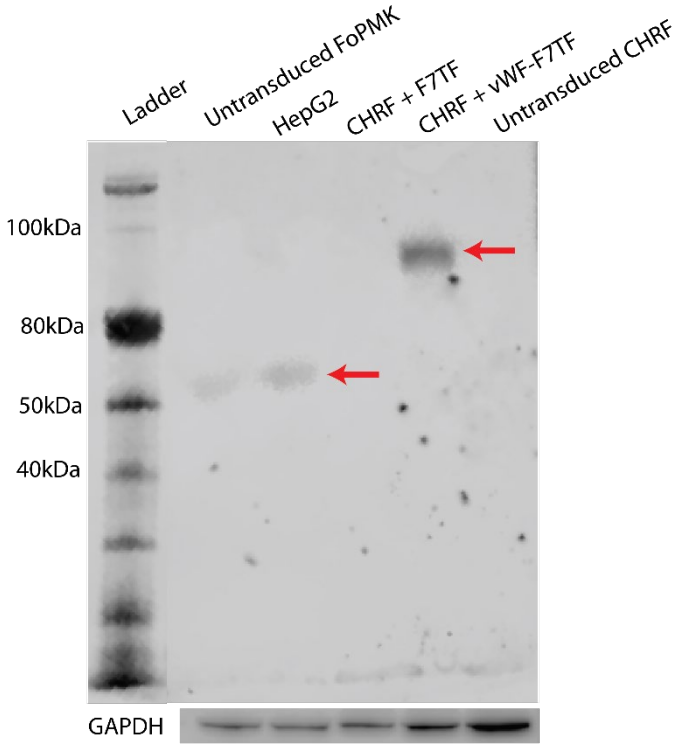

Figure 3.13. *Denaturing Western blot showing untransduced FoP-MK and CHRF cell lysates as negative controls, HepG2 cell lysates as a positive control, alongside CHRFs transduced with either F7TF or vWF-F7TF. Visible bands are highlighted with a red arrow. Blots were stripped and restained for GAPDH as a loading control. Western blots were repeated for an n=3.*

3.10 A chromogenic assay was established to measure functional activity of rFVIIa

This standard curve (Figure 3.14) established using serial dilutions of NovoSeven suggest that the minimum required concentration of rFVIIa to see a statistically significant difference lies between 100ng/ml and 1000ng/ml, and below this concentration, this functional assay become unreliable and indistinguishable from noise. This also established the antibody discovered in Figure 3.11 as being able to bind activated rFVIIa (further lending evidence to the results obtained using the same antibody in intracellular flow assays and Western blots such as Figure 3.13) at an epitope that does not inhibit enzymatic function.

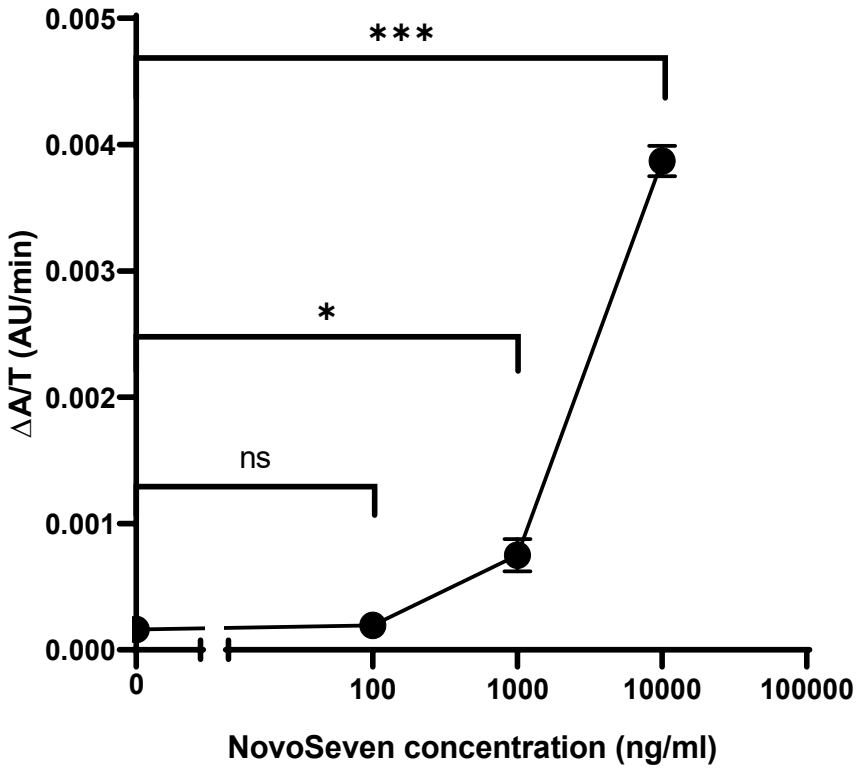

Figure 3.14. *The antibody found in Figure 3.11 was used to set up a chromogenic FVIIa assay (section 2.3.4). NovoSeven was used at 0, 100, 1000 and 10,000ng/ml concentrations to establish a dose-response relationship, while measuring the change in absorbance over time. n=3, one way ANOVA with multiple comparisons applying Bonferroni's correction. * p < 0.05 *** p < 0.01 Data shown as mean ± SEM.*

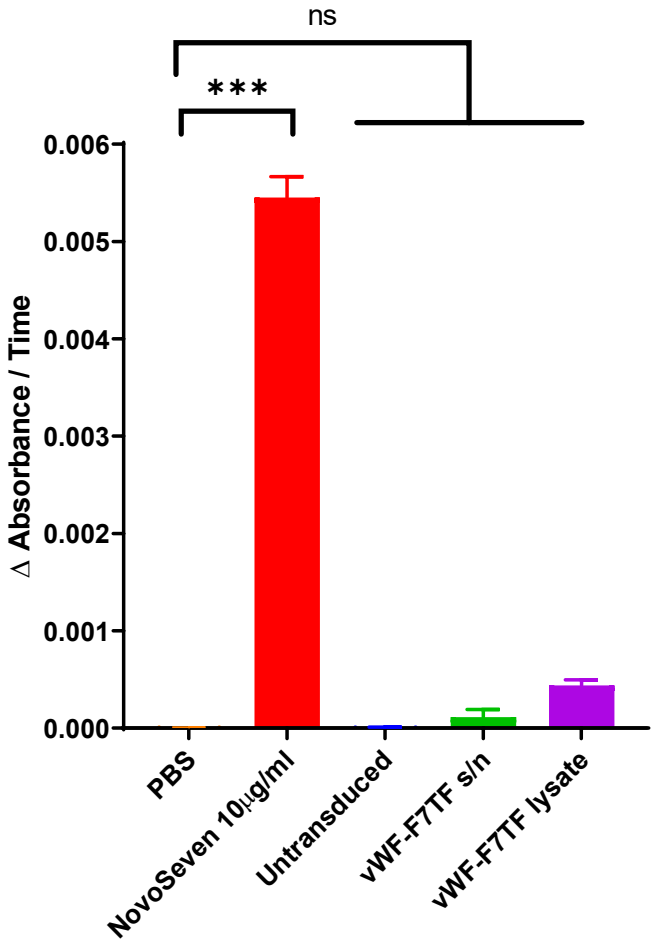

Figure 3.15. *Chromogenic assay results from the same samples as in Figure 3.9, on untransduced lysates as a negative control, Novoseven as a positive control and the supernatants and lysates from cells transduced with vWF-FVII. One-way ANOVA. n=3, data shown as mean ± SEM.*

The chromogenic assay in Figure 3.15 showed that although there was a small amount of enzymatic activity detected by the assay from both the supernatants and lysates, this was not large enough to be statistically significant from the untransduced controls.

3.11 Confirmation of the presence of vWF-F7TF in FoPMKs was obtained through ELISA, intracellular flow cytometry and measured over time

Megakaryocytes produced from BobC iPSCs through forward programming were transduced with the lentiviral constructs from Figure 3.7 (Figure 3.16). They were assayed with the intracellular flow cytometry assay established in Figure 3.12 for expression of FVII. FoP-MKs transduced with vWF-F7TF showed a significant expression of FVII, while those transduced with F7TF showed no signal different to the secondary-only or untransduced controls (Figure 3.17). Successful production of vWF-F7TF was further confirmed and quantified through ELISA (Figure 3.18B). This showed that the vWF-F7TF was detected in the lysates, as well as in the supernatants suggesting the platelets given off by this culture may contain vWF-F7TF, or that this was somehow otherwise being released into the culture.

Finally, these cultures were assayed over the duration of their cell culture to test whether expressed protein levels remained stable over time (Figure 3.18), and this confirmed that it remains highly expressed up to 50 days post transduction. After this point, the culture lost viability as has been observed in virally transduced forward programmed megakaryocytes beyond day 110 (Moreau *et al.*, 2016). Cells staining positive for only CD41 are thought to be immature precursors that have not fully differentiated.

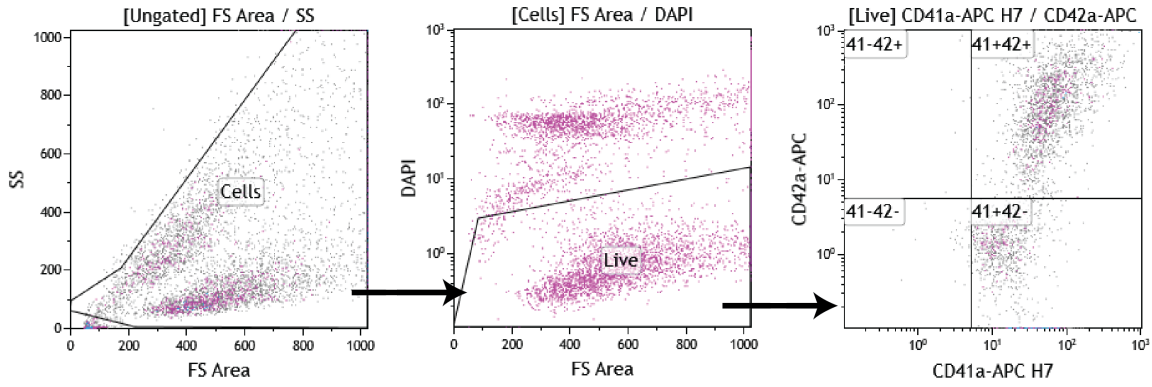

Figure 3.16. *Gating strategy for FoPMKs to ensure they are impermeable to DNA staining (DAPI negative, indicating viability) and positive for two common megakaryocyte markers (CD41 and CD42) before all experiments were performed. n=3*

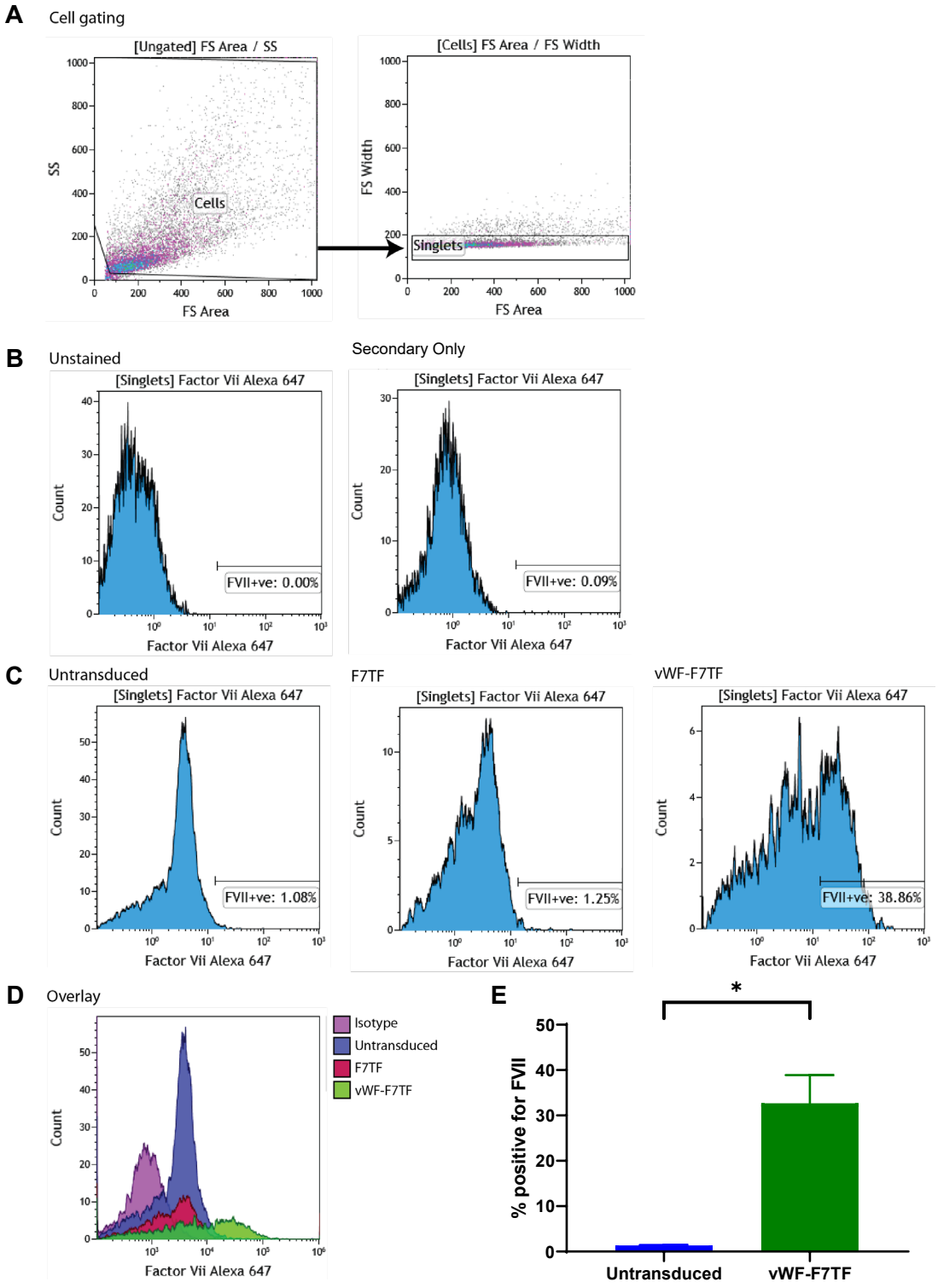

Figure 3.17. *Intracellular flow cytometry data from FoPMKs untransduced or transduced with either F7TF or vWF-F7TF. (A) Cell gating strategy used to isolate singlets (B) FVII staining from unstained untransduced cells and secondary-only stained cells. (C) Representative flow plots for untransduced cells, cells transduced with F7TF and vWF-F7TF (D) Overlay plot of FVII staining. (E) Quantification for n=3, two tailed t-test * p < 0.05; data shown is mean ± SEM.*

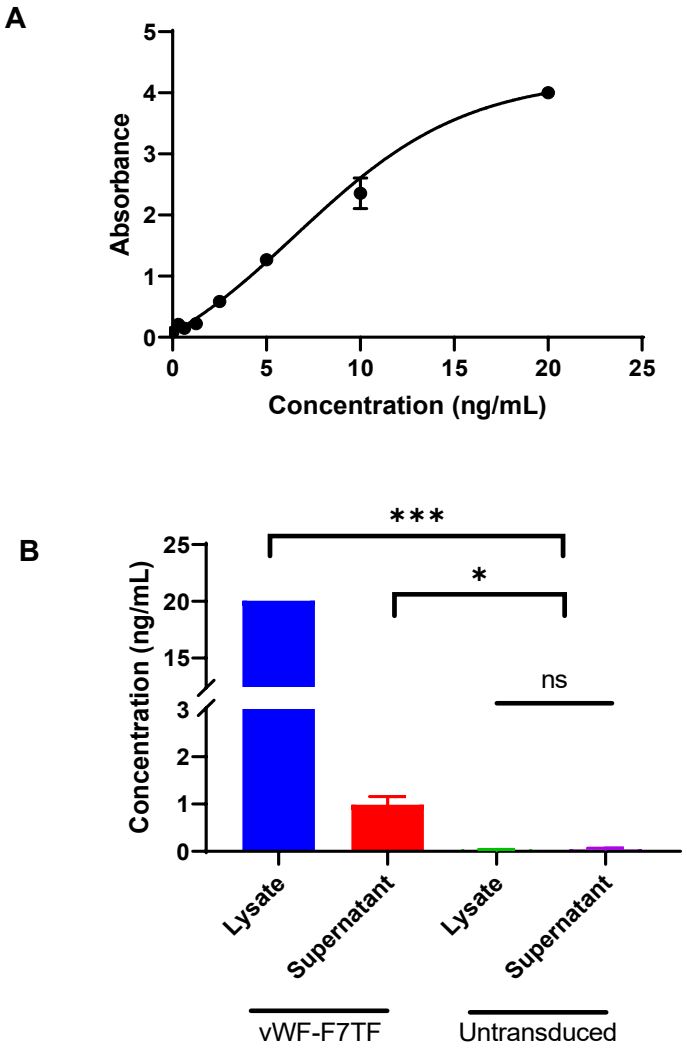

Figure 3.18. *ELISA evidence of FVII expression in transduced vs untransduced FoPMKs. (A) Standard curve for ELISA. (B) ELISA of lysates and supernatants from forward programmed MKs transduced and untransduced with lentivirus expressing the modified rFVIIa sequence. Data shown as mean ± SEM. N=3, One way ANOVA. * p < 0.05, *** p < 0.01*

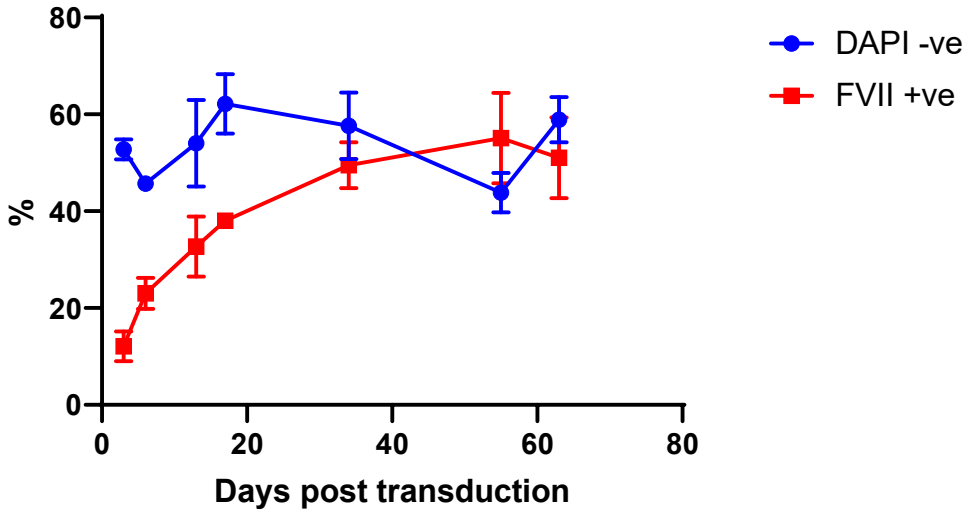

Figure 3.19. *Percentage of cells transduced with vWF-F7TF staining positive for FVII over time, overlaid with the DAPI negative (live cell) percentage over the same time period. n=3 transductions for 7 timepoints.*

3.12 Immunofluorescence reveals that this fusion protein is located in the VEGF-containing subpopulation of α–granules in forward-programmed megakaryocytes

Having established its presence, immunofluorescence was used to identify whether vWF-F7TF correctly localised to the α–granules. Previous work (Figure 3.1) had established that this vWF leader sequence attached to GFP co-localised with thrombospondin, a common α–granule marker. Immunofluorescence data from a co-staining of FVII and thrombospondin are shown in Figure 3.20; no co-localisation was observed between the thrombospondin and vWF-FVII in transduced cells.

As noted by Figure 3.20A, only secondary antibody staining does not result in the visualisation of any granular objects. Untransduced FoP-MKs, co-stained for thrombospondin and FVII, show green granular objects staining positive for thrombospondin but not for FVII (Figure 3.20B). FoP-MKs transduced with vWF-F7TF (Figure 3.20C) show the presence of granular objects within the cytoplasm of these cells staining for either green (thrombospondin) or red (FVII) but not both. No co-localisation events were observed.

Other markers were co-stained with FVII to identify which type of organelle the vWF-F7TF had been directed to. A literature review suggested that α–granules come in two subtypes, endostatin positive and VEGF positive, and that these two subtypes do not overlap with one another (Italiano *et al.*, 2008). A co-stain for FVII and endostatin showed similar results to that for thrombospondin with no co-localisation (Figure 3.19). A co-stain for VEGF showed some co-localisation with vWF-F7TF (Figure 3.20).

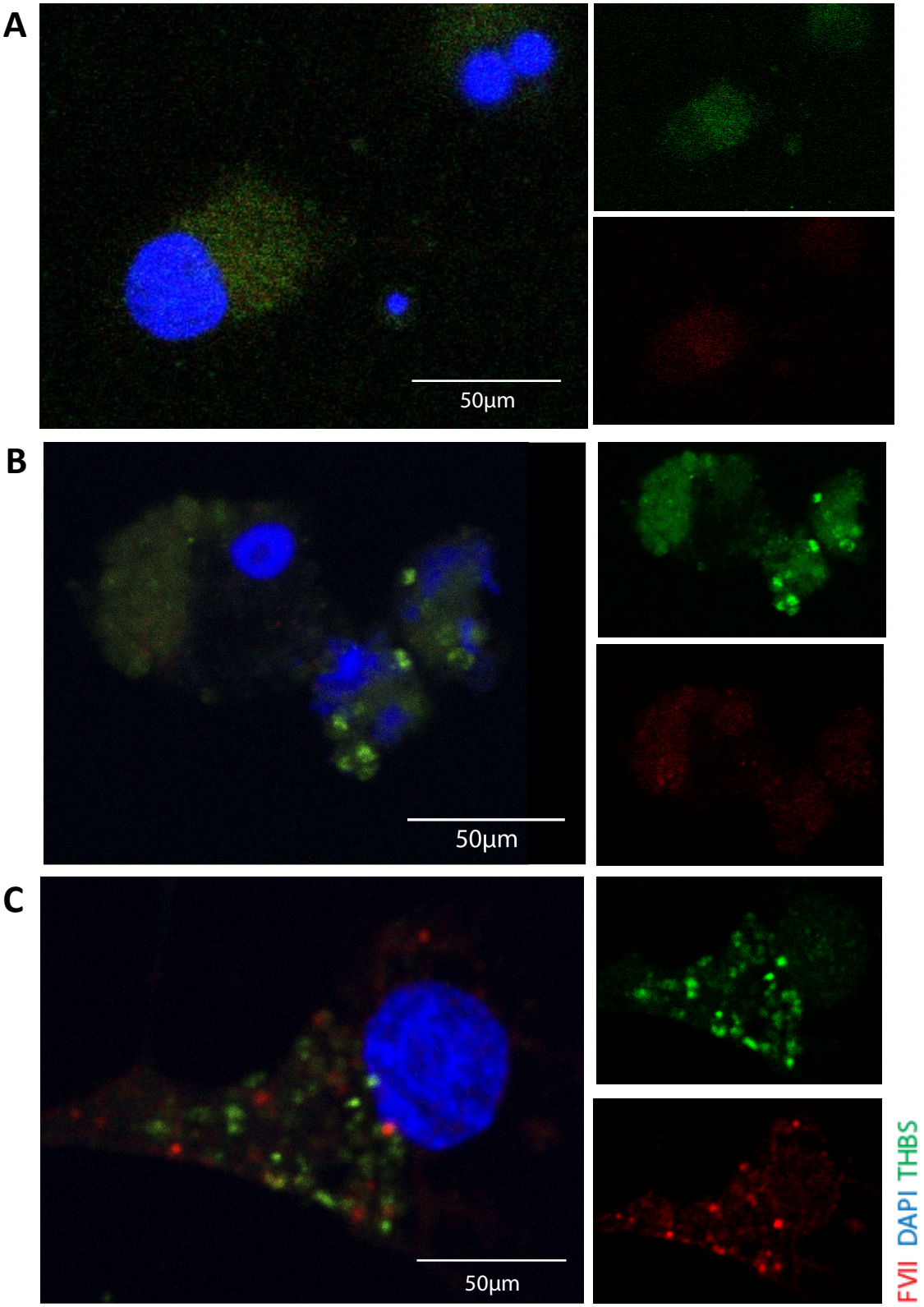

Figure 3.20. *Immunofluorescence data for localisation of vWF-F7TF and thrombospondin (THBS). (A) Secondary antibody only control to establish the background fluorescence (B) Untransduced FoP-MKs staining for FVII (red, ab97614, secondary A21244) and THBS (green, ab1823, secondary A21121). (C) FoP-MKs transduced with vWF-F7TF stained for FVII (red) and THBS (green). Images are representative of n=3 technical repeats, on a Leica Sp5 confocal 63x.*

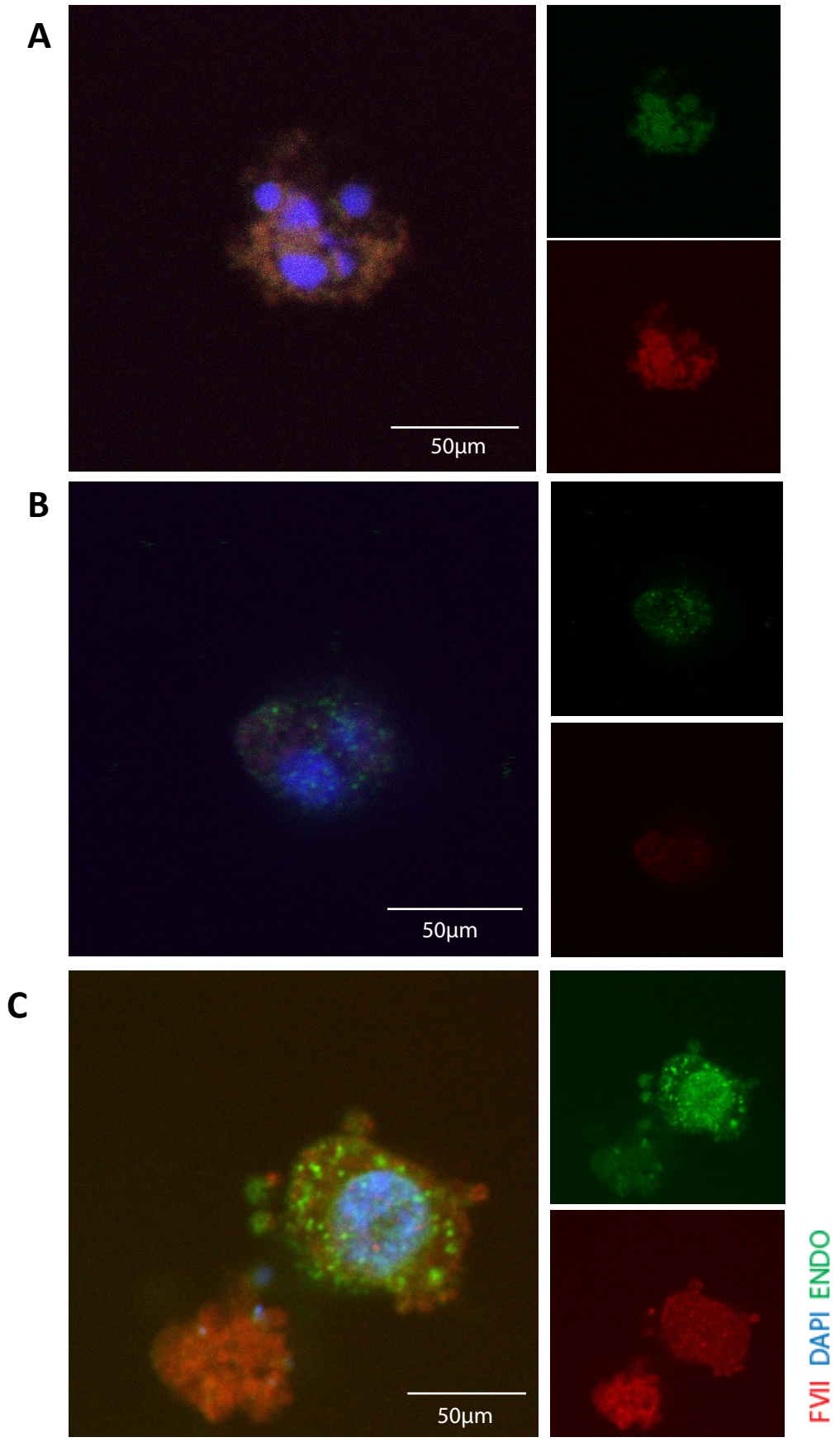

Figure 3.21. *Immunofluorescence data for localisation of vWF-F7TF and endostatin (ENDO). (A) Secondary antibody only control to establish the background fluorescence (B) Untransduced FoP-MKs staining for FVII (red, ab97614, secondary A21244) and ENDO (green, sc-514355, secondary A21121). (C) FoP-MKs transduced with vWF-F7TF stained for FVII (red) and ENDO (green). Images are representative of n=3 technical repeats, on a Leica Sp5 confocal 63x.*

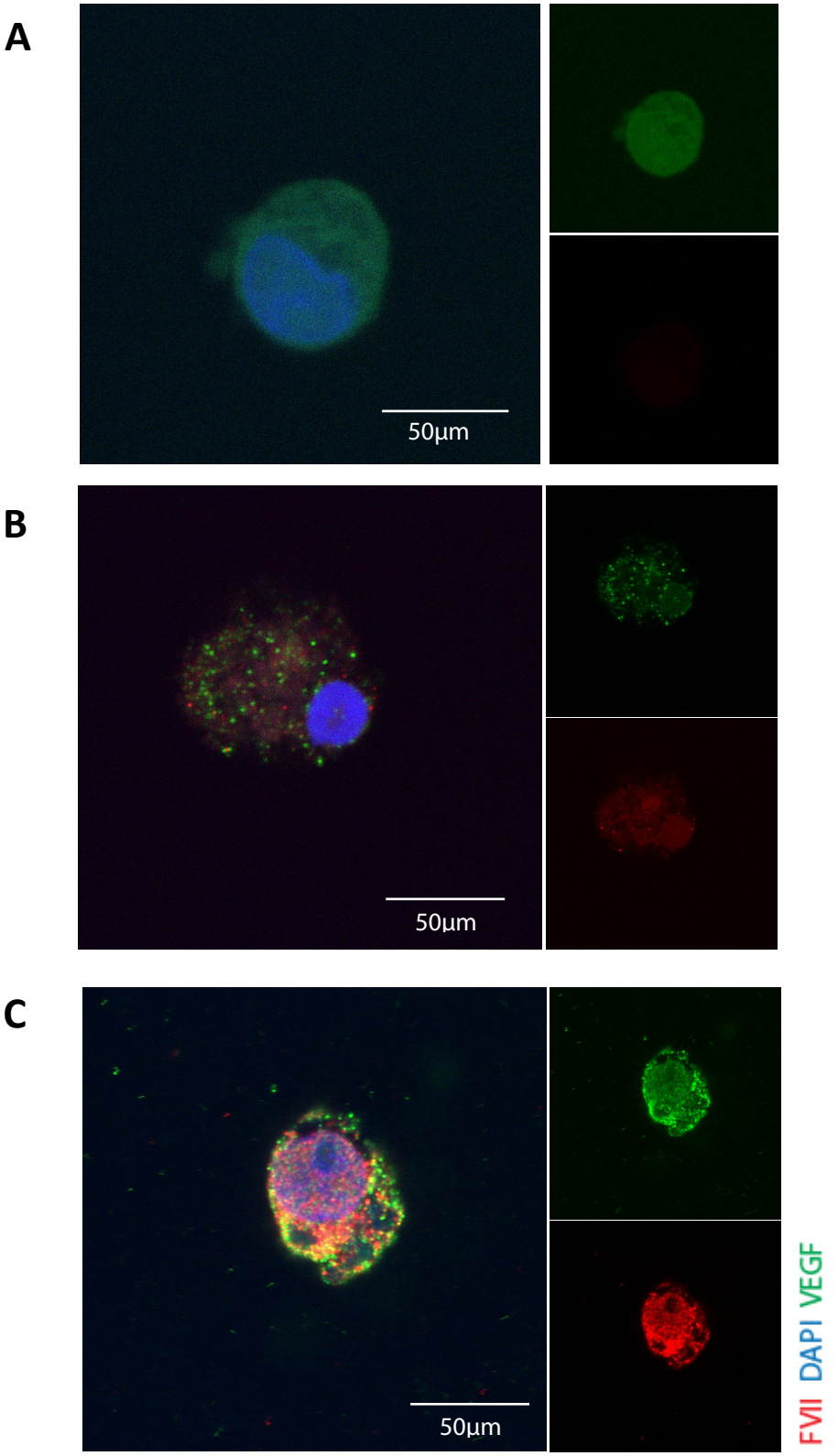

Figure 3.22. *Immunofluorescence data for localisation of vWF-F7TF and VEGF. (A) Secondary antibody only control to establish the background fluorescence (B) Untransduced FoP-MKs staining for FVII (red, ab97614, secondary A21244) and VEGF (green, NB100664SS, secondary A21121). (C) FoP-MKs transduced with vWF-F7TF stained for FVII (red) and VEGF (green). Images are representative of n=3 technical repeats, on a Leica Sp5 confocal 63x.*

3.13 The engineered furin and thrombin sites were functional as demonstrated by Western blot and able to reconstitute the wild-type rFVIIa upon activation

From two separate transductions, the full-length protein (Figure 3.21B) can be observed at ~95kDa (Figure 3.21A shows the molecular weights of the different components of this fusion protein), absent in the untransduced controls. Figure 3.21C demonstrates that the native tissue factor cleavage site has been replaced with a furin cleavage site. Excess furin causes further cleavage of the full-length transcript to a band seen at around 60kDa to demonstrate this.

Addition of thrombin (Figure 3.21C) results in cleavage at the thrombin cleavage site, demonstrating its functionality in releasing the heavy and light chains of endogenous FVIIa. The shift between these versions of the protein were quantified for several western blots and shown in Figure 3.21D, which demonstrates how additional furin results in further cleavage of the full-length protein, while addition of thrombin alone results in separation of the heavy and light chains.

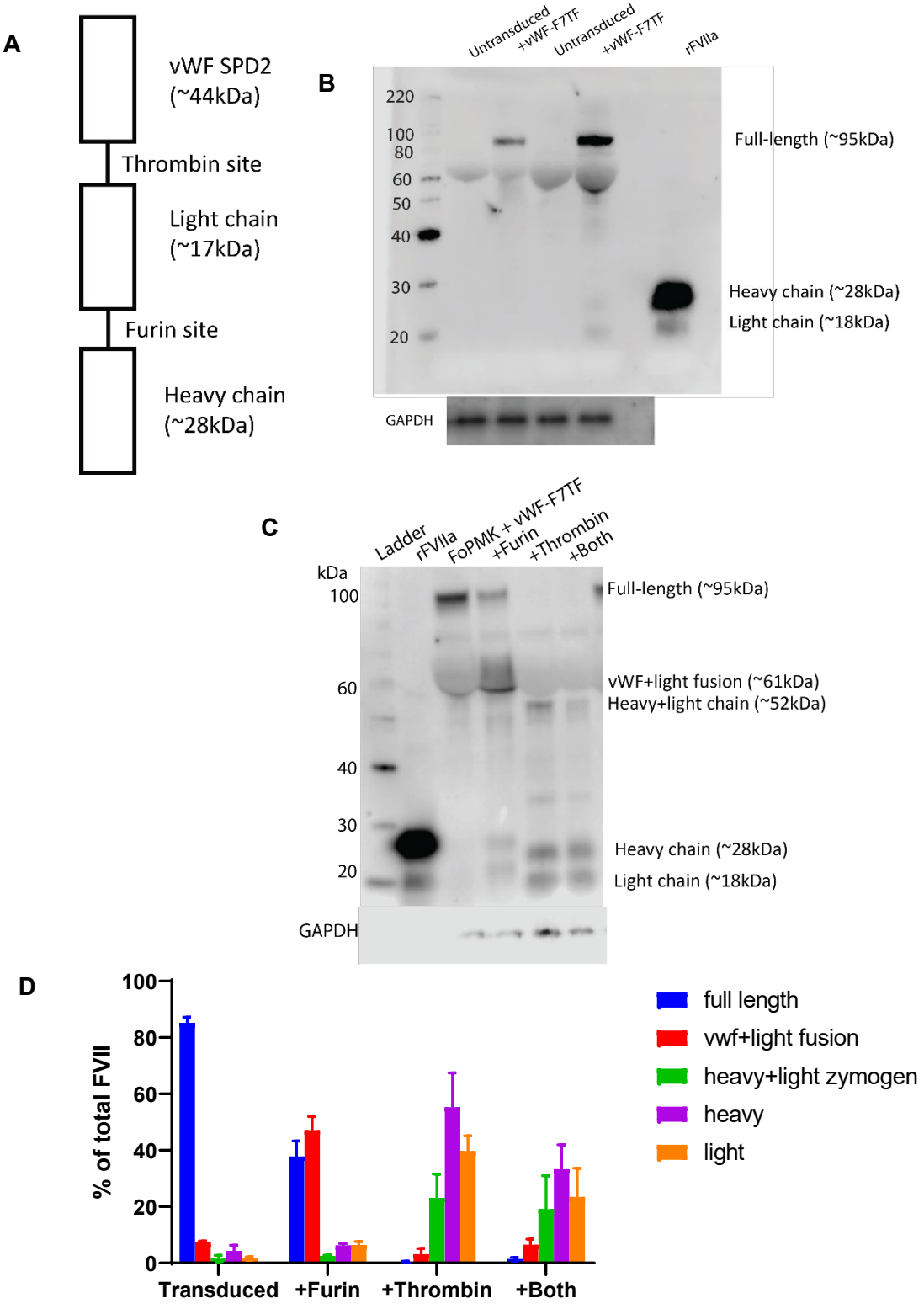

***Figure 3.23**. Western blot data on vWF-F7TF from FoPMK lysates (A) Schematic of the modifications made to the original FVII sequence and molecular weights of the different components (B) Reducing blot of untransduced and transduced (with vWF-F7TF) FoP-MKs from two separate cultures with a ladder and NovoSeven as a positive control. (C) Reducing blot showing the effect of adding either furin or thrombin or both to the lysates of transduced FoPMKs (D) Quantification of the bands with ImageStudio at five separate molecular weights from n=3 western blots with lysates from transduced FoPMKs incubated with either furin, thrombin or both; data shown as mean ± SEM.*

3.14 Functional chromogenic assays were unable to detect enzymatic activity from this fusion protein

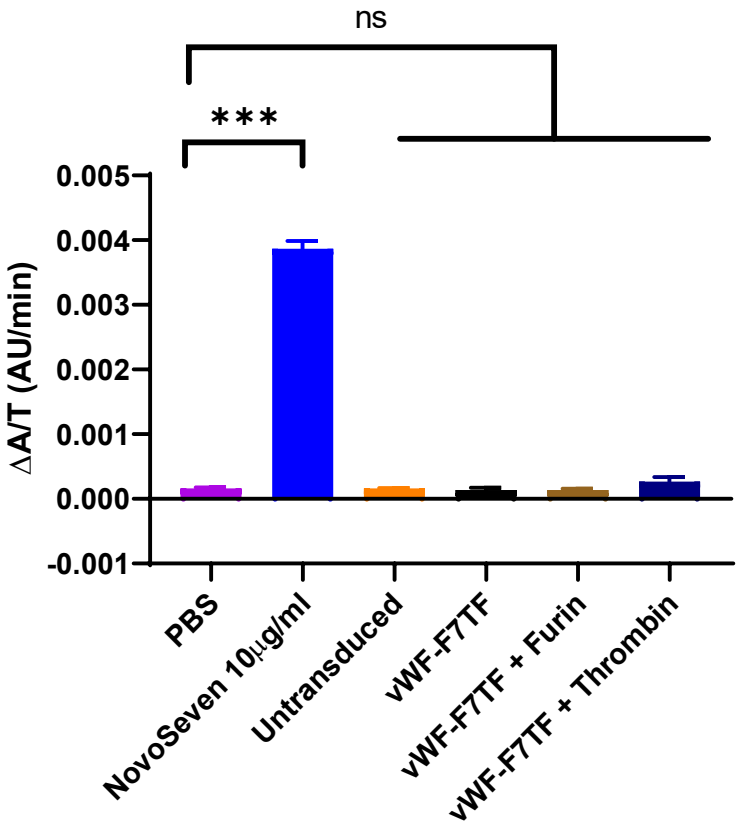

Figure 3.24. *Chromogenic assay results for vWF-F7TF produced in FoPMKs. PBS and NovoSeven were used as positive and negative controls, followed by lysates from untransduced FoP-MKs, lysates from FoPMKs transduced with vWF-F7TF without and then with subsequent incubation with either furin or thrombin. All lysate samples came from $10x10^6$ cells to normalise protein content. n=3, data shown as mean ± SEM.*

Chromogenic assays (as established from Figure 3.14) were used to evaluate functionality of the fusion protein produced from FoP-MKs (Figure 3.24). Although the negative and positive controls worked as expected, no significant differences were observed from PBS or untransduced controls. Lysates were also incubated with furin or thrombin to increase availability of the native form of FVIIa (as observed in Figure 3.21D). A small increase was observed in lysates incubated with thrombin, but this was not statistically significant.

3.15 Transduced FopMKs produce platelets loaded with vWF-F7TF

Having verified that vWF-F7TF was produced in megakaryocytes transduced with the lentivirus, platelets were collected from both untransduced and transduced cultures and analysed by intracellular flow cytometry to investigate whether this fusion protein was being subsequently packaged into platelets as would be expected of a protein in an α–granule (Figure 3.25). Isotype and secondary only control stainings were established on platelets from untransduced cultures, combining markers for maturity (CD42) and viability (Zombie) to ensure FVII was present in platelets and not artefactual remnants of cell culture (Figure 3.25A and Figure 3.25B). Combined staining showed a significant whole population shift of platelets (Figure 3.25C, Figure 3.25D, Figure 3.26A) in platelets from cultures transduced with vWF-F7TF compared to those from untransduced cultures. This was quantified and shown to be significant ($p < 0.05$) (Figure 3.25B).

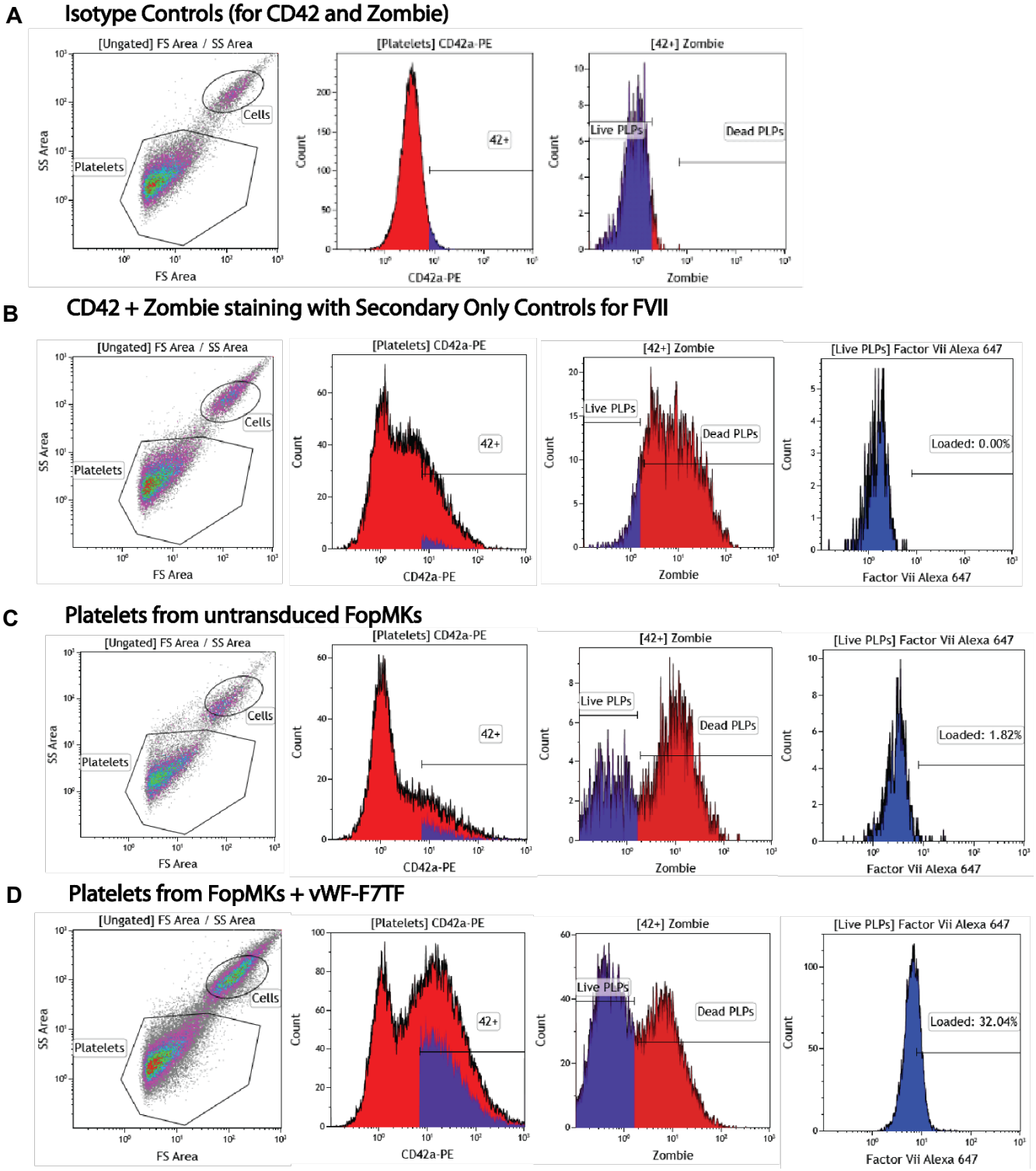

Figure 3.25. *Representative flow plots of intracellular flow experiments on platelets derived from FoPMK cultures. (A) Platelets from untransduced cultures were stained for isotypes for maturity (CD42) and viability (Zombie) (B) Platelets from untransduced cultures stained for CD42, Zombie and only the secondary antibody for FVII. (C) Platelets from untransduced cultures stained for all three markers (D) Platelets from FoPMK cultures transduced with vWF-F7TF*

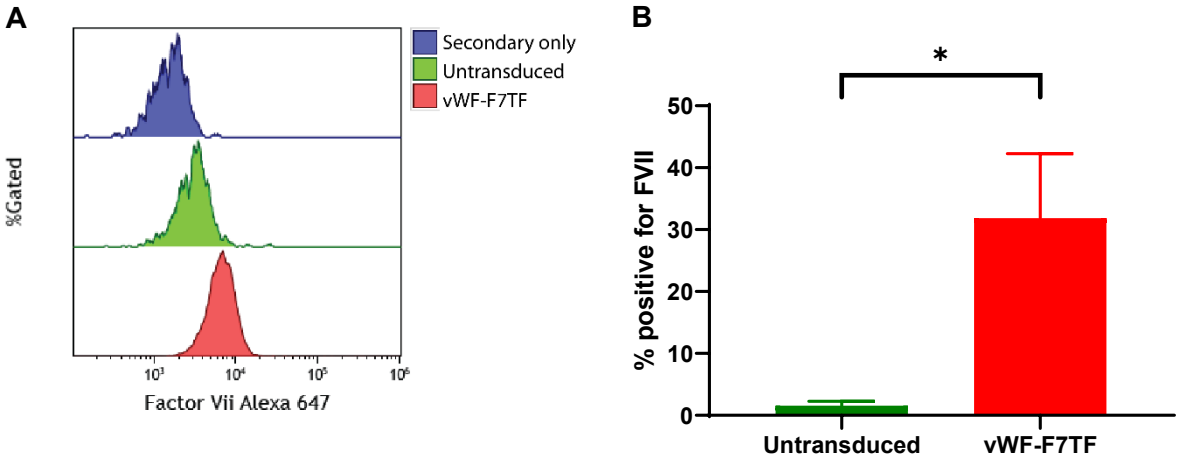

Figure 3.26. *Summarised flow data for platelets from untransduced and transduced FoPMK cultures. After CD42 and Zombie gating (A) Overlay plot of secondary only, untransduced and vWF-F7TF cultures. (B) Percentage gating positive for FVII for n=3, data shown as mean ± SEM. Two-tailed t-test, * $p < 0.05$*

3.16 Thrombin generation assays on platelets loaded with this fusion protein showed an effect

All parameters measured for the thrombin generation assay appeared to be increased for platelets containing vWF-F7TF compared to both untransduced platelets and human donor platelets, for every concentration of platelets tested (Figure 3.25A). A representative plot shows that the thrombin generation from *in vitro*-derived platelets differs considerably from that of donor platelets. The thrombin generation peak has a reduced lag time, increased peak height and an increased area under the curve, indicating higher total thrombin generation. Representative plots and subsequent quantification also show *in vitro*-derived platelets loaded with vWF-F7TF had an increased peak height and area under the curve when compared with untransduced *in vitro* platelets. All reactions were triggered with the use of RCLow, a solution of a low concentration of phospholipid micelles containing rhTF in Tris-Hepes-NaCl buffer.

There appeared to also be a dose-dependent relationship between the number of platelets and a response in peak thrombin generation (Figure 3.25B) and total thrombin generation (Figure 3.25C) for each of the conditions. This data shows that when modelled as a dose-response curve with non-linear regression, *in vitro* platelets have a higher V_{max} for thrombin generation (although this was not significant at the $p<0.05$ level), and that the addition of rFVIIa shifts this curve to the left, resulting in a lower EC_{50}. Non-linear regression calculated the EC_{50} values from the area under the curve of the donor, untransduced and vWF-F7TF platelets as 3.30 (1.45 to 10.1), 1.91 (0.623 to 4.94), 0.515 (0.281 to 0.937) respectively, reported as mean (95% confidence interval) to three significant figures. From this, the EC_{50} of total thrombin generation of vWF-F7TF-loaded *in vitro* platelets was found to be significantly ($p<0.05$) different to the donor platelets, while the untransduced *in vitro* platelets were not (Figure 3.28).

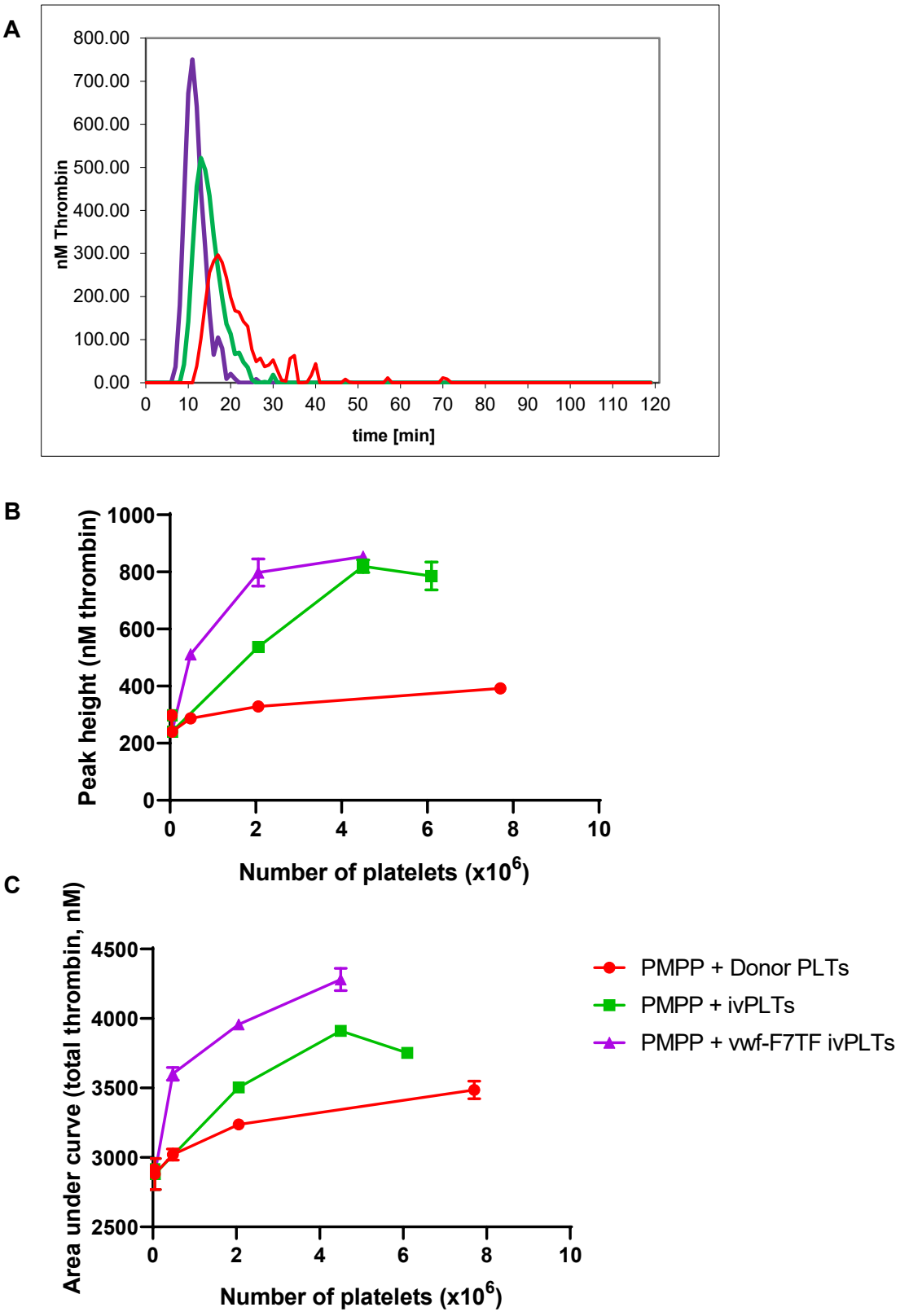

Figure 3.27. *Results from a thrombin generation assay on donor platelets (PLTs), platelets from an untransduced culture (ivPLTs) and platelets from a vWF-F7TF culture of FoPMKs (vwf-F7TF ivPLTs) mixed with platelet-and-microparticle-free plasma (PMPP) in a volume of 100µl. The reaction was triggered with the addition of RCLow (a solution of phospholipid micelles containing rhTF). (A) Shows a representative thrombin generation assay for the three conditions carried out for $2x10^6$ platelets. A dose response was plotted for parameters including (B) the peak thrombin generation and (C) the total thrombin generation. n=3, data shows mean ± SEM.*

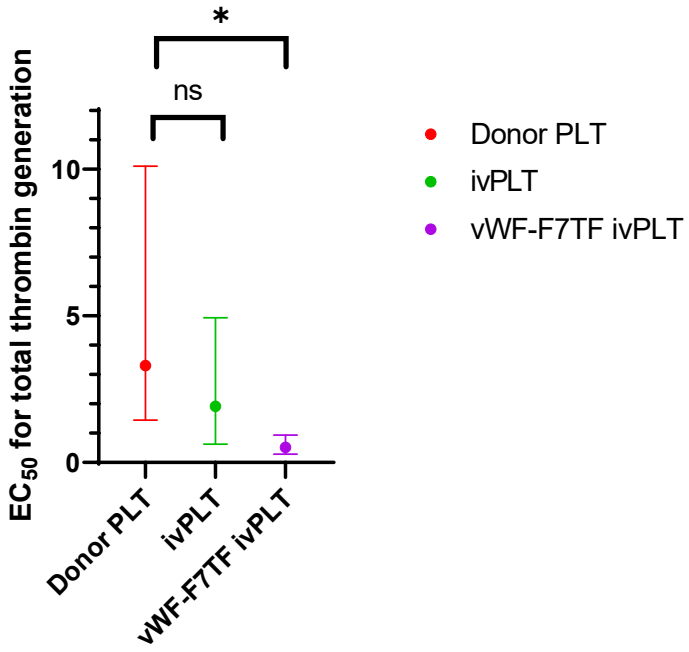

Figure 3.28. *Confidence intervals for the EC_{50} for total thrombin generation, derived from non-linear regression applied to the concentration curves in Figure 3.25C.*

3.17 Discussion

The success of the cloning was confirmed through Sanger sequencing of the entire length of the FVII sequence at each stage to confirm no point mutations or frameshifts (Figure 3.4D, Figure 3.5, Figure 3.7B and Figure 3.7D). The use of overlapping-extension PCR was necessary because of the lack of any suitable restriction sites near the tissue factor cleavage site for the insertion of the furin cleavage sequence. Gibson assembly was favoured for the insertion to pWPT for the ability to insert sequences without leaving restriction site scars that may impair function of the plasmid or the resulting protein (Gibson *et al.*, 2009).

CHRFs were chosen as an intermediate step in order to establish FVII assays before transferring these onto FoP-MKs as they are easier to culture and grow in large numbers, with the caveat that they do not represent a physiological system nor one suitable to generate platelets for human transfusion.

Using this monoclonal antibody found in Figure 3.11 to set up an intracellular flow assay, no appropriate isotype could be found as no details to the concentration of this antibody were given. As a substitute, a secondary only staining was used instead. This may explain why the untransduced cells appear to cause a shift compared to the secondary only control, although not as great a shift as transduced samples (Figure 3.17). Other possible reasons for this non-specific

staining of untransduced cells include the presence of non-specific binding sites in FoPMK system as observed in the untransduced FoPMK lane in Figure 3.13.

Clinically, the most common readout of FVIIa activity is the prothrombin time (PT), which measures the activity of the extrinsic pathway of coagulation, as well the associated international normalised ratio (INR) (Tripathi *et al.*, 2017). Traditionally, the PT is the time taken to form a clot measured in platelet poor plasma upon the addition of tissue. Although very useful clinically, this assay has some limitations in this context as the effect of FVIIa is measured indirectly and other factors can affect the PT. A shortened PT does not necessarily predict success of rFVIIa therapy in patients with bleeding, although a correction back to a normal range is suggested in the literature to be a better indicator (Pusateri and Park, 2005). Furthermore, the quantity of FVIIa required to see a noticeable difference is high (Bomken *et al.*, 2009). The quantity of protein produced from a small-scale cell culture system may not be sufficient to observe a difference. Finally, as the assay takes place in platelet-poor plasma, the effect of platelet-coagulation pathway synergy as hypothesised by the cell-based model of haemostasis is likely to be missed (Hoffman and Monroe, 2001).

The chromogenic assay in Figure 3.15 showed that although there was a small amount of enzymatic activity detected by the assay from both the supernatants and lysates, this was not large enough to be statistically significant from the untransduced controls. This is likely to be due to concentration of vWF-F7TF present in the samples; as seen in Figure 3.14, the minimum concentration required for a statistically significant result is at least 1000ng/ml. From Figure 3.9C, the concentration of vWF-F7TF in the lysates is at most 76ng/ml, far below this threshold. Therefore, it is difficult to conclude whether there is or is not any functional activity from this data as even the rFVIIa diluted to this level gave a statistically insignificant result.

The FoPMKs were monitored for their maturity (CD41 and CD42) and viability (DAPI) routinely to ensure they were live megakaryocytes to remove this as a confounding factor from all of the results obtained from these cells. ELISA data (Figure 3.18) and intracellular flow data (Figure 3.17) confirmed the presence of vWF-F7TF in these cells. Immunofluorescence data showed that the vWF-FVII did appear to be in some granular-like object within the cytoplasm (Figure 3.20) that did not co-localise with thrombospondin, the granule marker that previously co-localised with vWF-eGFP (Figure 3.1); this could be within a lysosome, other endosome or another subset of megakaryocyte granule. To rule this out, other granule markers were trialled and VEGF was found to co-localise with the vWF-

F7TF to a far greater degree than other granule markers (Figure 3.20). This means that the addition of the F7TF sequence has switched trafficking from one subtype of α-granule to another. This may be due to the addition specifically of the furin cleavage site, as furin is a chaperone protein known to be involved in protein trafficking in the secretory pathway (Thomas, 2002). This effect may be mediated by other unknown sequences in the endogenous FVII gene or other mechanisms, such as through homoaggregation (Hayward *et al.*, 1999). It remains unclear whether this will result in different stimuli triggering a differential release of rFVIIa-containing granules under certain circumstances and not others.

The absence of the F7TF protein without the vWF leader sequence was notable, as it was intended to be used as a control with the FoP-MKs. This was despite the eGFP without the vWF leader sequence being successfully expressed by Dr Annett Mueller (Figure 3.1). This could be attributed to a failure of transduction, but when measured by qPCR when titrating the lentivirus (Figure 3.8) it appeared to be successful. Furthermore, no protein expression was observed across three separate attempts at transduction for CHRFs and for FoPMKs. Therefore, although a failure of transduction cannot be ruled out it remains unlikely. Another reason why no protein was observed is perhaps that the F7TF protein was degraded or underwent further post-translational changes hindering the ability for binding to the antibody epitope immediately upon production in the cytoplasm. As the F7TF portion of the sequence is sufficient to switch trafficking towards a VEGF positive granule subpopulation, perhaps lacking the vWF leader sequence it is trafficked into lysosomal machinery for degradation. Mutations in the EGF-1 domain of FVII have been shown to result in clinical deficiencies of FVII due to altered sorting mechanics in functional studies (D'Andrea *et al.*, 2004).

At this point, the vWF-FVII has been detected structurally within the transduced FoP-MKs by a variety of techniques and localised into a specific subtype of α–granule within the FoP-MK. Next, other more functional in vitro assays were used to investigate whether the modifications made to the protein sequence were functioning as intended, and to test whether the fusion protein was still capable of acting as an enzyme. Although the chromogenic assay again returned an inconclusive answer (Figure 3.24), likely again due to the protein being present at a level orders of magnitude lower than required to observe a difference from the control, Western blot data (Figure 3.21) showed that the inserted furin and thrombin sequences were functioning as intended, with a shift in protein fragments observed upon towards the separated heavy and light chains.

Figure 3.21D showed a significant shift in profile of the fragments of the fusion protein upon the addition of thrombin. Not only were the native light and heavy chain produced, but the full-length protein was removed almost entirely with no corresponding increase in the zymogen FVII without separation of the heavy and light chains as might be expected just from the cleavage of the vWF leader sequence. This may suggest some end-product inhibition of furin; the cleavage of the thrombin site causing the final conformational change may free endogenous furin to further cleave the full-length protein. This may also be due to the non-specific antibody binding seen in untransduced samples (Figure 3.13) near the same molecular weight of the vWF SPD2+light protein, obscuring the true quantity of this form present.

Although the datasheet for the antibody states that it is a monoclonal antibody against one epitope, it is clear from this western blot data that the antibody is able to bind to both the heavy chain and the light chain, although the signal is strongest from the heavy chain (Figure 3.21B).

Previous work from the Ghevaert group has established a standardised assessment of in vitro-derived platelets through measurement of maturity (CD42b) and metabolic viability (Zombie) in anucleate platelets (Shepherd *et al.*, 2018). This was applied to the in vitro generated platelets from untransduced and transduced cultures here in order to establish the identity of these particles not purely based on size, in order to exclude as much general cellular debris as possible. The metabolic marker here used was Zombie-violet which is an amine-reactive dye permeable to compromised cell membranes (and so stains dead platelets positively); any non-protein debris will stain negatively, the same as a live platelet. This was preferable to the other major viability marker in use, Calcein, which stains live platelets, as this dye was shown to leak out of permeabilised platelets for the intracellular assay (Caillon *et al.*, 2013).

Intracellular flow data showed that the resultant platelets from these cultures were able to produce vWF-FVII containing platelets (Figure 3.26). These platelets were combined with functional clotting assays to investigate how this fusion protein took part in Figure 3.25. Under the hypothesis of the cell-based model of clotting (Figure 1.11), the interplay between the F7TF and platelet membrane would allow for a physiologically relevant amplification of any pro-clotting effects that are likely to translate to in vivo models more so than the supraphysiological levels of protein required for assays looking only at the enzymatic function of FVIIa in isolation, e.g. the chromogenic assays. Changes in parameters such as peak height and area under the curve have been associated clinically with changes in functional

haemostasis (van Veen, Gatt and Makris, 2008). Therefore, the data in Figure 3.25C suggests that the reduction in the EC_{50} of these vWF-F7TF-loaded platelets would result in faster clot formation *in vivo* compared to unloaded *in vitro* platelets or donor platelets, demonstrating the continued functionality of the fusion protein despite the modifications made to it. Note that non-viable cell fragments from culture have not been removed from the samples of ivPLTs which may influence results obtained.

There is evidence in the literature that platelets from in vitro megakaryocytes retain a more 'embryonic' phenotype and are hyperreactive compared to adult platelets; this appears to be borne out by the data from untransduced platelets in Figure 3.25A showing a tendency towards parameters that suggest a faster rate of clot formation, although this was not significantly ($p>0.05$) different to donor platelets from the nonlinear regression confidence intervals (Sim *et al.*, 2016).

Overall, the FVII gene was modified with a vWF leader sequence, a thrombin cleavage site and furin cleavage site. These were expressed successfully in FoPMKs and were sorted to their α-granules. The thrombin and furin sequence were verified to be functionally active and cleave under the designed circumstances to give the native rFVIIa heavy and light chains. These FoPMKs were able to produce platelets containing this vWF-F7TF fusion protein and were observed to result in an increased haemostatic effect *in vitro* compared to donor platelets and platelets from untransduced cultures.

4 Quantifying the accuracy of genome editing with CRISPR with whole-genome sequencing

4.1 Introduction

CRISPR is a technique to edit genomes through the creation of targeted double strand breaks (DSBs) derived from a prokaryotic immune system, providing significantly more versatility over older techniques such as ZFNs and TALENs (Jinek *et al.*, 2012). The technique has proven successful in a wide range of model organisms and systems, including in iPSCs initially for disease modelling (Horii *et al.*, 2013). Specificity it is derived from a targeting guide RNA to direct the formation of these DSBs. Cas9 scans and unwinds the genomic DNA to create an R loop, changing its confirmation to expose the nuclease domain and cleaving the DNA (Szczelkun *et al.*, 2014). The specificity of this guide RNA is therefore crucial to the avoidance of off-target effects, the formation of DSBs at genomic loci not intended by the design of the guide RNA. In applying this technique to cells in culture, often large numbers of cells are transfected with a plasmid to express both the Cas9 and the guide RNA, and the culture is subcloned and screened for the desired mutation. Other techniques have also proven successful, including the nucleofection of ribonucleoproteins (RNPs), pre-prepared Cas9 and guide RNA complexes directly into cells (Foster *et al.*, 2018).

The specificity of this technique is critical for ensuring its safety in its translation to a clinical setting; off-target mutations have been reported in previous genome editing technologies (Grau, Boch and Posch, 2013). These off-target effects can impair the fitness or functionality of the edited cells, or more problematically can generate oncogenic cell clones. Initially, certain guides (reported as ‘promiscuous’) were shown to have a high off-target activity while others were not; indicating that this question is very guide RNA-dependent (Fu *et al.*, 2013). These studies were at first focused on genomic loci predicted computationally to be similar to the target sequence, in vitro cleavage assays or high-throughput reporter screens (Mali *et al.*, 2013). Later, whole genome sequencing data supported the idea that the target specificity of CRISPR is very guide-dependent; in one study off-target activity varied widely from zero to as many as 151 off-targets (Tsai *et al.*, 2015). Other studies have identified DSB hot spots that vary between cell types which may contribute to cell-type specific off-target effects (Pratto *et al.*, 2014). One study using human iPSCs identified in addition to the on-target mutation, only one high frequency off-target not present in the reference genome (Yang *et al.*, 2014).

In response to this data, several techniques have been developed to mitigate the potential off-target effects of certain applications of CRISPR, including the double nickase system (Ran *et al.*, 2013). Combining two guide RNAs and two Cas9

enzymes, each tagged to a different fluorescent protein, this technique allows for an even higher genome editing specificity, reported to reduce off-target effects by 50 to 1,500-fold in cell lines without sacrificing on-target efficiency. This is reported to occur due to DNA cuts being made only when both nickases are binding, which is unlikely to occur in off-target regions of the genomes.

For the clinical translation of both FoPMK technology and the genetically engineered FVII reported in chapter 3, the transition away from a lentivirally delivered system to a genome edited system would be favoured to meet clinical good manufacturing practice (cGMP) standards. Lentiviral technology has several significant barriers for use in the clinic in the context of FoPMK technology. Firstly, the production of lentiviral vectors in a cell line must take place alongside any iPSC culture to continuously transduce these cells after differentiation in order to avoid silencing and with each culture lasting up to 110 days, this process would need to be repeated on a consistent basis (Moreau *et al.*, 2016). Secondly, the production of lentiviruses requires transient transfection with three to four different plasmids in each vector manufacturing batch, introducing significant opportunity for variation that is undesirable in a large-scale cGMP manufacturing process (Sanber *et al.*, 2015). Thirdly, the integration of the resulting lentivirus is not a controlled process. Although integration sites are not completely random, there are many reports of lentiviral vector integration inducing alternative splicing and aberrant transcript, the consequences of which remain unknown (Moiani *et al.*, 2012). There remains an element of stochasticity and unpredictability with this technique that is undesirable in a cGMP process which may impact the safety of the resulting product.

Ideally, the constructs generated in section 3 would be engineered into a genomic safe harbour such as AAVS1 or ROSA26 to prevent genomic silencing effects, removing the complexities associated with lentiviral vector production and simplifying the cell culture process. This approach has seen great success in iPSCs (Oceguera-Yanez *et al.*, 2016). Furthermore, genome editing allows for the creation of platelets with other biological benefits such as a lack of immunogenicity. Platelet transfusions often currently need to be matched for HLA immuno-compatibility with the recipient, which reduces the pool of suitable donors considerably. Patients with platelet transfusion refractoriness (the failure to achieve an acceptable increment in platelet count following transfusion) has been documented in 30-50% of patients who undergo regular platelet transfusions and has been described to be associated with the sensitisation against HLA antigens (Brand, 2001). As platelets only express HLA class I, through knockout of HLA

Class I, it may be possible to generate ‘universal’ platelets at scale from a single stem cell line (Traherne, 2008).

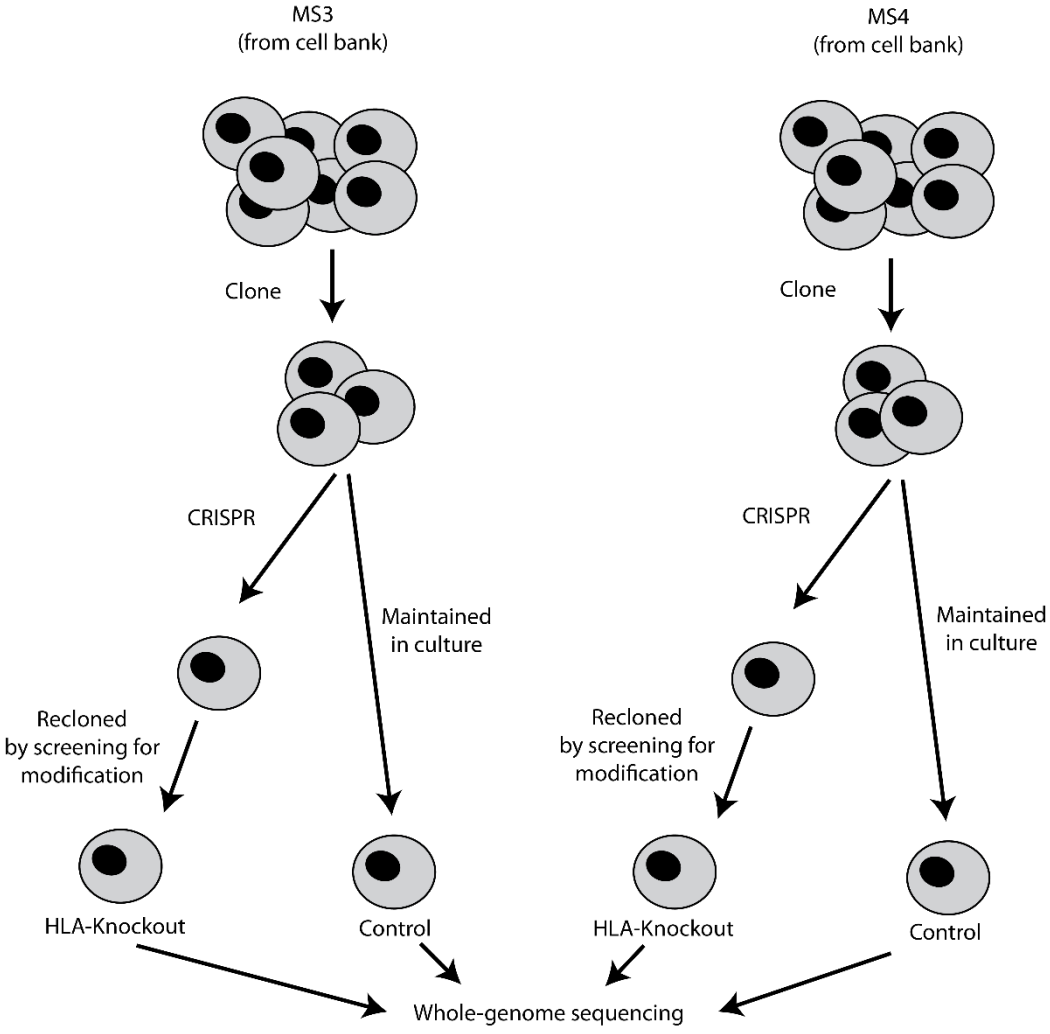

Figure 4.1. *Schematic of cell culture and CRISPR applied to generate samples for whole-genome sequencing*

A key component of the HLA Class I complex is β2-microglobulin (B2M) which forms the light chain not involved in antigen presentation but crucial in maintaining the overall structure of the complex (Arce-Gomez *et al.*, 1978). Mutations in B2M in patient have been shown to result in significant immunodeficiencies due to the failure of intracellular antigen presentation (Wani *et al.*, 2006). Mouse models with the gene knocked out showed a failure of CD8+ T cell development but otherwise generally healthy mice (Koller *et al.*, 1990). Previously, Dr Amanda Evans modified two iPSC lines (MS3 and MS4) by using the double nickase technique to knockout B2M. The samples generated for sequencing were successfully cultured as outlined in Figure 4.1, with the knockout being confirmed by PCR genotyping.

Alongside any off-target mutations introduced by the CRISPR technique, a confounding factor in any analysis is that other mutations have been reported to take place purely through the process of cell culture. This has been reported in iPSC culture, and is thought to be due to both adaptation to the conditions of cell culture, genetic drift as well as due to a lack of negative selection that would be present in vivo from a viable immune system (Thompson *et al.*, 2020).

Mutations broadly can be categorised into either single nucleotide variations (SNVs) that do not result in a frameshift, and insertion-deletions (indels) that may result in a frameshift. Many of the current techniques in the analysis of mutations come from the field of oncology. Different causes of mutation have been known to leave characteristic marks in the genome, for example, C:G>A:T transversions predominate in smoking-associated lung cancer, while C:G>T:A transversions are common in UV light-associated skin cancers (Hainaut and Pfeifer, 2001). A landmark paper looked at the profile of different types of single nucleotide polymorphisms and using unsupervised machine learning to cluster these for different drivers of mutational processes to obtain characteristic mutation signatures (Alexandrov *et al.*, 2013). An indel classification system has remained more elusive due to the more complex nature of these mutations, but recent work has attempted to apply a similar analysis (Alexandrov *et al.*, 2020).

4.2 Aims

Methods were developed to assess the off-target effects of genome editing in two stem cell lines both independently edited to be HLA-null using CRISPR with the double nickase system. Whole genome sequencing was used to identify any variation from the reference genome, with previously known variants filtered out to leave only the *de novo* mutations and compared between the control and knockout samples to remove the effect of the normal rate of mutation arising from the process of cell culture. Both SNP and indel frequencies were analysed, as well as the SNP mutation signature observed from these samples. The location of these mutations in the genome were also documented to assess their potential impact.

4.3 The SNV mutation rate in both modified cell lines appeared reduced compared to controls

All SNVs were called by comparing the control and knockout sequences to the reference genome, followed by filtering known single nucleotide polymorphisms (SNPs). As the cell culture period was known, the variants were quantified and measured as a rate of SNVs ocurring per day per base pair of DNA. In Figure

4.2A, the average rate of mutation measured was lower in the knockout than the corresponding control sample in both bases. When split by chromosome for MS3 in Figure 4.2B (control) and Figure 4.2C (knockout), the distribution of SNVs appear roughly similar, mostly distributed around the average, with a disproportionately large number of mutations ocurring in chromosome 21 and a disproportionately smaller number ocurring on the X chromosome. Similar results were observed in Figure 4.2D and Figure 4.2E for the MS4 line.

The genomic location of SNVs is important as a SNV in an exonic region may alter the amino acid sequence of the resultant protein with consequences for its function, while those in intronic or intergenic regions may not have such a direct effect on function. In Figure 4.3 the subset of SNVs that were obtained by comparing the control line to the knockout lines (as opposed to all four to the reference genome) and the genomic location of these were plotted. In Figure 4.3A the MS3 comparison shows the vast majority of the SNVs detected occur in intergenic regions, followed closely by intronic regions. Only a very small fraction of all the SNVs detected occur in exonic regions. In Figure 4.3B a similar result is obtained for the MS4 comparison, with slightly more SNVs observed in exonic regions than with the MS3 line.

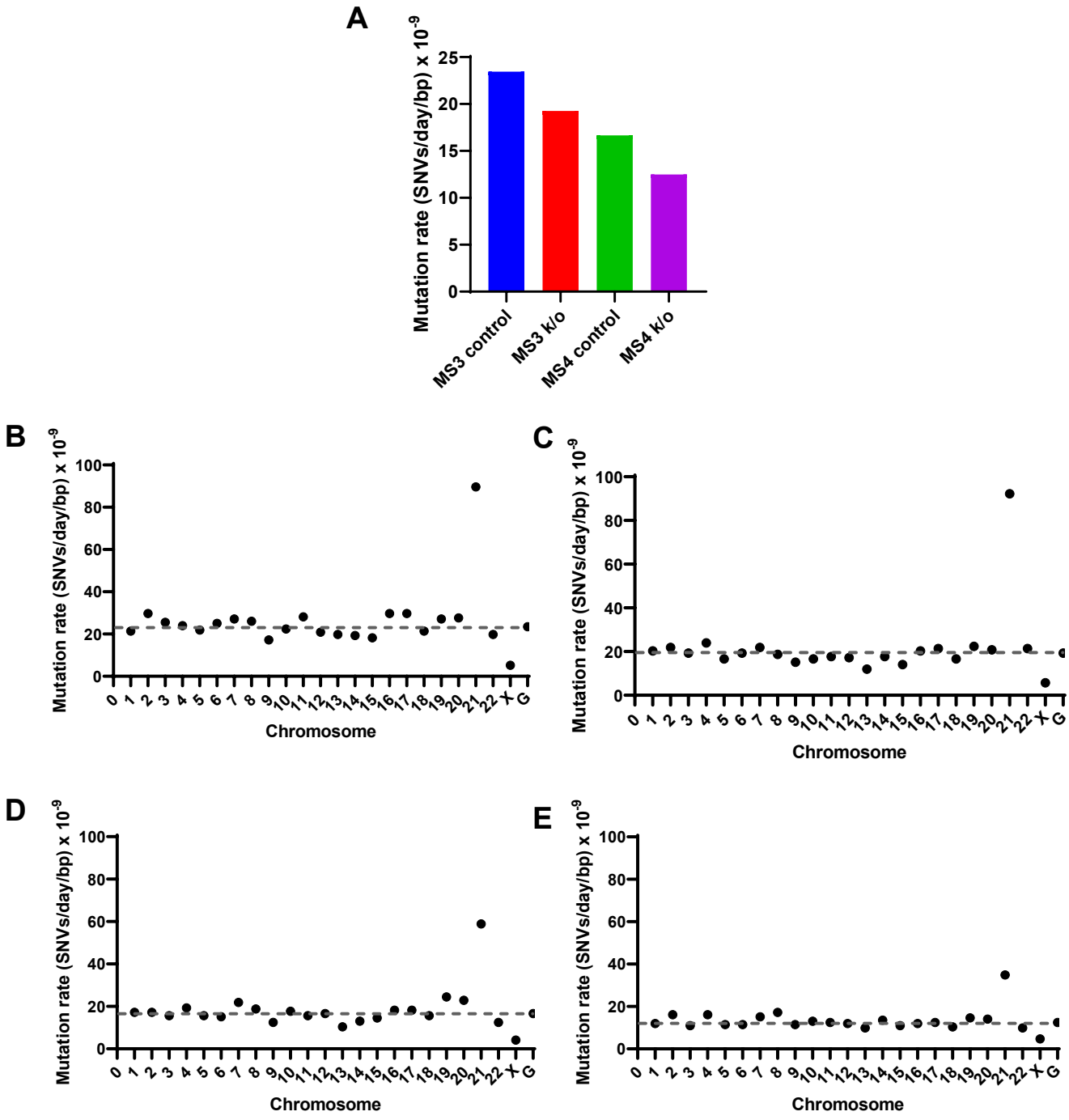

Figure 4.2. *Summarised SNV data from control and knockout samples from both cell lines. (A) The average mutation rate for each sample per day in cell culture per base pair. (B) The distribution of these mutations across each chromosome in the MS3 control sample (C) Chromosomal distribution of mutations in the MS3 knockout sample. (D) Chromosomal distribution of mutations in the MS4 control sample (E) Chromosomal distribution of mutations in the MS4 knockout sample. G – average across all chromosomes, plotted in (A).*

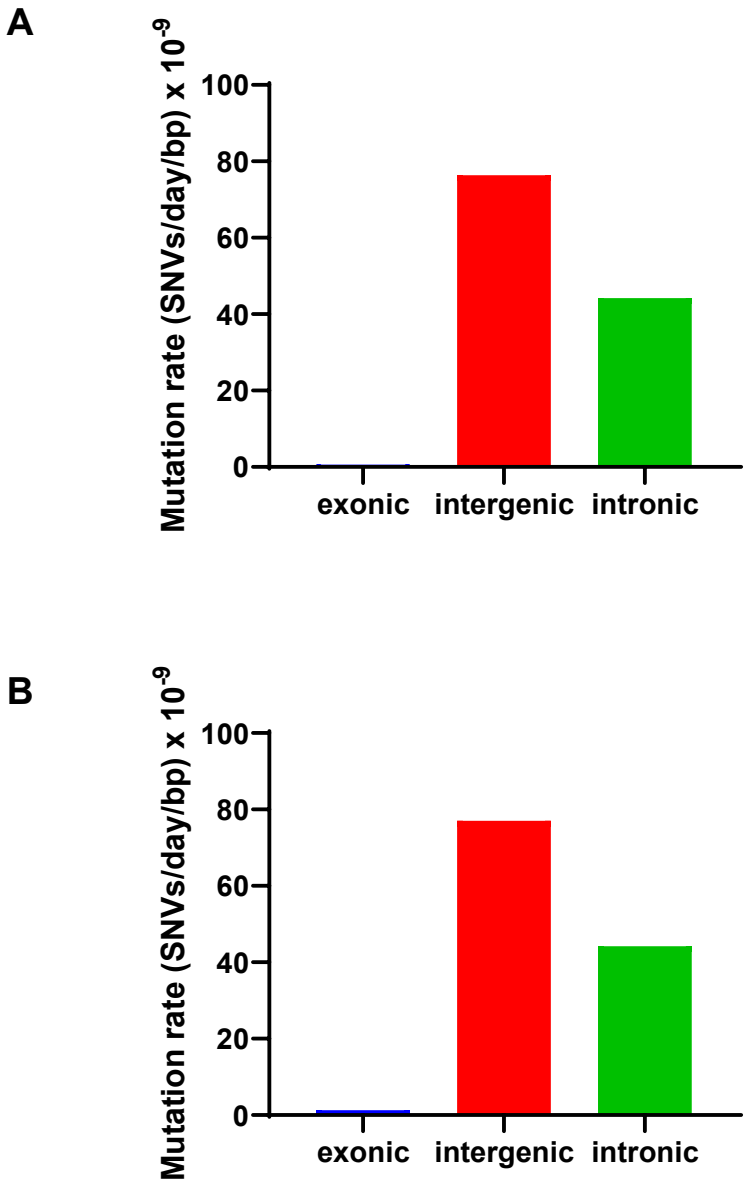

Figure 4.3. *Comparing the difference between the knockout and control lines to show the genomic region where the SNVs are located. (A) From the MS3 control vs knockout lines. (B) From the MS4 control vs knockout lines.*

4.4 SNV mutation signatures from modified cell lines were quantified

The mutational signatures of the SNVs observed in each of the four samples were also quantified to identify the process driving the formation of these mutations. In Figure 4.4, the main types of SNVs observed were C>T transitions followed by T>C transitions and this was consistent across all four samples and across the context of the surrounding two base pairs (e.g. ACA was likely to convert to ATA). No additional mutational signatures were observed in the knockout cells compared to the controls, indicating the same process was driving the acquisition of mutations independent of the CRISPR knockout modification.

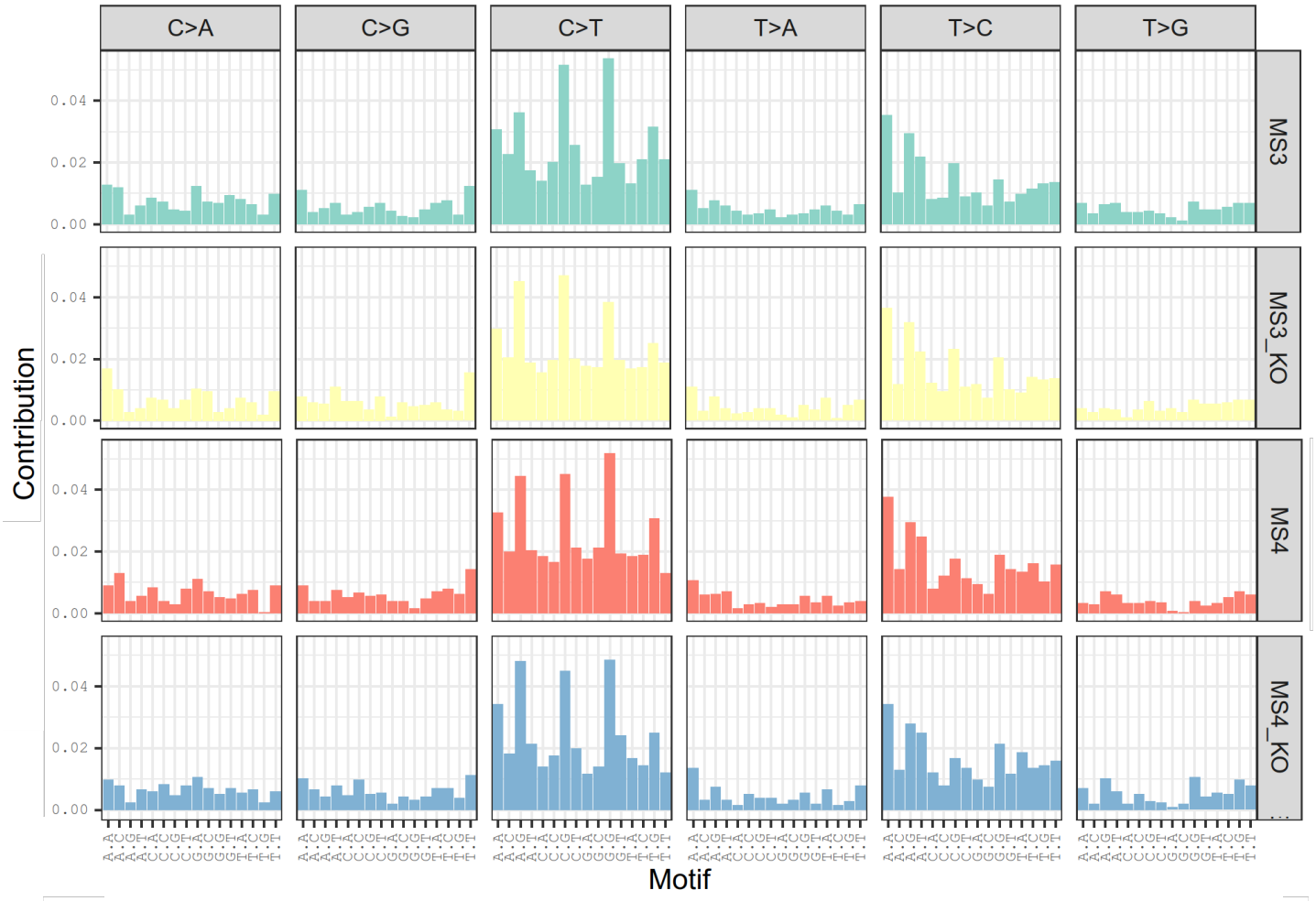

***Figure 4.4**. Results from quantifying the types of motifs and mutational signatures present in all four samples. Each column represents a different single nucleotide substitution, while the subcolumns indicate the context of the two bases surrounding the mutated base. Each bar represents the contribution of that mutation subtype to the overall mutational phenotype in the sample. Each row represents a different biological sample, either the control or knockout for MS3 and MS4.*

4.5 Indel frequency was also quantified in all samples

Similar to the SNV data, the indel frequency was quantified and the knockouts of MS3 had a slightly lower rate of mutation than the corresponding control (Figure 4.5A). MS4 had a higher rate of indels detected than its respective controls. On the chromosomal breakdown for MS3 (Figure 4.5B and Figure 4.5C), there appeared to not be any individual chromosome significantly contributing to the indel load on these cells; chromosome 17 and 19 appear to be consistently higher than the average, while chromosome 9, 22 and X appear to consistently be lower than the average. This pattern is repeated in the MS4 line (Figure 4.5D and Figure 4.5E). This suggests that the distribution of indels may not be random and that certain chromosomes have features more amenable to indels than others, or that common factors have resulted in the detection of artefacts in both cell lines at similar locations.

The types of indel occurring in these samples were also quantified in Figure 4.6. Variants were compared between knockout and control lines, and the types of the indels detected when performing this comparison were classified as complex, deletion or insertion. In both MS3 and MS4 comparisons, the vast majority of detected indels appear to be complex, consisting of both insertion and deletion of bases, followed by deletions. Although some purely insertion indels were detected in these samples, the proportion compared to the complex indels detected is very low.

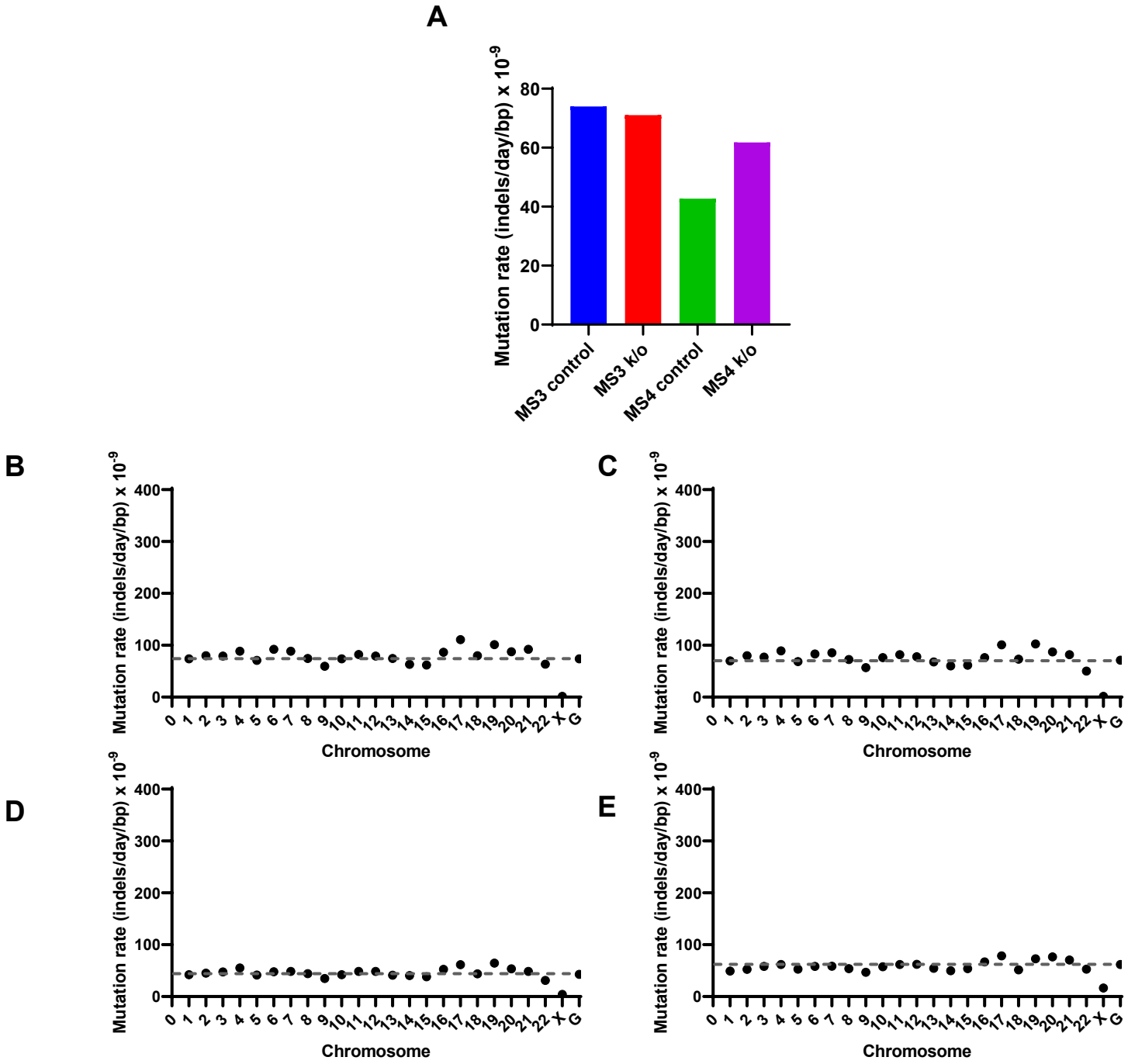

Figure 4.5. *Summarised indel data from control and knockout samples from both cell lines. (A) The average mutation rate for each sample per day in cell culture per base pair. (B) The distribution of these mutations across each chromosome in the MS3 control sample (C) Chromosomal distribution of mutations in the MS3 knockout sample. (D) Chromosomal distribution of mutations in the MS4 control sample (E) Chromosomal distribution of mutations in the MS4 knockout sample. G – average across all chromosomes, plotted in (A).*

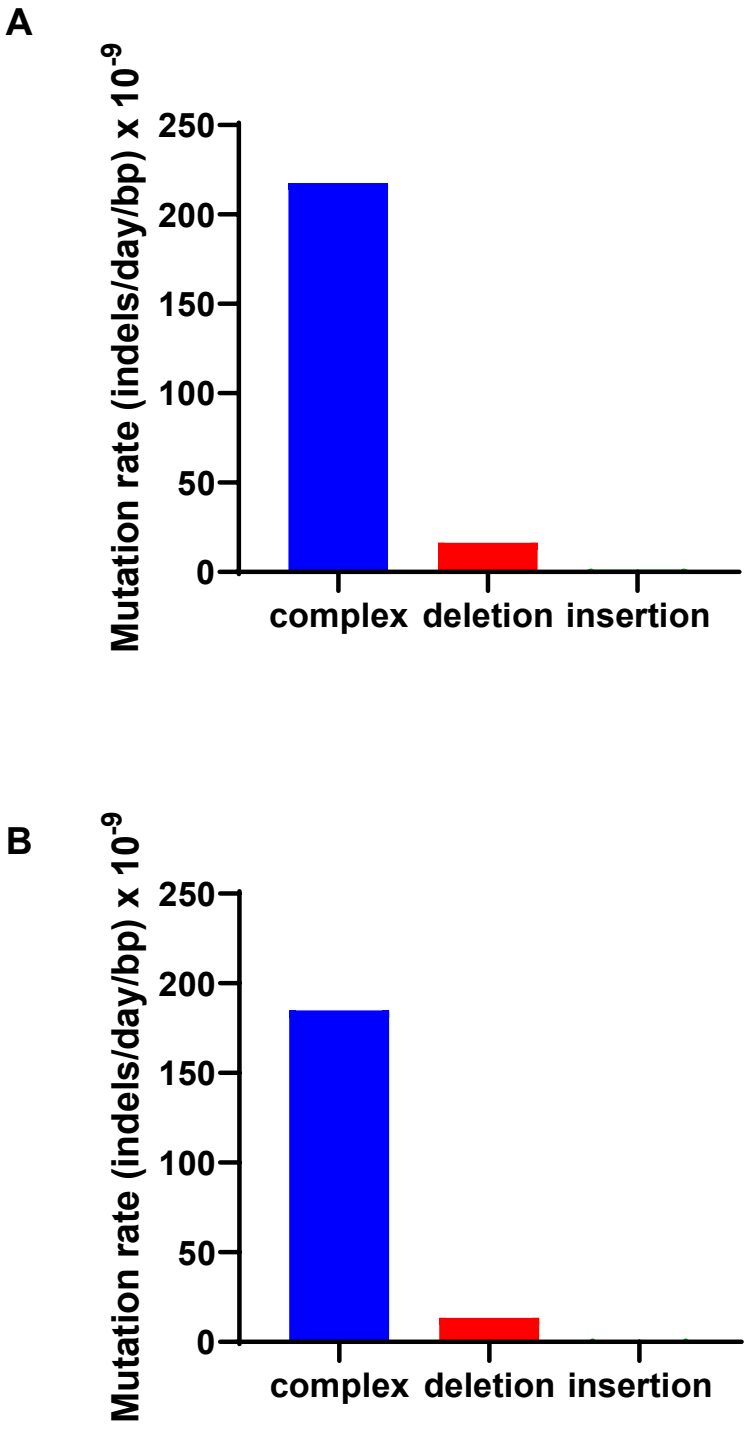

***Figure 4.6**. The different types of indels seen in comparing the KO to the control line in (A) MS3 and (B) MS4. Complex – a combination of insertions and deletions at the same locus.*

4.6 Circos plots visualise all SNV and indel data laid across the genome

By overlaying the SNV and indel data on top of one another, it becomes possible to identify areas rich in both; i.e. mutational hotspots. Circos plots were generated to visually identify such areas (Figure 4.7 and Figure 4.8); if a high incidence of indels and SNVs appeared at specific genomic loci in the knockouts but not the controls, this may indicate a mutational scar from on- or off-target effects of CRISPR.

The large number of complex indels were observed as the blue band spanning a large proportion of the plots in all four samples. There is a visible deletion stripe on chromosome 15 in both Figure 4.7B and Figure 4.8B absent in the controls Figure 4.7A and Figure 4.8A, indicating the location of B2M (chr15:44711487-44718877) thereby further confirming the success of the on-target effect of the CRISPR (Faber *et al.*, 1976).

Comparing Figure 4.7A and Figure 4.7B, a mutational hotspot identified in Figure 4.2B and Figure 4.2C is visible as an area with insertion, deletion and complex indels and SNVs in chromosome 21, but is present in both control and knockouts. Another potential hotspot was observed in chromosome 2, with an increase in concentration of SNVs and indels in the knockouts compared to the controls in MS3 (Figure 4.7A and Figure 4.7B).

The hotspot observed in chromosome 21 in MS3 is also present in the MS4 knockout plot (Figure 4.8B) and yet absent from the corresponding control (Figure 4.8A). The hotspot observed in chromosome 2 in MS3 is absent from the MS4 plots. However, a hotspot was identified on chromosome 20 with additional mutations in the knockout than the control in the MS4 line (Figure 4.8B) that was not present in MS3.

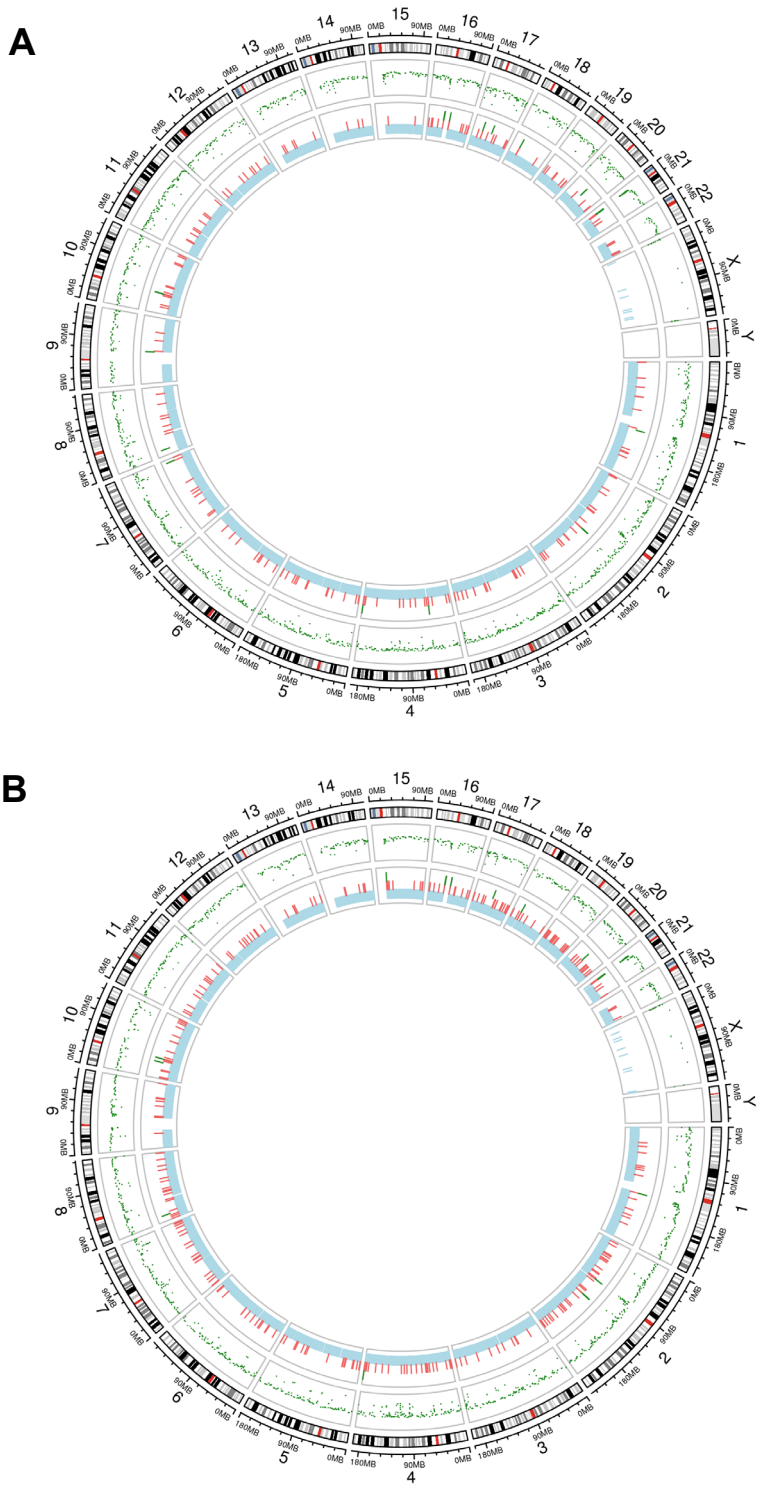

Figure 4.7. *Circos plot of MS3 (A) control and (B) knockout cell lines. The inner light blue ring represents the location of complex indels, with the red and green lines representing deletions and insertions respectively. The green dots represent the locations of the SNVs, with a position closer to the centre of the circle indicating a higher concentration of SNVs at that locus.*

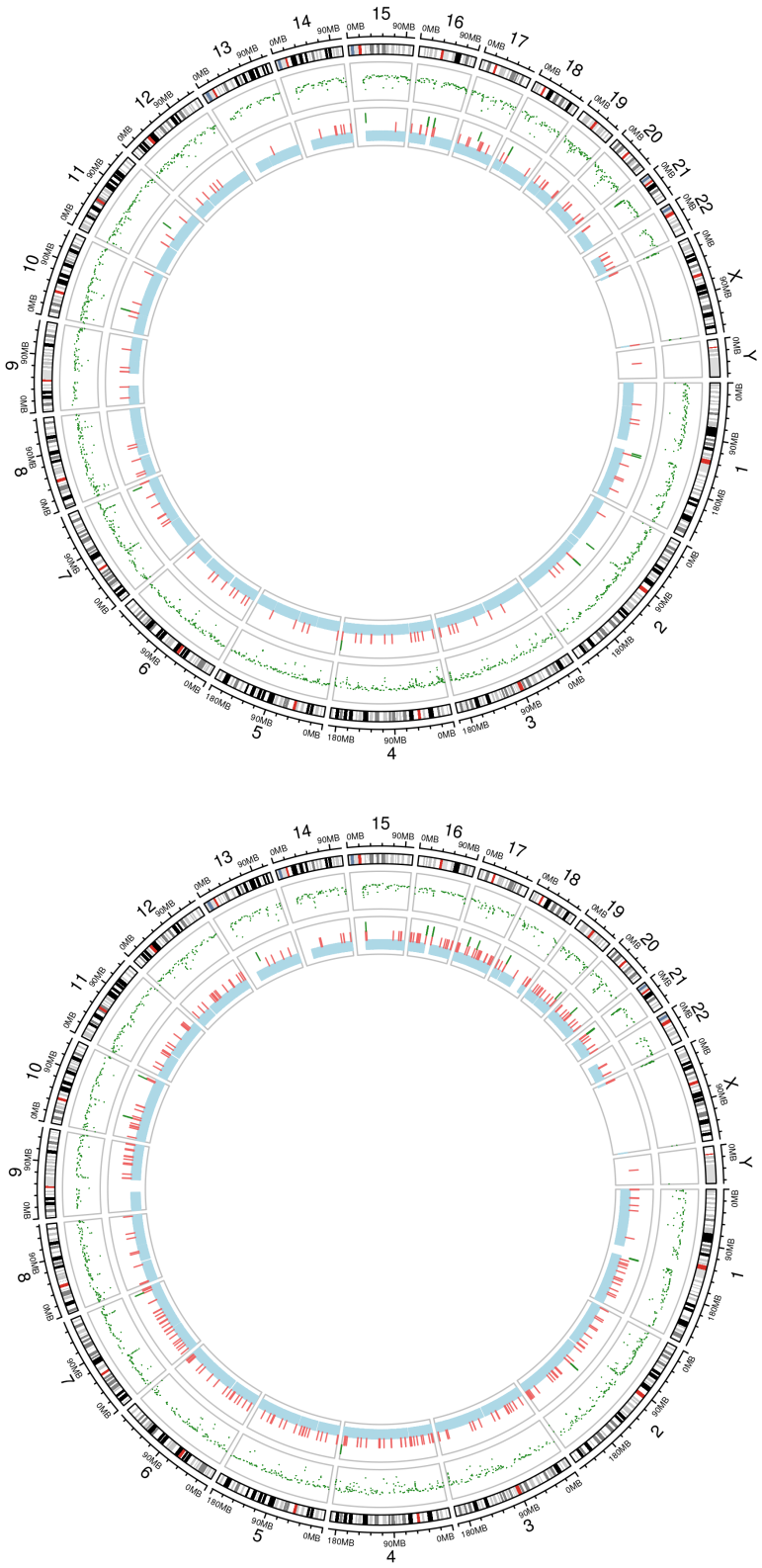

Figure 4.8 *Circos plot of MS4 (A) control and (B) knockout cell lines. The inner light blue ring represents the location of complex indels, with the red and green lines representing deletions and insertions respectively. The green dots represent the locations of the SNVs, with a position closer to the centre of the circle indicating a higher concentration of SNVs at that locus.*

4.7 Discussion

Notably, the findings from this analysis were from a single genome sequencing of each cell line at one point in time, ideally these would be repeated for biological replicates to allow for statistical analysis with a t-test to confirm the differences observed are not due to chance. The methodology, however, was established into a pipeline such that the analysis may be repeated on future samples.

As this methodology relied on comparison with a reference sequence and filtering out known SNPs, it remains possible that SNPs that are common but unreported were classified as de novo mutations despite existing prior to the experiment. Ideally, the parent culture from which both the control and knockout cultures would also be sequenced to get a true mutation rate over a known time period; many variant calls seen from comparison with the reference genome are likely to be variants rather than true mutations, mixed with the true mutations that have been observed to take place over the duration of a cell culture (Thompson *et al.*, 2020).

The many variants seen in common between the MS3 and MS4 lines is also of note as several studies have shown that pluripotent stem cells acquire mutations in cultures that confer a survival advantage to the stem cells so that within a few passages that whole culture is dominated by the mutant clone (Baker *et al.*, 2016; Merkle *et al.*, 2017).

In Figure 4.2A, the SNV mutation rate was reduced in the knockouts compared to the controls. This is likely due to genetic bottleneck effects from the re-cloning involved in CRISPR as outlined in Figure 4.1. The act of re-cloning likely reduced the genetic variation present in the wider culture resulting in an observed lower rate of mutation.

From the SNV data (Figure 4.2B,C,D and E), there were certain chromosomes (e.g. 21) predisposed to acquiring mutations than others and that this was not a random uniformly distributed process. This has been reported in the literature previously. Between 12.5% and 34% of all human pluripotent stem cell lines have been found to acquire specific non-random chromosomal abnormalities over time particularly in chromosome structure and number in chromosomes 1, 12, 17 and 20 that were reminiscent of changes also observed in cancers (Na *et al.*, 2014).

In Figure 4.3, both MS3 and MS4 have the vast majority of their mutations in intergenic or intronic regions. SNVs in exonic regions are a very small percentage of the total SNVs, which implies that most of the detected SNVs have no effect

on protein structure. However, intergenic regions are no longer thought of as 'junk DNA' and has been found to have an important role in gene regulation (Pennisi, 2012). The impact of the SNVs detected will therefore likely not affect protein function, but may affect protein expression through effects on gene regulation.

In Figure 4.3, the numbers of recorded mutations are much higher than those observed in Figure 4.2. This is likely because the comparisons in Figure 4.2 are with the reference genome, while in Figure 4.3 they are between the knockout and their matched controls. As the cultures have diverged over time, it is likely they have developed different sets of mutations independently, and this results in the inflated numbers seen here as both sets of mutations are included in the comparison in Figure 4.3 rather than one or the other seen in Figure 4.2.

The same analysis performed for SNVs in Figure 4.3 was not repeated for indels as the effect of an indel can reach far beyond the location in which it is detected. For example, a frameshift can affect the entire length of the protein or intronic sequence despite only being a 2bp change. Furthermore, unlike SNVs, indels can be large and span several different types of genomic region. For these reasons, it is not an appropriate analysis to apply to elucidate what effects the presence of these mutations might have on overall gene expression.

The mutation signature observed in Figure 4.4 has been designated SBS5 (of unknown origin) in the literature, and has been detected in most cell cultures, having been attributed to processes generating mutations throughout life at constant rates in all individuals (Alexandrov *et al.*, 2015; Petljak *et al.*, 2019).

From Figure 4.5A, the rates of indel formation are two- to three-fold higher than the rates of SNV occurrence seen in Figure 4.2A. In all the chromosomal breakdowns of mutation rates, the X chromosome is consistently lower than the average across the genome. This is likely due to a low coverage of sequencing reads across the X chromosome due to its highly repetitive regions and therefore an artefact of the experimental setup than a true lower mutation rate (Ross *et al.*, 2005).

From Figure 4.6, the vast majority of indels detected were complex (consisting of both insertion and deletion of elements). This may be another artefact of the sequencing technology used, as short read sequencing containing indels may not align with the genome at all or misalign with an incorrect part of the reference genome. There were very few insertions detected and this may reflect the tendency for NHEJ and HR to favour deletions in the DNA repair pathway (Mao

et al., 2008). This may also reflect the inability of short read sequencing to detect the insertion of mobile genetic elements such as LINE-1 (Teissandier *et al.*, 2019).

The circus plots in Figure 4.7 and Figure 4.8 confirm the success of the targeted deletion of the B2M locus. The appearance of other genetic mutation hotspots was noted, but not consistent between the MS3 and MS4 lines. This may be interpreted as CRISPR not causing any repeated off-target effects at specific off-target locations. This does not rule out the possibility of CRISPR causing random mutations throughout the genome, but Figure 4.2A and Figure 4.5A suggest that this is not the case either.

Overall, from this analysis, despite the limitations mentioned above, the data suggests that the double nickase technique with the specific guides used to knockout HLA in these iPSC lines was successful, and that it posed no additional mutational burden on these cells. On the contrary, the re-cloning process appeared to have reduced the genetic diversity of the cell culture.

Knowledge of the mutations present in these cells may provide an opportunity to spot harmful mutations that may occur by chance, for example in p53 as has been reported to have been acquired in certain stem cell lines previously (Merkle *et al.*, 2017). These issues become especially relevant when ensuring any transplant or transfusion of cells that have been designed to avoid immunogenicity (e.g. through B2M knockout) become tumorigenic. As iPSC-derived technologies such as forward-programming move to clinical translation, regulatory bodies will want to see evidence of safety and efficacy. These kinds of assays may provide further proof of the safety of genome-edited therapies as well as an opportunity for ongoing quality control as part of the manufacturing process. In one recent study, Ito and colleagues intend to translate the *in vitro* platelets they derived from immortalised MK cultures into human patients and techniques such as these may help to assure regulators that the resultant products will adhere to the Hippocratic principle of first doing no harm (Ito *et al.*, 2018).

This approach can be generalised and used as a pipeline for any other genome editing performed on iPSCs. For future work, ideally the direct parental cell culture from which both the control and edited cells were derived (Figure 4.1) would also be sequenced to accurately assess the effects of random mutations due to cell culture compared with those induced by the genome editing process.

5 Passive absorption results in platelets loaded with rFVIIa that have an improved haemostatic effect in vitro

5.1 Introduction

As described in Figure 1.6, the two main routes by which proteins are present within the α-granules of megakaryocytes and subsequently platelets are through protein synthesis and endocytosis. Previous work has shown that both MKs and platelets are able to passively endocytose and pinocytose certain proteins such as fibrinogen and immunoglobulins (synthesised by hepatocytes and B cells respectively) into these granules which are then released upon stimulation by agonists (Handagama, George, *et al.*, 1987).

Mass spectrometry data has shown that the contents of the α-granules are wide-ranging, a testament to the wide variety of roles that platelets play not just in thrombosis but also inflammation (Maynard *et al.*, 2007). Notably, not all proteins present in the plasma are endocytosed into the α-granules. For example, factor V is present in α-granules but not factor VII. This suggests that rather than being a passive process, endocytosis in this context is specific to certain proteins binding to specific receptors.

Clathrin-coated membranes were first noted in platelets in 1982 (Morgenstern, 1982). Clathrin-coated pits were shown to line the plasma membrane and open canalicular system (OCS), either existing by themselves or fused with secretory α-granules, shown to transfer plasma components to platelet granules (Behnke, 1989). Other studies show that both clathrin dependent and independent endocytosis take place in platelets. The data suggests cargo is delivered to α-granules and the endosomal-lysosome pathway respectively. These studies involve resting platelets with colloidal gold-tagged fibrinogen, now used as a marker for receptor-mediated endocytosis, and acid phosphatase, a marker for lysosomes (Behnke, 1992).

The endocytosis of rFVIIa into granular structures within cells is not unique to megakaryocytes and platelets. Studies with rFVIIa tagged with a fluorophore revealed that it accumulates in hepatocytes, in zones of calcified cartilage in bone, and other extravascular spaces containing tissue factor-expressing cells (Gopalakrishnan *et al.*, 2010). rFVIIa has also been shown to be endocytosed by endothelial cells through the endothelial cell protein C receptor (EPCR) (Ghosh *et al.*, 2007). This binding has also been shown to reduce its pro-coagulant activity (López-Sagaseta *et al.*, 2007).

Some studies suggest that in vivo, sequestration within megakaryocytes and shielding from the normal proteolytic and excretion mechanisms acting on proteins present in the plasma may be a reason for the efficacy of once-daily

rFVIIa injections for patients with haemophilia despite its plasma half-life of 2 hours. One group have shown that MEG-01 cells, from a human megakaryoblastic leukaemia cell line, were able to take up rFVIIa passively through the endothelial protein C receptor (EPCR). The platelets produced from this appear to subsequently contain rFVIIa (Schut *et al.*, 2017).

Hoffman and colleagues demonstrated that rFVIIa is able to bind weakly to activated platelet membranes and locally enhance thrombin generation (Hoffman and Monroe, 2010). This association has been described to take place through binding to GPIb-IX-V (Weeterings *et al.*, 2008). More recently, another group showed using intracellular flow cytometry that rFVIIa can be directly endocytosed by platelets of FVII-deficient patients, suggesting that this may also contribute to the prolonged half-life observed with rFVIIa (Lopez-Vilchez *et al.*, 2011).

5.2 Aims

Although the endocytosis of rFVIIa into platelets and megakaryocytes has been described before in the context of explaining the prolonged efficacy of rFVIIa beyond its theoretical plasma half-life, it has not been explored as a method to deliver rFVIIa using platelets for haemostatic effect in normal individuals for the treatment of acute haemorrhage.

To provide further evidence for the mechanisms described in the literature, *ex vivo* mouse megakaryocytes and human FoPMKs were used to investigate whether rFVIIa can be endocytosed outside of a transformed cell line, and whether these can then produce platelets that have loaded with rFVIIa in their granules. The preliminary results from Lopez-Vilchez and colleagues were also validated. Human donor platelets were also tested for their ability to directly endocytose rFVIIa into α-granules, not lysosomes, and maintain functional activity. This was performed in the context of augmenting a transfusion unit to improve its haemostatic effect. These resultant platelets were then assayed to see if they can then subsequently release this rFVIIa upon stimulation, and the effect of these loaded platelets in *in vitro* clotting assays were observed.

5.3 Mouse megakaryocytes and their resultant platelets were evaluated for their ability to endocytose rFVIIa

Mouse bone marrow-derived HSCs were harvested and differentiated into megakaryocytes in culture to evaluate their ability to endocytose rFVIIa (section 2.3.7). In Figure 5.1, they were evaluated for the presence of intracellular FVII by flow cytometry.

Gates were set up first by forward and side scatter and singlet events were gated for (Figure 5.1A). A Per/Cy7-only control was used to set up the gate for CD42d, a marker of mouse megakaryocytes. These gates were then used to set up the gating for FVII in Figure 5.1B, by using a control stained for CD42d but with only secondary antibody staining for FVII.

Mouse MKs not incubated with rFVIIa in this experiment showed 7.79 ± 0.778% positive for FVII (Figure 5.1C) while mouse MKs incubated with FVII reported 8.01 ± 0.826% positive for FVII (Figure 5.1D) (mean ± SEM). The overall difference was not statistically significant when compared in a paired t-test (n=3 for each condition, $p>0.05$) (Figure 5.2B).

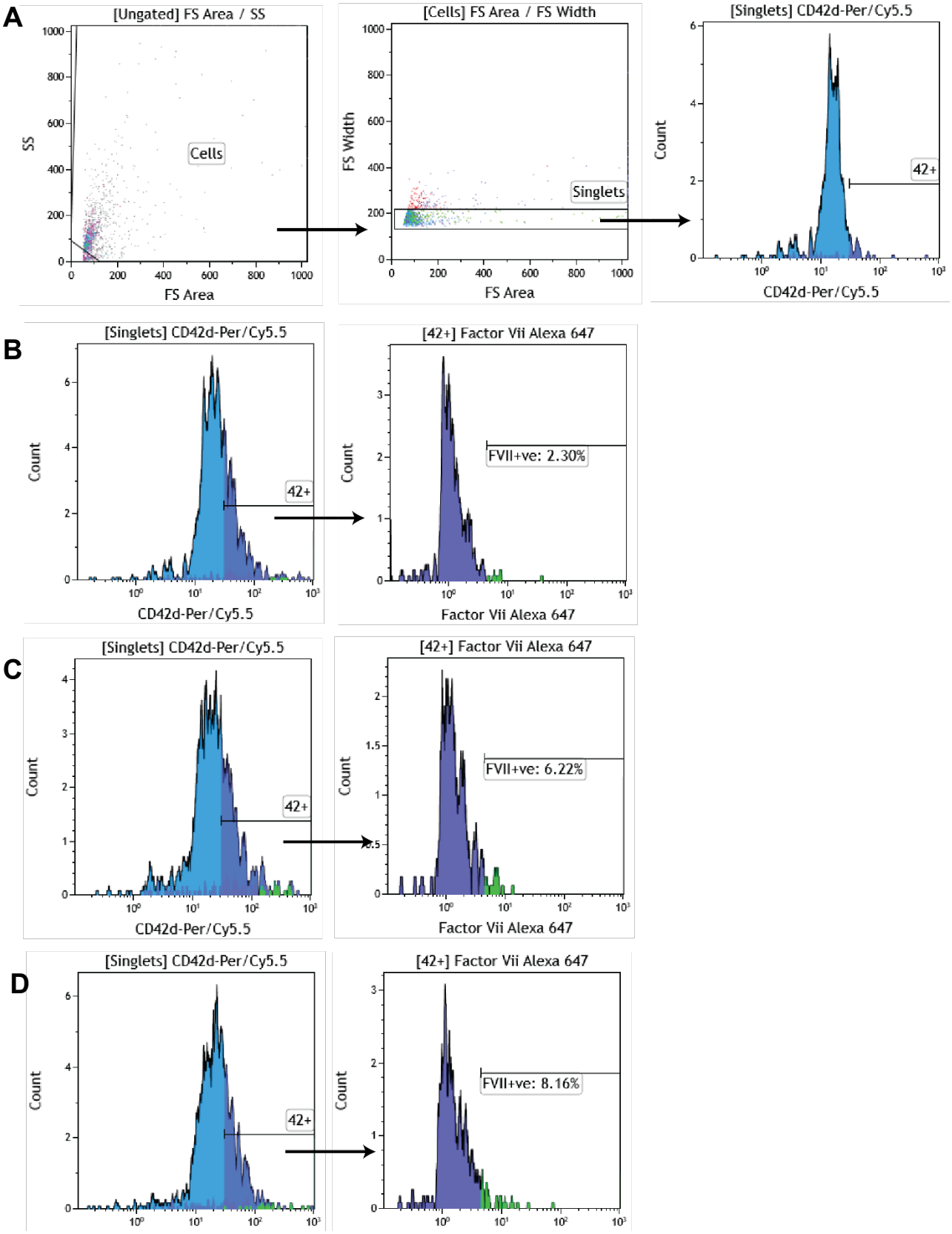

Figure 5.1. *Mouse MKs derived from bone marrow were incubated for 24 hours with or without recombinant FVII. They were washed to remove excess FVII and intracellular staining was performed defining MKs using the Ab against CD42d (A) Isotype control for CD42d. Gating strategy from FS/SS, to singlets to setting up the CD42d gate (B) Control for FVII staining. Gate setup for FVII with CD42d and secondary antibody only. (C) Mouse MKs incubated without rFVIIa (D) Mouse MKs incubated with rFVIIa*

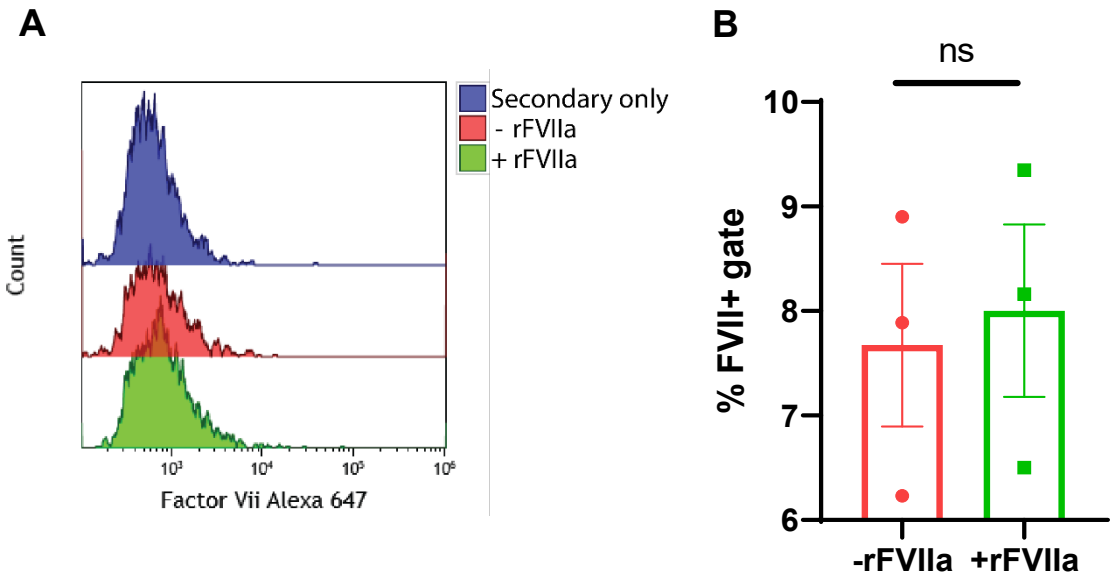

Figure 5.2. *Statistics from several experiments incubating mouse MKs with rFVIIa. (A) The FVII stainings from isotype, -rFVIIa and +rFVIIa were overlaid on a single plot. (B) % gating positive for FVII staining were quantified from biological replicates. n=3, a two-tailed paired t-test was performed at the $p < 0.05$ significance level, data shown as mean ± SEM.*

Although no statistically significant increase was seen in the MKs from Figure 5.2B, platelets were collected from each of these experiments to evaluate whether any rFVIIa had already been produced and packaged into the platelets.

For the experiments in Figure 5.3 and Figure 5.4, platelets from the MKs in Figure 5.1 and Figure 5.2 were collected and analysed by intracellular flow cytometry. Gates were first set up from the isotype control for CD42 (Figure 5.3A) on size and the gate for CD42d was set up. On the secondary-only control for FVII (Figure 5.3B), the gate for the FVII was set up after selecting the events positive for CD42d. On platelets from MKs not incubated with rFVIIa (Figure 5.3C) compared with platelets from MKs incubated with rFVIIa (Figure 5.3D), there was a slight increase in percentage of events staining positive for FVII (on average, from 7.81% to 9.56%, from Figure 5.4B), but this was not statistically significant at a $p<0.05$ level. An overlay plot showing the FVII stainings for a representative isotype, platelets from MKs without and with rFVIIa are shown in Figure 5.4A.

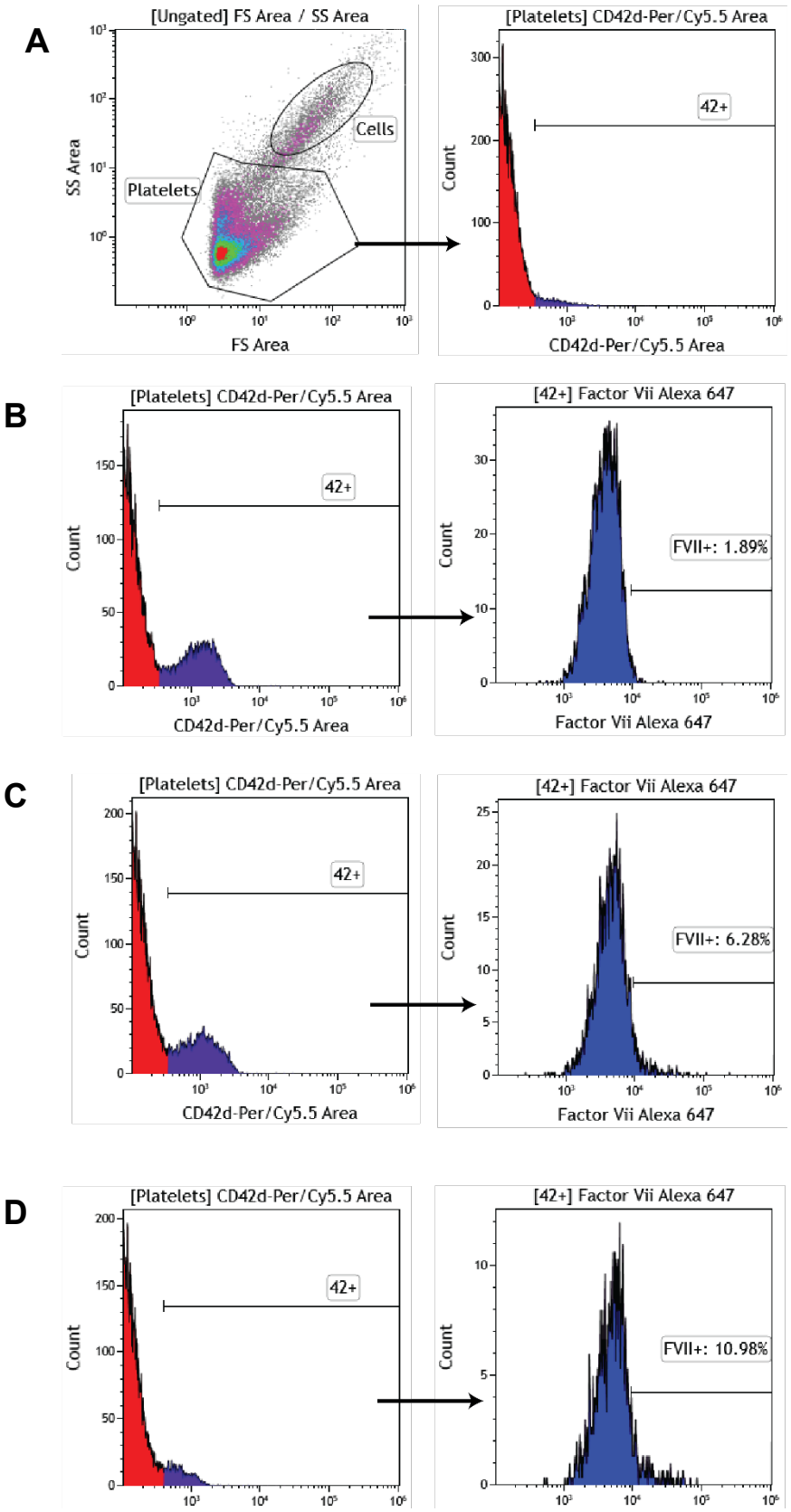

Figure 5.3. *Representative intracellular flow cytometry plots of platelets from mouse MKs incubated with or without rFVIIa. Platelets were defined by size and presence of CD42d. (A) Isotype control for CD42d. Gating strategy from FS/SS to set up the CD42d gate. (B) Secondary antibody only control for FVII. This was used to set the gates for %FVII+ve. (C) PLPs from MKs incubated without rFVIIa (D) PLPs from MKs incubated with rFVIIa.*

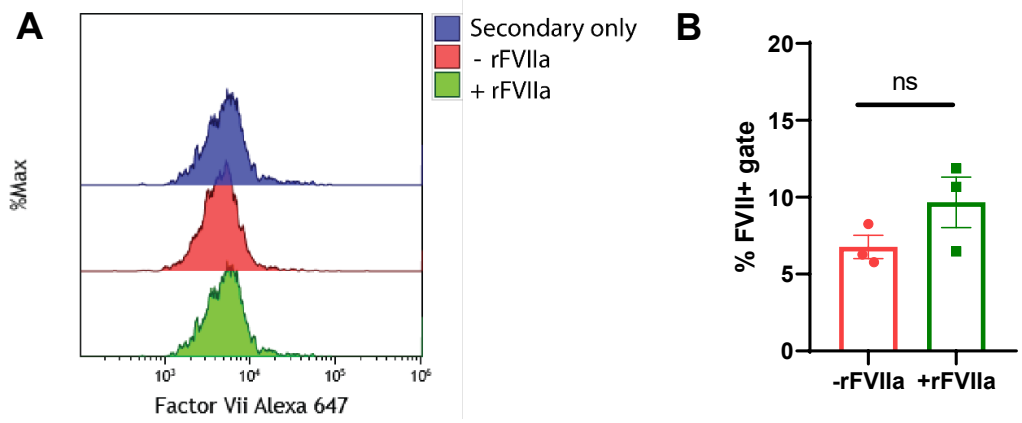

Figure 5.4. *Summary of statistics for intracellular staining of platelets from MKs incubated with or without rFVIIa. (A) Overlay plot showing secondary only control, platelets from MKs without rFVIIa and platelets from MKs with rFVIIa (B) Percentage of platelets staining positive for intracellular rFVIIa, n=3, two-tailed paired t-test at a significant level of p<0.05. Data shown as mean ± SEM.*

5.4 Forward-programmed megakaryocytes were able to endocytose rFVIIa into granules

Forward programmed megakaryocytes were first assessed for viability (DAPI negative) and megakaryocyte identity (through expression of both CD41 and CD42) before any experiments were performed (Figure 5.5) to ensure cells were at least >50% viable and >60% CD41+ and CD42+.

FoPMKs incubated with or without rFVIIa for 24 hours at 37ºC were fixed, permeabilised and stained for FVII before being analysed by flow cytometry. They were first gated on size to exclude debris (Figure 5.6A), and gating for FVII was established on a secondary only control (Figure 5.6B). FoPMKs incubated without rFVIIa showed on average 5.29% positive for FVII, likely non-specific binding (representative plot in Figure 5.6C and average from three experiments in Figure 5.6F), while those incubated with rFVIIa showed on average 45.5% positive, which proved a significant increase to a p<0.05 level.

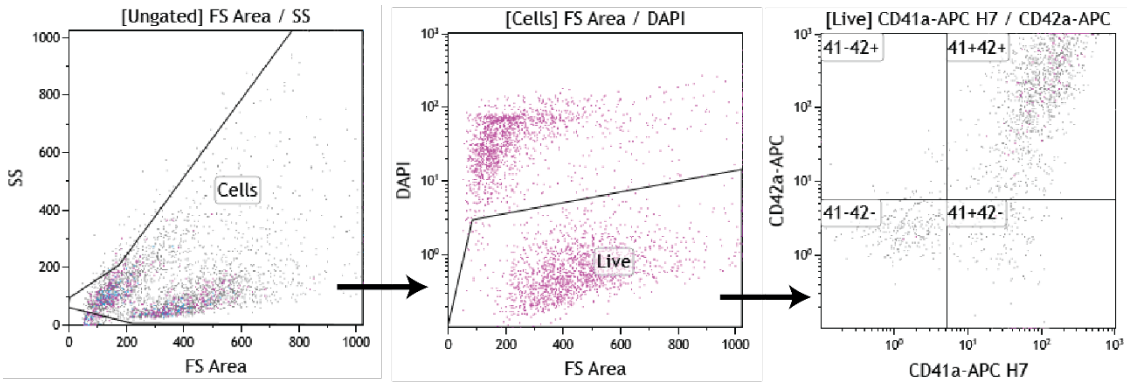

Figure 5.5. *Flow cytometry data to assess the viability of the FoPMK population (DAPI) and expression of markers for megakaryocytes (CD41 and CD42) to confirm their identity.*

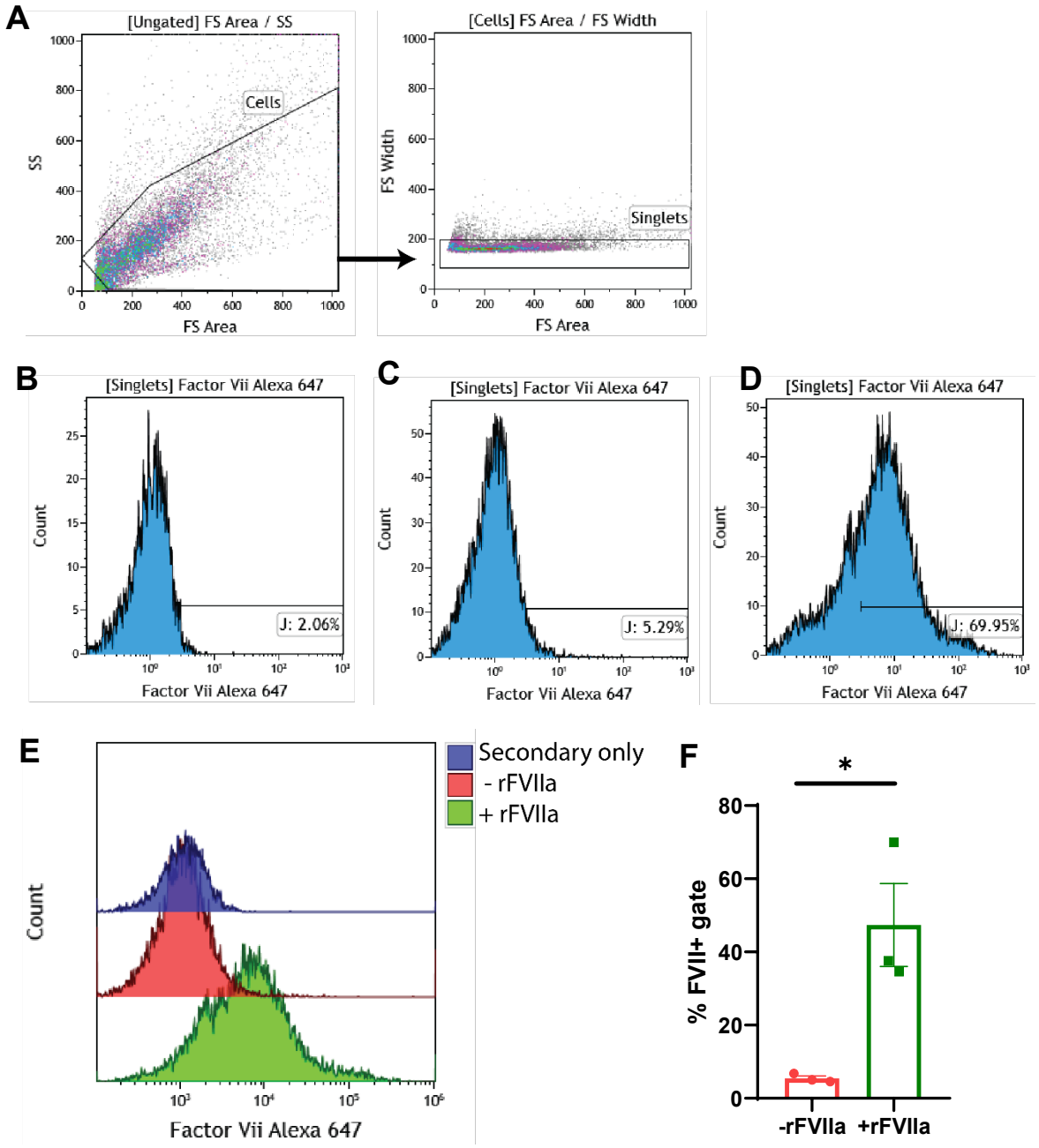

Figure 5.6. *Representative flow cytometry plots of FoPMKs incubated with and without rFVIIa for 24 hours before being washed and stained. (A) Cells were gated on FS/SS and then for singlet events (B) Secondary only staining was used to set up FVII gating (C) FoPKs not incubated with rFVIIa (E) FoPMKs incubated with rFVIIa (F) Overlay plot for FVII staining in secondary only control, without and with rFVIIa. (G) Quantified percentage of events in percentage gating FVII+ve under both conditions assessed by a two-tailed paired t-test, * p< 0.05, n=3; data shown as mean ± SEM.*

To verify that the rFVIIa was present intracellularly and not simply adsorbed to the surface of the megakaryocytes, flow staining was repeated with and without permeabilization and a marker for megakaryocytes (CD41) and viability (Zombie) (Figure 5.7). Gates were established first on FS/SS and then to select only singlet events. The gate for CD41 was established using an isotype control for this antibody (Figure 5.7A). Gating for Zombie was established on samples stained for CD41 but not Zombie (Figure 5.7B). Gating for FVII was then set up on samples stained for CD41 and Zombie but only the 647 secondary antibody (Figure 5.7C). FoPMKs were incubated with rFVIIa for 24 hours at 37ºC before being washed and stained for FVII either with or without permeabilization (Figure 5.7D-G). All controls used to establish the gating strategy were unpermeabilised. This was summarised in overlay flow plots (Figure 5.8A) and quantified for three biological replicates (Figure 5.8B), which confirmed a significant ($p<0.05$) difference between the FoPMKs incubated with rFVIIa and permeabilised compared with all other samples. From this data, FVII was confirmed to be present intracellularly in live megakaryocytes, and not adsorbed to their surface nor attached to dead cells.

Immunofluorescence data further confirmed the endocytosis of FVII into these cells. Secondary antibody staining established no granular objects seen without any primary antibodies and acted as a control for background fluorescence signal (Figure 5.9A). Confocal images showed the presence of granular objects staining for rFVIIa in the cytoplasm of these FoPMKs (Figure 5.9C) that were absent in FoPMKs not incubated with rFVIIa (Figure 5.9B). However, the granules did not appear to co-localise with thrombospondin, the marker used for α-granules in Figure 3.1.

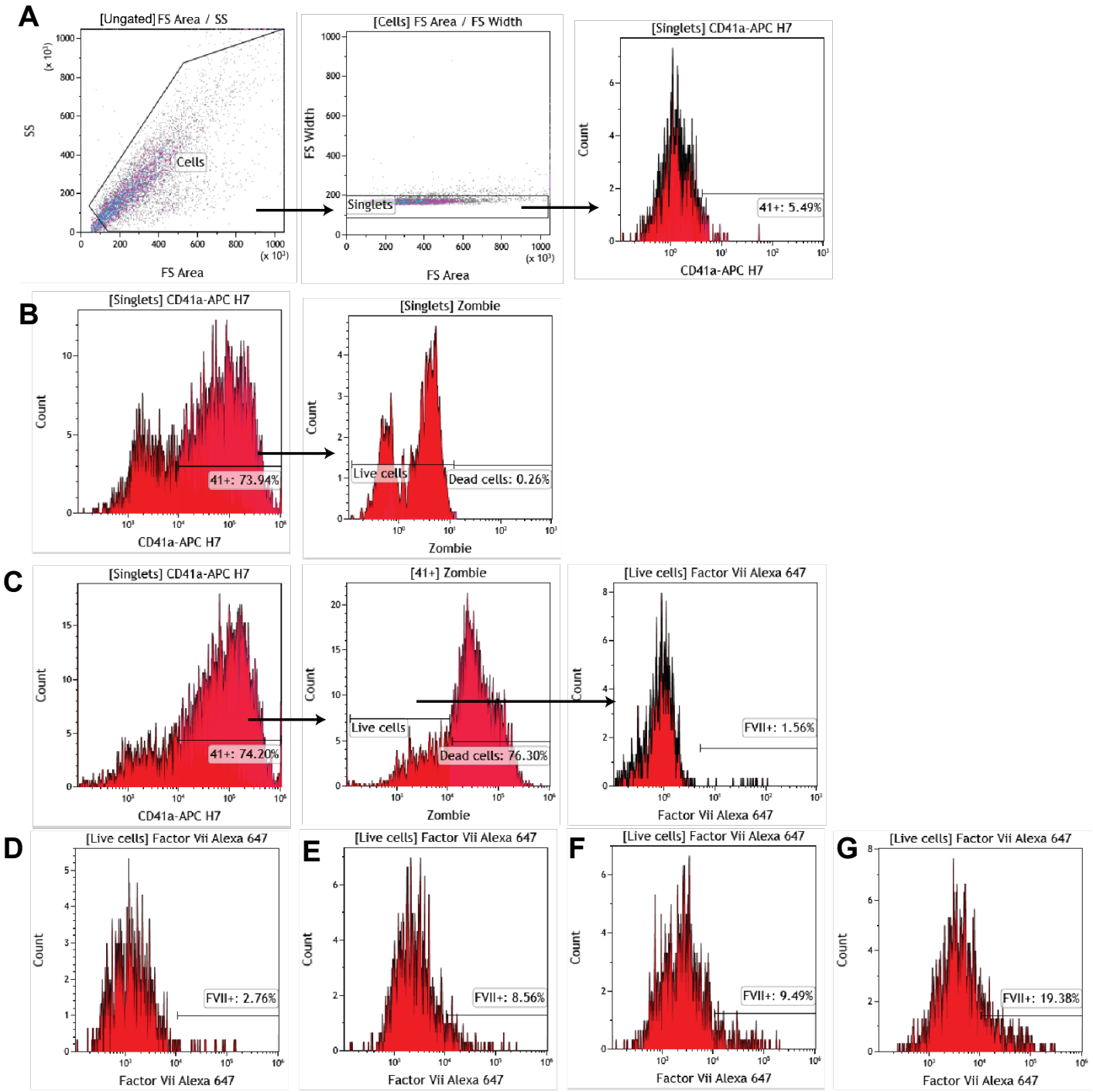

Figure 5.7. *Representative intracellular flow staining for FoPMKs incubated with and without rFVIIa with and without permeabilization. (A) Gating strategy set up first for cells, on size to exclude debris, then singlets, and then the CD41 gate was set with the isotype control (B) Gating for Zombie was set up on cells stained for CD41 but not Zombie (C) Gating for both CD41+ and Zombie-, the FVII gate was set up with a 647-secondary-only control (D) FoPMKs without permeabilization or incubation with rFVIIa (E) FoPMKs without permeabilization but with rFVIIa incubation (F) FoPMKs permeabilised but without rFVIIa incubation (G) FoPMKs permeabilised and with rFVIIa incubation*

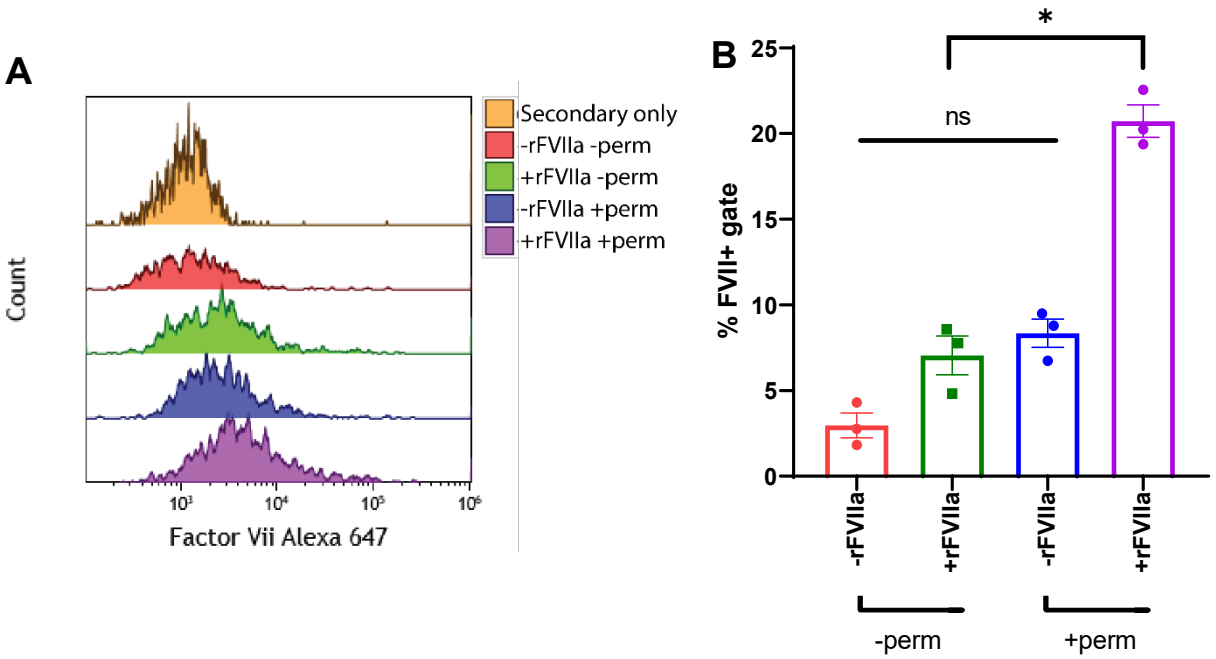

Figure 5.8. *Summarised flow data for CD41+Zombie- gated FoPMK cells on the number of events positive for FVII staining with and without permeabilization. (A) Overlay flow plots summarising the data in Figure 5.7 (B) Quantified percentages of cells staining positive for FVII; n=3, one-way ANOVA with Tukey's correction for multiple testing, * $p < 0.05$; data shown as mean ± SEM.*

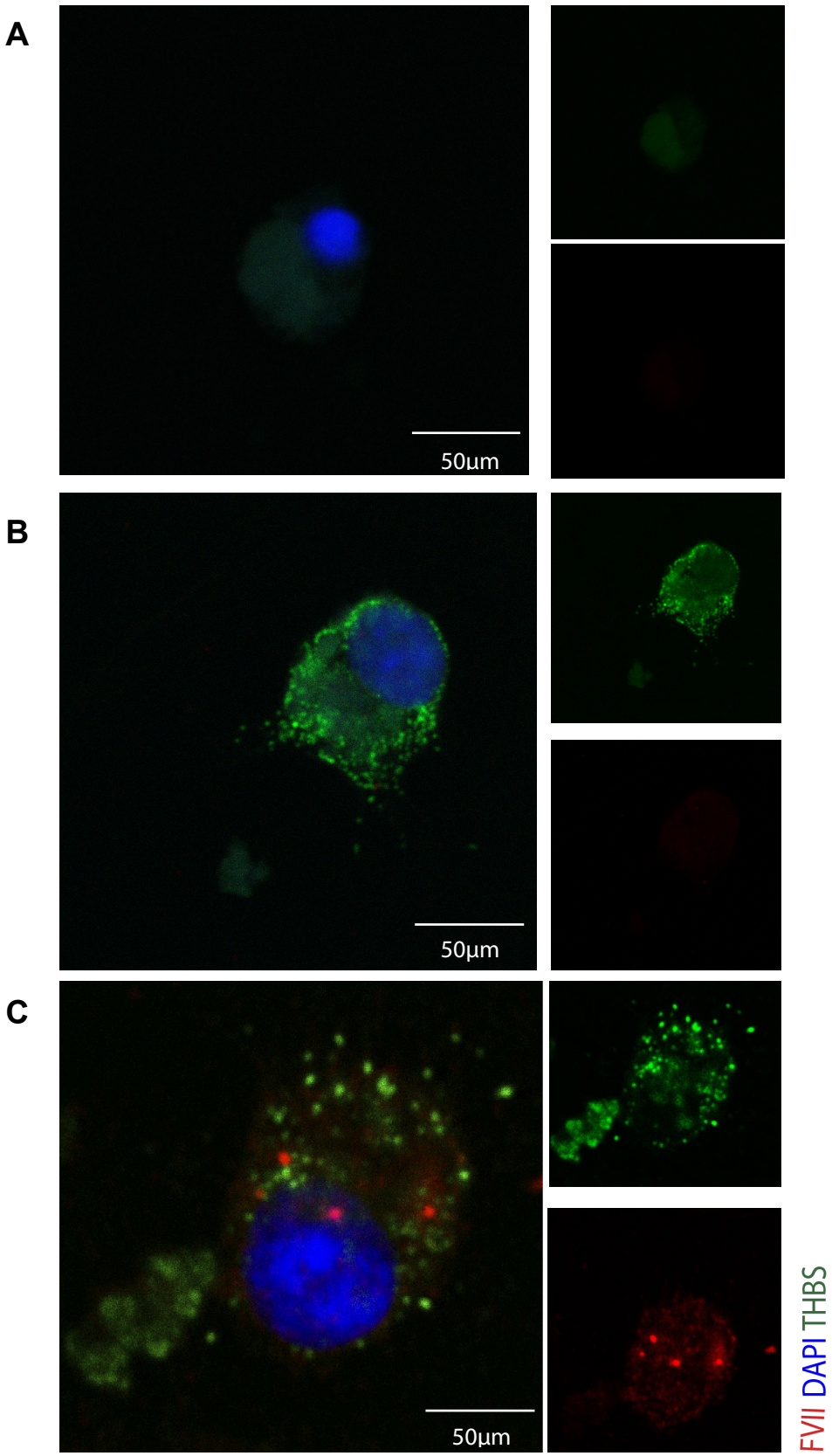

Figure 5.9. *Representative immunofluorescence photographs for forward programmed megakaryocytes incubated with and without rFVIIa. (A) Secondary only staining (B) Primary and secondary antibodies added, on cells not incubated with rFVIIa (C) Staining on cells incubate with rFVIIa for 24 hours at 37ºC. Staining was performed for FVII (red, ab97614, secondary A21244) and thrombospondin (THBS, green, ab1823, secondary A21121). n=3, on a Leica Sp5 confocal 63x*

Intracellular flow cytometry was used to assess whether the subsequent platelets produced by these MKs contained rFVIIa or not. MKs incubated with rFVIIa for 24 hours at 37ºC were then washed and cultured in RPMI for another 24 hours to elicit platelet release. Platelets were then collected from these cultures, fixed and stained for analysis.

Gating was established using isotype controls for gating on CD41/42 to establish platelet identity (Figure 5.10A). A control omitting Zombie was used to set up the Zombie gate for live platelets (Figure 5.10B). A 647-secondary only control was used to set up the FVII positive gate (Figure 5.10C). Platelets from the MKs not incubated with rFVIIa were measured (Figure 5.10D) and compared to platelets from MKs incubated with rFVIIa (Figure 5.10E).

Overlaid on top of each other, there was no observed difference between these two conditions (Figure 5.11A). Quantified from three biological replicates, platelets from MKs not incubated with rFVIIa showed an average of 9.36% positive for FVII, compared to 10.5% for platelets from MKs incubated with rFVIIa (Figure 5.11B). No significant increase was observed in FVII staining at the $p<0.05$ level.

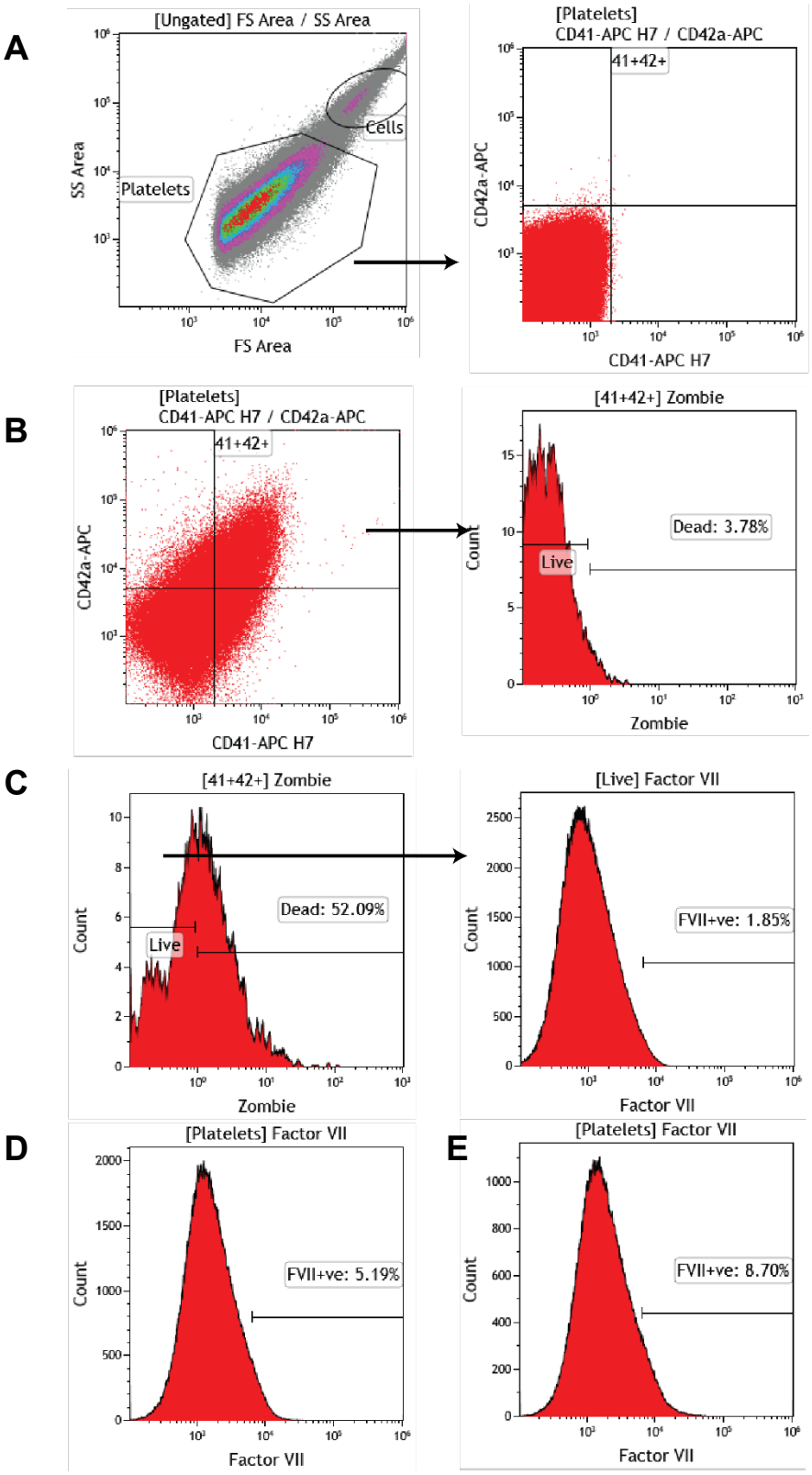

Figure 5.10. *Intracellular flow data in platelets from FoPMKs incubated with and without rFVIIa.(A) Gating strategy to set up CD41/42 gates on isotype control samples. (B) Gating strategy to set up Zombie gate on samples stained with CD41/42 but not Zombie (C) Gating strategy to set up FVII positive gate on samples stained with CD41, CD42, Zombie and 647-secondary only. (D) Representative FVII staining on platelets from FoPMKs incubated without rFVIIa. (E) Representative FVII staining on platelets from FoPMKs incubated with rFVIIa.*

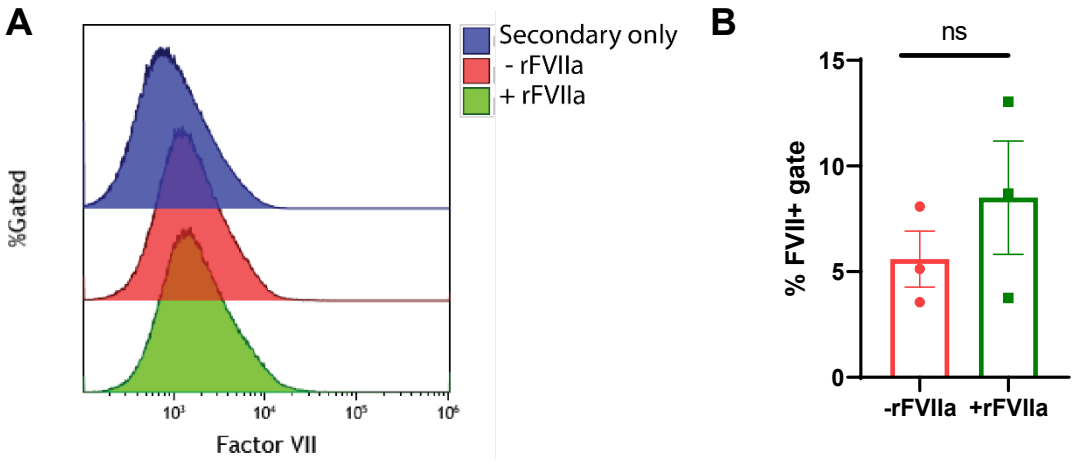

Figure 5.11. *Summary of flow data on platelets from FoPMKs incubated with or without rFVIIa (A) Overlay plots of PLPs from secondary only control, without and with rFVIIa (B) Quantified data; data shown as mean ± SEM, paired t-test performed at the p<0.05 significance level.*

5.5 Human platelets can directly endocytose rFVIIa

Intracellular flow cytometry was used to test whether human platelets are able to directly endocytose rFVIIa. Human donor platelets were incubated at room temperature for 1 hour with rFVIIa before being washed and analysed. Controls used to establish gating were unpermeabilised and incubated with 647-secondary only (Figure 5.12A). After gating on size and for only singlet events, the FVII gate was set. On platelets not incubated with rFVIIa and unpermeabilised, there was no significant difference between the samples incubated but not permeabilised and not incubated with rFVIIa but permeabilised (Figure 5.12B-D). However, there was a significant ($p<0.05$) difference between all three of these groups and the samples incubated with rFVIIa and permeabilised (Figure 5.12E,G) and was visible as a whole population shift on an overlay plot (Figure 5.12F). This suggested that rFVIIa was absorbed by the platelets and was present intracellularly, not weakly attached to the surface.

As there seemed to be evidence for endocytosis in the flow data, a FVII ELISA on platelet lysates were also performed to confirm this (Figure 5.13). Results from the samples show that the $10x10^6$ platelets incubated with 10µg/ml rFVIIa contained 13.9ng/ml of FVII in their lysate compared to 0.4ng/ml for the platelet sample incubated without, significant to $p<0.05$ (Figure 5.13B).

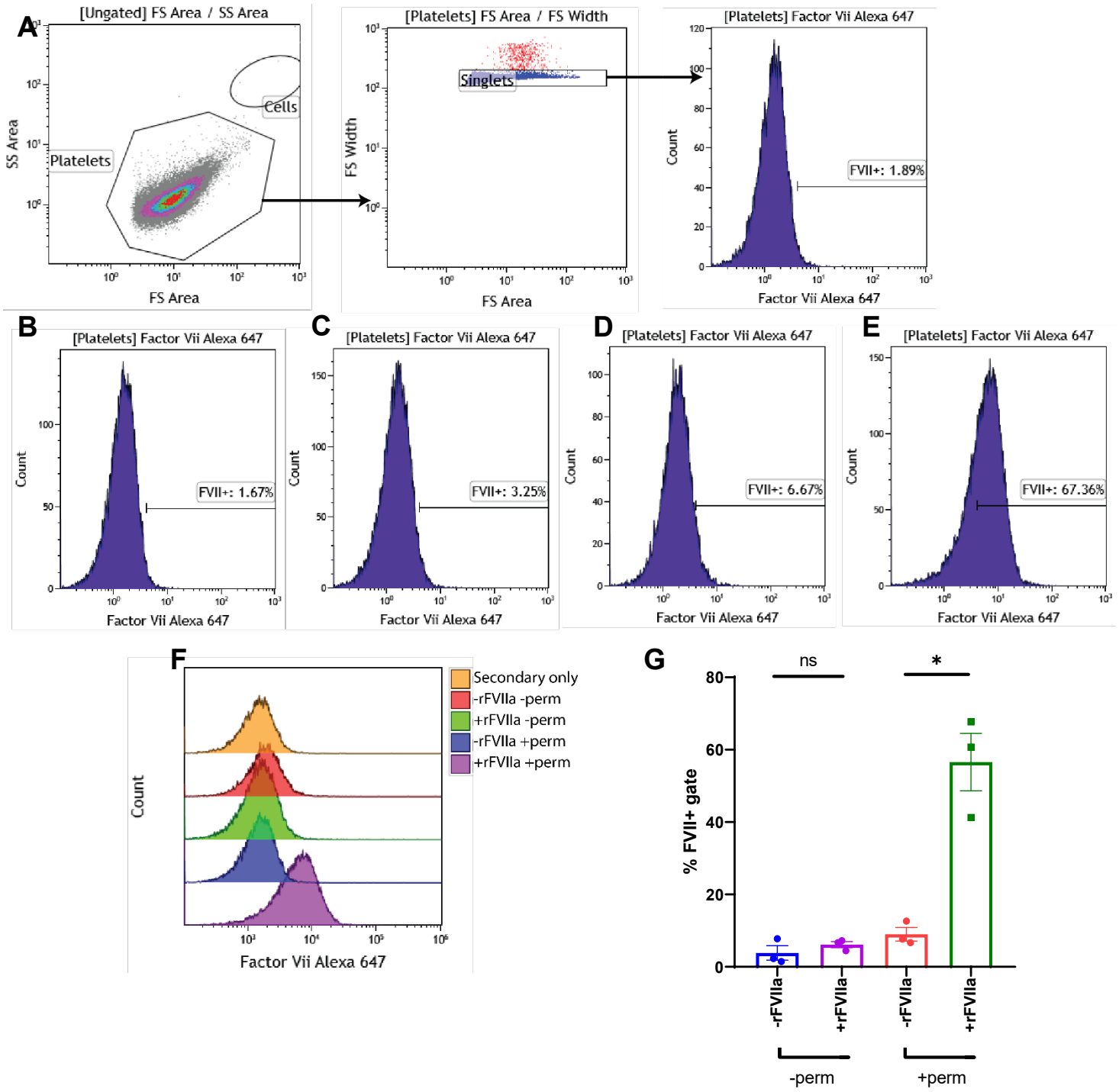

Figure 5.12. *Intracellular flow cytometry showing presence of intracellular rFVIIa in platelets incubated with rFVIIa for 1 hour. (A) Gating was set up on FS/SS and on singlet events alone. FVII gate was set up on unpermeabilised platelets with 647-secondary only (B) Platelets without rFVIIa incubation, without permeabilization (C) Platelets with rFVIIa incubation, without permeabilization (D) Platelets without rFVIIa incubation, with permeabilization (D) Platelets with rFVIIa incubation, with permeabilization (E) Overlay flow plots summarising this data (F) Quantified percentages across n=3 biological replicates, one-way ANOVA with Tukey's multiple testing correction, * $p < 0.05$; data shown as mean ± SEM.*

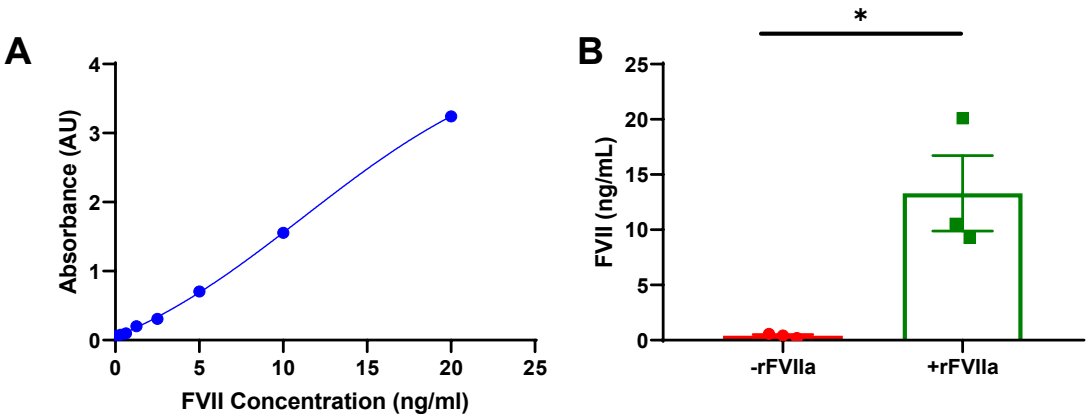

Figure 5.13. *Factor VII ELISA was performed to detect the presence of rFVIIa in the lysates of 10x10^6 platelets incubated with rFVIIa for 1 hour at room temperature and subsequently washed. n=3, data shown as mean ± SEM.(A) Standard curve for ELISA (B) ELISA results for lysates incubated with and without rFVIIa * p<0.05 from a two-tailed unpaired t-test*

5.6 These loaded platelets can release rFVIIa upon exposure to agonists

In order to test whether these loaded human donor platelets were able to release this absorbed rFVIIa, a releasate assay was performed where these samples were incubated with or without agonist, and the supernatant collected for analysis by ELISA. In Figure 5.14, the lysates further replicate the previous result in Figure 5.13 while acting as internal controls to verify that the platelets being used in this experiment were loaded with rFVIIa. The releasates from samples not incubated with rFVIIa did not show any detectable FVII, with or without agonist. The releasates of platelets incubated with rFVIIa showed a very small amount of rFVIIa not significantly different from those not incubated without agonist, while the releasate of platelets incubated with rFVIIa and agonist showed a significant ($p<0.01$) quantity of rFVIIa had been released. This shows that human platelets can absorb rFVIIa into their granules, and subsequently release this when challenged with an agonist.

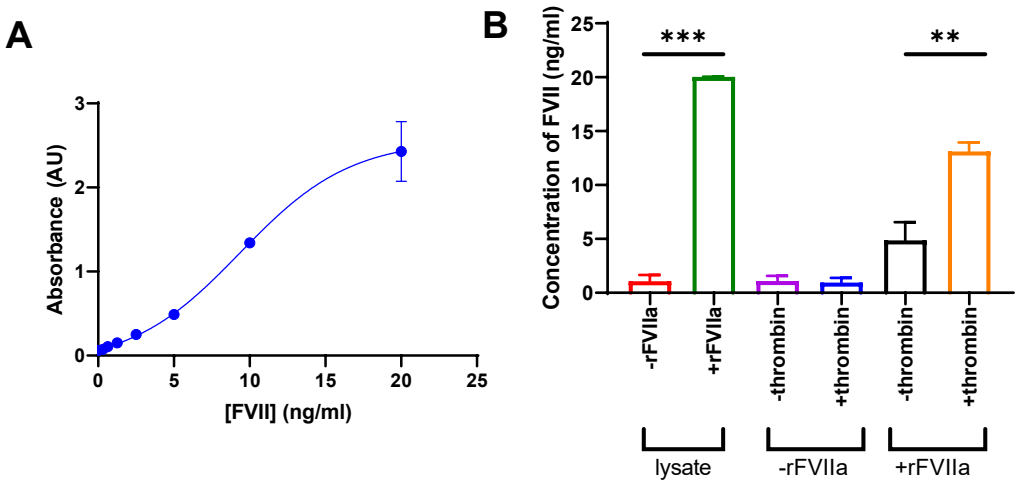

Figure 5.14. *Releasate assay performed on human donor platelets incubated with and without rFVIIa for 1 hour at room temperature. Samples were then washed and then incubated with either TAP lysis buffer (section 2.1.1.4), 1U thrombin or Tyrode's. A FVII ELISA was performed to quantify the presence of rFVIIa in each of these samples. N=3, error bars = SEM ** p<0.01 *** p < 0.001*

5.7 These platelets show improved haemostatic activity in a thrombin generation assay

A thrombin generation assay was performed to measure the effect of this intracellular rFVIIa in donor platelets on thrombus formation, and representative plots of the thrombin generation over time were observed to be very different between loaded and unloaded platelets (Figure 5.15A). A dose-dependent relationship between the parameters of the thrombin generation plot and concentration of platelets used was observed under both conditions, trending to indicate a faster thrombus formation (reduced lag time, increased peak height, reduced peak time, increased area under curve) with increasing platelet concentration (Figure 5.15B-E). Platelets loaded with rFVIIa showed a more pro-thrombotic phenotype compared to unloaded platelets at all concentrations, demonstrating a lower lag time, and time to peak, and a higher peak height and total area under the curve at both intermediate concentrations of platelets. The concentration curve for total thrombin generation (area under the thrombin generation curve) compared to the number of platelets was modelled using non-linear regression to calculate the EC_{50} of the donor and loaded platelets, which were 3.43 (2.777 to 4.274) and 0.331 (0.09411 to 0.6773) respectively, reported as the mean (95% confidence interval) to 3 significant figures (Figure 5.15E). This shows that the EC_{50} of loaded platelets was significantly ($p<0.05$) reduced for total thrombin generation compared to donor platelets (Figure 5.16).

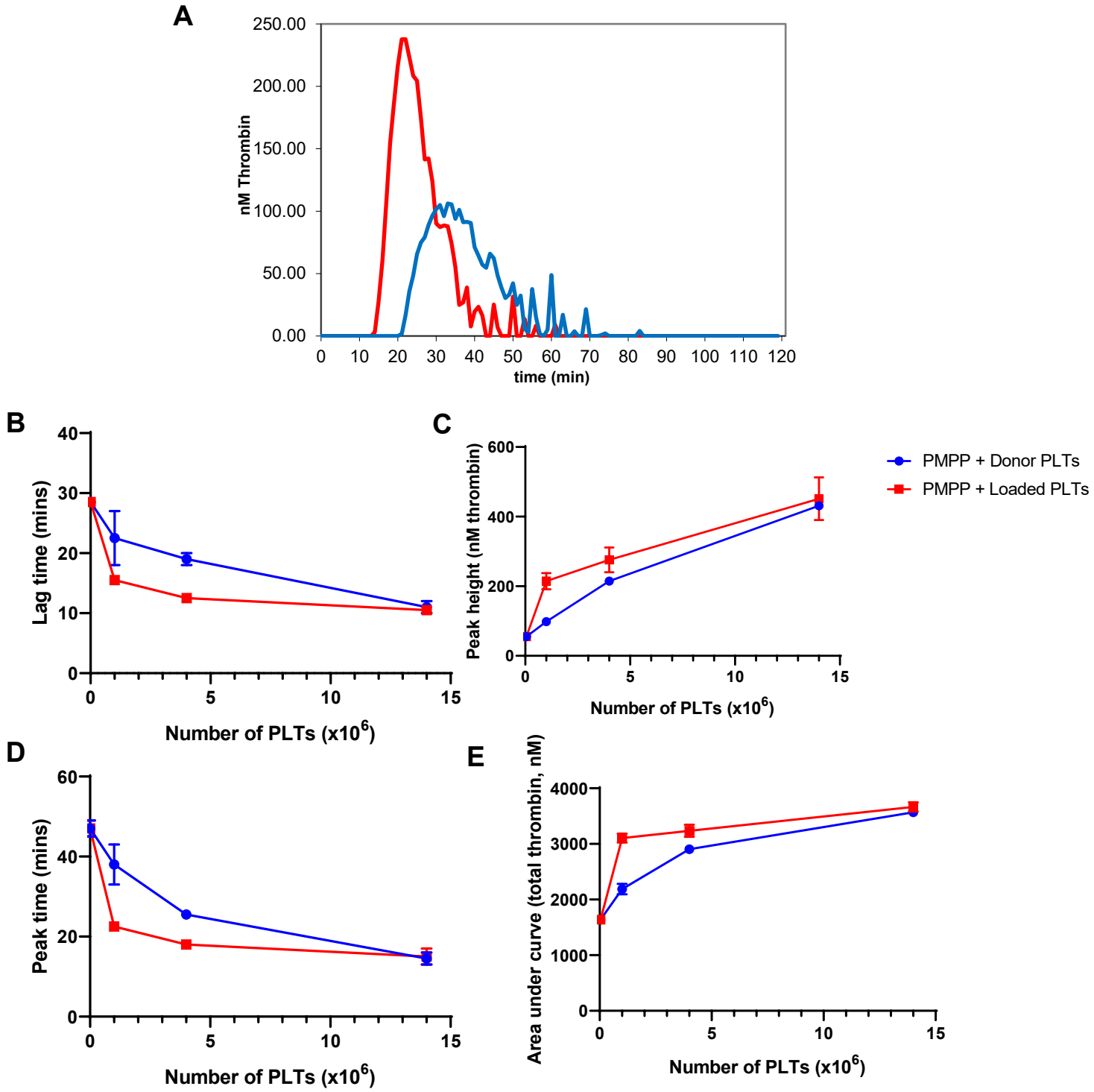

Figure 5.15. *Thrombin generation assay on three concentrations of donor platelets incubated with or without 10µg/ml rFVIIa for 1 hour at room temperature before being washed and analysed. Thrombin generation was performed in the presence of platelet and microparticle-free plasma (PMPP) in 100µl, triggered by the addition of RCLow (solution containing phospholipid micelles with rhTF) and measured for both conditions at three concentrations of platelets (PLTs) and repeated for n=3 biological replicates, data shown as mean ± SEM. (A) Representative thrombin generation plots for donor platelets vs loaded platelets at 1x10^6 platelets. (B) Lag time before onset of peak (C) Peak height (D) Time duration of peak in minutes (E) Area under the curve, representing total thrombin generation.*

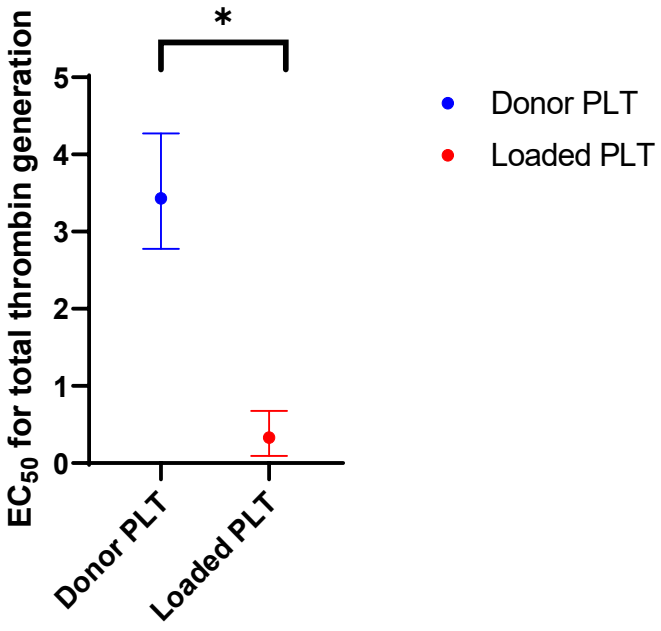

Figure 5.16. *Confidence intervals for the EC_{50} for total thrombin generation, derived from non-linear regression applied to the concentration curves in Figure 5.15E. The EC_{50} here refers to concentration needed for half of the maximal signal from the assay.*

5.8 Discussion

From Figure 5.1, there appeared to be a very slight increase in FVII staining in mouse megakaryocytes but this was not significant. Only one concentration of rFVIIa was used, for one incubation time which may not be sufficient for significant endocytosis. The number of mouse MKs cultured from bone marrow was small (Figure 5.1A) and the cells only survived for a short (<7 days) period of time, although other groups have reported cultures lasting for several weeks (Ho *et al.*, 2019). In Figure 5.4, there is a small increase in FVII staining (although not significant) from the platelets these MKs produce. One way to overcome some of these issues would be to combine this data with immunofluorescence, which would provide information on localisation of the rFVIIa.

However, conclusions from the mouse MK model are of limited applicability to a human system. Other groups have reported that the composition of platelet α-granules is species-specific and conclusions from the mouse system do not necessarily map onto human biology (Hoffman, 2005). The FoPMK system was adapted instead as it is likely more relevant for clinical translation and the numbers of megakaryocytes produced proved to be far greater than *ex vivo* mouse MK cultures (Figure 5.1A compared to Figure 5.6A).

Intracellular flow staining in Figure 5.7 was used to show that rFVIIa was endocytosed by live FoPMKs, and not dead cells that may absorb protein non-specifically. This data also confirmed that the rFVIIa was present inside of the cells, and not merely adsorbed to the surface. To do this experiment, a standard megakaryocyte marker (CD41) and dead cell marker (Zombie) was used as has been suggested in the literature to ensure all events seen were live MKs (Shepherd *et al.*, 2018). Zombie was used in place of other more commonly used viability stains, for example Calcein-AM, which leak out of permeabilised cells. The disadvantage to this is that Zombie only stains dead cell membranes, and so is a 'negative' dye where those staining negative are gated for, as opposed to a 'positive' dye like Calcein-AM which gives more confidence in the viability of its population. All controls were unpermeabilised to establish the assay gating strategy as permeabilization itself is likely to change the binding properties of the antibody due to more exposed non-specific binding sites. This perhaps explains the increase in percentage of events gating positive for the -rFVIIa condition between the unpermeabilized and permeabilized samples (Figure 5.8B).

The platelets produced from these MKs did not have any significant staining for FVII (Figure 5.11). From looking at the IF data, this may not be entirely surprising. From Figure 5.9C, it can be noted that unlike the genetically engineered FVII in chapter 3 (Figure 3.20), the rFVIIa endocytosed is not distributed across many different granules but localised to only a small number (3 in Figure 5.9C, compared to >29 thrombospondin granules and >14 for the vWF-F7TF in Figure 3.20C). This may indicate that the vast majority of the rFVIIa absorbed into the MKs are ending up in a small population of platelets, and most of the produced platelets remain unloaded. Like the FVII in chapter 3, the rFVIIa here did not co-localise with thrombospondin. This may suggest it is also similarly in a VEGF-positive granule. Alternatively, it may be possible that the rFVIIa taken up by these MKs ended up in granular structures unrelated to the α-granules, such as lysosomes or early endosomes, which were then not transferred to the resultant platelets from these MKs.

A limitation of the FoPMK approach is that it remains difficult to scale up to produce enough PLPs necessary for an in vivo mouse transfusion experiment, to ask whether these loaded platelets have a superior haemostatic effect in vivo. For a cost-benefit analysis, clinical translation, this may represent the worst of both worlds, being expensive to scale-up, while requiring addition of an expensive drug (the work in genetically engineering FVII into the granules in chapter 3 simplifies this to just the issue of scaling up FoPMK platelet production). To address this, human donor platelets were assessed for their ability to directly endocytose

rFVIIa, which would render the use of platelet loading far more accessible and easier to scale-up, despite requiring the use of an expensive drug.

Gates were set up only on size as donor platelet preparations gating only on FS/SS have been shown previously to be highly positive for CD41/42 and viable (Vučetić *et al.*, 2018). Unlike Hoffman and colleagues, flow cytometry data (Figure 5.12G) here suggests that rFVIIa is able to be directly endocytosed into platelets, and not just weakly attached to the surface (Hoffman and Monroe, 2010). This is more in line with results reported by Lopez-Vilchez and colleagues (Lopez-Vilchez *et al.*, 2011). However, these experiments do not rule out the weak attachment of rFVIIa *in vivo* from the plasma, as any excess rFVIIa was washed off in the experiments presented here.

From the combination of intracellular flow data and ELISA data it can be concluded that rFVIIa is present inside of the platelets incubated with the drug. Intracellular flow cytometry is able to answer whether the rFVIIa is present inside of the platelets or not (with and without permeabilization) (Figure 5.12G), and ELISA data is able to quantify the exact amount of rFVIIa absorbed (Figure 5.13), with the two approaches complementing one another. The ELISA data suggests that the vast majority of the rFVIIa added was in excess and was not absorbed. It may be possible to load many more platelets with the same concentration of rFVIIa used here.

The conclusions from one group suggest that the prolonged efficacy of rFVIIa lies due to its uptake by megakaryocytes and subsequent production of platelets (Schut *et al.*, 2017). Data generated here suggest that direct uptake by platelets in circulation may play a more fast-acting, and therefore much larger role.

From the releasate experiments (Figure 5.14), it can be quantified that approximately 40% of the absorbed rFVIIa was released in response to agonists, which may indicate why a dramatic difference was seen in the thrombin generation assay. The rFVIIa may exist as a dynamic equilibrium between the granules and the extracellular compartment, thus the FVII detected in the releasate of the no thrombin condition may be due to Le Chatelier's principle. Alternatively, it is possible that the centrifugation or other mechanical stimulus may have triggered some platelet activation independent of the thrombin.

The thrombin generation assay data (Figure 5.15) suggest that fewer loaded platelets are required for the same level of total thrombin generation due to the lowered EC_{50}, suggesting that they are more readily able to form clots. This is

likely to be of benefit both locally in thrombus formation. Intravital microscopy has previously established a small number of platelets being responsible for initiation of clotting after a laser injury, before recruiting others (Rosen *et al.*, 2001). Clinically, this might be applicable in giving platelet transfusions. As patients indicated for a transfusion typically have a low platelet count, the transfusion of loaded platelets may provide significantly more benefit than transfusion in patients with a normal platelet count.

The results of this are somewhat surprising given that FVII is present in large quantities in plasma but are not endocytosed by platelets in circulation as evidenced by mass spectrometry data from platelet α-granules (Maynard *et al.*, 2007). Meanwhile, these data show that FVIIa is readily taken up by donor platelets into their α-granules. This may be explained by the change in conformation in FVIIa compared to FVII, or some epitope created only when in complex with TF, that allows for binding to a receptor on platelets, perhaps EPCR. Speculatively, this might explain the ability of platelets to adsorb FVIIa on the surface of their cell membranes and not FVII in the cell-based model of haemostasis described in section 1.4.2.

To conclude, FoPMKs can endocytose rFVIIa and package it into granules, but this is not present in the subsequently produced platelets to a noticeable degree. By contrast, human platelets directly from a donor can endocytose rFVIIa and subsequently release it when stimulated with agonist. This results in them having better characteristics at forming thrombi in the thrombin generation assay, especially at low concentrations where the differences are most apparent.

6 A novel thrombocytopaenic mouse model for measuring haemostasis after human platelet transfusion

6.1 Introduction

Previous work in establishing a model for human platelet transfusion in vivo has met with success. Early attempts introduced platelets into an immunodeficient NSG mouse with survival of human platelets for several days when injected intravenously (Newman, Aster R and Boylan B., 2007). Later work showed that platelet transfusion through the tail vein is equivalent to the retro-orbital route used previously and may increase the survival time of the platelets (56% detectable in the circulation when injected retro-orbitally after 5 hrs, versus 84% when injected via the tail vein) (Fuhrmann *et al.*, 2016). However, these times remain far below the five to seven days seen with platelet transfusion into human recipients.

Work involving transplantation of human CD34+ stem cells to reconstitute human megakaryopoiesis in mice resulted in poor engraftment, and this was discovered to be due to rapid clearance of human platelets by mouse macrophages (Hu and Yang, 2012). Macrophage depletion with clondronate-liposomes was able to reverse this effect. However, these models have significant differences compared to clinical platelet transfusion, where patients with a low platelet count are transfused with human donor platelets to treat acute haemorrhage. This is not modelled by irradiation and transplantation of CD34+ stem cells for a long-term engraftment. By depleting the circulating mouse platelets, it would be possible to remove a major confounding factor in using a mouse model to assess the functionality of transfused human platelets, without requiring irradiation and subsequent transplantation of human stem cells into the mouse bone marrow niche.

There are several different techniques used to induce thrombocytopaenia in mice. Chemical approaches include the use of busulfan, but this is also associated with an associated leukopaenia which is undesirable as this effect is not limited to platelets (Qi and Hardwick, 2007). Genetic knockout of the c-Mpl receptor leads to a 85-90% drop in platelet counts, but the remaining platelets are still functional, and this does not appear to be a specific cell-targeted approach as seen by defects in other parts of haematopoiesis (Alexander *et al.*, 1996). More recent genetic approaches include using diphtheria toxin receptor under a platelet factor 4 promoter to allow for a platelet depletion specific to an individual mouse that is still able to receive transfusion of murine platelets (Wuescher, Nishat and Worth, 2019).

The gold standard for inducing thrombocytopenia in mice has been antibody-mediated depletion, mostly developed in a C57BL/6 background. Polyclonal antisera against mouse platelets have been used to cause a thrombocytopenia (Jenne *et al.*, 2011; Salas-Perdomo *et al.*, 2019). A specific monoclonal antibody targeting GPIIb/IIIa was shown to be effective in reducing platelet counts, but induced an anaphylactic response (Nieswandt *et al.*, 2003), whilst one instead targeting GP1b has been shown to effectively induce a thrombocytopenia for up to 96 hours without an allergic response (Nieswandt *et al.*, 2000). These models have been used to investigate bleeding disorder such as immune thrombocytopenic purpura (ITP), the role of platelets in immunity and neuroprotection. However, they have not been used with human platelet transfusion and it is unclear if these antibodies will cross-react with and clear human platelets.

The group of Koji Eto (Kyoto University), also working on in vitro-derived platelets, used NSG mice with irradiation-induced thrombocytopaenia, and an intravital laser-induced injury model to assess the formation of thrombi (Nakamura *et al.*, 2014). This approach has the same major limitations as described with irradiation. Furthermore, although the laser injury model shows that in vitro platelets form stable thrombi under imaging, it lends no functional evidence that these stable thrombi contribute significantly to haemostasis.

More recently, an antibody-mediated depletion model was published by the Bergmeier group, including a laser-induced injury and imaging of the resulting platelet recruitment (Paul and Bergmeier, 2020). This shows that it is possible for human donor platelets to be haemostatically active with the absence of endogenous mouse platelets. This shares the limitation of not directly measuring bleeding and has not been used with in vitro-derived platelets or platelets loaded with rFVIIa.

6.2 Aims

As described in the introduction, previous work has shown that human donor platelets can survive for several hours in the mouse circulation. In this chapter, thrombocytopaenia was induced through an antibody-mediated depletion of endogenous mouse platelets to limit the indirect effects of inducing a thrombocytopenia seen through other techniques. These mice then underwent a transfusion of human donor platelets and subsequently were subjected to a tail transection experiment to functionally measure haemostasis in the context of human platelet transfusion. This mouse model was then used to measure the

haemostatic effect of donor platelets loaded with rFVIIa compared to only donor platelets.

6.3 A polyclonal anti-mouse platelet antibody was able to lower mouse platelet counts, but showed cross-reactivity with human platelets

Mice were rendered thrombocytopaenic with a polyclonal rabbit anti-mouse platelet antiserum (see section 2.1.1.15). This was originally raised by taking C57BL/6 platelets and using these as an antigen in rabbits, and subsequently collecting the serum. Previous work had shown that it was effective at fully rendering C57/BL6 mice thrombocytopaenic (Hilton, Kile and Alexander, 2009). However, it had not been tested in an immunocompromised NRG/J mouse, which comes from a BALB/c background.

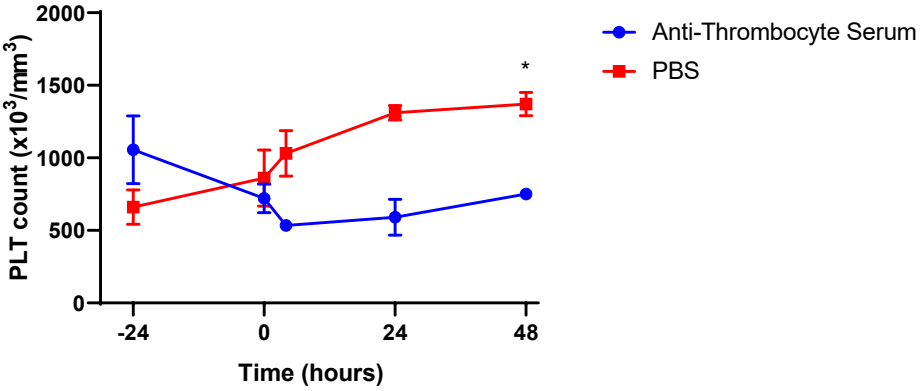

Figure 6.1. *NRG/J mice treated with anti-thrombocyte antiserum. NRG/J mice were given i.v. anti-thrombocyte antiserum or PBS and bled via the tail vein at -24, 4, 24 and 48 hours post-injection. n=3, results show mean±SEM, *** p=0.0006. A two-way repeated measures ANOVA was performed with a Geisser-Greenhouse correction. Comparisons were performed at each time-point and a Bonferroni correction was applied.*

The anti-mouse thrombocyte antiserum showed mixed results (Figure 6.1). Mice given the depletion antiserum had a reduction in their platelet count compared to baseline to 68% of the original level, eventually dropping to 56% by 24 hours, while control mice had an increase in platelet counts. Although the platelet count was lowered in the mice that received the antiserum intravenously, this was only to 68% of baseline compared with a 99% decrease seen in the literature (Salas-Perdomo *et al.*, 2019). For this model, the ultimate purpose was to reduce the mouse platelet count to be as low as possible to measure the effects of only the human platelets, for which a 68% reduction is unsuitable. Furthermore, the control mice platelet count increased over the course of the experiment. Alongside this,

it was noted that by comparing other blood parameters between baseline and 48 hours, the lymphocyte percentage had reduced in both experimental groups, with a corresponding increase in the granulocyte percentage (Table 6.1). The white blood count had also trended towards increasing, although this was not statistically significant.

	Anti-Thrombocyte serum			**PBS**		
	Baseline	**48 hours**		**Baseline**	**48 hours**	
PLT	1,055.33±468.95	750.00±75.64		661.00±237.17	1,370.33±161.58	*
WBC	2.97±3.74	4.50±1.91		1.97±1.84	3.65±0.30	
LYM%	49.93±12.61	29.33±0.74	*	52.50±13.88	32.20±2.60	*
MON%	14.83±1.92	14.37±0.87		13.00±5.90	15.40±0.40	
GRA%	35.23±10.95	56.30±1.53	*	34.50±8.63	52.40±3.00	*
EOS%	3.47±2.26	1.73±0.44		6.50±5.30	2.00±0.80	
RBC	6.03±1.81	8.83±2.55		3.77±1.94	8.58±1.64	
MCV	49.33±0.67	50.33±0.67		49.00±1.15	50.00±0.00	
MCH	16.37±0.29	16.33±0.07		16.83±0.68	16.35±0.10	
MCHC	33.13±0.64	32.50±0.53		34.20±1.81	32.60±0.00	
RDW	15.10±0.31	15.43±0.29		14.87±0.13	15.45±0.10	
MPV	5.20±0.35	5.67±0.24		5.10±0.12	4.95±0.10	

Table 6.1. *Complete blood counts reported from mice of both groups compared at baseline (-24 hours) and 48 hours post-injection. Data shown as mean ± 95% CI. * $p<0.05$, two-way-ANOVA with Sidak's multiple comparison tests.*

The anti-mouse thrombocyte antiserum was added to human donor platelets (Figure 6.2) in order to assess whether the polyclonal nature of this antiserum would cross-react with any human platelets given as a transfusion, which would diminish the utility of this approach.

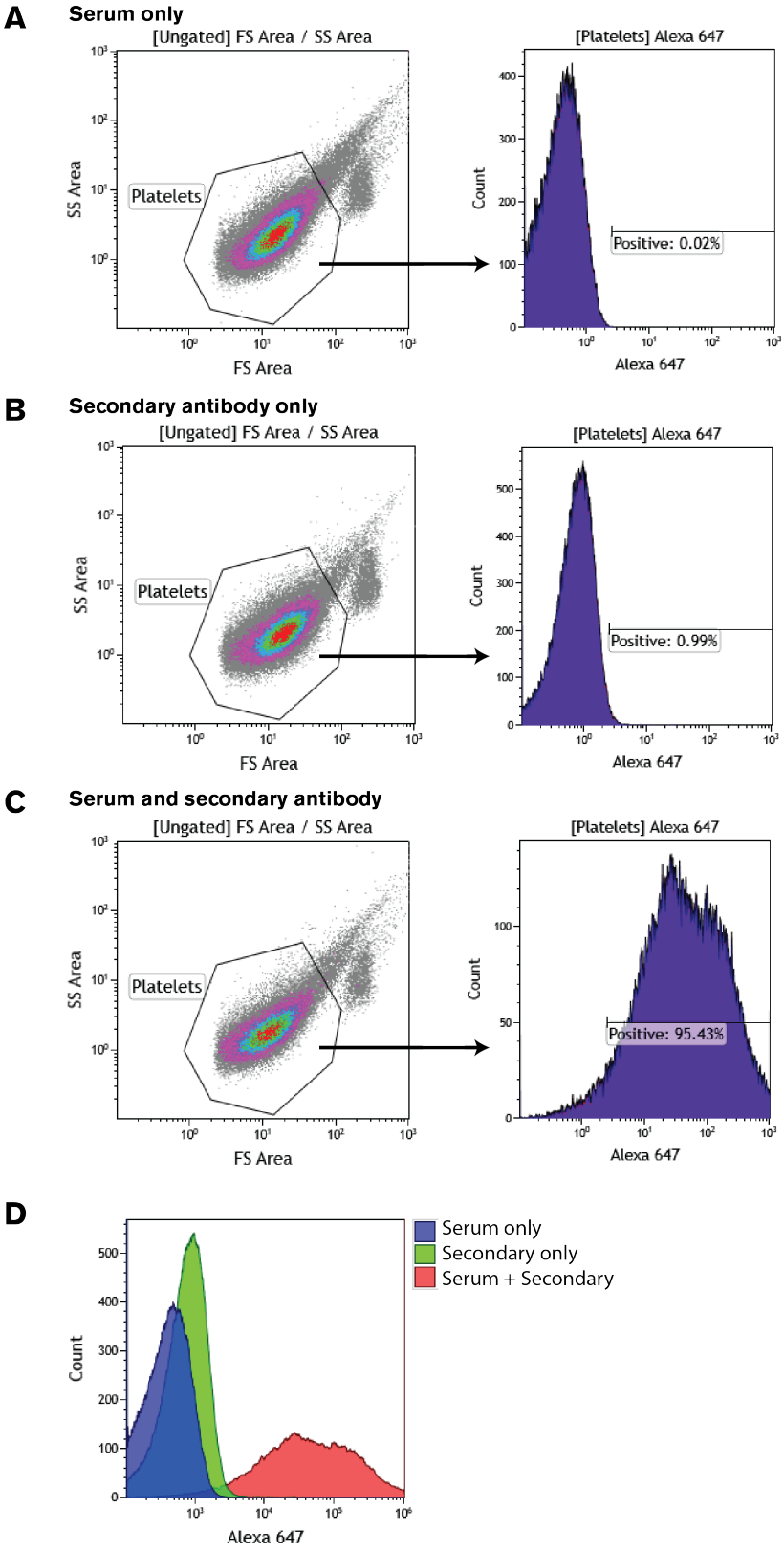

Figure 6.2. *Flow cytometry data on the binding of anti-mouse thrombocyte serum onto human platelet samples. Representative flow plots are shown, n=1. (A) Serum was incubated with human donor platelets without a secondary antibody. (B) Secondary antibody A21244 (section 2.1.1.15) only with human donor platelets. (C) Serum with human donor platelets and secondary antibody. (D) An overlay plot of all three conditions was created in Kaluza.*

From the flow cytometry data (Figure 6.2), it is clear that there is an observed difference from human platelets with this antiserum, from a 1% positive gating in the secondary antibody only staining to a 95.44% positive gating with the serum. In Figure 6.2A, with only the serum, no signal is seen from the platelets. This was used to set the platelet gate. In Figure 6.2B, with only the secondary antibody (section 2.1.1.15), no signal is seen from the platelets in the Alexa-647 channel. This was used to set the positive gate. In Figure 6.2C, with both the serum and the secondary antibodies, a significant shift is seen. Finally, in Figure 6.2D, an overlay plot shows the shift seen, indicating this polyclonal serum is able to cross-react with human donor platelets. The gates were set using the serum-only and secondary-only as controls, and the platelets incubated with both the serum and the secondary antibody showed 91.3% of the platelets in the positive gate.

6.4 Immunocompromised NRG/J mice were rendered thrombocytopaenic with a monoclonal anti-GP1b antibody that does not cross-react with human platelets

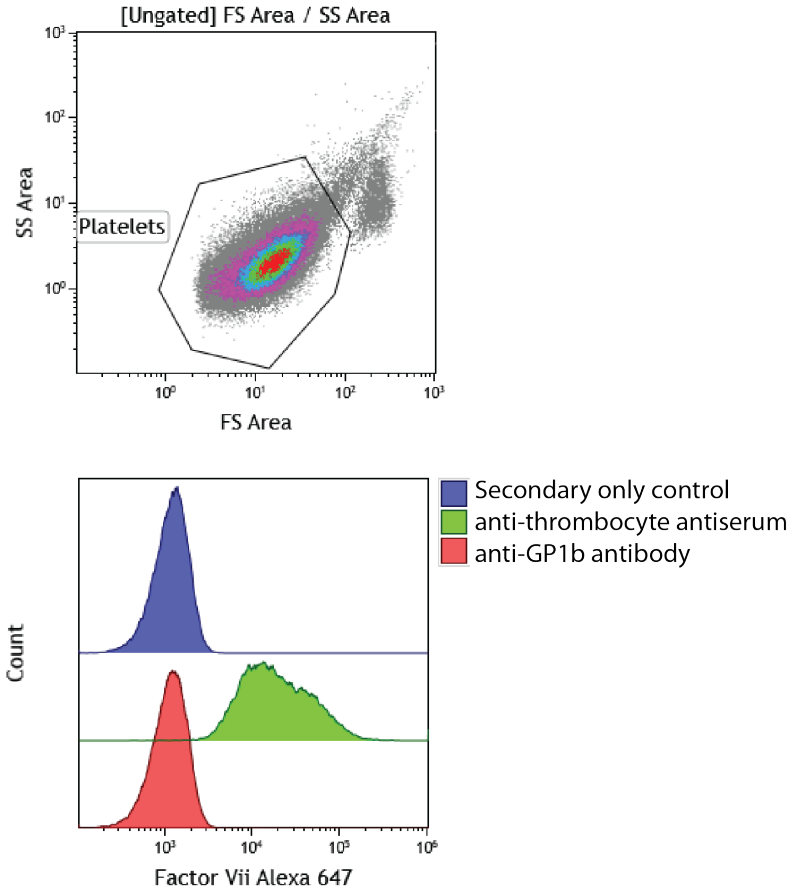

Figure 6.3. *A monoclonal anti-GP1b antibody does not bind to human platelets. Representative flow (n=1) overlay plots of anti-platelet antiserum (section 2.1.1.15) (green) binding to human platelets, used as a positive control. The secondary antibody-only A21244 (section 2.1.1.15) was used as a negative control (blue). Results from the anti-GP1b antibody are shown in red.*

In contrast to the anti-thrombocyte serum, which here was used as a positive control, the anti-GP1b monoclonal antibody showed no cross-reactivity with human platelets (Figure 6.3). There was no detectable difference between the anti-GP1b signal compared with the secondary antibody only control.

A time course experiment was performed to measure the scale of the thrombocytopenia that is was possible to induce in these mice, as well as the duration of this platelet depleted period (Figure 6.4A). When platelet counts were plotted over time, the non-depleted group showed a steady platelet count of 1467 ± 69 PLTx10^3/mm^3, whereas the group given the antibody showed a rapid thrombocytopaenia to 68 ± 10 PLTx10^3/mm^3 within 1hr of the injection. This depletion lasted for at least 48 hours post injection. After this period, a rapid rise in platelet count to pre-depletion levels was seen between 48 and 96 hours post injection, followed by a reactive thrombocytosis above the normal platelet count that was observed between 96 and 168 hours post injection. There was no steady increase in platelet count seen with the vehicle control in Figure 6.4A as was observed with the previous antiserum (Figure 6.1).

From Figure 6.4B, flow data on blood taken from IVC of control and treated mice show that the platelets normally seen in the platelet gate are almost completely absent from the treated mouse blood, providing further evidence of platelet depletion. No evidence for any other blood parameter being altered was observed in either experimental group between the treatments or between baseline and 48 hours (Table 6.2).

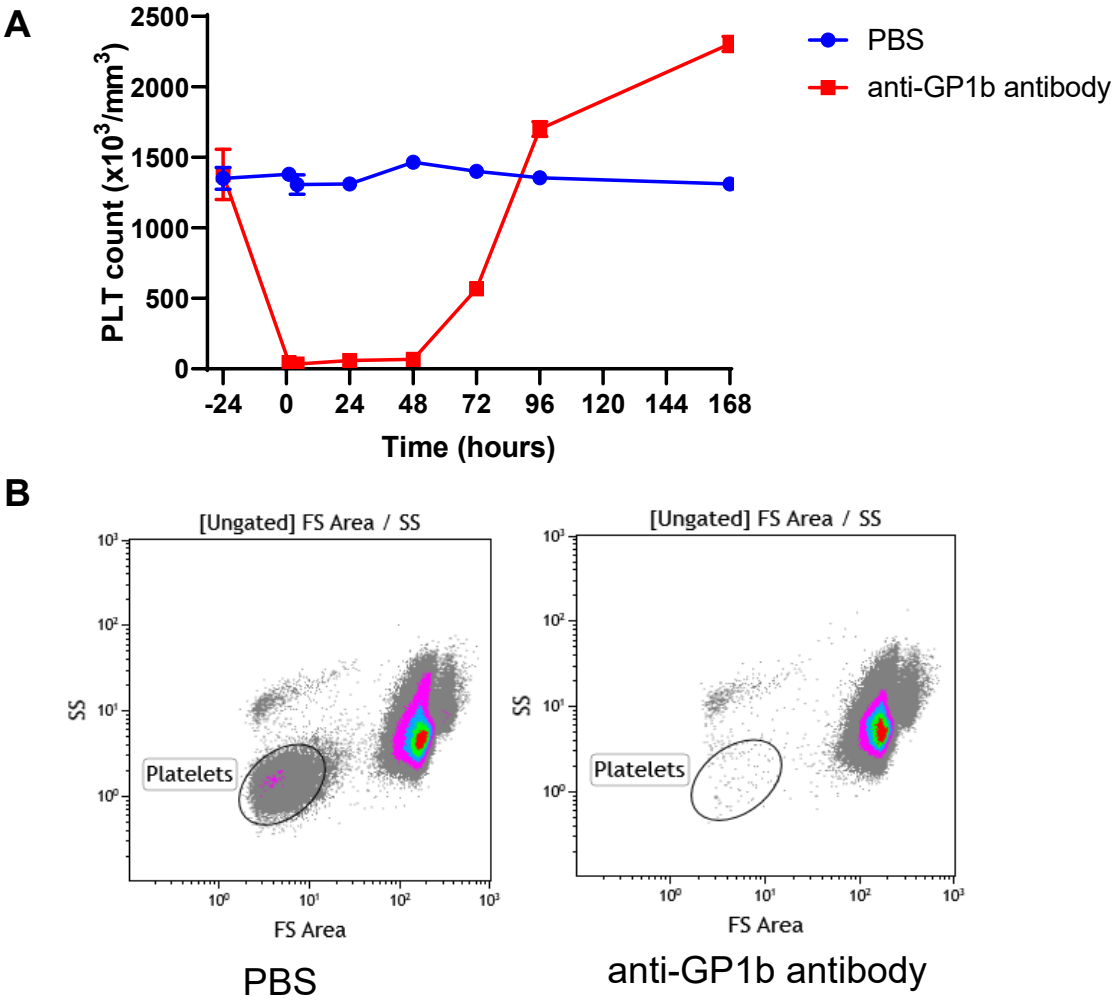

Figure 6.4. *A monoclonal anti-GP1b antibody was able to induce a >99% thrombocytopaenia for 48 hours in NRG/J mice. (A) Time course data of platelet counts for the control and mice treated with anti-Gp1b antibody (section 2.1.1.15), Tail vein bleeds were performed -24, 1, 24, 48, 72, 96 and 168 hrs post platelet depletion. Results show mean ± SEM, n=3, p<0.01 (B) Flow data on blood taken from IVC of control and treated mice with the platelet gate highlighted.*

	Anti-GP1b antibody			PBS		
	Baseline	**48 hours**		**Baseline**	**48 hours**	
PLT	1,378.50±357.00	68.00±10.00	*	1,350.50±155.00	1,466.50±69.00	
MPV	5.00±0.20	9.30±1.40		4.90±0.00	4.85±0.10	
Hb	15.50±1.00	14.95±0.70		15.40±1.00	16.25±0.30	
WBC	2.60±0.00	3.00±0.80		2.20±0.40	2.35±0.30	
LYM%	36.80±8.80	37.00±2.40		33.45±7.10	36.10±5.40	
MON%	16.65±0.70	16.50±0.00		15.15±0.70	15.25±0.70	
GRA%	46.55±9.50	46.50±2.40		51.40±7.80	48.65±6.10	
EOS%	1.60±0.40	1.05±0.30		1.50±0.80	1.45±0.90	
LYM#	0.90±0.20	1.05±0.30		0.65±0.30	0.80±0.00	
MON#	0.40±0.00	0.45±0.10		0.25±0.10	0.30±0.00	
GRA#	1.30±0.20	1.50±0.40		1.30±0.00	1.25±0.30	
EOS#	0.04±0.01	0.03±0.00		0.03±0.02	0.03±0.02	
RBC	9.49±0.43	9.36±0.41		9.37±0.81	10.09±0.40	
HCT	47.65±2.70	47.05±2.50		47.30±4.60	51.00±1.80	
MCV	50.50±1.00	50.50±1.00		50.50±1.00	50.50±1.00	
MCH	16.30±0.40	16.00±0.00		16.45±0.30	16.15±0.30	
MCHC	32.45±0.30	31.80±0.20		32.55±0.90	31.95±0.50	
RDW	15.35±0.30	15.50±0.20		14.95±0.10	15.25±0.10	

Table 6.2. *Complete blood counts reported from mice of both groups compared at baseline (-24 hours) and 48 hours post-injection. Data shown as mean ± 95% CI. * p<0.05, two-way-ANOVA with Sidak's multiple comparison tests.*

6.5 Thrombocytopaenic mice were transfused with donor platelets and the haemostatic effect was measured through a tail transection

Thrombocytopenic mice were then used for a tail transection experiment to measure haemostasis. The weight of the tail transected and haemoglobin concentration from the mice were examined to show no significant differences between the groups apart from the platelet count (Figure 6.5A,B,C).

Next, the volume of blood loss in the first four minutes of the experiment showed the greatest difference between the three groups (Figure 6.6A). The undepleted group showed very little blood loss (10.4 ± 3.70 µL), while the depleted group showed a significant volume of blood loss (275 ± 38.1 µL), approximately a third of the estimated circulating volume of these mice). The depleted group that were transfused with human donor platelets showed a significant ($p<0.05$) reduction in the volume of blood lost compared to the depleted only group (71.8 ± 30.3 µL).

A plot of the cumulative blood loss over time (Figure 6.6C) showed that this effect was sustained over the course of the twenty minute experiment, although the addition of the cumulative errors from each volume calculation compounded when summing them together, making it difficult to draw any statistically significant conclusions after the first four minutes.

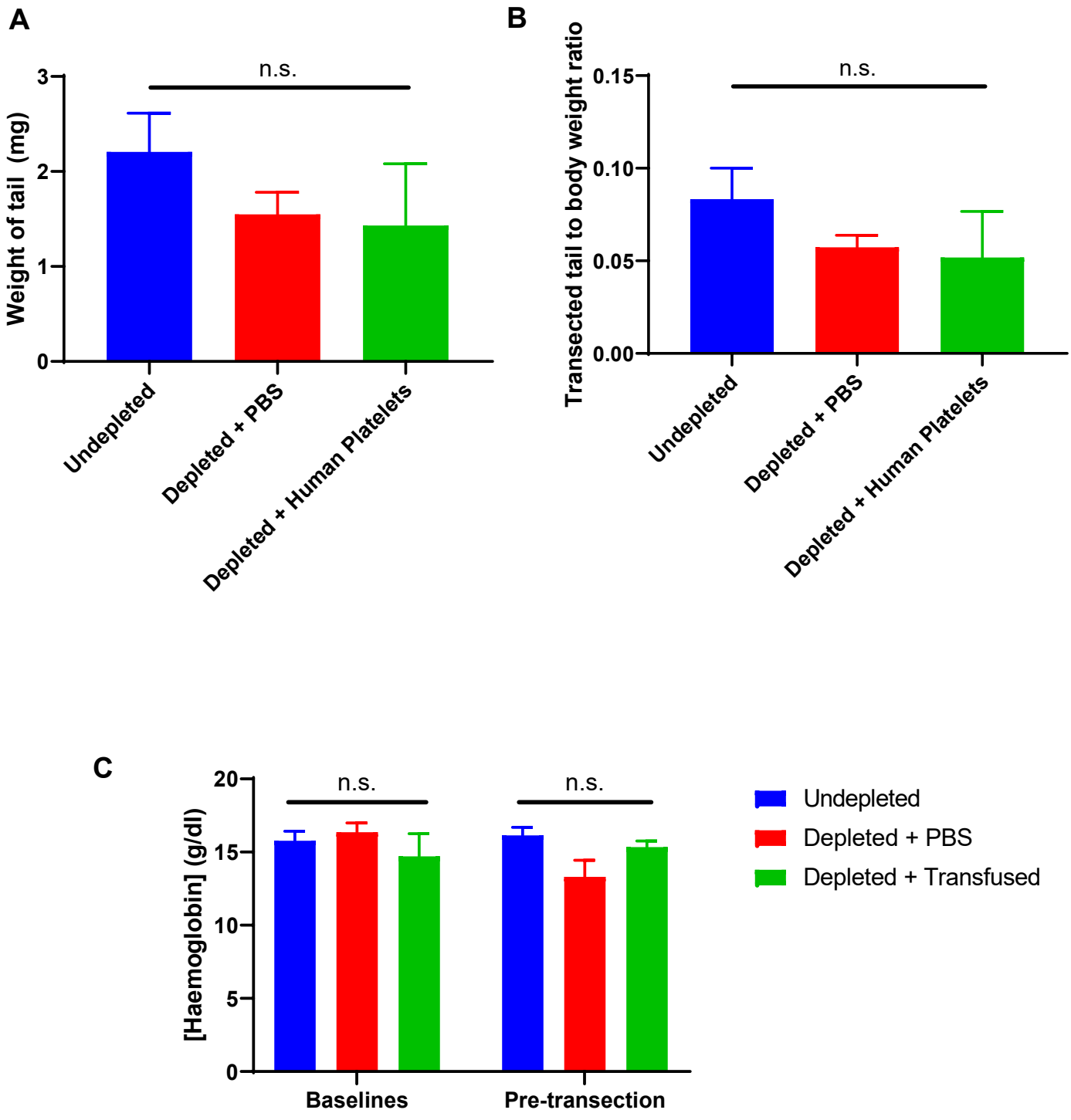

Figure 6.5. *Controls for the haemostasis tail transection experiment. (A) The weight of tail transected (B) The weight of tail transected normalised to mouse body weight (C) The circulating blood haemoglobin concentrations as measured by a complete blood count, at baseline (-24 hours) or shortly before the transection (-1hr). n=3, ANOVA. Error bars represent SEM.*

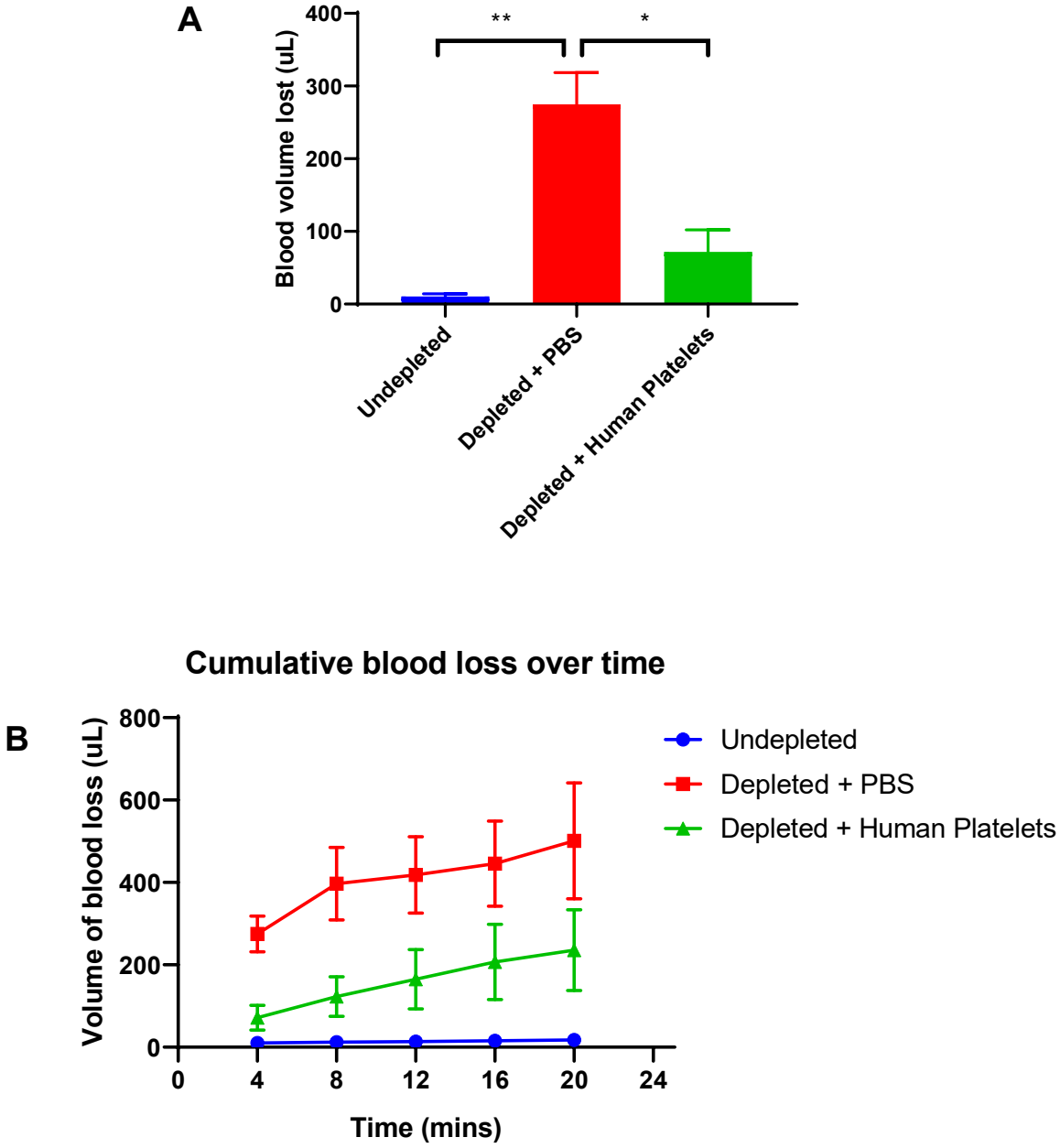

Figure 6.6. *Summary of haemostasis mouse model from mice that were undepleted, depleted of platelets and depleted and subsequently transfused with 100x10^6 human donor platelets. (A) The total blood volume lost in the first four minutes in all three groups. One way ANOVA, *p <0.05 **p<0.01 (B) The amount of cumulative blood volume loss over the full 20 minutes of the experiment in all three groups. n=3 per group, results show mean±SEM*

6.6 Passively loaded platelets have a superior haemostatic effect to unloaded platelets in an in vivo mouse model

Finally, this mouse model was used to evaluate the functionality of the human donor platelets loaded through endocytosis (chapter 5) *in vivo*. As the undepleted mice appeared to consistently show little to no bleeding in previous experiments (Figure 6.6B), this was omitted for the following experiment as it would be unethical to use more mice than necessary. Instead, the main controls in this experiment were platelet-depleted and given a PBS transfusion which was expected to show a significant blood loss, platelet-depleted and given a human donor platelet transfusion, expected to show a reduction, and platelet-depleted mice given a transfusion of rFVIIa loaded platelets.

The weight of the tail transected and circulating haemoglobin concentration from the mice were examined to show no significant differences between the groups apart from the platelet count (Figure 6.7A,B,C).

Next, the volume of blood loss in the first four minutes of the experiment showed significant ($p<0.05$) differences between the three groups (Figure 6.8A). The platelet-depleted group showed a large volume of blood loss (167 ± 19.5 µL). The depleted group that were transfused with human donor platelets showed a significant ($p<0.05$) reduction in the volume of blood lost compared to the depleted only group (66.6 ± 11.0 µL). Finally, the group of mice transfused with the donor platelets loaded with rFVIIa showed a reduction from this (20.7± 2.64 µL). It was noted that there was no overlap between any of the three groups at this timepoint.

A plot of the cumulative blood loss over time (Figure 6.8B) showed that this effect trended over the course of the twenty minute experiment, with the average blood loss from the loaded donor platelet group being consistently below the average blood loss from the donor platelet group at all time points, although the compounding error of the cumulative blood loss makes it difficult to draw statistically significant conclusions.

The rate of blood loss appears to be steady at 11.4±4.08µL/min (mean±SEM) for the group transfused with donor platelets only, while the rate of blood loss appears to be biphasic with an inflection point at 12 minutes for the group transfused with loaded donor platelets with the first 12 minutes progressing at a rate of 5.72±0.676µL/min and the latter 12 minutes progressing at 16.4±4.11µL/min (data from Figure 6.8B and Figure 6.9). The variability in blood loss was also noted to be lower in these first twelve minutes of loaded platelet transfusion compared to the latter 12 minutes or the donor platelets only.

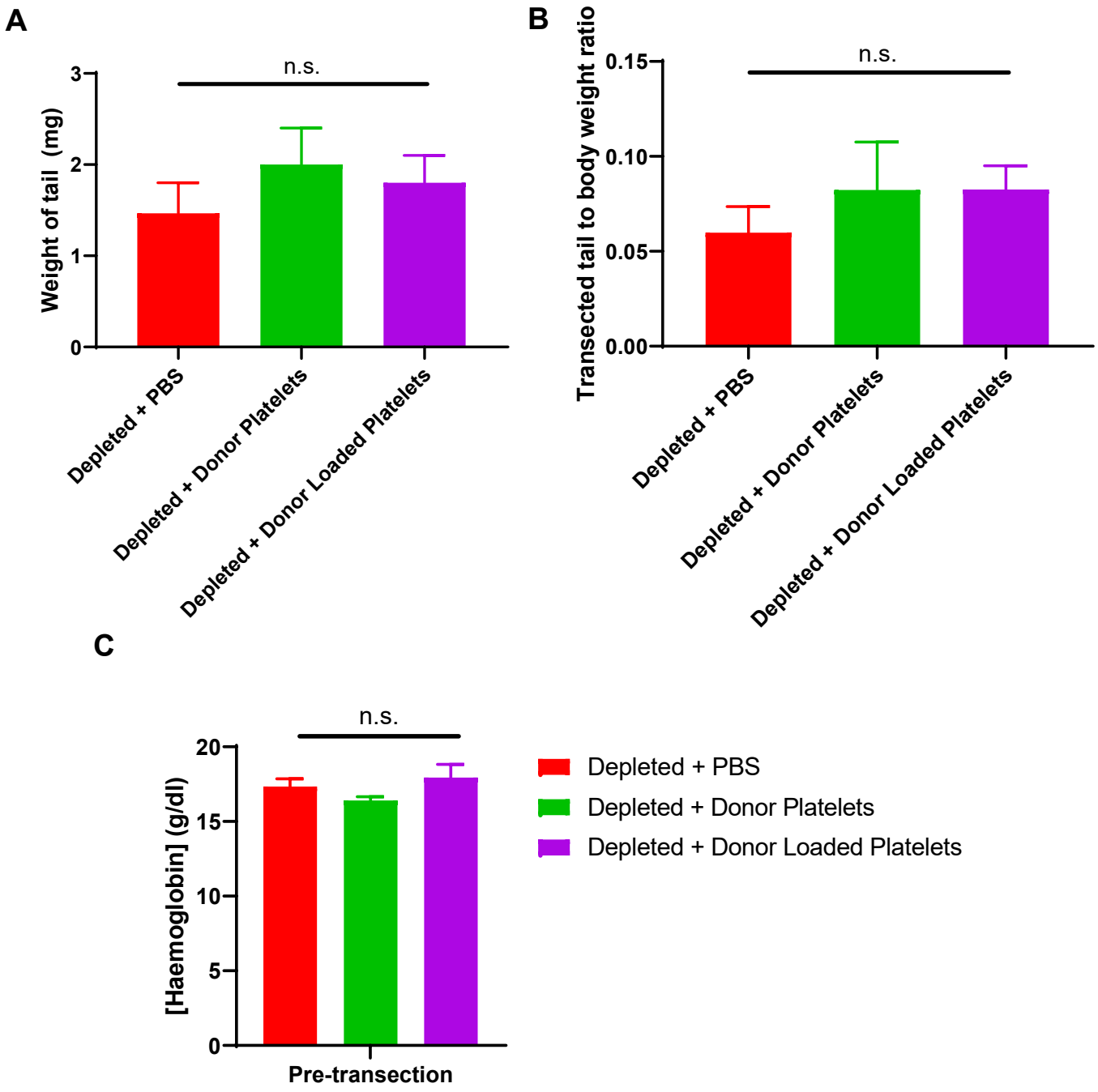

Figure 6.7. *Controls for the haemostasis tail transection experiment. (A) The weight of tail transected (B) The weight of tail transected normalised to mouse body weight (C) The circulating blood haemoglobin concentrations as measured by a complete blood count, shortly before the transection (-1hr). n=3, ANOVA. Error bars represent SEM.*

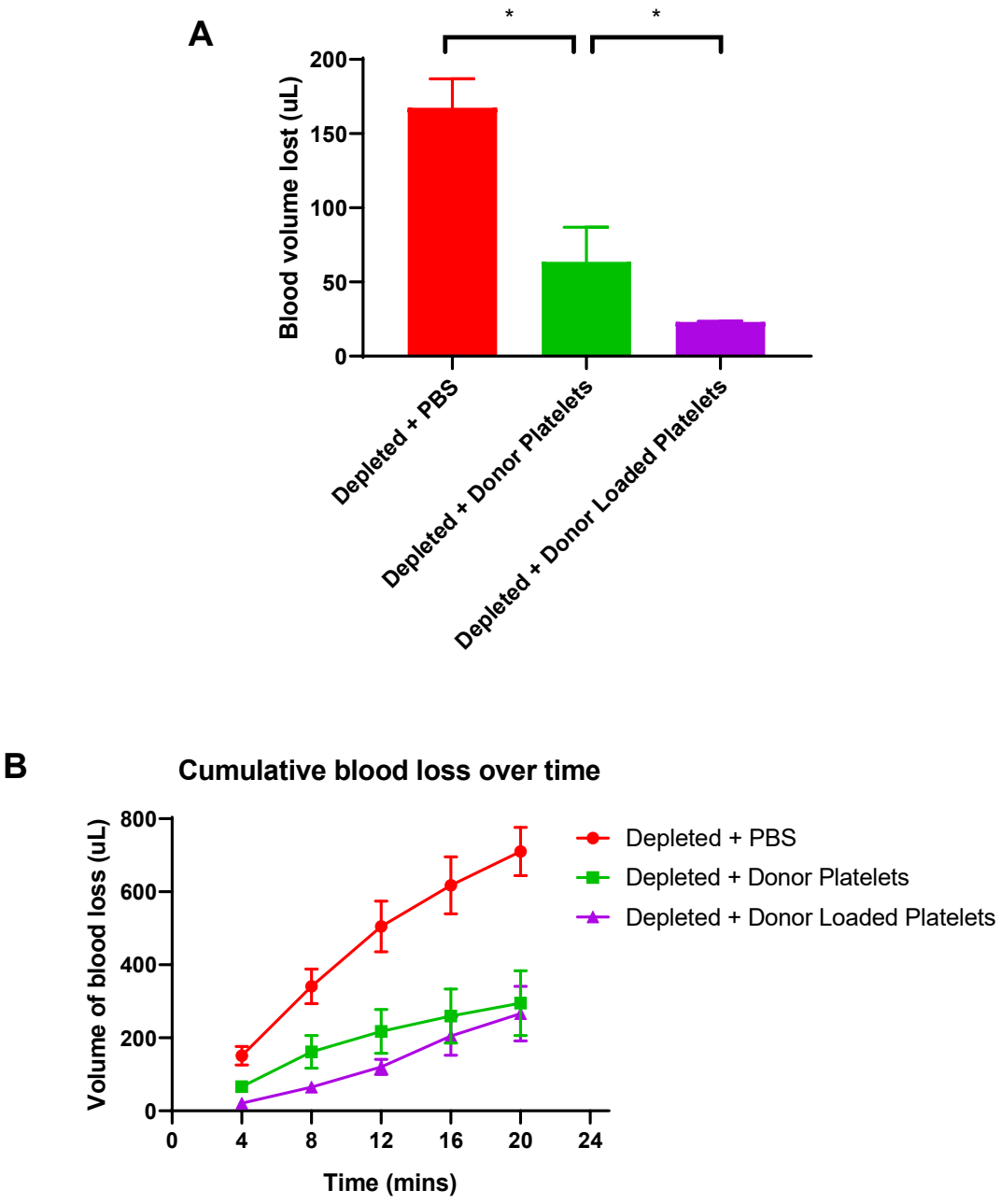

Figure 6.8. *Summary of haemostasis mouse model from mice that were depleted of platelets and transfused with 100x10^6 human donor platelets, and depleted and transfused with 100x10^6 human donor platelets loaded with rFVIIa. (A) The total blood volume lost in the first four minutes in all three groups. One way ANOVA, *p <0.05 **p<0.01 (B) The amount of cumulative blood volume loss over the full 20 minutes of the experiment in all three groups. n=3 per group, results show mean±SEM*

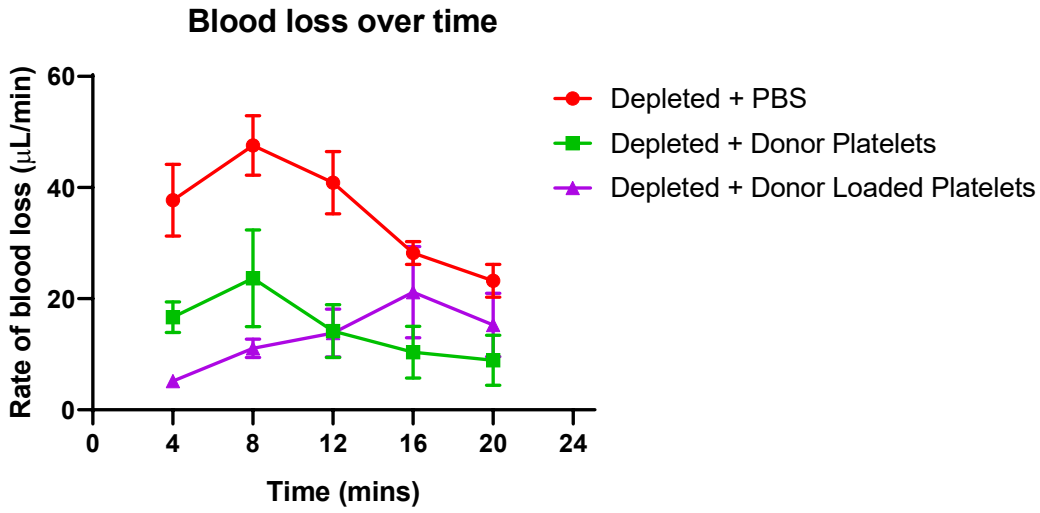

Figure 6.9. *Rate of blood loss for each individual timepoint (non-cumulative) plotted for the three groups of mice (n=3 in each group, all depleted of mouse platelets and then transfused with either PBS, donor platelets or donor loaded platelets). Data shown as mean±SEM.*

6.7 Discussion

From Figure 6.6, although the platelet count was lowered in the mice that received the antiserum intravenously, this was only to a modest degree. Differences between the BALB/c background of the NRG/J mice and C56BL/6 mice the serum was raised from could be a reason why the same dose previously reported to result in a full depletion had a substandard effect in the NRG/J mice (Hilton, Kile and Alexander, 2009; Salas-Perdomo *et al.*, 2019). This effect may be counteracted by increasing the dose of antiserum used and could be used to alter the magnitude of thrombocytopaenia. Furthermore, the control mice platelet count increased over the course of the experiment. This could be due to an inflammatory reaction, or perhaps a physiological response to the dilution of the platelet count through the intravenous injection of 100uL of fluid. From Table 6.1, it is possible that an inflammatory reaction is responsible for this effect as the percentage of granulocytes increased with a concordant decrease in the percentage of lymphocytes, suggesting an acute bacterial infection in both groups. Bacterial infection has been demonstrated to result in a rise in platelet counts in the literature (Bordin *et al.*, 1995).

From Figure 6.2, the signal from human platelets with this antiserum may be due either to non-specific binding, or binding to shared antigens present in both human and mouse platelets that the anti-thrombocyte serum is able to bind to. However, this feature renders this antiserum unsuitable for model development as it is likely to clear the human platelets from circulation as well as the mouse

platelets. Mice given the depletion antiserum appear to have a reduction in their platelet count compared to baseline to around 68% of the original level before steadily recovering over 48 hours towards the baseline, while control mice appear to experience an increase in platelet counts above the baseline platelet count.

Figure 6.4A shows clearly that the platelet count was depleted significantly ($p < 0.01$) through use of the anti-GP1b antibody and this represented a superior choice compared with the anti-thrombocyte antiserum. The antibody may have opsonised the platelets both in circulation and those newly produced, leading to Fc-dependent clearance by macrophages as seen in immune thrombocytopenic purpura (ITP) (Harrington *et al.*, 1951). The platelet-sized objects seen in the flow gates in Figure 6.4B may be very newly formed platelets, as evidenced by the increase in MPV; although no association has been found between steady-state platelet turnover and platelet size in humans (Mezzano *et al.*, 1981), Burstein and colleagues found that larger platelets are released after administration of IL-6 (Burstein *et al.*, 1992). Alternatively, these could be platelets that do not express CD42b on their surface, reported to correlate with decreased responses to agonist (Blair, Michelson and Frelinger, 2018). The dose of the antibody as suggested by the manufacturer was reported to increase the length of the period of platelet-depletion and not to modulate the degree of platelet depletion, suggesting the dose affects the half-life of the antibody in the circulation, but that any dose used is far in excess of that needed to opsonise all platelets in the circulation owing to its specificity. The reactive thrombocytosis seen post 96 hours is likely mediated by increased TPO production as a homeostatic response to the low platelet count, which is perhaps why it occurs after three days (as TPO acts on the level of the stem cell to stimulate thrombopoiesis) (Dettke *et al.*, 1998). This mouse model could therefore be also used as a model to discover novel factors involved in stimulation of reactive thrombopoiesis.

The only parameter measured to demonstrate the antibody does not interact with human platelets was binding; the antibody may also stimulate other functionality without long-term binding, for example, platelet activation. Interaction between vWF and GP1b is sufficient to promote platelet aggregation and similar effects have been previously reported by antibodies against GP1b through activating GP1b-IX in a shear-independent manner by inducing unfolding of the mechanosensory domain therein, leading to downstream platelet signalling (Quach, Chen and Li, 2018).

There are many factors that might influence the level of blood loss from these mice and several measurements were taken in order to ensure that conditions

that could affect the level of blood loss unrelated to the activity of platelets were kept as consistent as possible (Figure 6.5). Firstly, the weight of the tail that had been transected was collected and weighed (Figure 6.5A), and this showed no significant difference between the three groups. This indicates that the amount of tail transected and therefore the injury sustained was similar in all three groups. One confounder is the total body weight of the mice; 1g of tail to a 20g mouse is more significant an injury compared to a 30g mouse. For this reason, the ratio of transected tail to total body weight was also compared (Figure 6.5B) which again revealed no significant difference. Secondly, the circulating haemoglobin concentration were compared between all three groups (Figure 6.5C), both at the baseline bleeds taken 24 hours before the experiment and in the blood samples taken shortly before the experiment to confirm platelet depletion. A vastly different haemoglobin concentration may affect the calculations of volume of blood loss as it is based upon a haemoglobin assay of the saline that the mice bleed into. There was no significant difference between any of the groups at either timepoint, indicating that the platelet depletion had no significant effect on the haemoglobin levels in the mice.

Other blood parameters measured in the complete blood counts from these mice also showed no difference between the experimental groups apart from in the platelet count (Table 6.2), suggesting that the antibody is able to specifically deplete platelets and not affect other cell types. This suggests that any significant difference is solely due to platelet-related haemostasis and not differences in the coagulation cascade. Platelets are known to be a source of cytokines, microparticles and other factors, however, so the possibility that there exist other indirect consequences of platelet depletion on haemostasis that were not measured here remains (Maynard *et al.*, 2007).

A time course of the remainder of the experiment (Figure 6.6) shows how the rate of blood loss slows in all three groups over the twenty minutes of the experiment. This may be due to the significant levels of blood loss experienced by the depletion only group, and that with a reduced circulating volume, other factors such as blood pressure became the primary driving factors behind the rate of blood loss. Other possible factors to explain this effect may be the formation of a thrombus in all three groups that slowed the rate of blood loss.

The final experiment in Figure 6.8 shows that the loaded platelets described have a significantly ($p<0.05$) improved haemostatic response *in vivo* in the first four minutes of the experiment. This also appeared biphasic, with the trend being the rate of blood loss in the first 12 minutes being much lower in the loaded platelets,

before speeding up in the latter half of the experiment. The dynamics of the effects of loaded platelets on blood loss also appear to be different to the donor platelets from the individual timepoint data (Figure 6.9). This might suggest that the loaded platelets are being used up in the first part of the experiment, while slowing blood loss and maintaining the mouse blood pressure. In the latter part of the experiment, this suggests that after having been used up, the mice were able to bleed more than the same timepoint of mice transfused with only donor platelets as the other group had already lost a large proportion of their circulating blood volume. The peak of blood loss present in the depleted mice at eight minutes is lessened in magnitude in the mice transfused with donor platelets, and is shifted 8 minutes to the right in the mice transfused with loaded donor platelets (Figure 6.9).

However, it was also noted that the final cumulative blood loss was very similar between the unloaded donor platelet transfusion and the loaded platelet transfusion groups. This could be a feature of the relatively low number of platelets being transfused in this model. With an approximate pre-depletion platelet count of $1000x10^3$ platelets/μL and a blood volume of 1mL, this represents about 10^9 platelets in circulation. Comparatively, with a transfusion of only 10^8 platelets, or 10% of the original platelet count, this may not be sufficient to restore full haemostasis. This low number of platelets was chosen to amplify any differences between the groups, while still being sufficient for some degree of haemostasis. It would be difficult to assess differences between the groups when all of them have little-to-no bleeding as observed with the undepleted controls (Figure 6.6A), or when all groups bleed profusely and was chosen as in humans a platelet count of $100x10^3$/μl is clinically sufficient for haemostasis. This may mean however that all of the circulating platelets given by transfusion were used up in the first four minutes, or technical issues such as clots being dislodged when moving from one tube to another may have an effect on the later timepoints.

Alternatively, the effect of rFVIIa being at the very initiation of the clotting cascade (Figure 1.11) may imply it is specifically this initial part of the clotting process that is being accelerated. Evidence of this is that the rate of blood loss appears to be steady for the group transfused with donor platelets only (Figure 6.8 and Figure 6.9), while the rate of blood loss appears to be biphasic with an inflection point at 12 minutes for the group transfused with loaded donor platelets with the first 12 minutes progressing much more slowly and the latter 12 minutes increasing, suggesting that the loaded platelets are being used up in the first half of the experiment.

Figure 5.14 suggests that perhaps a small amount of rFVIIa is released without agonist stimulation from these platelets. Although this would likely be diluted by the blood volume of the mouse compared to the targeted delivery of the rFVIIa to the site of bleeding and would not result in a therapeutic dose if administered at this level directly to the mice, it may be prudent to include this as another control group if this experiment were to be repeated with rFVIIa-loaded platelets.

Overall, inducing a thrombocytopenia is possible, specifically depleting mouse platelets for 48 hours while not affecting any other blood parameters. The antibody used does not cross-react with human platelets. This creates a significant bleeding phenotype in these immunodeficient mice. Human platelets can be transfused into this model, survive in the circulation for the length of the experiment and have a significant effect on reducing bleeding in mice.

7 FINAL DISCUSSION

7.1 Introduction

Platelets, being small anucleate cells with granules that are released upon activation, have great potential as a novel drug delivery system. The benefits of this approach include the ability to potentially improve the safety profile and reducing the required dose of drugs that are already in clinical use, by only exposing the active drug in areas of platelet activation, to eventually provide significant improvements over currently available treatments.

As platelets normally activate in areas of thrombus formation, rFVIIa was chosen as a candidate to augment the thrombotic potential of platelets selectively in areas of bleeding for the treatment of acute haemorrhage. This project aimed to develop tools to load platelet granules with rFVIIa, assess the success of this and their efficacy for the treatment of bleeding *in vivo* as a proof-of-concept for using platelets as a delivery system. This was done through exploring the two routes that proteins normally take for trafficking to platelet granules, synthesis and endocytosis.

7.2 Loading platelet granules with non-endogenous proteins

7.2.1 *Loading platelet granules through an expression cassette in a forward-programmed megakaryocyte system*

Firstly, a modified form of the FVII was designed, cloned and transduced into FoPMKs. The transduction of FoPMKs was shown to be successful through a variety of techniques including ELISA, flow cytometry, Western blot and IF. The modified FVII was then localised using IF into granules within these FoPMKs. ELISA data also suggested that the modified FVIIa was present in the resultant platelets in the supernatant and flow cytometry was used to demonstrate further that the platelets produced by these MKs in a liquid culture system contained this modified protein.

The importance of these results lies in the generalisability of the targeting system used. Previous work had only showed that when fused to FVIII that the resultant fusion protein ended up in granules in *ex vivo* megakaryocytes from dogs (Du *et al.*, 2013). Work by Dr Annett Mueller from the Ghevaert group showed that this, when fused to GFP could be used to load platelet granules more generally, and that this was not specific to only FVIII.

Evidence in this thesis has shown that it is possible to load arbitrary clotting factors such as rFVIIa, but also that cleavage sequences such as a thrombin cleavage site can be inserted to result in the release of the original protein from

the vWF-based targeting system upon activation. Finally, the data here has elucidated how this targeting strategy affects the subtype of α-granule that these proteins may be targeted to, which has previously not been investigated.

7.2.2 *Validation of the functionality of the modified FVII*

After having verified the presence of the modified FVII structurally, it was then validated functionally. First, Western blots were used to show that the addition of exogenous enzyme was able to cleave the modified FVII at the appropriate inserted cleavage sequences. Thrombin alone was sufficient to cleave the full-length protein into the heavy and light chain seen in the native rFVIIa, thought to be due to the presence of intracellular furin in the lysates.

Next, thrombin generation assays showed a clear difference between the platelets produced by the FoPMKs transduced with the vWF-F7TF compared to donor platelets and those produced from untransduced FoPMKs. This was notable both in the raw thrombin generation graphs at intermediate concentrations of platelets, but also in the calculated EC_{50} values derived from the concentration curve of platelets when observing the total thrombin generation from this assay.

The trends shown in all parameters of this assay suggest that the platelets produced from transduced FoPMKs are able to generate more thrombin, and therefore form clots more rapidly, than those from untransduced FoPMKs and donor platelets. However, this is an *in vitro* model system to recreate the process of clotting and so caution should be taken when interpreting this result for translation to *in vivo* models.

Importantly, this also demonstrates that the proteins delivered using this system such as FVIIa do not undergo such irreversible structural changes due to the addition of the large (~40kDa) vWF SPD2 domain as to render them non-functional. This suggests that, when scaled up in the future, this would create platelets containing a version of FVII that would convert into its native active enzymatic form upon platelet activation and subsequently have an effect on thrombin generation, as the Western blot data suggests that without thrombin this does not take place. This may then provide a further safety mechanism for this drug over the commercially available rFVIIa, in requiring thrombin to be present before the rFVIIa is enzymatically active in its native form.

7.2.3 *Endocytosis as a technique to load platelet granules*

Platelets were shown to be able to directly endocytose rFVIIa into their granules through a short incubation at room temperature, and the efficacy of these loaded platelets was demonstrated in releasate assays and in thrombin generation assays (chapter 5). Flow cytometry was used to demonstrate that platelets are able to directly endocytose and internalise the protein, and ELISA was used to show that they are able to release it upon stimulation with thrombin. Thrombin generation assays showed similar results to those seen from the platelets loaded through the expression cassette, with a higher total thrombin generation observed at intermediate concentrations from the raw thrombin generation graph as well as a reduction in the EC_{50} for these loaded platelets compared to donor platelets.

Difficulty remains in directly comparing the activity of the rFVIIa in these platelets loaded through endocytosis with those from the lentiviral transduction, as the amount of protein absorbed or synthesised per granule or platelet is likely subject to considerable variation between the two systems. However, despite this caveat, the reduction in EC_{50} values appears similar.

Importantly, taken together with the results from the expression cassette, this shows that this effect on total thrombin generation is caused by the selective release of rFVIIa by platelets in response to thrombin, regardless of the very different techniques used to actually load the granules.

7.2.4 *Demonstrating the in vivo potential of loaded platelets*

Finally, the most important finding of this work was that these loaded platelets demonstrate efficacy in an *in vivo* model of haemostasis. The platelets loaded by endocytosis might be predicted to result in a faster rate of clot formation from the faster, sharper peak seen from the thrombin generation assay. The result from this *in vivo* was demonstrated to result in a significant ($p<0.05$) reduction in blood volume loss in the first 4 minutes from a transfusion and tail transection model *in vivo* (chapter 6).

This work builds on all the results of previous chapters in demonstrating that the effects seen from these loaded platelets from in vitro assays translate to an *in vivo* system, opening the door to encourage the development of even more sophisticated techniques to generate these platelet products at scale to address some of the current issues with platelet transfusion and rFVIIa administration.

7.3 Further work

7.3.1 *How much rFVIIa is present in loaded platelet granules?*

One question that remains relating to this work is in accurately quantifying how much of the protein is packaged into each granule or into each platelet. This would help to compare the effective doses of loaded platelets with the doses of rFVIIa used in the literature in clinical trials (Gill *et al.*, 2009). This would also help in estimating the high local concentration of rFVIIa generated in areas of platelet activation and allow further mathematical modelling of this.

The total amount may vary from platelet to platelet, and likely will need to be standardised for each preparation as some granules may contain more rFVIIa than others, and some platelets may contain more granules than others. The techniques used to load the platelets may also affect this, as suggested by the IF data in Figure 5.9 showing few granules in MKs loaded through endocytosis, compared to Figure 3.20 loaded through the expression cassette showing many more granules positive for rFVIIa per megakaryocyte.

Finally, this could then be used to directly quantify the effective dose of rFVIIa required for efficacy compared to the current standard for treatment to test the hypothesis that the rFVIIa is delivered to create a high local concentration of the protein in areas of bleeding and that this has a similar effect *in vivo* to systemically dosed rFVIIa. This also raises the question of whether the FVIIa released by loaded platelets remains bound to the platelet surface or if it is released into the interstitial space.

7.3.2 *Do loaded platelets continue to keep rFVIIa sequestered in vivo?*

The data in chapter 5 showed that even the no thrombin condition of loaded platelets, expected not to have any FVII in their releasate, did show a small amount of FVII detected. Questions that remain to be explored are whether this is significant *in vivo*, whether this matters for the safety of loaded platelets and whether the platelets are able to only release the rFVIIa at sites of bleeding or if they release the rFVIIa in other locations.

This observed FVII in the supernatant may have been left over from an incomplete washing of the excess rFVIIa, or it may have been released from the loaded platelets themselves. The latter may occur due to accidental activation of the platelets, for example, through mechanical manipulation, or perhaps it may represent a situation where the contents of these granules are somewhat leaky to the extracellular compartment. This effect has been previously observed in the

spontaneous release of neurotransmitters from synaptic granules in neurones (Fatt and Katz, 1950; Kavalali, 2018). Platelet granules, being similar to synaptic vesicles in many respects, may undergo similar processes.

Theoretically, despite this apparent leakiness of the platelet granule contents, the efficacy of the loaded platelets should derive from a high local concentration of rFVIIa in areas of platelet activation, and a dilution to very low plasma concentrations in the general circulation. This would however require further work and different mouse models to address and to quantify its impact.

7.3.3 *How are the different granule populations formed and do they undergo differential release?*

The immunofluorescence data from chapters 3 and 5 raise questions about the trafficking of proteins in megakaryocytes, and implies that the sorting of proteins in these cells is not as linear as has been previously assumed. For example, although the vWF-SPD2 fragment attached to GFP results in GFP expression from thrombospondin-containing granules (Figure 3.1), the same vWF-SPD2 fragment attached to FVII does not (Figure 3.20). Instead, this appears to direct the fusion protein to an alternative subpopulation of granule that contains VEGF but not thrombospondin or endostatin. Some papers suggest that the different subpopulations serve antagonistic functions (pro- and anti-angiogenic), and are released in response to different agonists, although both appear to be released upon exposure to thrombin (Italiano *et al.*, 2008). An open question remains as to how the FVII portion of the protein is able to partially override the vWF-SPD2 portion of the domain, given the size of this fragment, and whether this may be differentially released in response to certain agonists.

Although GFP was expressed in the cytoplasm when the SPD2 domain is removed, the same cannot be said for FVII without this domain. Despite being at a high titre when detected by qPCR in HCT116 cells (Figure 3.8), attempts to detect the resultant protein by Western blot and flow cytometry in FoPMKs failed. This may suggest that the protein is somehow being degraded and being taken directly to the proteosome, or that it is being misfolded and thus not binding to the antibody or that its expression is being silenced, which may be how *in vivo*, certain coagulation factors such as Factor V are expressed by MKs whereas others such as Factor VII are not (Maynard *et al.*, 2007).

The vWF-F7TF protein produced was also not present in every granule containing VEGF. There was a population containing both, as well as population of granules

containing either one or the other. This might imply some stochasticity to the distribution and sorting of proteins into granules, with some granules ending up with more of certain proteins than others, and other studies have previously found little functional co-clustering of proteins within α-granules (Kamykowski *et al.*, 2011). Another explanation for this is that the expression of GFP was measured using direct fluorescence compared to the expression of vWF-F7TF, measured using immunofluorescence. The use of antibody staining may make the immunofluorescence technique more sensitive to the amount of protein present in a way that the direct fluorescence methodology is not.

Finally, when comparing the synthesis route compared to the endocytosis route looking only at the MKs, the number of granules staining positive for FVII when the MKs are incubated for 24 hours with the protein remain small compared to the number detected when the vWF-F7TF is expressed through lentiviral transduction. There also appears to be some evidence of platelet heterogeneity in the literature (Kempton *et al.*, 2005). Combined with the stochasticity of the vWF-F7TF produced through synthesis and the limited number of granules observed through endocytosis, there also appears to be some evidence of this heterogeneity from data in this thesis.

7.4 Future perspectives and challenges

7.4.1 *Genomic safe harbour integration*

The construct introduced in chapter 3 may be introduced into a genomic safe harbour site in the inducible FoPMKs to result in an inducible stem cell line that can be forward programmed to produce rFVIIa-loaded platelets.

Challenges that remain with this approach include the need to discover novel safe harbour sites for this insertion to take place. The doxycycline inducible FoPMK system currently makes use of both well-characterised safe harbour sites, AAVS1 and ROSA26. Insertion of a third sequence would require the discovery of another reliable safe harbour sequence that remains immune to silencing effects when the iPSCs are differentiated into FoPMKs, and this discovery could be attempted using a gene-trap approach or follow-up of predicted safe harbour sites from whole-genome sequencing studies (Pellenz *et al.*, 2019).

This approach could be combined with the work in chapter 4 to ensure the resultant cell lines remain absent of any known deleterious or dangerous mutations and CRISPR used to insert the vWF-F7TF construct into this genomic site. Combined with improvements in bioreactor technology and further scaling

up, this alternative source of rFVIIa-loaded platelets could be evaluated with the mouse model established in chapter 6. If this occurs, it will also be necessary to explore whether the amount of vWF-F7TF being produced in this system per megakaryocyte and per granule is the same as that observed in the lentiviral system in order to make an accurate comparison between them.

7.4.2 *Producing platelets on a larger scale*

This work complements studies looking at novel bioreactor technologies that might allow for *in vitro*-derived platelets to be extracted at a much larger scale than is currently possible. Current bioreactor technologies appear to result in approximately 10-100 platelets per input MK, even when incorporating microfluidic devices and turbulence to recreate the mechanical stresses of MKs in bone marrow. Compared to the thousands produced from MKs in bone marrow *in vivo*, this indicates an order of magnitude of improvement is still possible.

This increase in thrombopoiesis would be necessary to offset the otherwise prohibitive costs involved in scaling up MK culture. For a standard human transfusion unit of $5x10^{10}$ platelets, roughly £200 (NHS Blood & Transplant, 2016), at present this would optimistically require the culture of approximately $5x10^{8}$ MKs, which when seeded at an optimal concentration of $0.5x10^{6}$ MKs/mL would require approximately 1L of cell culture media, alone already £330 (CellGenix, 2020), every two days along with associated cytokines.

Improvements to *in vitro* thrombopoiesis technologies, e.g. new bioreactor designs or additional soluble factors to stimulate platelet release, may address some of these issues. From the work in chapter 3, if it is possible to achieve a similar haemostatic effect with fewer platelets in a transfusion unit, this may also independently bring *in vitro* derived platelets closer to clinical translation. Key considerations for clinical translation are ensuring stem cell-derived therapies are safe, effective and affordable, as defined by the International Society for Stem Cell Research guidelines from 2016 (Daley *et al.*, 2016).

The use of CRISPR to integrate these exogenous genetic sequences into the self-renewing iPSC lines used for differentiation will eliminate the use of lentivirus. Lentiviral transduction, although a useful laboratory technique, is often expensive to produce and utilise on a large scale for platelet production as well as in a cGMP facility, and has safety issues when considering its random genomic integration leaves open the potential for a malignant transformation of the FoPMK culture, requiring constant screening for abnormal insertion and the presence of replication-competent viruses (Milone and O'Doherty, 2018). These have all been

documented issues when other therapies such as with chimeric antigen receptor (CAR) T-cells in the field of cancer immunotherapy (Oldham, Berinstein and Medin, 2015). Elimination of lentivirus would simplify the culture process to be fully inline, allowing it to take place fully in a CL1 facility and render vWF-F7TF MK culture more scalable by reducing the costs and number of reagents required, complexity of cell culture, allowing it to more easily be translated into a cGMP facility and the quality assurance thereafter would be more straightforward.

When combined with other work looking to knockout B2M and render platelets immuno-compatible with a large number of people, it is possible that in the future there will be one cGMP-compliant stem cell line engineered with all of the appropriate modifications to be able to produce platelets that do not require HLA-matching and provide additional benefits such as rFVIIa delivery compared to platelets from donor blood. A similar approach has been taken with B2M knockouts to generate universally immuno-compatible CAR T cells (Ren *et al.*, 2017).

7.4.3 In vivo *modelling of haemostasis*

One limitation of the work in this thesis is that much of the work is either with *in vitro* models that attempt to recreate the process of clotting (such as the thrombin generation assay) and *in vivo* work that takes place in a model system in mice that has limitations in its applicability to human platelet transfusion in a clinical context. For example, the main readout of the tail transection assay was the first four minutes of blood loss. The later time points appeared less informative due to three possible sources of experimental error. The significant percentage of circulating blood volume being lost is likely to have affected the blood pressure at later time points in the assay, which makes a direct comparison of blood volume lost between timepoints difficult. Any clot formed may have been dislodged by the movement of the tail from one tube to another. This makes later time points more unreliable, and measurement errors compound when measuring cumulative blood loss through this technique. Other mouse models may need to be explored to investigate these effects further, such as those looking at platelet survival (Fuhrmann *et al.*, 2016).

The purpose of the *in vivo* model explored here is very different to and does not attempt to model long-term safety due to technical limitations, not least being that the mice are terminated within twenty minutes of the transfusion. Even in an immunocompromised mouse model, human platelets are cleared within hours without the addition of other substances such as clodronate liposomes which

deplete macrophages and may alter the physiology of the mice in other ways, which may alter the behaviour of these platelets compared to if they were transfused into a human patient (Newman, Aster R and Boylan B., 2007). These factors make it difficult to assess the incidence of increased thrombosis (e.g. in heart attacks and cerebrovascular accidents) with this form of therapy. As a key consideration of the use of rFVIIa in the clinic is the safety profile, especially when approaching regulatory agencies for these therapies. There is, however, a theoretical benefit of being able to use a lower overall dose of the drug and therefore reduce the incidence of adverse events. Future work may look at other *in vivo* models of haemostasis that also look at the safety aspects of these products.

7.4.4 *Clinical trials*

As was previously described in the introduction (section 1.5), current treatments for acute haemorrhage involve blood products such as fresh frozen plasma, activated prothrombin complex concentrates, as well as platelet transfusion. The addition of donor platelets loaded through endocytosis as a therapeutic option may provide another product that could be derived from blood donors. This may allow for the transfusion of fewer platelets, resulting in less immune sensitisation of the recipient and allow the current limited platelet supply to treat more patients than is possible at present.

Many of the surgical tools used for haemostasis also require a knowledge of where the bleeding is occurring from (Behrens, Sikorski and Kofinas, 2014). A targeted therapy that can be administered systemically could provide benefits over these current treatments for patients bleeding from an unknown source and as demonstrated in the in vivo model, where the tail transection was carried out immediately after transfusion, a significant difference was observed in the first four minutes of bleeding.

For patients receiving rFVIIa in an acute setting for haemorrhage that likely will also require a transfusion at some point, the targeted delivery of this drug with the transfusion may result in a much lower dose of the drug being required to observe a benefit. The increased cost-effectiveness for rFVIIa that may justify its use more often clinically. This technique could also offer potential safety benefits through a reduction in thrombotic events as has been observed with the comparatively high doses of rFVIIa currently in clinical use.

This could provide an ideal patient population with which to use this as an intervention in a clinical trial setting. Blood products are already common

treatments for haemorrhage and so this may offer an opportunity to assess safety and efficacy of these products when compared to standard therapies that have known adverse events, allowing for the maintenance of clinical equipoise.

The double-blinded control arm could be the current standard of trauma care with normal donor platelets used as a transfusion when required, while the experimental arm could be transfusion with these loaded platelets. The outcomes measured in such a trial would be the number of units of platelet transfusion required and quantity of blood loss as intermediate endpoints, as well as the percentage survival of these patients as an endpoint. Platelets have an advantage over other therapeutics in that they can also be removed quickly through plasmapheresis if any adverse events were detected with these loaded platelets.

7.4.5 *Platelet granules as a drug delivery system beyond rFVIIa*

In this thesis, only rFVIIa was used as a payload for these platelets. This will however pave the way for further possible cargo proteins suitable for delivery. Example of some of these possibilities include the delivery of thymosin β4, shown in in vitro cultures to stimulate cardiomyocyte regeneration to areas of infarcted myocardium where platelets have been observed to accumulate (Shrivastava *et al.*, 2010). Platelets might also be used to deliver anti-thrombotic agents to existing clots, such as tissue plasminogen activator (t-PA) (Greineder *et al.*, 2013). Due to their important immunomodulatory and angiogenic roles, platelets are often recruited by tumours and so there exist opportunities to deliver cytotoxic agents to certain cancers (Labelle, Begum and Hynes, 2014). Some of this has been attempted through covalent linkage of anti-PD1 antibodies to the surface of platelets, but it may be possible to further sequester these agents within platelet granules to further reduce their off-target effects (Zhang *et al.*, 2018).

This versatility is likely to provide a significant competitive advantage to *in vitro*-derived platelets compared to other efforts to develop synthetic platelet alternatives based on nanoparticles which may not share the same biological interactions as real platelets and often depend on materials that, unlike stem cells, are not able to self-renew which may drive costs up (Shukla *et al.*, 2017).

Potential ways in which platelets could be used as a drug delivery system include being targeted to areas where platelets normally degranulate (Figure 7.1A), e.g. in coagulation or other instances where there is endothelial damage, such as myocardial infarction (Gidlöf *et al.*, 2013). Platelets could also be engineered to express receptors that bind proteins of interest from the blood preventing their action, and as they last for up to ten days, be more effective than antibodies

(Figure 7.1B). Both of these could be coupled together to result in a targeted delivery system that could degranulate in response to a particular stimulus or context, such as in tumours using the Warberg effect, or at times of high sugar in diabetes (Figure 7.1C). Finally, the platelets may simply be used to protect recombinant proteins from degrading in the blood, which might be especially useful in diseases where enzymes are missing from the blood, e.g. inborn errors of metabolism (Figure 7.1D).

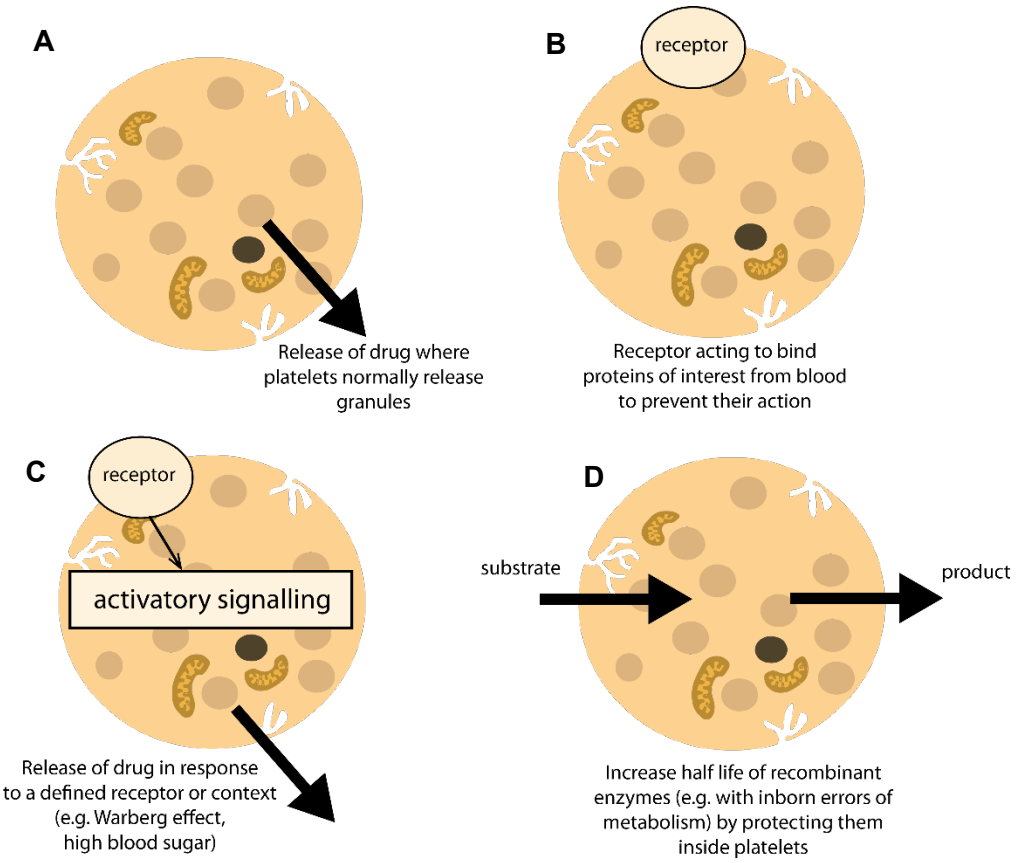

***Figure 7.1**. Potential ways in which platelets could be used as a drug delivery system.*

7.5 Conclusions

Overall, this thesis demonstrates two methods for successfully loading platelet α-granules with FVIIa, lentiviral transduction of their precursor megakaryocytes (with methods developed to assess off-target effects of CRISPR if integrated into a genomic safe harbour site) and direct endocytosis by platelets. Both techniques result in platelets that show improved haemostatic properties with *in vitro* assays. A novel mouse model for human platelet transfusion and subsequent haemostasis was established using immunocompromised thrombocytopenic NRG/J mice and this was subsequently used to show an improvement in haemostasis following transfusion of platelets loaded with rFVIIa.

8 Bibliography

Acar, M. *et al.* (2015) 'Deep imaging of bone marrow shows non-dividing stem cells are mainly perisinusoidal', *Nature*. Nature Publishing Group, 526(7571), pp. 126–130. doi: 10.1038/nature15250.

Achneck, H. E. *et al.* (2010) 'A Comprehensive Review of Topical Hemostatic Agents', *Annals of Surgery*, 251(2), pp. 217–228. doi: 10.1097/SLA.0b013e3181c3bcca.

Ahmed, S. G., Ibrahim, U. A. and Hassan, A. W. (2007) 'Adequacy and pattern of blood donations in north-eastern Nigeria: The implications for blood safety', *Annals of Tropical Medicine and Parasitology*. Ann Trop Med Parasitol, 101(8), pp. 725–731. doi: 10.1179/136485907X241442.

Ala, F. *et al.* (2012) 'External Financial Aid to Blood Transfusion Services in Sub-Saharan Africa: A Need for Reflection', *PLoS Medicine*. Public Library of Science, 9(9), p. e1001309. doi: 10.1371/journal.pmed.1001309.

Albers, C. A. *et al.* (2012) 'Compound inheritance of a low-frequency regulatory SNP and a rare null mutation in exon-junction complex subunit RBM8A causes TAR syndrome', *Nature Genetics*. Nature Publishing Group, 44(4), pp. 435–439. doi: 10.1038/ng.1083.

Alexander, W. S. *et al.* (1996) 'Studies of the c‐Mpl Thrombopoietin Receptor through Gene Disruption and Activation', *Stem Cells*. Wiley, 14(S1), pp. 124–132. doi: 10.1002/stem.5530140716.

Alexandrov, L. B. *et al.* (2013) 'Deciphering signatures of mutational processes operative in human cancer', *Cell reports*. 2013/01/10. Cell Press, 3(1), pp. 246–259. doi: 10.1016/j.celrep.2012.12.008.

Alexandrov, L. B. *et al.* (2015) 'Clock-like mutational processes in human somatic cells', *Nature genetics*. 2015/11/09, 47(12), pp. 1402–1407. doi: 10.1038/ng.3441.

Alexandrov, L. B. *et al.* (2020) 'The repertoire of mutational signatures in human cancer', *Nature*. 2020/02/05. Nature Publishing Group UK, 578(7793), pp. 94–101. doi: 10.1038/s41586-020-1943-3.

Aljamali, M. N. *et al.* (2008) 'Long-term expression of murine activated factor VII is safe, but elevated levels cause premature mortality', *The Journal of Clinical Investigation*. The American Society for Clinical Investigation, 118(5), pp. 1825–1834. doi: 10.1172/JCI32878.

American Red Cross (2019) *One-two punch of winter storms, canceled blood drives straining Red Cross blood supply*. Available at: https://www.redcrossblood.org/local-homepage/news/article/one-two-punch-of-winter-storms--canceled-blood-drives-straining-.html (Accessed: 4 February 2020).

Andrews, R. K. and Berndt, M. C. (2004) 'Platelet physiology and thrombosis',

Thrombosis Research. Pergamon, 114(5–6), pp. 447–453. doi: 10.1016/J.THROMRES.2004.07.020.

Arce-Gomez, B. *et al.* (1978) 'The genetic control of HLA-A and B antigens in somatic cell hybrids: requirement for beta2 microglobulin.', *Tissue antigens*. England, 11(2), pp. 96–112. doi: 10.1111/j.1399-0039.1978.tb01233.x.

Aschoff, L. (1893) 'Ueber capilläre Embolie von riesenkernhaltigen Zellen', *Archiv für Pathologische Anatomie und Physiologie und für Klinische Medicin*. Springer-Verlag, 134(1), pp. 11–25. doi: 10.1007/BF01924893.

Augustsson, C. and Persson, E. (2014) 'In vitro evidence of a tissue factor-independent mode of action of recombinant factor VIIa in hemophilia', *Blood*. American Society of Hematology, 124(20), pp. 3172–3174. doi: 10.1182/blood-2014-05-576892.

Avecilla, S. T. *et al.* (2004) 'Chemokine-mediated interaction of hematopoietic progenitors with the bone marrow vascular niche is required for thrombopoiesis', *Nature Medicine*. Nat Med, 10(1), pp. 64–71. doi: 10.1038/nm973.

Avvisati, G. *et al.* (1980) 'Evaluation of a New Chromogenic Assay for Factor VII and its Application in Patients on Oral Anticoagulant Treatment', *British Journal of Haematology*. John Wiley & Sons, Ltd, 45(2), pp. 343–352. doi: 10.1111/j.1365-2141.1980.tb07153.x.

Baker, D. *et al.* (2016) 'Detecting Genetic Mosaicism in Cultures of Human Pluripotent Stem Cells', *Stem Cell Reports*. Cell Press, 7(5), pp. 998–1012. doi: 10.1016/j.stemcr.2016.10.003.

Barker, J. E. (1994) 'SI/SI(d) hematopoietic progenitors are deficient in situ', *Experimental Hematology*, 22(2), pp. 174–177.

Bartley, T. D. *et al.* (1994) 'Identification and cloning of a megakaryocyte growth and development factor that is a ligand for the cytokine receptor Mpl', *Cell*. Elsevier, 77(7), pp. 1117–1124. doi: 10.1016/0092-8674(94)90450-2.

Bastian, L. S. *et al.* (1999) 'Regulation of the megakaryocytic glycoprotein IX promoter by the oncogenic Ets transcription factor Fli-1.', *Blood*. United States, 93(8), pp. 2637–2644.

Bates, I. *et al.* (2008) 'Maternal mortality in sub-Saharan Africa: The contribution of ineffective blood transfusion services', *BJOG: An International Journal of Obstetrics and Gynaecology*. BJOG, pp. 1331–1339. doi: 10.1111/j.1471-0528.2008.01866.x.

Becker, A. J., McCulloch, E. A. and Till, J. E. (1963) 'Cytological demonstration of the clonal nature of spleen colonies derived from transplanted mouse marrow cells', *Nature*. Nature Publishing Group, 197(4866), pp. 452–454. doi: 10.1038/197452a0.

Becker, R. P. and De Bruyn, P. P. H. (1976) 'The transmural passage of blood cells into myeloid sinusoids and the entry of platelets into the sinusoidal circulation; a scanning electron microscopic investigation', *American Journal of*

Anatomy. Am J Anat, 145(2), pp. 183–205. doi: 10.1002/aja.1001450204.

Behnke, O. (1989) 'Coated pits and vesicles transfer plasma components to platelet granules.', *Thrombosis and haemostasis*. Germany, 62(2), pp. 718–722.

Behnke, O. (1992) 'Degrading and non-degrading pathways in fluid-phase (non-adsorptive) endocytosis in human blood platelets.', *Journal of submicroscopic cytology and pathology*. Italy, 24(2), pp. 169–178.

Behnke, O. and Forer, A. (1998) 'From megakaryocytes to platelets: Platelet morphogenesis takes place in the bloodstream', *European Journal of Haematology, Supplement*. John Wiley & Sons, Ltd, 60(61), pp. 3–24. doi: 10.1111/j.1600-0609.1998.tb01052.x.

Behrens, A. M., Sikorski, M. J. and Kofinas, P. (2014) 'Hemostatic strategies for traumatic and surgical bleeding', *Journal of biomedical materials research. Part A*. 2013/12/12, 102(11), pp. 4182–4194. doi: 10.1002/jbm.a.35052.

Bernad, A. *et al.* (1994) 'Interleukin-6 is required in vivo for the regulation of stem cells and committed progenitors of the hematopoietic system', *Immunity*, 1(9), pp. 725–731. doi: 10.1016/S1074-7613(94)80014-6.

Bezinover, D. *et al.* (2018) 'Perioperative coagulation management in liver transplant recipients', *Transplantation*. Lippincott Williams and Wilkins, pp. 578–592. doi: 10.1097/TP.0000000000002092.

Bikard, D. *et al.* (2013) 'Programmable repression and activation of bacterial gene expression using an engineered CRISPR-Cas system', *Nucleic Acids Research*, 41(15), pp. 7429–7437. doi: 10.1093/nar/gkt520.

Birkenfeld, J. *et al.* (2007) 'GEF-H1 Modulates Localized RhoA Activation during Cytokinesis under the Control of Mitotic Kinases', *Developmental Cell*. Cell Press, 12(5), pp. 699–712. doi: 10.1016/j.devcel.2007.03.014.

Blagoveshchenskaya, A. D. *et al.* (2002) 'Selective and signal-dependent recruitment of membrane proteins to secretory granules formed by heterologously expressed von Willebrand factor', *Molecular Biology of the Cell*. American Society for Cell Biology, 13(5), pp. 1582–1593. doi: 10.1091/mbc.01-09-0462.

Blair, P. and Flaumenhaft, R. (2009) 'Platelet α-granules: Basic biology and clinical correlates', *Blood Reviews*. Churchill Livingstone, 23(4), pp. 177–189. doi: 10.1016/J.BLRE.2009.04.001.

Blair, T. A., Michelson, A. D. and Frelinger, A. L. (2018) 'Mass Cytometry Reveals Distinct Platelet Subtypes in Healthy Subjects and Novel Alterations in Surface Glycoproteins in Glanzmann Thrombasthenia', *Scientific Reports*. Nature Publishing Group, 8(1). doi: 10.1038/s41598-018-28211-5.

Bomken, C. *et al.* (2009) 'Recombinant Activated Factor VII (rFVIIa) in the Management of Major Obstetric Haemorrhage: A Case Series and a Proposed Guideline for Use', *Obstetrics and gynecology international*. 2010/02/03. Hindawi Publishing Corporation, 2009, p. 364843. doi: 10.1155/2009/364843.

Bordin, J. O. *et al.* (1995) 'Bacterial infection-associated improvement of platelet counts in two patients with chronic and unresponsive idiopathic thrombocytopenic purpura with normal platelet survival studies', *British Journal of Haematology*. Br J Haematol, 90(2), pp. 332–335. doi: 10.1111/j.1365-2141.1995.tb05154.x.

Brand, A. (2001) 'Alloimmune platelet refractoriness: incidence declines, unsolved problems persist.', *Transfusion*. United States, pp. 724–726. doi: 10.1046/j.1537-2995.2001.41060724.x.

Brouard, N. *et al.* (2017) 'A unique microenvironment in the developing liver supports the expansion of megakaryocyte progenitors', *Blood Advances*. American Society of Hematology, 1(21), pp. 1854–1866. doi: 10.1182/bloodadvances.2016003541.

Bruns, I. *et al.* (2014) 'Megakaryocytes regulate hematopoietic stem cell quiescence through CXCL4 secretion', *Nature Medicine*. Nature Publishing Group, 20(11), pp. 1315–1320. doi: 10.1038/nm.3707.

Di Buduo, C. A. *et al.* (2015) 'Programmable 3D silk bone marrow niche for platelet generation ex vivo and modeling of megakaryopoiesis pathologies', *Blood*. American Society of Hematology, 125(14), pp. 2254–2264. doi: 10.1182/blood-2014-08-595561.

Burstein, S. *et al.* (1992) 'Thrombocytopoiesis in normal and sublethally irradiated dogs: response to human interleukin-6', *Blood*. American Society of Hematology, 80(2), pp. 420–428. doi: 10.1182/blood.v80.2.420.bloodjournal802420.

Caillon, L. *et al.* (2013) 'Biophysical Investigation of the Membrane-Disrupting Mechanism of the Antimicrobial and Amyloid-Like Peptide Dermaseptin S9', *PLOS ONE*. Public Library of Science, 8(10), p. e75528.

Capecchi, M. R. (2005) 'Gene targeting in mice: Functional analysis of the mammalian genome for the twenty-first century', *Nature Reviews Genetics*. Nat Rev Genet, pp. 507–512. doi: 10.1038/nrg1619.

Castaman, G. and Matino, D. (2019) 'Hemophilia A and B: Molecular and clinical similarities and differences', *Haematologica*. Ferrata Storti Foundation, pp. 1702–1709. doi: 10.3324/haematol.2019.221093.

CellGenix (2020) *CellGenix GMP SCGM*. Available at: https://cellgenix.com/products/gmp-scgm/ (Accessed: 24 October 2020).

Chaing, S. *et al.* (1994) 'Severe factor VII deficiency caused by mutations abolishing the cleavage site for activation and altering binding to tissue factor', *Blood*, 83(12).

Chen, C. H. *et al.* (2017) 'α-granule biogenesis: from disease to discovery', *Platelets*. Taylor & Francis, 28(2), pp. 147–154. doi: 10.1080/09537104.2017.1280599.

Chen, J. Y. *et al.* (2016) 'Hoxb5 marks long-term haematopoietic stem cells and reveals a homogenous perivascular niche', *Nature*. Nature Publishing Group, 530(7589), pp. 223–227. doi: 10.1038/nature16943.

Cheng, Q. *et al.* (2010) ‘A role for factor XIIa-mediated factor XI activation in thrombus formation in vivo’, *Blood*. Blood, 116(19), pp. 3981–3989. doi: 10.1182/blood-2010-02-270918.

Cherry, A. B. C. and Daley, G. Q. (2012) ‘Reprogramming cellular identity for regenerative medicine’, *Cell*. Cell Press, pp. 1110–1122. doi: 10.1016/j.cell.2012.02.031.

Choi, E. S. *et al.* (1995) ‘Recombinant human megakaryocyte growth and development factor (rhumgdf), a ligand for c‐mpl, produces functional human platelets in vitro’, *Stem Cells*. John Wiley & Sons, Ltd, 13(3), pp. 317–322. doi: 10.1002/stem.5530130313.

Chow, A. *et al.* (2011) ‘Bone marrow CD169+ macrophages promote the retention of hematopoietic stem and progenitor cells in the mesenchymal stem cell niche’, *Journal of Experimental Medicine*. Rockefeller University Press, 208(2), pp. 761–771. doi: 10.1084/jem.20101688.

Clifford, L. and Kor, D. J. (2016) ‘Blood products’, in *Surgical Intensive Care Medicine, Third Edition*. Springer International Publishing, pp. 473–493. doi: 10.1007/978-3-319-19668-8_35.

Cong, L. *et al.* (2013) ‘Multiplex genome engineering using CRISPR/Cas systems’, *Science*. American Association for the Advancement of Science, 339(6121), pp. 819–823. doi: 10.1126/science.1231143.

Cowan, K. (2017) *Strategies to reduce inappropriate use of platelet transfusions*, *Nursing Times*. Available at: https://www.nursingtimes.net/clinical-archive/haematology/strategies-to-reduce-inappropriate-use-of-platelet-transfusions-30-01-2017/ (Accessed: 24 September 2019).

Crane, G. M., Jeffery, E. and Morrison, S. J. (2017) ‘Adult haematopoietic stem cell niches’, *Nature Reviews Immunology*. Nature Publishing Group, pp. 573–590. doi: 10.1038/nri.2017.53.

Crittenden, J. R. *et al.* (2004) ‘CalDAG-GEFI integrates signaling for platelet aggregation and thrombus formation’, *Nature Medicine*. Nat Med, 10(9), pp. 982–986. doi: 10.1038/nm1098.

Czogalla, K. J. *et al.* (2017) ‘Warfarin and Vitamin K compete for binding to Phe55 in human VKOR’, *Nature Structural and Molecular Biology*. Nature Publishing Group, 24(1), pp. 77–85. doi: 10.1038/nsmb.3338.

D’Andrea, G. *et al.* (2004) ‘Molecular characterization of a factor VII deficient patient supports the importance of the second epidermal growth factor-like domain.’, *Haematologica*. Italy, 89(8), pp. 979–984.

Dager, W. E., Roberts, A. J. and Nishijima, D. K. (2019) ‘Effect of low and moderate dose FEIBA to reverse major bleeding in patients on direct oral anticoagulants’, *Thrombosis Research*. Elsevier Ltd, 173, pp. 71–76. doi: 10.1016/j.thromres.2018.11.009.

Daley, G. Q. *et al.* (2016) ‘Setting Global Standards for Stem Cell Research and

Clinical Translation: The 2016 ISSCR Guidelines', *Stem cell reports*. 2016/05/12. Elsevier, 6(6), pp. 787–797. doi: 10.1016/j.stemcr.2016.05.001.

Datta, N. S. *et al.* (1996) 'Novel alterations in CDK1/cyclin B1 kinase complex formation occur during the acquisition of a polyploid DNA content', *Molecular Biology of the Cell*. American Society for Cell Biology, 7(2), pp. 209–223. doi: 10.1091/mbc.7.2.209.

Davie, E. W. and Ratnoff, O. D. (1964) 'Waterfall sequence for intrinsic blood clotting', *Science*. Science, 145(3638), pp. 1310–1312. doi: 10.1126/science.145.3638.1310.

Dettke, M. *et al.* (1998) 'Increase in endogenous thrombopoietin in healthy donors after automated plateletpheresis', *Transfusion*. Blackwell Publishing Inc., 38(5), pp. 449–453. doi: 10.1046/j.1537-2995.1998.38598297213.x.

Dexter, T. M., Allen, T. D. and Lajtha, L. G. (1977) 'Conditions controlling the proliferation of haemopoietic stem cells in vitro', *Journal of Cellular Physiology*. John Wiley & Sons, Ltd, 91(3), pp. 335–344. doi: 10.1002/jcp.1040910303.

Dickneite, G. and Pragst, I. (2009) 'Prothrombin complex concentrate vs fresh frozen plasma for reversal of dilutional coagulopathy in a porcine trauma model', *BJA: British Journal of Anaesthesia*, 102(3), pp. 345–354. doi: 10.1093/bja/aen391.

Ding, L. *et al.* (2012) 'Endothelial and perivascular cells maintain haematopoietic stem cells', *Nature*. NIH Public Access, 481(7382), pp. 457–462. doi: 10.1038/nature10783.

Du, L. M. *et al.* (2013) 'Platelet-targeted gene therapy with human factor VIII establishes haemostasis in dogs with haemophilia A', *Nature Communications*. Nature Publishing Group, 4, pp. 1–11. doi: 10.1038/ncomms3773.

Duke, W. W. (1910) 'The relation of blood platelets to hemorrhagic disease: Description of a method for determining the bleeding time and coagulation time and report of three cases of hemorrhagic disease relieved by transfusion', *Journal of the American Medical Association*. American Medical Association, 55(14), pp. 1185–1192. doi: 10.1001/jama.1910.04330140029009.

Ebbe, S. (1976) 'Biology of megakaryocytes.', *Progress in hemostasis and thrombosis*. United States, 3, pp. 211–229.

Elagib, K. E. *et al.* (2017) 'Neonatal expression of RNA-binding protein IGF2BP3 regulates the human fetal-adult megakaryocyte transition', *Journal of Clinical Investigation*. American Society for Clinical Investigation, 127(6), pp. 2365–2377. doi: 10.1172/JCI88936.

Eliades, A., Papadantonakis, N. and Ravid, K. (2010) 'New roles for cyclin E in megakaryocytic polyploidization', *Journal of Biological Chemistry*. J Biol Chem, 285(24), pp. 18909–18917. doi: 10.1074/jbc.M110.102145.

Erban, S. B., Kinman, J. L. and Schwartz, J. S. (1989) 'Routine Use of the Prothrombin and Partial Thromboplastin Times', *JAMA: The Journal of the*

American Medical Association. American Medical Association, 262(17), pp. 2428–2432. doi: 10.1001/jama.1989.03430170090034.

Escolar, G. and White, J. G. (1991) 'The platelet open canalicular system: A final common pathway', *Blood Cells*, 17(3), pp. 467–485.

Estcourt, L. J. *et al.* (2017) 'Guidelines for the use of platelet transfusions', *British Journal of Haematology*. Blackwell Publishing Ltd, 176(3), pp. 365–394. doi: 10.1111/bjh.14423.

Faber, H. E. *et al.* (1976) 'beta2-microglobulin locus on human chromosome 15.', *Somatic cell genetics*. United States, 2(2), pp. 141–153. doi: 10.1007/BF01542627.

Fatt, P. and Katz, B. (1950) 'Some observations on biological noise.', *Nature*. England, 166(4223), pp. 597–598. doi: 10.1038/166597a0.

Feghhi, S. *et al.* (2016) 'Glycoprotein Ib-IX-V Complex Transmits Cytoskeletal Forces That Enhance Platelet Adhesion', *Biophysical Journal*. Biophysical Society, 111(3), pp. 601–608. doi: 10.1016/j.bpj.2016.06.023.

Ford, C. E. *et al.* (1956) 'Cytological identification of radiation-chimæras', *Nature*. Nature Publishing Group, 177(4506), pp. 452–454. doi: 10.1038/177452a0.

Foster, A. J. *et al.* (2018) 'CRISPR-Cas9 ribonucleoprotein-mediated co-editing and counterselection in the rice blast fungus', *Scientific Reports*, 8(1), p. 14355. doi: 10.1038/s41598-018-32702-w.

Frisch, B. J. and Calvi, L. M. (2014) 'Hematopoietic stem cell cultures and assays', *Methods in molecular biology (Clifton, N.J.)*, 1130, pp. 315–324. doi: 10.1007/978-1-62703-989-5_24.

Fu, Y. *et al.* (2013) 'High-frequency off-target mutagenesis induced by CRISPR-Cas nucleases in human cells', *Nature Biotechnology*, 31(9), pp. 822–826. doi: 10.1038/nbt.2623.

Fuhrmann, J. *et al.* (2016) 'Assessment of human platelet survival in the NOD/SCID mouse model: Technical considerations', *Transfusion*. Blackwell Publishing Inc., 56(6), pp. 1370–1375. doi: 10.1111/trf.13602.

Gallwitz, M. *et al.* (2012) 'The extended cleavage specificity of human thrombin', *PLoS ONE*. Edited by W. Xu. CRC Press Inc, 7(2), p. e31756. doi: 10.1371/journal.pone.0031756.

Gao, Y. *et al.* (2012) 'Role of RhoA-Specific Guanine Exchange Factors in Regulation of Endomitosis in Megakaryocytes', *Developmental Cell*. Dev Cell, 22(3), pp. 573–584. doi: 10.1016/j.devcel.2011.12.019.

García-Roa, M. *et al.* (2017) 'Red blood cell storage time & transfusion: Current practice, concerns & future perspectives', *Blood Transfusion*. SIMTI Servizi Sri, pp. 222–231. doi: 10.2450/2017.0345-16.

Gaur, M. *et al.* (2006) 'Megakaryocytes derived from human embryonic stem

cells: A genetically tractable system to study megakaryocytopoiesis and integrin function', *Journal of Thrombosis and Haemostasis*. John Wiley & Sons, Ltd, 4(2), pp. 436–442. doi: 10.1111/j.1538-7836.2006.01744.x.

Geddis, A. E. (2010) 'Megakaryopoiesis', *Seminars in Hematology*. NIH Public Access, 47(3), pp. 212–219. doi: 10.1053/j.seminhematol.2010.03.001.

Gerrard, J. M., White, J. G. and Peterson, D. A. (1978) 'The platelet dense tubular system: its relationship to prostaglandin synthesis and calcium flux', *Thrombosis and Haemostasis*, pp. 224–231. doi: 10.1055/s-0038-1648656.

Ghadimi, K., Levy, J. H. and Welsby, I. J. (2016) 'Prothrombin Complex Concentrates for Bleeding in the Perioperative Setting', *Anesthesia and Analgesia*. Lippincott Williams and Wilkins, pp. 1287–1300. doi: 10.1213/ANE.0000000000001188.

Ghosh, S. *et al.* (2007) 'Endothelial cell protein C receptor acts as a cellular receptor for factor VIIa on endothelium', *The Journal of biological chemistry*. 2007/02/27, 282(16), pp. 11849–11857. doi: 10.1074/jbc.M609283200.

Giammona, L. M. *et al.* (2006) 'Nicotinamide (vitamin B3) increases the polyploidisation and proplatelet formation of cultured primary human megakaryocytes', *British Journal of Haematology*. Br J Haematol, 135(4), pp. 554–566. doi: 10.1111/j.1365-2141.2006.06341.x.

Gibson, D. G. *et al.* (2009) 'Enzymatic assembly of DNA molecules up to several hundred kilobases', *Nature Methods*. Nature Publishing Group, 6(5), pp. 343–345. doi: 10.1038/nmeth.1318.

Gidlöf, O. *et al.* (2013) 'Platelets activated during myocardial infarction release functional miRNA, which can be taken up by endothelial cells and regulate ICAM1 expression', *Blood*, 121(19), pp. 3908–3917. doi: 10.1182/blood-2012-10-461798.

Gill, R. *et al.* (2009) 'Safety and efficacy of recombinant activated factor VII: A randomized placebo-controlled trial in the setting of bleeding after cardiac surgery', *Circulation*, 120(1), pp. 21–27. doi: 10.1161/CIRCULATIONAHA.108.834275.

El Golli, N. *et al.* (2005) 'Evidence for a granule targeting sequence within platelet factor 4', *Journal of Biological Chemistry*. American Society for Biochemistry and Molecular Biology, 280(34), pp. 30329–30335. doi: 10.1074/jbc.M503847200.

Goncalves, K. A. *et al.* (2016) 'Angiogenin Promotes Hematopoietic Regeneration by Dichotomously Regulating Quiescence of Stem and Progenitor Cells', *Cell*. Cell Press, 166(4), pp. 894–906. doi: 10.1016/j.cell.2016.06.042.

Gopalakrishnan, R. *et al.* (2010) 'Bio-distribution of pharmacologically administered recombinant factor VIIa (rFVIIa).', *Journal of thrombosis and haemostasis : JTH*, 8(2), pp. 301–310. doi: 10.1111/j.1538-7836.2009.03696.x.

Gordon, J. W. and Ruddle, F. H. (1981) 'Integration and stable germ line transmission of genes injected into mouse pronuclei', *Science*, 214(4526), pp.

1244 LP – 1246. doi: 10.1126/science.6272397.

Grau, J., Boch, J. and Posch, S. (2013) 'TALENoffer: genome-wide TALEN off-target prediction', *Bioinformatics*, 29(22), pp. 2931–2932. doi: 10.1093/bioinformatics/btt501.

Greineder, C. F. *et al.* (2013) 'Advanced drug delivery systems for antithrombotic agents', *Blood*. 2013/06/24. American Society of Hematology, 122(9), pp. 1565–1575. doi: 10.1182/blood-2013-03-453498.

Grover, S. P. and Mackman, N. (2019) 'Intrinsic Pathway of Coagulation and Thrombosis', *Arteriosclerosis, Thrombosis, and Vascular Biology*. Lippincott Williams and Wilkins, 39(3), pp. 331–338. doi: 10.1161/ATVBAHA.118.312130.

Gurdon, J. B., Elsdale, T. R. and Fischberg, M. (1958) 'Sexually mature individuals of Xenopus laevis from the transplantation of single somatic nuclei', *Nature*. Nature Publishing Group, 182(4627), pp. 64–65. doi: 10.1038/182064a0.

Gurney, A. L. *et al.* (1994) 'Thrombocytopenia in c-mpl-deficient mice', *Science*. American Association for the Advancement of Science, 265(5177), pp. 1445–1447. doi: 10.1126/science.8073287.

Hainaut, P. and Pfeifer, G. P. (2001) 'Patterns of p53 G-->T transversions in lung cancers reflect the primary mutagenic signature of DNA-damage by tobacco smoke.', *Carcinogenesis*. England, 22(3), pp. 367–374. doi: 10.1093/carcin/22.3.367.

Handagama, P. J., Feldman, B. F., *et al.* (1987) 'In vitro platelet release by rat megakaryocytes: effect of metabolic inhibitors and cytoskeletal disrupting agents.', *American journal of veterinary research*. United States, 48(7), pp. 1142–1146.

Handagama, P. J., George, J. N., *et al.* (1987) 'Incorporation of a circulating protein into megakaryocyte and platelet granules', *Proceedings of the National Academy of Sciences of the United States of America*. National Academy of Sciences, 84(3), pp. 861–865. doi: 10.1073/pnas.84.3.861.

Harrington, W. J. *et al.* (1951) 'Demonstration of a thrombocytopenic factor in the blood of patients with thrombocytopenic purpura.', *The Journal of laboratory and clinical medicine*. United States, 38(1), pp. 1–10.

Harrison, P. and Cramer-Martin, E. (1993) 'Platelet α-granules', *Blood Reviews*. Churchill Livingstone, 7(1), pp. 52–62. doi: 10.1016/0268-960X(93)90024-X.

Hart, A. *et al.* (2000) 'Fli-1 is required for murine vascular and megakaryocytic development and is hemizygously deleted in patients with thrombocytopenia', *Immunity*. Cell Press, 13(2), pp. 167–177. doi: 10.1016/S1074-7613(00)00017-0.

Hart, T. *et al.* (2015) 'High-Resolution CRISPR Screens Reveal Fitness Genes and Genotype-Specific Cancer Liabilities', *Cell*. Cell Press, 163(6), pp. 1515–1526. doi: 10.1016/j.cell.2015.11.015.

Hayward, C. P. M. *et al.* (1999) 'Multimerin processing by cells with and without

pathways for regulated protein secretion', *Blood*, 94(4), pp. 1337–1347. doi: 10.1182/blood.v94.4.1337.416k20_1337_1347.

Hedner, U. and Erhardtsen, E. (2000) 'Future possibilities in the regulation of the extrinsic pathway: rFVIIa and TFPI.', *Annals of medicine*. England, 32 Suppl 1, pp. 68–72.

Hedner, U. and Kisiel, W. (1983) 'Use of human factor VIIa in the treatment of two hemophilia A patients with high-titer inhibitors.', *The Journal of clinical investigation*. American Society for Clinical Investigation, 71(6), pp. 1836–41. doi: 10.1172/JCI110939.

Hegyi, E., Heilbrun, L. K. and Nakeff, A. (1990) 'Immunogold probing of platelet factor 4 in different ploidy classes of rat megakaryocytes sorted by flow cytometry.', *Experimental hematology*, 18(7), pp. 789–93.

Heijnen, H. F. G. *et al.* (1998) 'Multivesicular bodies are an intermediate stage in the formation of platelet α-granules', *Blood*, 91(7), pp. 2313–2325. doi: 10.1182/blood.v91.7.2313.2313_2313_2325.

Heijnen, H. F. G. (2019) 'WPBs and α-granules: More and more look-alike?', *Blood*. American Society of Hematology, pp. 2634–2636. doi: 10.1182/blood-2019-02-900878.

Heilmann, E. *et al.* (1994) 'Dog platelets accumulate intracellular Fibrinogen as they age', *Journal of Cellular Physiology*, 161(1), pp. 23–30. doi: 10.1002/jcp.1041610104.

Hersh, E. M. *et al.* (1965) 'Causes of Death in Acute Leukemia: A Ten-Year Study of 414 Patients From 1954-1963', *JAMA: The Journal of the American Medical Association*. American Medical Association, 193(2), pp. 105–109. doi: 10.1001/jama.1965.03090020019005.

Hilton, D. J., Kile, B. T. and Alexander, W. S. (2009) 'Mutational inhibition of c-Myb or p300 ameliorates treatment-induced thrombocytopenia', *Blood*. The American Society of Hematology, 113(22), pp. 5599–5604. doi: 10.1182/blood-2008-12-195255.

Himburg, H. A. *et al.* (2014) 'Pleiotrophin mediates hematopoietic regeneration via activation of RAS', *Journal of Clinical Investigation*. American Society for Clinical Investigation, 124(11), pp. 4753–4758. doi: 10.1172/JCI76838.

Hirsh, J. *et al.* (2001) 'Mechanism of Action and Pharmacology of Unfractionated Heparin', *Arteriosclerosis, Thrombosis, and Vascular Biology*. Lippincott Williams and Wilkins, 21(7), pp. 1094–1096. doi: 10.1161/hq0701.093686.

Ho, Y.-H. *et al.* (2019) 'Remodeling of Bone Marrow Hematopoietic Stem Cell Niches Promotes Myeloid Cell Expansion during Premature or Physiological Aging', *Cell Stem Cell*. Elsevier, 25(3), pp. 407-418.e6. doi: 10.1016/j.stem.2019.06.007.

Hock, H. *et al.* (2004) 'Tel/Etv6 is an essential and selective regulator of adult hematopoietic stem cell survival', *Genes and Development*. Cold Spring Harbor

Laboratory Press, 18(19), pp. 2336–2341. doi: 10.1101/gad.1239604.

Hoffman, M. (2005) 'One more way that mice and men are different', *Journal of Thrombosis and Haemostasis*. John Wiley & Sons, Ltd, 3(3), pp. 448–449. doi: 10.1111/j.1538-7836.2005.01220.x.

Hoffman, M. and Monroe, D. M. (2010) 'Platelet binding and activity of recombinant factor VIIa.', *Thrombosis research*. United States, 125 Suppl, pp. S16-8. doi: 10.1016/j.thromres.2010.01.025.

Hoffman, M. and Monroe, D. M. 3rd (2001) 'A cell-based model of hemostasis.', *Thrombosis and haemostasis*. Germany, 85(6), pp. 958–965.

Horii, T. *et al.* (2013) 'Generation of an ICF syndrome model by efficient genome editing of human induced pluripotent stem cells using the CRISPR system.', *International journal of molecular sciences*, 14(10), pp. 19774–19781. doi: 10.3390/ijms141019774.

Hu, Z. and Yang, Y. G. (2012) 'Full reconstitution of human platelets in humanized mice after macrophage depletion', *Blood*, 120(8), pp. 1713–1716. doi: 10.1182/blood-2012-01-407890.

Ichikawa, M. *et al.* (2004) 'AML-1 is required for megakaryocytic maturation and lymphocytic differentiation, but not for maintenance of hematopoietic stem cells in adult hematopoiesis', *Nature Medicine*. Nature Publishing Group, 10(3), pp. 299–304. doi: 10.1038/nm997.

Italiano, J. E. *et al.* (2008) 'Angiogenesis is regulated by a novel mechanism: Pro- and antiangiogenic proteins are organized into separate platelet α granules and differentially released', *Blood*, 111(3), pp. 1227–1233. doi: 10.1182/blood-2007-09-113837.

Itkin, T. *et al.* (2012) 'FGF-2 expands murine hematopoietic stem and progenitor cells via proliferation of stromal cells, c-Kit activation, and CXCL12 down-regulation', *Blood*, 120(9), pp. 1843–1855. doi: 10.1182/blood-2011-11-394692.

Ito, T. *et al.* (1996) 'Recombinant human c-Mpl ligand is not a direct stimulator of proplatelet formation in mature human megakaryocytes', *British Journal of Haematology*. Blackwell Publishing Ltd, 94(2), pp. 387–390. doi: 10.1046/j.1365-2141.1996.d01-1813.x.

Ito, Y. *et al.* (2018) 'Turbulence Activates Platelet Biogenesis to Enable Clinical Scale Ex Vivo Production', *Cell*. Cell Press, 174(3), pp. 636-648.e18. doi: 10.1016/j.cell.2018.06.011.

Ivanciu, L., Krishnaswamy, S. and Camire, R. M. (2014) 'New insights into the spatiotemporal localization of prothrombinase in vivo.', *Blood*. The American Society of Hematology, 124(11), pp. 1705–1714. doi: 10.1182/blood-2014-03-565010.

Ivanov, I. I. *et al.* (2019) 'Platelet P-selectin triggers rapid surface exposure of tissue factor in monocytes', *Scientific Reports*, 9(1), p. 13397. doi: 10.1038/s41598-019-49635-7.

Jacobson, L. O. *et al.* (1951) 'Recovery from radiation injury', *Science*. American Association for the Advancement of Science, 113(2940), pp. 510–511. doi: 10.1126/science.113.2940.510.

Jenne, C. N. *et al.* (2011) 'The Use of Spinning-Disk Confocal Microscopy for the Intravital Analysis of Platelet Dynamics in Response to Systemic and Local Inflammation', *PLOS ONE*. Public Library of Science, 6(9), p. e25109.

Jesty, J. *et al.* (1996) 'Initiation of the tissue factor pathway of coagulation in the presence of heparin: Control by antithrombin III and tissue factor pathway inhibitor', *Blood*. American Society of Hematology, 87(6), pp. 2301–2307. doi: 10.1182/blood.v87.6.2301.bloodjournal8762301.

Jinek, M. *et al.* (2012) 'A programmable dual-RNA-guided DNA endonuclease in adaptive bacterial immunity', *Science*. American Association for the Advancement of Science, 337(6096), pp. 816–821. doi: 10.1126/science.1225829.

Jurlander, B. *et al.* (2001) 'Recombinant Activated Factor VII (rFVIIa): Characterization, Manufacturing, and Clinical Development', *Seminars in Thrombosis and Hemostasis*, 27(4), p. 373. doi: 10.1055/s-2001-16971.

Kamykowski, J. *et al.* (2011) 'Quantitative immunofluorescence mapping reveals little functional coclustering of proteins within platelet α-granules', *Blood*, 118(5), pp. 1370–1373. doi: 10.1182/blood-2011-01-330910.

Kaplan, J. E. and Saba, T. M. (1978) 'Platelet removal from the circulation by the liver and spleen.', *The American journal of physiology*, 235(3), pp. H314-20. doi: 10.1152/ajpheart.1978.235.3.H314.

Karakikes, I. *et al.* (2015) 'Human Induced Pluripotent Stem Cell-Derived Cardiomyocytes: Insights into Molecular, Cellular, and Functional Phenotypes', *Circulation Research*. Lippincott Williams and Wilkins, pp. 80–88. doi: 10.1161/CIRCRESAHA.117.305365.

Kaufman, D. S. *et al.* (2001) 'Hematopoietic colony-forming cells derived from human embryonic stem cells', *Proceedings of the National Academy of Sciences of the United States of America*. National Academy of Sciences, 98(19), pp. 10716–10721. doi: 10.1073/pnas.191362598.

Kaushansky, K. (2005) 'The molecular mechanisms that control thrombopoiesis.', *The Journal of clinical investigation*. American Society for Clinical Investigation, 115(12), pp. 3339–47. doi: 10.1172/JCI26674.

Kavalali, E. T. (2018) 'Spontaneous neurotransmission: A form of neural communication comes of age', *Journal of neuroscience research*. 2017/12/08, 96(3), pp. 331–334. doi: 10.1002/jnr.24207.

Kempton, C. L. *et al.* (2005) 'Platelet heterogeneity: variation in coagulation complexes on platelet subpopulations.', *Arteriosclerosis, thrombosis, and vascular biology*. United States, 25(4), pp. 861–866. doi: 10.1161/01.ATV.0000155987.26583.9b.

Kiel, M. J. *et al.* (2005) 'SLAM family receptors distinguish hematopoietic stem and progenitor cells and reveal endothelial niches for stem cells', *Cell*, 121(7), pp. 1109–1121. doi: 10.1016/j.cell.2005.05.026.

Kim, Y. G., Cha, J. and Chandrasegaran, S. (1996) 'Hybrid restriction enzymes: Zinc finger fusions to Fok I cleavage domain', *Proceedings of the National Academy of Sciences of the United States of America*. Proc Natl Acad Sci U S A, 93(3), pp. 1156–1160. doi: 10.1073/pnas.93.3.1156.

Kimura, S. *et al.* (1998) 'Hematopoietic stem cell deficiencies in mice lacking c-Mpl, the receptor for thrombopoietin', *Proceedings of the National Academy of Sciences of the United States of America*. National Academy of Sciences, 95(3), pp. 1195–1200. doi: 10.1073/pnas.95.3.1195.

Koller, B. H. *et al.* (1990) 'Normal development of mice deficient in beta 2M, MHC class I proteins, and CD8+ T cells.', *Science (New York, N.Y.)*. United States, 248(4960), pp. 1227–1230. doi: 10.1126/science.2112266.

Konieczna, I. M. *et al.* (2013) 'Administration of nicotinamide does not increase platelet levels in mice', *Blood Cells, Molecules, and Diseases*. Blood Cells Mol Dis, 50(3), pp. 171–176. doi: 10.1016/j.bcmd.2012.11.007.

Kuhl, C. *et al.* (2005) 'GATA1-Mediated Megakaryocyte Differentiation and Growth Control Can Be Uncoupled and Mapped to Different Domains in GATA1', *Molecular and Cellular Biology*. American Society for Microbiology, 25(19), pp. 8592–8606. doi: 10.1128/mcb.25.19.8592-8606.2005.

Kunisaki, Y. *et al.* (2013) 'Arteriolar niches maintain haematopoietic stem cell quiescence', *Nature*. NIH Public Access, 502(7473), pp. 637–643. doi: 10.1038/nature12612.

Labelle, M., Begum, S. and Hynes, R. O. (2014) 'Platelets guide the formation of early metastatic niches', *Proceedings of the National Academy of Sciences*, 111(30), p. E3053 LP-E3061. doi: 10.1073/pnas.1411082111.

Landsteiner, K. (1900) 'Zur Kenntnis der antifermentativen, lytischen und agglutinierenden Wirkungen des Blutserums und der Lymphe ("Anti-fermentative, lytic and agglutinating effects of blood serum and lymph")', *Zentralblatt Bakteriologie*, 27, pp. 357–362.

Lauritzen, B. *et al.* (2019) 'Administration of recombinant FVIIa (rFVIIa) to concizumab-dosed monkeys is safe, and concizumab does not affect the potency of rFVIIa in hemophilic rabbits.', *Journal of thrombosis and haemostasis : JTH*. England, 17(3), pp. 460–469. doi: 10.1111/jth.14380.

Lecine, P. *et al.* (1998) 'Mice lacking transcription factor NF-E2 provide in vivo validation of the proplatelet model of thrombocytopoiesis and show a platelet production defect that is intrinsic to megakaryocytes.', *Blood*. United States, 92(5), pp. 1608–1616.

Lefrançais, E. *et al.* (2017) 'The lung is a site of platelet biogenesis and a reservoir for haematopoietic progenitors', *Nature*. Nature Publishing Group, 544(7648), pp. 105–109. doi: 10.1038/nature21706.

Levanon, D. *et al.* (2001) 'Spatial and temporal expression pattern of Runx3 (Aml2) and Runx1 (Aml1) indicates non-redundant functions during mouse embryogenesis', *Mechanisms of Development*. Elsevier, 109(2), pp. 413–417. doi: 10.1016/S0925-4773(01)00537-8.

Levine, R. F., Hazzard, K. C. and Lamberg, J. D. (1982) 'The significance of megakaryocyte size.', *Blood*. United States, 60(5), pp. 1122–1131.

Levy, J. H. *et al.* (2017) 'What is the evidence for platelet transfusion in perioperative settings?', *Vox Sanguinis*. Blackwell Publishing Ltd, 112(8), pp. 704–712. doi: 10.1111/vox.12576.

Levy, L. and Woodfield, D. G. (1984) 'The transfusion of HLA-matched platelets to thrombocytopenic patients resistant to random donor platelets.', *The New Zealand medical journal*. New Zealand, 97(766), pp. 719–721.

Li, T. *et al.* (2011) 'Modularly assembled designer TAL effector nucleases for targeted gene knockout and gene replacement in eukaryotes.', *Nucleic acids research*, 39(14), pp. 6315–6325. doi: 10.1093/nar/gkr188.

Lichtman, M. A. *et al.* (1978) 'Parasinusoidal location of megakaryocytes in marrow: A determinant of platelet release', *American Journal of Hematology*. John Wiley & Sons, Ltd, 4(4), pp. 303–312. doi: 10.1002/ajh.2830040402.

López-Sagaseta, J. *et al.* (2007) 'Binding of factor VIIa to the endothelial cell protein C receptor reduces its coagulant activity.', *Journal of thrombosis and haemostasis : JTH*. England, 5(9), pp. 1817–1824. doi: 10.1111/j.1538-7836.2007.02648.x.

Lopez-Vilchez, I. *et al.* (2011) 'Redistribution and hemostatic action of recombinant activated factor VII associated with platelets', *American Journal of Pathology*. Elsevier Inc., 178(6), pp. 2938–2948. doi: 10.1016/j.ajpath.2011.02.026.

Lord, B. I., Testa, N. G. and Hendry, J. H. (1975) *The Relative Spatial Distributions of CFUS and CFUC in the Normal Mouse Femur*, *Blood*.

Lordier, L. *et al.* (2008) 'Megakaryocyte endomitosis is a failure of late cytokinesis related to defects in the contractile ring and Rho/Rock signaling', *Blood*. American Society of Hematology, 112(8), pp. 3164–3174. doi: 10.1182/blood-2008-03-144956.

Lordier, L. *et al.* (2012) 'RUNX1-induced silencing of non-muscle myosin heavy chain IIB contributes to megakaryocyte polyploidization', *Nature Communications*. Nature Publishing Group, 3(1), pp. 1–10. doi: 10.1038/ncomms1704.

Lu, S.-J. *et al.* (2011) 'Platelets generated from human embryonic stem cells are functional in vitro and in the microcirculation of living mice.', *Cell research*. Nature Publishing Group, 21(3), pp. 530–45. doi: 10.1038/cr.2011.8.

Lüscher, T. F. (1993) '5 Platelet-vessel wall interaction: Role of nitric oxide, prostaglandins and endothelins', *Bailliere's Clinical Haematology*. Baillieres Clin

Haematol, 6(3), pp. 609–627. doi: 10.1016/S0950-3536(05)80191-X.

Macfarlane, R. G. (1964) 'An enzyme cascade in the blood clotting mechanism, and its function as a biochemical amplifier [23]', *Nature*. Nature, pp. 498–499. doi: 10.1038/202498a0.

Mali, P. *et al.* (2013) 'CAS9 transcriptional activators for target specificity screening and paired nickases for cooperative genome engineering', *Nature Biotechnology*, 31(9), pp. 833–838. doi: 10.1038/nbt.2675.

Mao, Z. *et al.* (2008) 'DNA repair by nonhomologous end joining and homologous recombination during cell cycle in human cells', *Cell cycle (Georgetown, Tex.)*, 7(18), pp. 2902–2906. doi: 10.4161/cc.7.18.6679.

Margaritis, P. *et al.* (2004) 'Novel therapeutic approach for hemophilia using gene delivery of an engineered secreted activated Factor VII', 113(7), pp. 1025–1031. doi: 10.1172/JCI200420106.The.

Maroney, S. A. *et al.* (2011) 'Murine hematopoietic cell tissue factor pathway inhibitor limits thrombus growth.', *Arteriosclerosis, thrombosis, and vascular biology*, 31(4), pp. 821–826. doi: 10.1161/ATVBAHA.110.220293.

Maynard, D. M. *et al.* (2007) 'Proteomic analysis of platelet α-granules using mass spectrometry', *Journal of Thrombosis and Haemostasis*. J Thromb Haemost, 5(9), pp. 1945–1955. doi: 10.1111/j.1538-7836.2007.02690.x.

McCulloch, E. A. and Till, J. E. (1960) 'The Radiation Sensitivity of Normal Mouse Bone Marrow Cells, Determined by Quantitative Marrow Transplantation into Irradiated Mice', *Radiation Research*. JSTOR, 13(1), p. 115. doi: 10.2307/3570877.

Mehringer, S. L. *et al.* (2018) 'Activated Factor 7 Versus 4-Factor Prothrombin Complex Concentrate for Critical Bleeding Post–Cardiac Surgery', *Annals of Pharmacotherapy*. SAGE Publications Inc., 52(6), pp. 533–537. doi: 10.1177/1060028017752365.

Méndez-Ferrer, S. *et al.* (2010) 'Mesenchymal and haematopoietic stem cells form a unique bone marrow niche', *Nature*. Nature Publishing Group, 466(7308), pp. 829–834. doi: 10.1038/nature09262.

Merkle, F. T. *et al.* (2017) 'Human pluripotent stem cells recurrently acquire and expand dominant negative P53 mutations', *Nature*. Nature Publishing Group, 545(7653), pp. 229–233. doi: 10.1038/nature22312.

Mezzano, D. *et al.* (1981) 'Evidence that platelet buoyant density, but not size, correlates with platelet age in man', *American Journal of Hematology*. Am J Hematol, 11(1), pp. 61–76. doi: 10.1002/ajh.2830110108.

Miao, C. H. *et al.* (1992) 'Liver-specific expression of the gene coding for human factor X, a blood coagulation factor.', *The Journal of biological chemistry*. United States, 267(11), pp. 7395–7401.

Michelson, A. (2007) *Platelets*. 2nd edn, *Platelets*. 2nd edn. Elsevier Inc. doi:

10.1016/B978-0-12-369367-9.X5760-7.

Mikkola, H. K. A. and Orkin, S. H. (2006) ‘The journey of developing hematopoietic stem cells’, *Development*. The Company of Biologists Ltd, pp. 3733–3744. doi: 10.1242/dev.02568.

Miller, C. H. (2019) ‘Mixing Studies’, in *Transfusion Medicine and Hemostasis*. Elsevier, pp. 783–784. doi: 10.1016/b978-0-12-813726-0.00130-6.

Milone, M. C. and O’Doherty, U. (2018) ‘Clinical use of lentiviral vectors’, *Leukemia*, 32(7), pp. 1529–1541. doi: 10.1038/s41375-018-0106-0.

Mirzaahmadi, S. *et al.* (2011) ‘Expression of recombinant human coagulation factor VII by the Lizard Leishmania expression system.’, *Journal of biomedicine & biotechnology*. Hindawi Limited, 2011, p. 873874. doi: 10.1155/2011/873874.

Moiani, A. *et al.* (2012) ‘Lentiviral vector integration in the human genome induces alternative splicing and generates aberrant transcripts’, *The Journal of Clinical Investigation*. The American Society for Clinical Investigation, 122(5), pp. 1653–1666. doi: 10.1172/JCI61852.

Moreau, T. *et al.* (2016) ‘Large-scale production of megakaryocytes from human pluripotent stem cells by chemically defined forward programming’, *Nature Communications*, 7, p. 11208. doi: 10.1038/ncomms11208.

Morgenstern, E. (1982) ‘Coated membranes in blood platelets.’, *European journal of cell biology*. Germany, 26(2), pp. 315–318.

Morrison, S. J. and Scadden, D. T. (2014) ‘The bone marrow niche for haematopoietic stem cells’, *Nature*. NIH Public Access, pp. 327–334. doi: 10.1038/nature12984.

Morrison, S. J. and Weissman, I. L. (1994) ‘The long-term repopulating subset of hematopoietic stem cells is deterministic and isolatable by phenotype’, *Immunity*, 1(8), pp. 661–673. doi: 10.1016/1074-7613(94)90037-X.

Mukai, H. Y. *et al.* (2006) ‘Transgene Insertion in Proximity to thec-myb Gene Disrupts Erythroid-Megakaryocytic Lineage Bifurcation’, *Molecular and Cellular Biology*. American Society for Microbiology, 26(21), pp. 7953–7965. doi: 10.1128/mcb.00718-06.

Muntean, A. G. *et al.* (2007) ‘Cyclin D-Cdk4 is regulated by GATA-1 and required for megakaryocyte growth and polyploidization’, *Blood*. Blood, 109(12), pp. 5199–5207. doi: 10.1182/blood-2006-11-059378.

Murphy, S. and Gardner, F. H. (1971) ‘Platelet storage at 22 degrees C; metabolic, morphologic, and functional studies.’, *The Journal of clinical investigation*. American Society for Clinical Investigation, 50(2), pp. 370–377. doi: 10.1172/JCI106504.

Na, J. *et al.* (2014) ‘Aneuploidy in pluripotent stem cells and implications for cancerous transformation’, *Protein and Cell*. Higher Education Press, 5(8), pp. 569–579. doi: 10.1007/s13238-014-0073-9.

Nagasawa, T. *et al.* (1996) 'Defects of B-cell lymphopoiesis and bone-marrow myelopoiesis in mice lacking the CXC chemokine PBSF/SDF-1', *Nature*, 382(6592), pp. 635–638. doi: 10.1038/382635a0.

Nakamura, S. *et al.* (2014) 'Expandable megakaryocyte cell lines enable clinically applicable generation of platelets from human induced pluripotent stem cells', *Cell Stem Cell*. Cell Press, 14(4), pp. 535–548. doi: 10.1016/j.stem.2014.01.011.

Nakamura, Y., Gojobori, T. and Ikemura, T. (2000) 'Codon usage tabulated from the international DNA sequence databases: status for the year 2000.', *Nucleic Acids Res.*, 28, p. 292.

Nakorn, T. N., Miyamoto, T. and Weissman, I. L. (2003) 'Characterization of mouse clonogenic megakaryocyte progenitors', *Proceedings of the National Academy of Sciences of the United States of America*, 100(1), pp. 205–210. doi: 10.1073/pnas.262655099.

Nascimento, B., Goodnough, L. T. and Levy, J. H. (2014) 'Cryoprecipitate therapy', *British journal of anaesthesia*. 2014/06/27. Oxford University Press, 113(6), pp. 922–934. doi: 10.1093/bja/aeu158.

Neumüller, J., Ellinger, A. and Wagner, T. (2015) 'Transmission Electron Microscopy of Platelets FROM Apheresis and Buffy-Coat-Derived Platelet Concentrates', in *The Transmission Electron Microscope - Theory and Applications*. InTech. doi: 10.5772/60673.

Newman, P. J., Aster R and Boylan B. (2007) 'Human platelets circulating in mice: applications for interrogating platelet function and survival, the efficacy of antiplatelet therapeutics, and the molecular basis of platelet immunological disorders', *Journal of Thrombosis and Haemostasis*, 5((Suppl 1)), pp. 305–309.

NHS Blood & Transplant (2016) *NHSBT Price List 2016-17*. Available at: https://web.archive.org/web/20180603111712/http://hospital.blood.co.uk/media/28230/component-price-list-2016-2017.pdf (Accessed: 4 February 2020).

NICE (2020) *BNF: British National Formulary*. NICE. Available at: https://bnf.nice.org.uk/medicinal-forms/factor-viia-recombinant.html (Accessed: 23 June 2020).

Nichols, K. E. *et al.* (2000) 'Familial dyserythropoietic anaemia and thrombocytopenia due to an inherited mutation in GATA 1', *Nature Genetics*. Nat Genet, 24(3), pp. 266–270. doi: 10.1038/73480.

Nieswandt, B. *et al.* (2000) 'Identification of critical antigen-specific mechanisms in the development of immune thrombocytopenic purpura in mice.', *Blood*. United States, 96(7), pp. 2520–2527.

Nieswandt, B. *et al.* (2003) 'Targeting of platelet integrin alphaIIbbeta3 determines systemic reaction and bleeding in murine thrombocytopenia regulated by activating and inhibitory FcgammaR.', *International immunology*. England, 15(3), pp. 341–349. doi: 10.1093/intimm/dxg033.

Nishikii, H., Kurita, N. and Chiba, S. (2017) 'The road map for megakaryopoietic

lineage from hematopoietic stem/progenitor cells', *Stem Cells Translational Medicine*. Wiley Blackwell, 6(8), pp. 1661–1665. doi: 10.1002/sctm.16-0490.

Nishimura, S. *et al.* (2015) 'IL-1α induces thrombopoiesis through megakaryocyte rupture in response to acute platelet needs', *Journal of Cell Biology*. Rockefeller University Press, 209(3), pp. 453–466. doi: 10.1083/jcb.201410052.

Nombela-Arrieta, C. *et al.* (2013) 'Quantitative imaging of haematopoietic stem and progenitor cell localization and hypoxic status in the bone marrow microenvironment', *Nature Cell Biology*. NIH Public Access, 15(5), pp. 533–543. doi: 10.1038/ncb2730.

Nowell, P. C. *et al.* (1956) 'Growth and continued function of rat marrow cells in x-radiated mice.', *Cancer research*. American Association for Cancer Research, 16(3), pp. 258–61.

O'Hara, P. J. *et al.* (1987) 'Nucleotide sequence of the gene coding for human factor VII, a vitamin K-dependent protein participating in blood coagulation', *Proceedings of the National Academy of Sciences of the United States of America*. National Academy of Sciences, 84(15), pp. 5158–5162. doi: 10.1073/pnas.84.15.5158.

Oceguera-Yanez, F. *et al.* (2016) 'Engineering the AAVS1 locus for consistent and scalable transgene expression in human iPSCs and their differentiated derivatives', *Methods*, 101, pp. 43–55. doi: https://doi.org/10.1016/j.ymeth.2015.12.012.

Oldham, R. A., Berinstein, E. M. and Medin, J. A. (2015) 'Lentiviral vectors in cancer immunotherapy.', *Immunotherapy*. England, 7(3), pp. 271–284. doi: 10.2217/imt.14.108.

Omatsu, Y. *et al.* (2010) 'The Essential Functions of Adipo-osteogenic Progenitors as the Hematopoietic Stem and Progenitor Cell Niche', *Immunity*, 33(3), pp. 387–399. doi: 10.1016/j.immuni.2010.08.017.

Ono, N. *et al.* (2014) 'Vasculature-associated cells expressing nestin in developing bones encompass early cells in the osteoblast and endothelial lineage', *Developmental Cell*. Cell Press, 29(3), pp. 330–339. doi: 10.1016/j.devcel.2014.03.014.

Pabinger, I. *et al.* (2017) 'Tranexamic acid for treatment and prophylaxis of bleeding and hyperfibrinolysis', *Wiener Klinische Wochenschrift*. Springer-Verlag Wien, 129(9–10), pp. 303–316. doi: 10.1007/s00508-017-1194-y.

Pang, L. *et al.* (2006) 'Maturation stage-specific regulation of megakaryopoiesis by pointed-domain Ets proteins', *Blood*. American Society of Hematology, 108(7), pp. 2198–2206. doi: 10.1182/blood-2006-04-019760.

Patel-Hett, S. *et al.* (2011) 'The spectrin-based membrane skeleton stabilizes mouse megakaryocyte membrane systems and is essential for proplatelet and platelet formation', *Blood*, 118(6), pp. 1641–1652. doi: 10.1182/blood-2011-01-330688.

Patel, S. R. *et al.* (2005) 'Differential roles of microtubule assembly and sliding in proplatelet formation by megakaryocytes.', *Blood*, 106(13), pp. 4076–4085. doi: 10.1182/blood-2005-06-2204.

Patel, S. R., Hartwig, J. H. and Italiano, J. E. (2005) 'The biogenesis of platelets from megakaryocyte proplatelets', *Journal of Clinical Investigation*. American Society for Clinical Investigation, pp. 3348–3354. doi: 10.1172/JCI26891.

Paul, D. S. and Bergmeier, W. (2020) 'Novel Mouse Model for Studying Hemostatic Function of Human Platelets.', *Arteriosclerosis, Thrombosis, and Vascular Biology*. Ovid Technologies (Wolters Kluwer Health), 40, pp. 1891–1904. doi: 10.1161/atvbaha.120.314304.

Paul, F. *et al.* (2015) 'Transcriptional Heterogeneity and Lineage Commitment in Myeloid Progenitors', *Cell*, 163(7), pp. 1663–1677. doi: 10.1016/j.cell.2015.11.013.

Pellenz, S. *et al.* (2019) 'New Human Chromosomal Sites with "Safe Harbor" Potential for Targeted Transgene Insertion', *Human gene therapy*. 2019/03/28. Mary Ann Liebert, Inc., publishers, 30(7), pp. 814–828. doi: 10.1089/hum.2018.169.

Pennisi, E. (2012) 'ENCODE Project Writes Eulogy for Junk DNA', *Science*, 337(6099), pp. 1159 LP – 1161. doi: 10.1126/science.337.6099.1159.

Peters, R. and Harris, T. (2018) 'Advances and innovations in haemophilia treatment', *Nature Reviews Drug Discovery*. Nature Publishing Group, 17(7), pp. 493–508. doi: 10.1038/nrd.2018.70.

Petljak, M. *et al.* (2019) 'Characterizing Mutational Signatures in Human Cancer Cell Lines Reveals Episodic APOBEC Mutagenesis', *Cell*. Cell Press, 176(6), pp. 1282-1294.e20. doi: 10.1016/j.cell.2019.02.012.

Petronczki, M. *et al.* (2007) 'Polo-like Kinase 1 Triggers the Initiation of Cytokinesis in Human Cells by Promoting Recruitment of the RhoGEF Ect2 to the Central Spindle', *Developmental Cell*. Dev Cell, 12(5), pp. 713–725. doi: 10.1016/j.devcel.2007.03.013.

Pick, M. *et al.* (2007) 'Differentiation of Human Embryonic Stem Cells in Serum-Free Medium Reveals Distinct Roles for Bone Morphogenetic Protein 4, Vascular Endothelial Growth Factor, Stem Cell Factor, and Fibroblast Growth Factor 2 in Hematopoiesis', *STEM CELLS*. Wiley, 25(9), pp. 2206–2214. doi: 10.1634/stemcells.2006-0713.

Pratto, F. *et al.* (2014) 'Recombination initiation maps of individual human genomes', *Science*, 346(6211), p. 1256442. doi: 10.1126/science.1256442.

Provenzale, I. *et al.* (2019) 'Whole Blood Based Multiparameter Assessment of Thrombus Formation in Standard Microfluidic Devices to Proxy In Vivo Haemostasis and Thrombosis', *Micromachines*. MDPI, 10(11), p. 787. doi: 10.3390/mi10110787.

Pusateri, A. E. and Park, M. S. (2005) 'Mechanistic implications for the use and

monitoring of recombinant activated factor VII in trauma', *Critical care (London, England)*. 2005/10/07. BioMed Central, 9 Suppl 5(Suppl 5), pp. S15–S24. doi: 10.1186/cc3781.

Qi, B. and Hardwick, J. M. (2007) 'A Bcl-xL Timer Sets Platelet Life Span', *Cell*. Cell Press, pp. 1035–1036. doi: 10.1016/j.cell.2007.03.002.

Quach, M. E., Chen, W. and Li, R. (2018) 'Mechanisms of platelet clearance and translation to improve platelet storage', *Blood*. American Society of Hematology, pp. 1512–1521. doi: 10.1182/blood-2017-08-743229.

Radley, J. M. and Haller, C. J. (1982) 'The demarcation membrane system of the megakaryocyte: a misnomer?', *Blood*. United States, 60(1), pp. 213–219.

Ran, F. A. *et al.* (2013) 'Double nicking by RNA-guided CRISPR Cas9 for enhanced genome editing specificity.', *Cell*, 154(6), pp. 1380–1389. doi: 10.1016/j.cell.2013.08.021.

Rao, L. V and Rapaport, S. I. (1990) 'Factor VIIa-catalyzed activation of factor X independent of tissue factor: its possible significance for control of hemophilic bleeding by infused factor VIIa.', *Blood*. United States, 75(5), pp. 1069–1073.

Rao, V. K. *et al.* (2014) 'Factor VIII inhibitor bypass activity and recombinant activated factor vii in cardiac surgery', *Journal of Cardiothoracic and Vascular Anesthesia*. W.B. Saunders, 28(5), pp. 1221–1226. doi: 10.1053/j.jvca.2014.04.015.

Raslova, H. *et al.* (2004) 'FLI1 monoallelic expression combined with its hemizygous loss underlies Paris-Trousseau/Jacobsen thrombopenia', *Journal of Clinical Investigation*. The American Society for Clinical Investigation, 114(1), pp. 77–84. doi: 10.1172/JCI21197.

Ren, J. *et al.* (2017) 'Multiplex Genome Editing to Generate Universal CAR T Cells Resistant to PD1 Inhibition', *Clinical Cancer Research*, 23(9), pp. 2255 LP – 2266. doi: 10.1158/1078-0432.CCR-16-1300.

Ren, Q. *et al.* (2007) 'Endobrevin/VAMP-8 is the primary v-SNARE for the platelet release reaction', *Molecular Biology of the Cell*. American Society for Cell Biology, 18(1), pp. 24–33. doi: 10.1091/mbc.E06-09-0785.

Ren, Q., Ye, S. and Whiteheart, S. W. (2008) 'The platelet release reaction: Just when you thought platelet secretion was simple', *Current Opinion in Hematology*. Curr Opin Hematol, pp. 537–541. doi: 10.1097/MOH.0b013e328309ec74.

Rosen, E. D. *et al.* (2001) 'Laser-induced noninvasive vascular injury models in mice generate platelet- and coagulationdependent thrombi', *American Journal of Pathology*. Elsevier Inc., 158(5), pp. 1613–1622. doi: 10.1016/S0002-9440(10)64117-X.

Ross, M. T. *et al.* (2005) 'The DNA sequence of the human X chromosome.', *Nature*, 434(7031), pp. 325–337. doi: 10.1038/nature03440.

Rudin, N., Sugarman, E. and Haber, J. E. (1989) 'Genetic and physical analysis

of double-strand break repair and recombination in Saccharomyces cerevisiae.', *Genetics*. Genetics Society of America, 122(3), pp. 519–534.

Salas-Perdomo, A. *et al.* (2019) 'Role of the S1P pathway and inhibition by fingolimod in preventing hemorrhagic transformation after stroke', *Scientific Reports*. Nature Publishing Group, 9(1). doi: 10.1038/s41598-019-44845-5.

Sanber, K. S. *et al.* (2015) 'Construction of stable packaging cell lines for clinical lentiviral vector production.', *Scientific reports*, 5, p. 9021. doi: 10.1038/srep09021.

Sarode, R. *et al.* (2013) 'Efficacy and safety of a 4-factor prothrombin complex concentrate in patients on vitamin K antagonists presenting with major bleeding: A randomized, plasma-controlled, phase IIIb study', *Circulation*. NIH Public Access, 128(11), pp. 1234–1243. doi: 10.1161/CIRCULATIONAHA.113.002283.

Savage, B., Saldívar, E. and Ruggeri, Z. M. (1996) 'Initiation of platelet adhesion by arrest onto fibrinogen or translocation on von Willebrand factor', *Cell*. Cell Press, 84(2), pp. 289–297. doi: 10.1016/S0092-8674(00)80983-6.

Scherer, S. and Davis, R. W. (1979) 'Replacement of chromosome segments with altered DNA sequences constructed in vitro', *Proceedings of the National Academy of Sciences of the United States of America*. Proc Natl Acad Sci U S A, 76(10), pp. 4951–4955. doi: 10.1073/pnas.76.10.4951.

Schmitt, A. *et al.* (2001) 'Of mice and men: Comparison of the ultrastructure of megakaryocytes and platelets', *Experimental Hematology*. Elsevier Inc., 29(11), pp. 1295–1302. doi: 10.1016/S0301-472X(01)00733-0.

Schofield, R. (1978) 'The relationship between the spleen colony-forming cell and the haemopoietic stem cell.', *Blood cells*, 4(1–2), pp. 7–25.

Schulze, H. *et al.* (2006) 'Characterization of the megakaryocyte demarcation membrane system and its role in thrombopoiesis', *Blood*, 107(10), pp. 3868–3875. doi: 10.1182/blood-2005-07-2755.

Schut, A. M. *et al.* (2017) 'In vitro uptake of recombinant factor VIIa by megakaryocytes with subsequent production of platelets containing functionally active drug', *British Journal of Haematology*, 178(3), pp. 482–486. doi: 10.1111/bjh.14149.

Sehgal, S. and Storrie, B. (2007) 'Evidence that differential packaging of the major platelet granule proteins von Willebrand factor and fibrinogen can support their differential release', *Journal of Thrombosis and Haemostasis*. J Thromb Haemost, 5(10), pp. 2009–2016. doi: 10.1111/j.1538-7836.2007.02698.x.

Seita, J. and Weissman, I. L. (2010) 'Hematopoietic stem cell: Self-renewal versus differentiation', *Wiley Interdisciplinary Reviews: Systems Biology and Medicine*. NIH Public Access, pp. 640–653. doi: 10.1002/wsbm.86.

Semple, J. W., Italiano, J. E. and Freedman, J. (2011) 'Platelets and the immune continuum', *Nature Reviews Immunology*. Nature Publishing Group, 11(4), pp. 264–274. doi: 10.1038/nri2956.

Shattil, S. J. and Newman, P. J. (2004) 'Integrins: Dynamic scaffolds for adhesion and signaling in platelets', *Blood*. Blood, pp. 1606–1615. doi: 10.1182/blood-2004-04-1257.

Shepherd, J. H. *et al.* (2018) 'Structurally graduated collagen scaffolds applied to the ex vivo generation of platelets from human pluripotent stem cell-derived megakaryocytes: Enhancing production and purity', *Biomaterials*. Elsevier Ltd, 182, pp. 135–144. doi: 10.1016/j.biomaterials.2018.08.019.

Shivdasani, R. A. *et al.* (1997) 'A lineage-selective knockout establishes the critical role of transcription factor GATA-1 in megakaryocyte growth and platelet development.', *The EMBO journal*, 16(13), pp. 3965–3973. doi: 10.1093/emboj/16.13.3965.

Shrivastava, S. *et al.* (2010) 'Thymosin β4 and cardiac repair', *Annals of the New York Academy of Sciences*, 1194(1), pp. 87–96. doi: 10.1111/j.1749-6632.2010.05468.x.

Shukla, M. *et al.* (2017) 'In vitro characterization of SynthoPlate™ (synthetic platelet) technology and its in vivo evaluation in severely thrombocytopenic mice', *Journal of thrombosis and haemostasis : JTH*, 15(2), pp. 375–387. doi: 10.1111/jth.13579.

Siddiqui, F. A. *et al.* (2002) 'The presence and release of tissue factor from human platelets.', *Platelets*. England, 13(4), pp. 247–253. doi: 10.1080/09537100220146398.

Sim, X. *et al.* (2016) 'Understanding platelet generation from megakaryocytes: implications for in vitro-derived platelets', *Blood*. 2016/01/19. American Society of Hematology, 127(10), pp. 1227–1233. doi: 10.1182/blood-2015-08-607929.

Siminovitch, L., McCulloch, E. A. and Till, J. E. (1963) 'The distribution of colony-forming cells among spleen colonies', *Journal of Cellular and Comparative Physiology*. Wiley, 62(3), pp. 327–336. doi: 10.1002/jcp.1030620313.

Simon, T. L. (1994) 'The collection of platelets by apheresis procedures.', *Transfusion medicine reviews*, 8(2), pp. 132–45. doi: 10.1016/s0887-7963(94)70105-x.

Smart, N. *et al.* (2007) 'Thymosin beta4 induces adult epicardial progenitor mobilization and neovascularization.', *Nature*. England, 445(7124), pp. 177–182. doi: 10.1038/nature05383.

Smethurst, P. A. (2016) 'Aging of platelets stored for transfusion.', *Platelets*, 27(6), pp. 526–34. doi: 10.3109/09537104.2016.1171303.

Spangrude, G. J., Heimfeld, S. and Weissman, I. L. (1988) 'Purification and characterization of mouse hematopoietic stem cells', *Science*. American Association for the Advancement of Science, 241(4861), pp. 58–62. doi: 10.1126/science.2898810.

Stachura, D. L., Chou, S. T. and Weiss, M. J. (2006) 'Early block to erythromegakaryocytic development conferred by loss of transcription factor

GATA-1', *Blood*. Blood, 107(1), pp. 87–97. doi: 10.1182/blood-2005-07-2740.

Stirling, Y. (1995) 'Warfarin-induced changes in procoagulant and anticoagulant proteins', *Blood Coagulation & Fibrinolysis*, 6(5).

Stoffel, R., Wiestner, A. and Skoda, R. C. (1996) 'Thrombopoietin in thrombocytopenic mice: evidence against regulation at the mRNA level and for a direct regulatory role of platelets.', *Blood*. United States, 87(2), pp. 567–573.

Stothard, P. (2000) 'The sequence manipulation suite: JavaScript programs for analyzing and formatting protein and DNA sequences.', *BioTechniques*, 28(6), pp. 1102–1104.

Stroncek, D. F. and Rebulla, P. (2007) *Platelet transfusions*, *The Lancet*. doi: 10.1016/S0140-6736(07)61198-2.

Sturgeon, C. M. *et al.* (2014) 'Wnt signaling controls the specification of definitive and primitive hematopoiesis from human pluripotent stem cells', *Nature Biotechnology*. Nature Publishing Group, 32(6), pp. 554–561. doi: 10.1038/nbt.2915.

Sun, J. *et al.* (2014) 'Clonal dynamics of native haematopoiesis', *Nature*. Nature Publishing Group, 514(7522), pp. 322–327. doi: 10.1038/nature13824.

Suryadinata, R., Sadowski, M. and Sarcevic, B. (2010) 'Control of cell cycle progression by phosphorylation of cyclin-dependent kinase (CDK) substrates.', *Bioscience reports*. Portland Press, pp. 243–255. doi: 10.1042/BSR20090171.

Suzuki, D. *et al.* (2020) 'iPSC-Derived Platelets Depleted of HLA Class I Are Inert to Anti-HLA Class I and Natural Killer Cell Immunity', *Stem Cell Reports*, 14(1), pp. 49–59. doi: 10.1016/j.stemcr.2019.11.011.

Szczelkun, M. D. *et al.* (2014) 'Direct observation of R-loop formation by single RNA-guided Cas9 and Cascade effector complexes', *Proceedings of the National Academy of Sciences*, 111(27), pp. 9798 LP – 9803. doi: 10.1073/pnas.1402597111.

Tablin, F., Castro, M. and Leven, R. M. (1990) 'Blood platelet formation in vitro. The role of the cytoskeleton in megakaryocyte fragmentation.', *Journal of cell science*. England, 97 (Pt 1), pp. 59–70.

Takahashi, K. and Yamanaka, S. (2006) 'Induction of Pluripotent Stem Cells from Mouse Embryonic and Adult Fibroblast Cultures by Defined Factors', *Cell*, 126(4), pp. 663–676. doi: 10.1016/j.cell.2006.07.024.

Takahashi, K. and Yamanaka, S. (2016) 'A decade of transcription factor-mediated reprogramming to pluripotency', *Nature Reviews Molecular Cell Biology*. Nature Publishing Group, pp. 183–193. doi: 10.1038/nrm.2016.8.

Tangelder, G. J. *et al.* (1985) 'Distribution of blood platelets flowing in arterioles', *American Journal of Physiology - Heart and Circulatory Physiology*. American Physiological Society Bethesda, MD . doi: 10.1152/ajpheart.1985.248.3.h318.

Teissandier, A. *et al.* (2019) 'Tools and best practices for retrotransposon analysis using high-throughput sequencing data', *Mobile DNA*, 10(1), p. 52. doi: 10.1186/s13100-019-0192-1.

Thomas, G. (2002) 'Furin at the cutting edge: from protein traffic to embryogenesis and disease', *Nature reviews. Molecular cell biology*, 3(10), pp. 753–766. doi: 10.1038/nrm934.

Thomas, M. and Storey, R. (2015) 'The role of platelets in inflammation', *Thrombosis and Haemostasis*. Schattauer GmbH, 114(09), pp. 449–458. doi: 10.1160/TH14-12-1067.

Thompson, O. *et al.* (2020) 'Low rates of mutation in clinical grade human pluripotent stem cells under different culture conditions', *Nature Communications*, 11(1), p. 1528. doi: 10.1038/s41467-020-15271-3.

Thon, J. N. *et al.* (2014) 'Platelet bioreactor-on-a-chip.', *Blood*, 124(12), pp. 1857–67. doi: 10.1182/blood-2014-05-574913.

Thon, J. N., Schubert, P. and Devine, D. V. (2008) 'Platelet Storage Lesion: A New Understanding From a Proteomic Perspective', *Transfusion Medicine Reviews*. Transfus Med Rev, pp. 268–279. doi: 10.1016/j.tmrv.2008.05.004.

Traherne, J. A. (2008) 'Human MHC architecture and evolution: implications for disease association studies.', *International journal of immunogenetics*, 35(3), pp. 179–192. doi: 10.1111/j.1744-313X.2008.00765.x.

Tripathi, M. M. *et al.* (2017) 'Clinical evaluation of whole blood prothrombin time (PT) and international normalized ratio (INR) using a Laser Speckle Rheology sensor', *Scientific reports*. Nature Publishing Group UK, 7(1), p. 9169. doi: 10.1038/s41598-017-08693-5.

Tripodi, A. (2016) 'Thrombin Generation Assay and Its Application in the Clinical Laboratory', *Clinical Chemistry*, 62(5), pp. 699–707. doi: 10.1373/clinchem.2015.248625.

Tsai, S. Q. *et al.* (2015) 'GUIDE-seq enables genome-wide profiling of off-target cleavage by CRISPR-Cas nucleases', *Nature Biotechnology*, 33(2), pp. 187–197. doi: 10.1038/nbt.3117.

Turecek, P. L. *et al.* (2004) 'FEIBA: mode of action.', *Haemophilia : the official journal of the World Federation of Hemophilia*. England, 10 Suppl 2, pp. 3–9. doi: 10.1111/j.1365-2516.2004.00934.x.

Varnum-Finney, B. *et al.* (2011) 'Notch2 governs the rate of generation of mouse long- and short-term repopulating stem cells', *Journal of Clinical Investigation*. American Society for Clinical Investigation, 121(3), pp. 1207–1216. doi: 10.1172/JCI43868.

Védy, D. *et al.* (2009) 'Bacterial contamination of platelet concentrates: pathogen detection and inactivation methods', *Hematology Reports*. PAGEPress Publications, 1(1), p. 5. doi: 10.4081/hr.2009.e5.

van Veen, J. J., Gatt, A. and Makris, M. (2008) 'Thrombin generation testing in routine clinical practice: are we there yet?', *British journal of haematology*. England, 142(6), pp. 889–903. doi: 10.1111/j.1365-2141.2008.07267.x.

Vermeer, C. (1984) 'The vitamin K-dependent carboxylation reaction', *Molecular and Cellular Biochemistry*. Kluwer Academic Publishers, pp. 17–35. doi: 10.1007/BF00239604.

Visnjic, D. *et al.* (2004) 'Hematopoiesis is severely altered in mice with an induced osteoblast deficiency', *Blood*, 103(9), pp. 3258–3264. doi: 10.1182/blood-2003-11-4011.

Vodyanik, M. A. *et al.* (2005) 'Human embryonic stem cell-derived CD34+ cells: Efficient production in the coculture with OP9 stromal cells and analysis of lymphohematopoietic potential', *Blood*, 105(2), pp. 617–626. doi: 10.1182/blood-2004-04-1649.

Vučetić, D. *et al.* (2018) 'Flow cytometry analysis of platelet populations: usefulness for monitoringthe storage lesion in pooled buffy-coat platelet concentrates', *Blood transfusion = Trasfusione del sangue*. 2016/12/21. Edizioni SIMTI - SIMTI Servizi Srl, 16(1), pp. 83–92. doi: 10.2450/2016.0193-16.

Waddington, C. H. (1957) *The Strategy of the Genes: A Discussion of Some Aspects of Theoretical Biology.* London: George Allen and Unwin.

Wang, B. and Zheng, J. (2016) 'Platelet generation in vivo and in vitro', *SpringerPlus*. SpringerOpen. doi: 10.1186/s40064-016-2384-1.

Wang, X. *et al.* (2005) 'Effects of factor IX or factor XI deficiency on ferric chloride-induced carotid artery occlusion in mice', *Journal of Thrombosis and Haemostasis*. J Thromb Haemost, 3(4), pp. 695–702. doi: 10.1111/j.1538-7836.2005.01236.x.

Wang, Y. *et al.* (2015) 'Comparative analysis of human ex vivo-generated platelets vs megakaryocyte-generated platelets in mice: A cautionary tale', *Blood*. American Society of Hematology, 125(23). doi: 10.1182/blood-2014-08-593053.

Wani, M. A. *et al.* (2006) 'Familial hypercatabolic hypoproteinemia caused by deficiency of the neonatal Fc receptor, FcRn, due to a mutant beta2-microglobulin gene.', *Proceedings of the National Academy of Sciences of the United States of America*, 103(13), pp. 5084–5089. doi: 10.1073/pnas.0600548103.

Waugh, D. S. (2011) 'An overview of enzymatic reagents for the removal of affinity tags', *Protein expression and purification*. 2011/08/19. Academic Press, 80(2), pp. 283–293. doi: 10.1016/j.pep.2011.08.005.

Weeterings, C. *et al.* (2008) 'The glycoprotein Ib-IX-V complex contributes to tissue factor-independent thrombin generation by recombinant factor VIIa on the activated platelet surface.', *Blood*. United States, 112(8), pp. 3227–3233. doi: 10.1182/blood-2008-02-139113.

Weissman, I. L. (2014) 'Clonal Origins of the Hematopoietic System: The Single

Most Elegant Experiment', *The Journal of Immunology*. The American Association of Immunologists, 192(11), pp. 4943–4944. doi: 10.4049/jimmunol.1400902.

Weyrich, A. S. *et al.* (2004) 'Change in protein phenotype without a nucleus: Translational control in platelets', *Seminars in Thrombosis and Hemostasis*. Semin Thromb Hemost, pp. 491–498. doi: 10.1055/s-2004-833484.

WHO (2015) *Guidelines For the Treament of Malaria*. 3rd edn. Edited by Dr P Olumese. Geneva.

WHO (2016) *The 2016 global status report on blood safety and availability*. Geneva PP - Geneva: World Health Organization.

Wiesner, K. *et al.* (2018) 'Haematopoietic stem cells: Entropic landscapes of differentiation', *Interface Focus*, 8(6). doi: 10.1098/rsfs.2018.0040.

Wilmut, I. *et al.* (1997) 'Viable offspring derived from fetal and adult mammalian cells', *Nature*. Nature Publishing Group, 385(6619), pp. 810–813. doi: 10.1038/385810a0.

Witte, D. P. *et al.* (1986) 'Megakaryoblastic leukemia in an infant. Establishment of a megakaryocytic tumor cell line in athymic nude mice.', *Cancer*, 58(2), pp. 238–44.

Wood, J. P. *et al.* (2014) 'Biology of tissue factor pathway inhibitor', *Blood*. American Society of Hematology, pp. 2934–2943. doi: 10.1182/blood-2013-11-512764.

Wright, I. S. (1962) 'The nomenclature of blood clotting factors.', *Canadian Medical Association journal*. Canadian Medical Association, 86(8), pp. 373–374. doi: 10.1055/s-0038-1655480.

Wuescher, L. M., Nishat, S. and Worth, R. G. (2019) 'Characterization of a transgenic mouse model of chronic conditional platelet depletion', *Research and Practice in Thrombosis and Haemostasis*. Wiley, 3(4), pp. 704–712. doi: 10.1002/rth2.12255.

Yang, L. *et al.* (2014) 'Targeted and genome-wide sequencing reveal single nucleotide variations impacting specificity of Cas9 in human stem cells', *Nature Communications*, 5(1), p. 5507. doi: 10.1038/ncomms6507.

Yusa, K. *et al.* (2011) 'Targeted gene correction of α1-antitrypsin deficiency in induced pluripotent stem cells.', *Nature*, 478(7369), pp. 391–394. doi: 10.1038/nature10424.

Zakrzewski, W. *et al.* (2019) 'Stem cells: Past, present, and future', *Stem Cell Research and Therapy*. BioMed Central Ltd. doi: 10.1186/s13287-019-1165-5.

Zambidis, E. T. *et al.* (2005) 'Hematopoietic differentiation of human embryonic stem cells progresses through sequential hematoendothelial, primitive, and definitive stages resembling human yolk sac development', *Blood*, 106(3), pp. 860–870. doi: 10.1182/blood-2004-11-4522.

Zhang, X. *et al.* (2018) ‘Engineering PD-1-Presenting Platelets for Cancer Immunotherapy’, *Nano Letters*. American Chemical Society, 18(9), pp. 5716–5725. doi: 10.1021/acs.nanolett.8b02321.

Zhao, M. *et al.* (2012) ‘FGF signaling facilitates postinjury recovery of mouse hematopoietic system’, *Blood*. The American Society of Hematology, 120(9), pp. 1831–1842. doi: 10.1182/blood-2011-11-393991.

Zhao, M. *et al.* (2014) ‘Megakaryocytes maintain homeostatic quiescence and promote post-injury regeneration of hematopoietic stem cells’, *Nature Medicine*. Nature Publishing Group, 20(11), pp. 1321–1326. doi: 10.1038/nm.3706.

Zheng, J. *et al.* (2011) ‘Angiopoietin-like protein 3 supports the activity of hematopoietic stem cells in the bone marrow niche’, *Blood*. The American Society of Hematology, 117(2), pp. 470–479. doi: 10.1182/blood-2010-06-291716.

Zhou, B. O. *et al.* (2014) ‘Leptin-receptor-expressing mesenchymal stromal cells represent the main source of bone formed by adult bone marrow’, *Cell Stem Cell*. Cell Press, 15(2), pp. 154–168. doi: 10.1016/j.stem.2014.06.008.

Zimmet, J. M. *et al.* (1997) ‘A role for cyclin D3 in the endomitotic cell cycle.’, *Molecular and Cellular Biology*. American Society for Microbiology, 17(12), pp. 7248–7259. doi: 10.1128/mcb.17.12.7248.

Zimmet, J. and Ravid, K. (2000) ‘Polyploidy: Occurrence in nature, mechanisms, and significance for the megakaryocyte-platelet system’, *Experimental Hematology*. Exp Hematol, pp. 3–16. doi: 10.1016/S0301-472X(99)00124-1.